The potential of poly (ADP-ribose) polymerase (PARP) inhibitors to improve plant growth and yield: novel crop protection agents under stressed conditions

A thesis submitted by

Luke Alan Cartwright

A thesis submitted in partial fulfilment of the requirements for the degree of Doctor of Philosophy

The University Of Sheffield.

Department of Animal and Plant Sciences

University of Sheffield

Sheffield

S10 2TN

United Kingdom

September 2017

Abstract

Chemical inhibition of the activity of poly (ADP-ribose) polymerases (PARPs) is associated with enhanced stress tolerance and growth in response to a broad range of abiotic plant stressors. This led to the suggestion that PARP inhibitors might have application in future crop protection strategies. However, the vast majority of studies to date have involved short-term, *in vitro* assays which are not representative of the conditions crop plants experience in the field. This work aimed to quantify the impact of chemical PARP inhibitor application on photosynthesis, growth and yield *in planta,* under well-watered and droughted conditions. In Chapter 2, a protocol for the quantification of the impact of drought stress on photosynthesis was developed, mainly using chlorophyll fluorescence imaging. In Chapter 3, the impacts of PARP inhibitors on photosynthesis, growth and survival in response to drought were measured. PARP inhibitors enhanced survival to severe stress but there was a cost associated with application under well-watered and moderate drought conditions. Chlorophyll fluorescence and growth measurements indicated that PARP inhibitors also had a damaging effect. Results from Chapter 4 suggested that PARP and PSII inhibitors had broadly negative impacts on yield. There was a strong relationship between growth (maximum plant object sum area) and yield under stress, which enabled the effects that compounds had on yield to be predicted approximately 40 days earlier than measuring at harvest. By fitting a model to the growth data it was possible to predict the impacts even earlier still. In Chapter 5, application of a PARP inhibitor reduced stomatal conductance but did not alter opening/closing kinetics, indicating the compound had an anti-transpirant effect. The enhanced stress tolerance of PARP-deficient plants likely protected against severe drought. However, a trade-off arises because of the costs associated with application under more moderate conditions. If PARP inhibitors are to be used in agriculture the cost/benefit balance will have to be carefully considered.

Declaration

None of the work in this thesis has been submitted to support an application for another degree of qualification at this or any other University.

Acknowledgements

I would like to thank Doctor Stephen Rolfe for his supervision and support throughout this project. Additionally I would like to thank my co-supervisors Professor Julie Gray, Professor Joe Harrity and Doctor Stephen Lindell for their help along the way. I would like to thank all those who supported me during my time at Bayer and in particular Doctor Dirk Schmutzler and Doctor Jan Dittgen for their input.

I would like to acknowledge the Biotechnology and Biological Sciences Research Council and Bayer for funding this project.

Finally I need to thank those who have supported me personally over the course of the four years, all of whom I have told in person.

Abbreviations

3ABA	3-aminobenzamide
3MB	3-methoxybenzamide
A	Carbon assimilation
ABA	Abscisic acid
AMP	Adenosine monophosphate
ATP	Adenosine triphosphate
ARC	Adenosine diphosphate ribosyl cyclase
BABA	ß-aminobutyric acid
Ca^{2+}	Calcium
cADPR	Cyclic adenosine diphosphate ribose
CO_2	Carbon dioxide
Col-0	*Arabidopsis thaliana* ecotype Columbia (wild-type)
dat	Days after transfer (of plants into climate chamber)
dH_2O	Distilled water
DMSO	Dimethyl sulfoxide
DNA	Deoxyribonucleic acid
F_v/F_m	Maximum quantum yield of photosystem II
g_s	Stomatal conductance
GUS	ß-glucuronidase reporter system
H_2O_2	Hydrogen peroxide
INA	Isonicotinamide
LEA proteins	Late embryogenesis abundant proteins
MAPK	Mitogen-activated protein kinases
MERO	Methyl ester of rapeseed oil
NAD^+	Nicotinamide adenine dinucleotide
Nic (also NA)	Nicotinamide
NPQ	Non-photochemical quenching
NUDX	Nucleotide diphosphate linked to some moiety X
OST1	Open stomata 1
PAR (μmol m^{-2} s^{-1})	Photosynthetically active radiation
PAR	Poly (ADP-ribosyl)ation
PARG	Poly (ADP-ribose) glycohydrolase
PARP	Poly (ADP-ribose) polymerase
PCD	Programmed cell death
ΦPSII (also Y_II)	Quantum yield of photosystem II
ΦNO	Quantum yield of non-regulated energy dissipation
PP2Cs	Protein phosphatase 2Cs

PSII	Photosystem II
PYR/PYL/RCARs	Pyrabactin resistance/pyrabactin resistance-like/regulatory component of ABA receptor
*q*L	Fraction of open reaction centres of PSII (Lake model)
*q*P	Fraction of open reaction centres of PSII (Puddle model)
RCs	Reaction centres
RGB imaging	Red, green, blue imaging
RNA	Ribonucleic acid
RNAi	RNA interference
ROS	Reactive oxygen species
RuBP	Ribulose 1,5-bisphosphate
SLAC1	S-type anion channel 1
SnRK2s	SNF1-related protein kinase 2s
TAIR	The Arabidopsis Information Resource
TFs	Transcription factors
TTC	2,3,5-triphenyltetrazolium-chloride
WT	Wild-type

Table of contents

Compounds used in this thesis

For confidentiality the chemical structures of the compounds that were supplied by Bayer Crop Science cannot be provided. Instead, each compound's BCS- code (Bayer identification) is assigned a common name for referral in this work (see table below). Some information about each compounds activity is detailed below.

BCS-code	Assigned name
CO80755	Compound 1
CK52259	Compound 2
AF22791	Compound 3
CN85321	Compound 4

Compound 1 showed good inhibition of the PARP II enzyme from *Arabidopsis thaliana* with a pIC_{50} value of 6.4 (IC_{50} = 400 nM) and showed almost no herbicidal activity with a Bayer activity index (AI) of 2. The PSII inhibition value was not determined.

Compound 2 showed strong PARP inhibition with a pIC_{50} value of 7.4 (IC_{50} = 40 nM), but was a weak inhibitor of the PSII enzyme from *Spinacia oleracea* with a pIC_{50} value of < 5 (IC_{50} < 10 µM) and a weak herbicide with an AI of 118.

Compound 3 was a poor PARP inhibitor with a pIC_{50} < 5.3 (IC_{50} < 5 µM), but a good inhibitor of the PSII with a pIC_{50} value of 6 (IC_{50} = 1 µM) and was a moderately strong herbicide with an AI of 266.

Compound 4 was also a poor PARP inhibitor with a pIC_{50} < 5.3 (IC_{50} < 5 µM), but a good inhibitor of the PSII with a pIC_{50} value of 5.1 (IC_{50} = 1 µM) and was a moderate herbicide with an AI of 169.

Chapter 1

1. General Introduction

1.1. Introduction

In their 2015 report 'World Population Prospects: The 2015 Revision, Key Findings and Advanced Tables', the United Nations Department of Economic and Social Affairs estimated that the current 7.3 billion world population will reach 9.7 billion in 2050 and 11.2 billion in 2100 (United Nations, 2015). This population increase, alongside changing consumption patterns necessitates an increase in food production. In 'The State of Food and Agriculture: Climate Change, Agriculture and Food Security' the Food and Agricultural Organization projected that by 2050 global food demand will be at least 60% higher than 2006 levels (Food and Agriculture Organization, 2016).

There was a similar demand for food production increases in the middle of the last century which was mainly addressed by practices born out of the 'Green Revolution' (The Royal Society, 2009). Such practices included: the introduction of new crop varieties which were higher yielding or more stress tolerant than their predecessors; the incorporation of chemicals such as fertilisers, pesticides and herbicides into crop management regimes; and an expansion of the irrigation infrastructure. These improvements and others meant that the majority of the goals of the 'Green Revolution' were broadly achieved. However, nearly five decades on the scale of the negative environmental impacts of some unsustainable practices have been realised. For example, in 2009 the European Commission published 'Directive 2009/128/EC', a framework for the sustainable use of pesticides which banned several chemicals and some practices (such as aerial spraying) that had been successful in increasing crop yields over several decades (European Union, 2009). In the future food production will need to be intensified without the use of harmful synthetic chemicals, without large increases in the use of non-renewable energy or water for irrigation, and without the provision of more land for cultivation.

Additionally climate change threatens to hinder attempts to sustainably intensify food production. Depending on geography and the localised conditions, climate change is expected to lead to both increases and decreases in agricultural yields until about 2030. Although, beyond 2030 the negative impacts of climate change on crop productivity will become increasingly severe in all areas of the globe (Food and

Agriculture Organization, 2016). Furthermore, some of the indirect consequences of a changing climate will become ever more apparent as evidenced by the changes in the demographics of plant pests and diseases (Evans *et al.*, 2008; Gornall *et al.*, 2010). In any case most scientists agree that many agricultural regions are already at risk from declining water availability, temperature changes and soil degradation; conditions which are counter to raising crop productivity.

Advances in molecular genetics and a better understanding of crop physiology have been largely responsible for the 28-47% increase in crop production since 1985 (Foley *et al.*, 2011). However, future enhancements in crop yields are not likely to result from practices such as selective breeding and current policy restricts the potential impact of genetic modification, particularly across the European continent. Crop protection strategies which reduce losses to abiotic and biotic stresses provide routes to intensify production. Oerke & Dehne (2004) estimated that between 1996 and 1998 the yields of the eight major crop species globally were reduced by around 30% by abiotic and biotic stressors. They also suggested that these actual losses would double without the intervention of classical crop protection strategies, including some of the pesticides which are now banned after the European Commission Directive of 2009. Evidently successful reduction of the amount of crops lost to stress would significantly increase global yields.

1.2. The impact of drought on plant biochemistry, physiology and growth

Drought is a major problem which causes significant crop losses worldwide with ~ 40% of global land area situated in arid climates and > 307 million hectares equipped with artificial irrigation systems (Fedoroff *et al.*, 2010; Dubois *et al.*, 2017; Zhang & Sonnewald, 2017). Most crops grow in suboptimal conditions which prevent them from achieving their full genetic growth and reproductive potential (Atkinson & Urwin, 2012). This is evident when maximum and average yields for a crop are compared. For example, in a record year wheat yields in the US can be eight times higher than the recorded average (Boyer, 1982). Wang *et al.*, (2003) suggested that

abiotic stressors reduce average yields of major crop plants by more than 50%. In 2012 alone, drought resulted in the loss of US$23 billion worth of crops in the US and US$3.5 billion worth across the EU (Statista, 2016).

Unfavourable conditions such as drought can impair essential physiological functions and disrupt cellular organisation (Shao *et al.*, 2008; Krasensky & Jonak, 2012). Additionally drought can affect plants differently depending on the duration, the intensity and the developmental stage at which it occurs. From an agricultural perspective drought is considered primarily in terms of its impact on yield and the timing of water shortage during the growing season (e.g. leaf development, heading, flowering) has a much larger effect than the intensity of stress *per se* (Pinheiro & Chaves, 2011).

The water flow of a plant is largely controlled by the rate of transpiration (Chavarria & dos Santos, 2012). The absorption of water by roots reduces the water potential in the soil in contact with the roots. This draws water from the surrounding soil towards the transpiring plant. The water absorbtion by roots is related to its suface that is in direct contact with the soil. As such, younger and longer roots with more root hairs are essential for increasing the contact surface and maintaining water absorption capacity. Additionally, the proportion and distribution of roots is important for meeting a plants water requirments (Chavarria & dos Santos, 2012; Comas *et al.,* 2013). In humid areas plants do not require extensive root systems. In contrast, dry regions necessitate more root investment and plants typically have higher root:shoot ratios. Water flows continously from the roots through the xylem to the intracellular spaces in leaves where it is lost to the atmosphere through stomata. The flow of water though the xylem is greatly influenced by the xylem diameter and xylem vessels with larger diameters have greater hydraulic conductivity (Zach *et al.,* 2010). Xylem diameter is variable throughout the growing season, being larger in vessels formed during the early part of the growing cycle. However, in most plants the cross-sectional area of the xylem is proportional to the surface area of the transpiring leaf.

Stomata form the interface between the leaf and air and accordingly control the water potential gradient between the two (Flexas & Medrano, 2002; Chaves & Oliveira, 2004). Small changes in the relative humidity of the air can lead to large

changes in the water potential gradient between the leaf and the air, meaning that stomata control the water stability of a plant. The route of water between the leaf and air depends on stomatal resistance, which is determined by stomatal aperture, and the resistance in the boundary layer resistance closest to the leaf surface. As drought develops, stomatal closure becomes main control of resistance. Additionally to stomata, the cuticle provides resistance to transpiration (Burghardt & Riederer, 2003). Generally speaking the hydraulic resistance of the cuticle is low in tropical plants and comparatively higher in xerophytic plants, demonstrating the eveolutionary adaptation to water limitation. ABA can promote cuticle deposition in response to drought (Martin *et al.,* 2017).

Water deficit is first perceived by the roots and results in adaptive stomatal closure and photosynthetic electron transport downregulation (Zhang & Sonnewald, 2017). Stomata close to limit transpirational water loss during periods of high vapour pressure deficit, during which there is a large difference between the amount of water the air can hold when saturated and the amount it is holding at that time. Such conditions are likely to occur during periods of high air temperature and low humidity. Decreased CO_2 diffusion through the stomata to Rubisco is considered to be the primary cause of reduced photosynthetic rate under mild to moderate drought (Chaves, 2002; Chaves *et al.*, 2009). Photosynthesis is affected when light capture and utilisation becomes imbalanced as electron transport rate and carboxylation efficiency decrease (Zhang & Sonnewald, 2017). This situation arises when reduced stomatal conductance is concurrent with sustained high irradiance and the rate of production of reducing power outweighs the usage in the Calvin cycle (Pinheiro & Chaves, 2011). In such circumstances, increases in thermal energy dissipation processes from within the photosynthetic machinery compete with photochemistry for absorbed light and can provide effective protection against damage from over-excitation (Pinheiro & Chaves, 2011; Roach & Krieger-Liszkay, 2014; Ruban, 2016). Likewise increases in the activities of alternative electron sinks such as cyclic electron transport, the Mehler reaction or photorespiration can also reduce the rate of production of reducing power (Ort & Baker, 2002; Miyake, 2010; Foyer *et al.*, 2012; Shikanai, 2014).

Nevertheless over-excitation of the photosystems can result in the generation of harmful reactive oxygen species (ROS) which cause protein denaturation, membrane lipid peroxidation and the oxidation of DNA and RNA. ROS are scavenged by antioxidative metabolites and enzymes which protect the photosynthetic machinery against excess excitation energy that is not dissipated through electron transport, heat dissipation or photorespiration (Ort & Baker, 2002; Wang *et al.*, 2003; Foyer *et al.*, 2012). Levels of superoxide dismutase, ascorbate peroxidase and glutathione reductase have been shown to increase during drought stress (Chaves, 2002). On the other hand it has been demonstrated that ROS play a beneficial role in the response to abiotic stress (Choudhury *et al.*, 2017). For example, the production of ROS in the chloroplasts or mitochondria can divert electrons away from the photosynthetic apparatus where they could damage the antennae. ROS are then detoxified in some of the processes alluded to earlier. Additionally, ROS have been implicated as vital molecules in a variety of stress-responsive signal transduction pathways and in the priming of defences to abiotic stress. ROS can also mediate metabolism to prevent the over-accumulation of toxic intermediates. Mutants deficient in ROS production or detoxification were found to be more susceptible to abiotic stressors and less able to regulate endogenous response pathways (Suzuki *et al.*, 2012).

On a biochemical level, drought can limit the production and activity of Rubisco and inhibit Rubisco activase and other photosynthetic enzymes, although there is some suggestion that these restrictions develop during prolonged or severe drought (Lawlor & Cornic, 2002; Lawlor, 2002). Inhibition of photosynthetic metabolism reduces the levels of assimilates for sucrose and starch production. Additionally drought inhibits sucrose phosphate synthase activity altering the ratio of sucrose/starch. Glucose, fructose and sucrose are important signalling molecules in stress response and a plants' ability to maintain defence pathways can be inhibited if stores of these metabolites are depleted (Chaves *et al.*, 2009; Pinheiro & Chaves, 2011). Plants also rely on a suite of osmolytes to maintain water status and cellular stabilisation. Among them, glycine betaine, proline, aminobutyric acid and putrescine have been shown to accumulate during drought (Valliyodan & Nguyen, 2006; Langridge *et al.*, 2006). Cellular proteins can also be prevented from unfolding

by binding with late embryogenesis abundant (LEA) proteins. These proteins accumulate during late seed development when dehydration occurs and their protective role against drought stress is the same.

Both physiological and biochemical responses to drought are regulated by the induction of ABA-dependent and ABA-independent gene expression pathways (Zhang & Sonnewald, 2017). Low soil water potential triggers the biosynthesis and translocation of ABA from the roots to the leaves via the xylem, where it reduces stomatal conductance at the transcriptional and post-transcriptional levels. Additionally guard cells can autonomously synthesise ABA allowing them to respond to changes in atmospheric humidity (Bauer *et al.*, 2017). Water shortage in leaves inhibits starch degradation and induces starch synthesis resulting in decreased concentrations of soluble sugars, reduced turgor pressure and consequent stomatal closure (Zhang & Sonnewald, 2017). The current model of ABA dynamics suggests that when ABA is absent, the protein family pyrabactin resistance 1/PYR-like/regulatory component of ABA receptors (PYR1/PYLs/RCARs) form homodimers and do not interact with downstream clade A phosphatases type-2C (PP2Cs) (Raghavendra *et al.*, 2010). PP2Cs therefore bind and inactivate SNF1-related kinases (SnRK2 kinases) and downstream targets remain inactivated. Conversely, when ABA concentrations increase PYR1/PYLs/RCARs forms a complex with PP2Cs unblocking SnRK2 kinase and triggering gene expression cascades. Most drought response pathways are ABA-dependent, although several ABA-independent genes have now been identified which mostly contain dehydration elements in their promoter regions and are activated by Apetala2 transcription factors (Zhang & Sonnewald, 2017).

At a metabolite level there is a high level of connectivity between drought, photosynthesis, ROS, ABA and sugars (sucrose and starch in particular) (Figure 1A; Pinheiro & Chaves, 2011). Interaction between hormonal pathways including ABA, ethylene and auxins are also predominant. At a gene/protein level, sugars, ROS and ABA are well represented pathways linking drought and photosynthesis (Figure 1B). Members of the bZIP (basic leucine zipper domain) and one from ABI3 (abscisic acid insensitive) families of transcription factors (TFs) are ABA-dependent (Saibo *et al.*,

2009). bZIP TFs are associated with Rubisco regulation whereas ABI3 regulates stomatal aperture (Brady *et al.*, 2003; Saibo *et al.*, 2009).

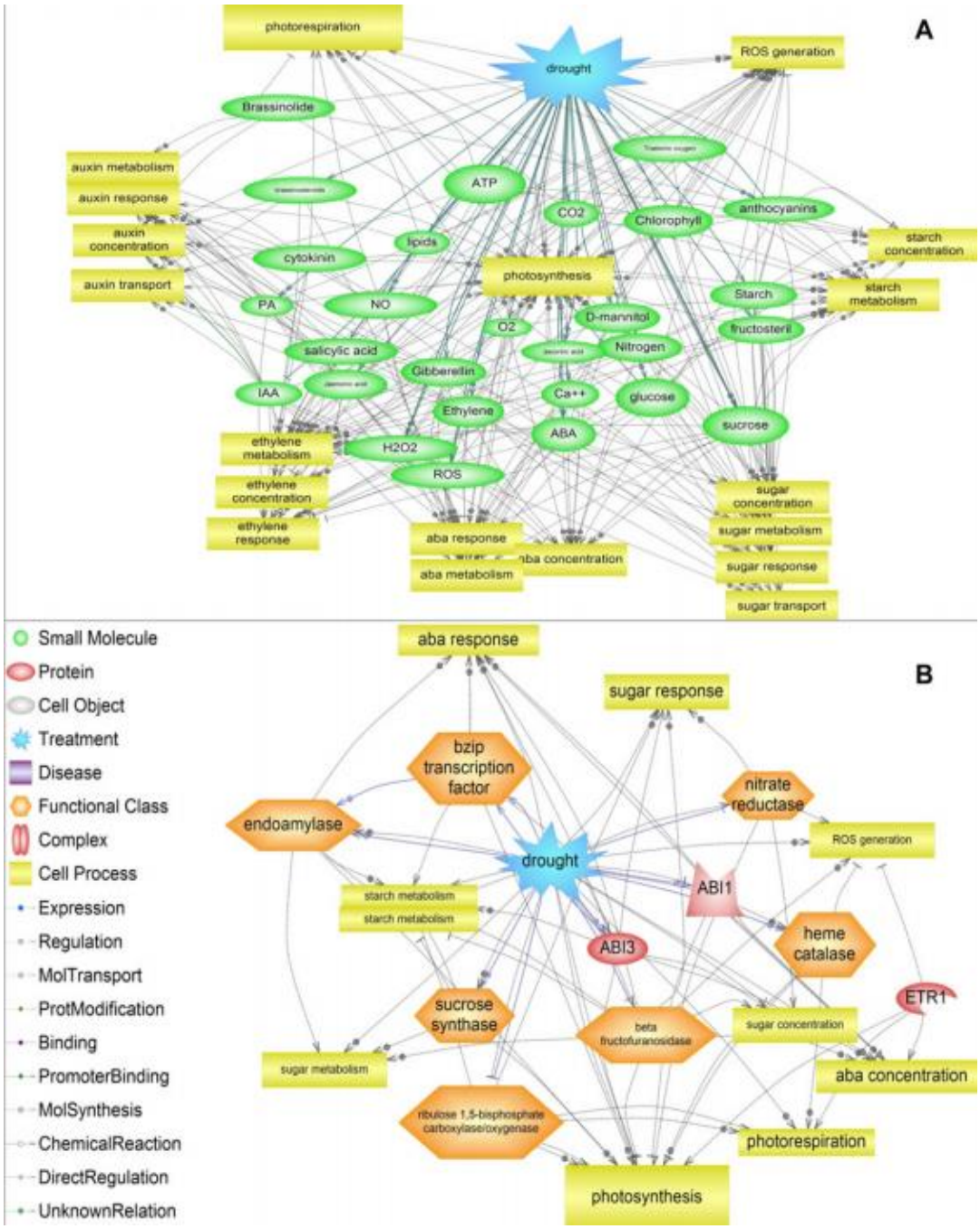

Figure 1A-B. Biological networks generated for drought and photosynthesis interactions from the literature available between 1995 and 2010 using Pathway Studio software. A = small molecules (local connectivity ≥ 6), B = proteins/genes (local connectivity ≥ 6). Taken from Pinheiro & Chaves, (2011).

Reduced net carbon gain as a result of decreased photosynthetic rate can lead to a reduction in growth rate, biomass accumulation and yield (Chaves, 2002). In

Arabidopsis, leaf growth is driven first by cell division, then by the subsequent cell expansion (Dubois *et al.*, 2017). Both of these processes have been shown to be repressed when drought was applied to Arabidopsis and maize, even when plants maintained leaf hydraulics (Baerenfaller *et al.*, 2012; Bonhomme *et al.*, 2012; Clauw *et al.*, 2015). The rapid induction of molecular cross-talk between DELLA signalling proteins and ethylene repressed leaf growth under *in vitro* osmotic stress, although this response was not replicated in soil-applied drought (Claeys *et al.*, 2012; Baerenfaller *et al.*, 2012; Dubois *et al.*, 2013). The response of yield to drought is covered in more detail in Chapter 4.

To acclimate to a particular stress plants must tailor their molecular, biochemical and physiological responses to suit the incident environmental conditions (Mittler, 2006). It is widely accepted that the simultaneous occurrence of multiple abiotic stressors is more lethal to crops than an individual stress condition. For example, it is common for plants in drought stricken areas to concurrently suffer from heat stress. Molecular and metabolomic analyses have revealed that the responses to drought and heat stress in combination are unique and cannot be extrapolated from the responses when the stresses are applied individually (Rizhsky *et al.*, 2004). In fact, often different stressors cause antagonistic responses. To alleviate heat stress a plant might open its stomata but this would be inappropriate if the plant was simultaneously experiencing drought stress.

Combined drought and heat wave caused significantly more financial damage than other major weather disasters in the US between 1980 and 2004 (Figure 2A; Rizhsky *et al.*, 2002, 2004; Mittler, 2006). Physiological characterisation of plants subjected to drought or heat stress or both, revealed that the combination led to several unique responses including high respiration, low photosynthetic rate, stomatal closure and high leaf temperature (Figure 2B). Starch breakdown and increased mitochondrial activity and energy production are likely to play central roles in drought and heat response (Rizhsky *et al.*, 2004). Transcriptomic studies revealed that > 770 transcripts were altered in Arabidopsis in response to the stress combination, but not by drought or heat (Mittler, 2006). Several metabolites including sugars differentially accumulated. For example proline, which is considered to be essential in drought

response, was strongly supressed during combined drought and heat. It is logical to suggest that different stress conditions result in the activation of different response pathways which can act synergistically or antagonistically.

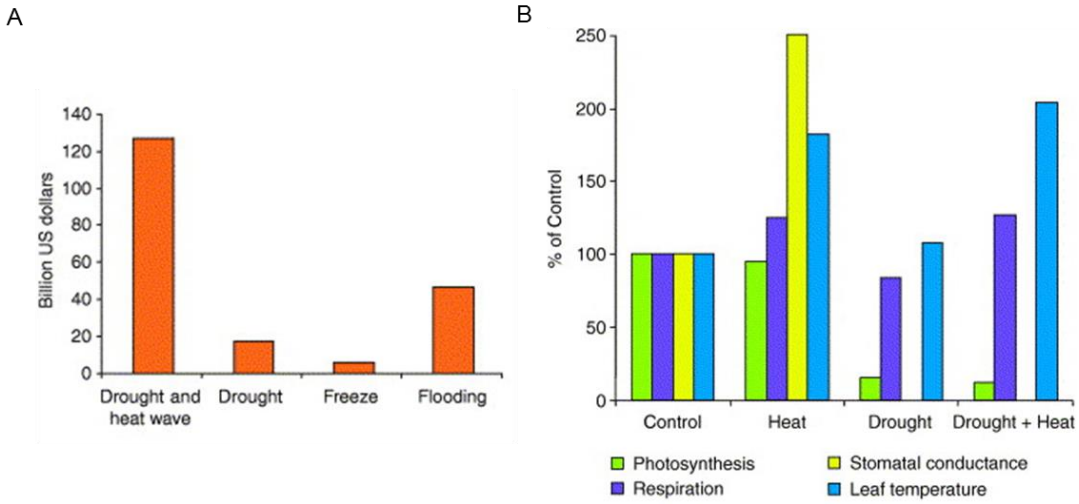

Figure 2A-B. (A) The total of all US weather disasters costing US$1 billion on more between 1980 and 2004 (excluding hurricanes, tornadoes and wildfires). Total damage was normalised to the US$ 2002 value. (B) Unique physiological characteristics of drought and heat stress combination. A combination of drought and heat stress is shown to be different from drought or heat stress by having a new combination of physiological parameters. Taken from Mittler, (2006).

Cross-talk between co-activated pathways is regulated at different levels and involves; mitogen-activated protein kinases (MAPK) cascades, transcription factors, stress hormones (e.g. ABA), calcium and ROS signalling, and receptor/signalling complexes (Fraire-velázquez *et al.*, 2011; Suzuki *et al.*, 2012; Ashraf & Harris, 2013; Kohli *et al.*, 2013; Roychoudhury *et al.*, 2013). For example, in Arabidopsis ethylene has been shown to play a vital role in drought and heat response and increased expression of the transcriptional co-factor MBF1c was shown to enhance tolerance to the stress combination by activating ethylene signal transduction pathways (Mittler & Blumwald, 2010). Consequently for a plant to mitigate against environmental insults effectively, it must correctly determine the nature and intensity of the stressors and activate the appropriate suite of response pathways. Recent research has uncovered many of the underlying components implicating:

small RNAs (Sunkar *et al.*, 2007); transcription factors (Mazzucotelli *et al.*, 2008); kinase cascades (Cristina-Rodriguez *et al.*, 2010); redox signals (Pinheiro & Chaves, 2011); ROS (Dinakar *et al.*, 2012; Suzuki *et al.*, 2012) and phytohormones (Kohli *et al.*, 2013; Roychoudhury *et al.*, 2013; Santino *et al.*, 2013) in signalling or gene expression regulation roles as part of sophisticated stress-response networks. However much work is yet to be done to establish the precise nature of stress-mediated cross-talk and several authors have called for more combinatorial stress investigations (Rizhsky *et al.*, 2004; Mittler, 2006; Atkinson & Urwin, 2012).

Drought and heat stress differentially affect morphology. While drought can result in decreased leaf area and increased root growth to minimise water loss and maximise water uptake, heat stress can lead to thin, elongated leaves with high specific leaf area and reduced root growth (Vile *et al.*, 2012). In contrast, drought and heat similarly affect flowering time, seed abortion and final yield, although there is some evidence to suggest that stress can accelerate flowering (Mittler, 2006; Takeno, 2016). This emergency response to produce the next generation, even when they themselves may not be able to survive, is most likely triggered by an increase in salicylic acid content which counteracts the action of flowering inhibitors. Furthermore, subsequent generations of drought stressed *Brassica rapa* lines were also found to flower earlier (Franks, 2011).

Over evolutionary time two water strategies have developed as a result of different climatic and and environmental conditions: isohydric and anisohydric (Sade *et al*. 2012; Sade & Moshelion 2014). Plants adopting the isohydric strategy attempt to maintain a constant leaf water potential when water is abundant or scarce (i.e. under droughted conditions), by reducing stomatal conductance to limit transpirational losses. In contrast, anisohydric plants have more variable leaf water potential because they keep their stomata open to maintain photosynthetic rates during times of water scarcity and lowering water potential. This risky approach can be beneficial under well-watered conditions because plants can sustain high CO_2 concentrations at in the mesophyll for photosynthetic electron transport, but a plant may become endangered during severe drought. From an agronomic point of view, any factor that leads to an increase in crop productivity under stress may be said to be a beneficial

trait. Due to their higher stomatal conductance and carbon assimilation, anisohydric crops are most likely to display enhanced yield under optimal or moderate water availability. However, there is a need to determine the soil water content threshold at which these plants would lose their agronomic advantage.

Some stress responses are considered inappropriate in a crop context, particularly if plants over-respond to mild stress intensities in order to maximise survival chances. Over the last twenty years several novel technologies have emerged which aim to alleviate crop losses to stress in a sustainable way. These methods include the use of biopesticides (Gatehouse *et al.*, 2011; Nakasu *et al.*, 2014), strobilurin fungicides (Herms *et al.*, 2002) and plant defence priming (Luna *et al.*, 2015; Martinez-Medina *et al.*, 2017). Over the same period there has been a shift in the agri-science industry to generate environmentally safe chemicals which can protect crop yield. One example is the synthesis of inhibitors of the poly (ADP-ribose) polymerase (PARP) enzymes. The activity of this enzyme group can be considered an inappropriate over-response to abiotic stress. The work in this thesis aimed to investigate the mode of action of PARP inhibitors and measure their effects on plant growth and yield under drought stress.

1.3. Poly (ADP-ribosyl)ation and poly (ADP-ribose) polymerases

Plants have evolved to survive and reproduce in natural environments, not to have high yields in a crop ecosystems. In order to maximise their chance of survival plants can over-respond to moderate stress which is considered a maladaptation from an agricultural perspective. This is because many of these responses are energetically intensive and often occur at the expense or growth and potentially, yield. One such example is the activity of Poly (ADP-ribose) polymerases (PARPs). PARPs catalyse the post-translational ADP-ribosylation of target proteins, itself included, by adding (often multiple) ADP-ribose moieties from nicotinamide adenine dinucleotide (NAD^+), resulting in an ADP-ribosylated protein and a nicotinamide residue (Figure 3). This reaction is reversible and ADP-ribose groups can be cleaved from proteins by poly (ADP-ribose) glycohydrolases (PARGs), generating free ADP-ribose groups which

can be hydrolysed by nucleoside diphosphate linked to some moiety-X (NUDX) enzymes, yielding adenosine monophosphate (AMP) and ribose-5-phosphate. Auto-modified PARP and other poly (ADP-ribosyl)ated proteins have roles in chromatin structuring, the transcription and the replication of DNA, and in the recruitment of DNA repair proteins.

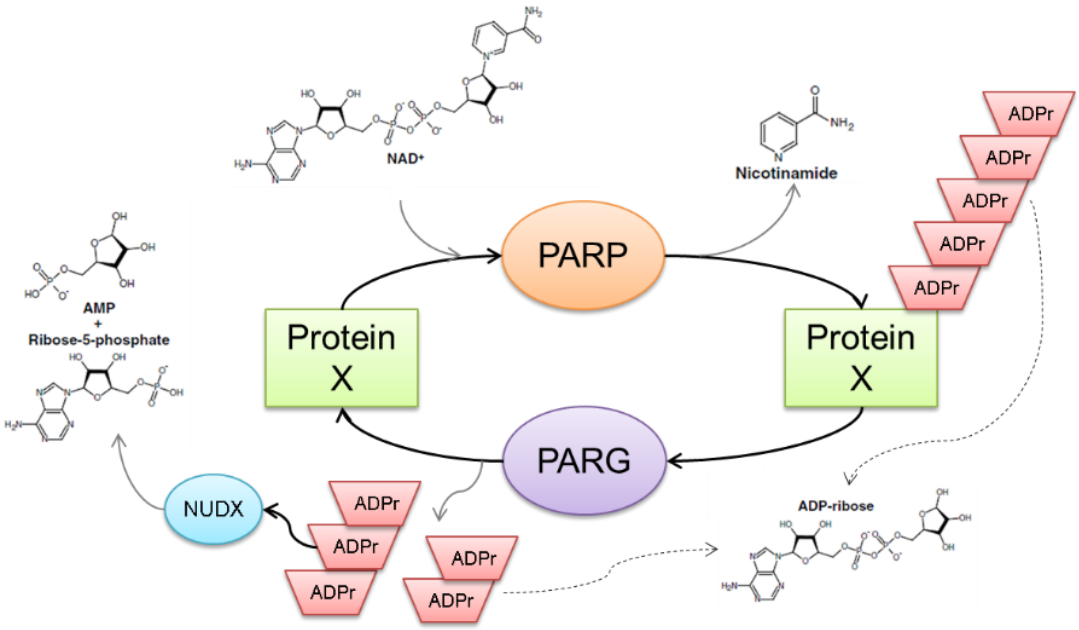

Figure 3. A model of poly (ADP-ribosyl)ation (PAR) in plants. Poly (ADP-ribose) polymerase (PARP) adds ADP-ribose groups onto target proteins generating ADP-ribosylated proteins and nicotinamide. The process is reversible and ADP-ribose can be removed from proteins through the activity of poly (ADP-ribose) glycohydrolases (PARG) generating free ADP-ribose, which is then cleaved into ribose-5-phosphate and AMP by the activity of nucleotide diphosphate linked to some moiety X (NUDX) enzymes. Adapted from Briggs & Bent, (2011).

In vivo PARP activity is greatly increased by conditions which result in DNA damage (Ikejima *et al.*, 1990; Babiychuk *et al.*, 1998). When PARP binds to DNA strand breaks it catalyses the ADP-ribosylation of specific nuclear proteins which leads to chromatin remodelling and the activation of DNA repair enzymes, particularly in replicating cells (Zhang *et al.*, 2003). It is hypothesised that when bound, PARP forms a protective block around the DNA strand break. PARP then auto-modifies through the addition of ADP-ribose groups to itself, releasing it from the nick site and allowing access for the now activated repair enzymes. High concentrations of nicotinamide can inhibit

PARP activity and delay the release of the enzyme from the nick site (Amor *et al.*, 1998; Zhang *et al.*, 2003; Briggs & Bent, 2011). Prolonged delay can initiate programmed cell death (PCD) at cell-cycle checkpoints. Previous studies have shown that plant nuclei contain low levels of PARPs in comparison to animal cells (Lepiniec *et al.*, 1995; Amor *et al.*, 1998). In animals, DNA-damaging agents post-translationally activate the constitutively abundant PARP proteins whereas in plants such as Arabidopsis, transcriptional activation leads to the production of PARPs, at a level regulated by the degree of DNA damage (Doucet-Chabeaud *et al.*, 2001). Additionally, because excessive NAD^+ consumption is considered a death signal the regulation of PARP activity at a gene expression level provides a method of preventing excessive NAD^+ consumption. The ratio of NAD^+/nicotinamide (i.e. PARP activity) therefore regulates whether a plant cell initiates DNA repair or PCD (Briggs & Bent, 2011). In soybean for example, overexpressing *AtPARP2* conferred protection against low ROS concentrations, but promoted cell death at high ROS levels (Amor *et al.*, 1998). The same group showed that soybean cell suspensions were protected from oxidative stress-induced PCD by PARP inhibition.

Strong PARP activation, such as that which can result from abiotic stress, leads to numerous consequences which can affect cellular regulation. PARP over-activation leads to: energy metabolite depletion (e.g. ATP, NAD^+), which can alter cellular redox state; mitochondrial overrespiration and subsequent ROS generation; and changes in gene expression, including ABA signalling (Briggs & Bent, 2011).

1.4. PARP homology is conserved among eukaryotes

The genomes of all eukaryotic organisms (with the exception of yeast) encode multiple PARP proteins, all bearing a conserved C-terminal catalytic PARP domain which binds and cleaves NAD^+. Arabidopsis encodes at least three putative PARPs, PARP1, PARP2 and PARP3; in addition to several structurally related proteins which lack enzymatic activity. PARP1 and PARP2 are believed to be involved in the aforementioned cellular processes as well as stress tolerance. Conversely PARP3, the most recently discovered, has been mainly implicated in seed development (Hunt &

Gray, 2009). To date several studies have used different nomenclature when describing Arabidopsis *PARP* loci information. TAIR loci details and those presented by some studies cited in this work are listed in Table 1. The Arabidopsis *parp* lines that were used in experiments in this work were classified using the TAIR loci nomenclature.

Table 1. Arabidopsis *PARP* nomenclature with the standard locus details from TAIR, (n.d.). Several papers to date have contradicted TAIR nomenclature.

Gene name	TAIR locus details	Doucet-Chabeaud *et al.*, (2001)	Briggs & Bent, (2011)	Schulz *et al.*, (2012)	Lamb *et al.*, (2012)	Jia *et al.*, (2013)
PARP1	At2g31320	At2g31320	At4g02390	Salk_097261C	At4g02390	At2g31320
PARP2	At4g02390	At4g02390	At2g31320	Salk_145153C	At2g31320	At4g02390
PARP3	At5g22470		At5g22470	Salk_108092C	At5g22470	-

Homologues of AtPARP1 have been characterised in other species such as maize (Babiychuk *et al.*, 1998), poplar and rice (Briggs & Bent, 2011). Furthermore there is evidence that plant PARPs are structurally related to mammalian PARPs (Babiychuk *et al.*, 1998; Doucet-Chabeaud *et al.*, 2001). The degree of protein domain conservation between some plant and animal PARPs is shown schematically in Figure 4. Based on the structures plant PARPs can be categorised into three groups: (i) those that possess two zinc-finger domains and thus resemble human PARP1; (ii) those that possess the PARP domain and the WGR superfamily but lack further N-terminal domains and resemble human PARP2; and (iii) those that resemble human PARP1 but lack zinc-fingers (Figure 4).

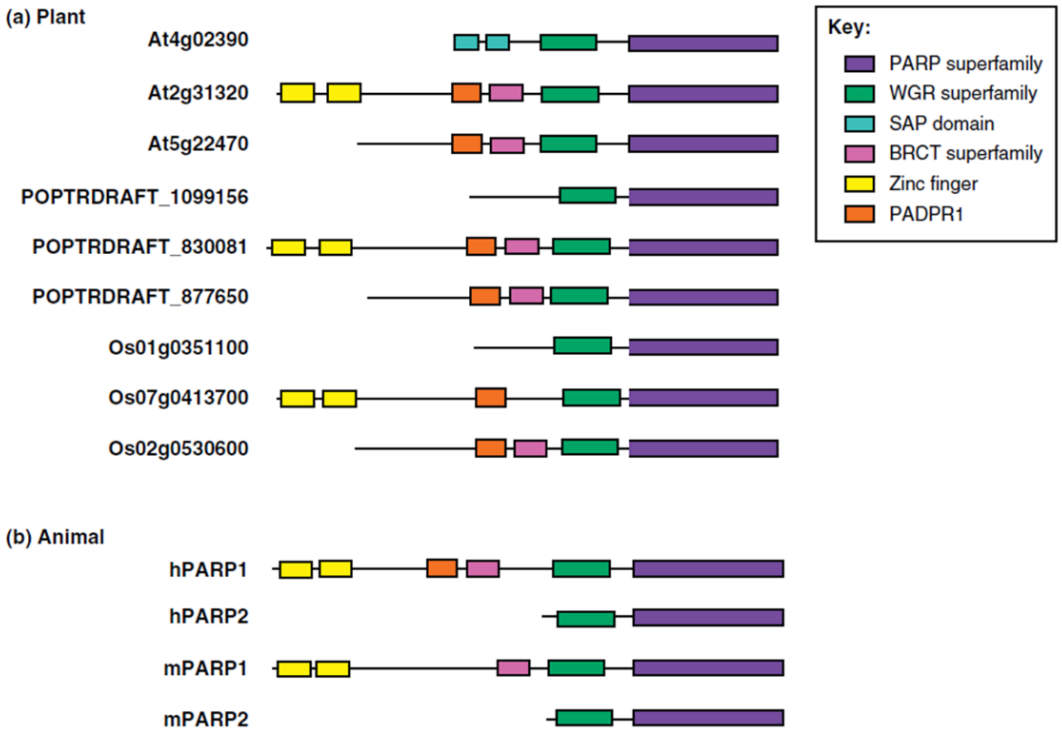

Figure 4. The conservation of protein domains across (a) plant and (b) animal poly (ADP-ribose) polymerases (PARP). Domains from Arabidopsis (At), poplar (POPDRAFT), rice (Os), human (h) and mouse (m) are shown. PARP superfamily = PARP catalytic domain; WGR superfamily = putative PARP nucleic acid binding domain; SAP domain = putative DNA and RNA binding domain; BRCT superfamily = protein-protein and DNA-protein break binding domain; Zinc finger = PARP-type DNA nick sensor; PADPR1 = unknown function, found in ADP-ribose synthetases. Taken from Briggs & Bent, (2011).

1.5. A brief history of PARP inhibition in plants

PARP inhibition was first described in plants around two decades ago and there has been growing interest ever since. Early studies supplemented media with chemical PARP inhibitors such as 3-methoxybenzamide (3-MB) and 3-aminobenzamide (3-ABA) (Figure 5A and B respectively). Genetic knock-down of PARP activity has been achieved using RNAi or cDNA technology but to date few studies have used knock-out lines. Several groups have reported that the genetic or chemical downregulation of PARP activity led to an increased tolerance to abiotic stressors such as oxidative stress (Amor *et al.*, 1998; Schulz *et al.*, 2012), ionising radiation (Doucet-Chabeaud *et al.*, 2001) and drought (Block *et al.*, 2004). In each case the enhanced resistance correlated with reduced poly ADP-ribose levels.

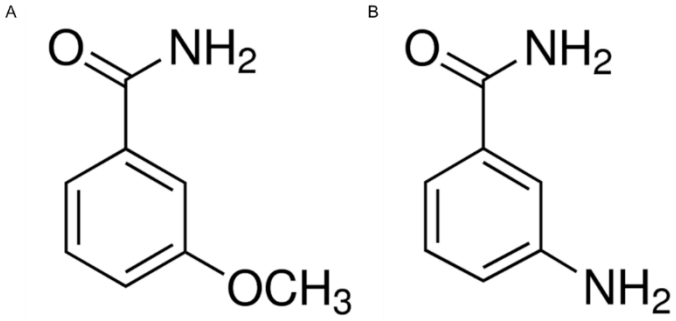

Figure 5A-B. Chemical structures of the PARP inhibitors (A) 3-methozybenzamide (3MB) and (B) 3-aminobenzamide (3-ABA).

In 1998 Amor *et al.,* suggested that PARP activation leads to NAD^+ depletion and subsequent cell death is induced through the generation of ROS. To assess the potential involvement of PARP proteins in the oxidative stress response they exogenously applied H_2O_2 to soybean culture cells and quantified the degree of PCD. They found that H_2O_2 treatment induced PCD, the extent of which was reduced following treatment with the PARP inhibitors 3ABA or nicotinamide (NIC), although the work did not detail any statistical analysis of the data (Figure 6). This suggests that plants which were able to maintain cellular NAD^+ stores under stress were better able to survive.

To substantiate these inhibitor results and determine the timing of the onset of PARP activation, they quantified the concentration of NAD^+ over a five hour period and observed two periods of NAD^+ depletion following stimulation with H_2O_2 (Figure 7). The first period, which occurred after thirty minutes, was quite severe and corresponded to the activation of PARP following the rapid ROS-induced DNA damage. NAD^+ concentrations then returned to normal after one hour. The second period, which began after two hours and was both gradual and continuous, can be attributed to the activity of endonucleases which produce the characteristic 50 kilobase DNA fragments following the initiation of PCD processes. Subsequently the group inferred that a link exists between stress-induced DNA damage and PARP activation.

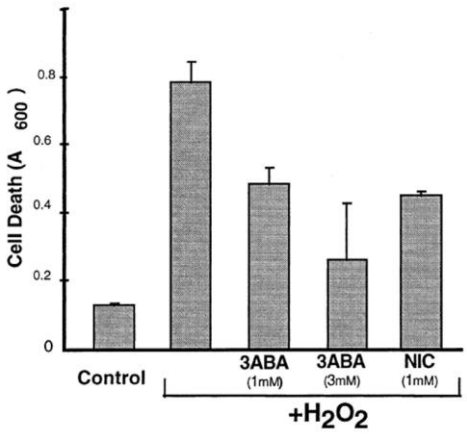

Figure 6. The effect of the PARP inhibitor 3-aminobenzamide (3ABA) and nicotinamide (NIC) on H_2O_2-induced cell death in soybean culture cells. Cells were preincubated with the indicated concentrations of compounds and then treated with 6 mM H_2O_2. Taken from Amor *et al.,* (1998).

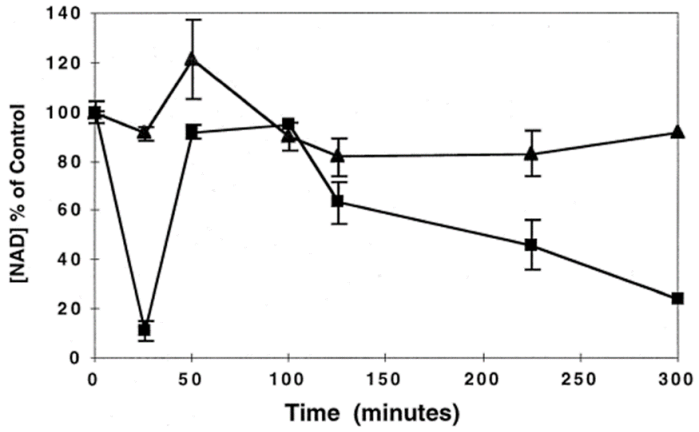

Figure 7. Changes in NAD concentration in soybean culture cells following treatment with H_2O_2. Cells were harvested at the indicated time points and total NAD content was measured in samples of 1 ml cells. Data presented as percentages of the NAD concentration in untreated cells which was around 100 µM/mg dry weight cells. ▲ untreated control cells, ■ 6 mM H_2O_2. Taken from Amor *et al.,* (1998).

In an attempt to establish a causal link between PARP activity and H_2O_2-induced PCD they transformed soybean cells with a recombinant PARP gene isolated from Arabidopsis. The Arabidopsis *app* gene constructs were introduced in either the sense or the antisense orientation, and the transformed cells were treated with either mild or severe H_2O_2 stress. They observed that when the sense transformed cells were subjected to mild H_2O_2 stress the degree of PCD was lower than the

corresponding antisense transformed cells (Figure 8). The reverse was true at severe stress where the level of PCD observed was higher in the sense transformed cells. They noted that the results of PCD inhibition from the inhibitor data in Figure 6 were consistent with the antisense PARP expression data in Figure 8. From these results they proposed that under moderate stress PARPs repair DNA damage initiating cell recovery. In contrast, after severe stress which causes extensive DNA damage, PARP activity is likely to result in apoptosis probably as a result of NAD^+ depletion. Overall the group had established a link between PARP activity, NAD^+ levels and the initiation of PCD. They had demonstrated that PARP inhibition enhanced survival in response to oxidative stress through the maintenance of NAD^+ homeostasis, an effect they were able to replicate through treatment with NAD^+.

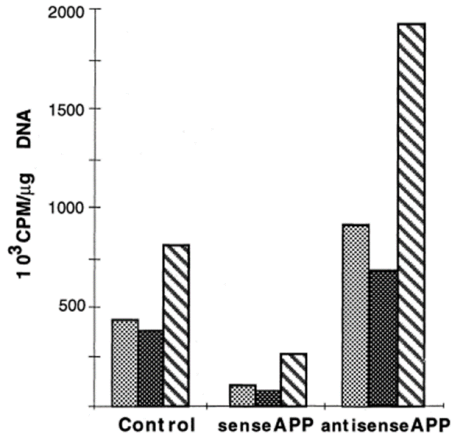

Figure 8. The effect of PARP expression on DNA nicks. Soybean culture cells were transformed with sense or antisense *app* constructs. Cells were treated with: water (light grey, dotted bars); 2 mM H_2O_2 (dark grey, dotted bars); or 10 mM H_2O_2 (dashed bar) for 120 min before they were harvested and nuclei were prepared. DNA nicks were estimated by nick translation in isolated nuclei and the incorporated label measured in a scintillation counter. Taken from Amor *et al.,* (1998).

Later in 2001 Doucet-Chabeaud *et al.,* recorded increases in *PARP1* and *PARP2* mRNA accumulation after exposing Arabidopsis to ionising radiation (Figure 9A-C). The level of *PARP2* transcripts increased following the application of drought or when the plants were cultivated on media containing cadmium, whereas no significant changes in *PARP1* mRNA were observed (Figure 10A-B). They suggested that PARP2 is involved

in a more general stress response whereas PARP1 is specifically activated by DNA breaks. This would form part of a growing consensus which suggested that PARP2 is implicated in the response to numerous abiotic stressors, where PARP1 primarily acts as a DNA-nick sensor initiating either repair or PCD depending on the degree of enzyme activation (recently suggested again in Rissel *et al.*, 2017).

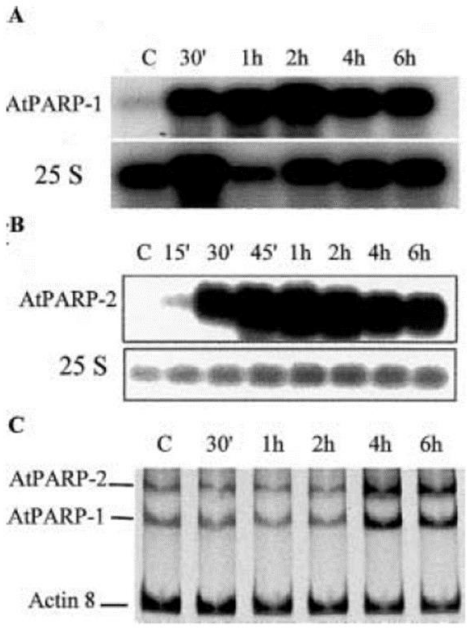

Figure 9A-C. Time course of *AtPARP1* (A) and *AtPARP2* (B) mRNA transcript accumulation following ionising irradiation or oxidative stress treatment. 5 µg aliquots of mRNA were prepared from untreated or 50 Gy gamma-irradiated leaves at the indicated time points and used for Northern analysis with *AtPARP1* and *AtPARP2* cDNA as probes. Filters were rehybridised with the constitutively expressed Arabidopsis ribosomal *25S* cDNA as a control. C: the time course of *AtPARP1* and *AtPARP2* mRNA accumulation in Arabidopsis cell suspensions following treatment with 5 mM H_2O_2 was followed by quantitative multiplex RT-PCR, in addition to Arabidopsis *ACT8* mRNA (actin 8) as a control. Taken from Doucet-Chabeaud *et al.,* (2001).

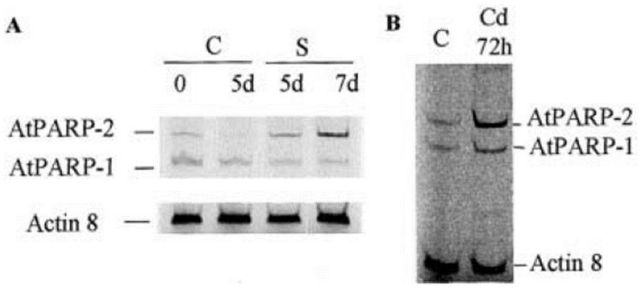

Figure 10A-B. The effect of dehydration (A) and cadmium treatment (B) on *AtPARP1* and *AtPARP2* mRNA expression. A: plants were cultivated with (C) or without (S) daily watering for the indicated time points. B: young plantlets were grown on nutrient media without (C) or in the presence (Cd) of 50 µM $CdCl_2$ for the suggested time. RNA extraction and qtRT-PCR with gene-specific primers for *AtPARP1*, *AtPARP2* and *ACT8* as a control were carried out according to normal protocols. Taken from Doucet-Chabeaud *et al.,* (2001).

In 2004 Block *et al.*, investigated how genetic and chemical downregulation of PARP activity affected tolerance to a broad range of abiotic stresses. They measured the effects of the PARP inhibitors 3MB, nicotinamide (NA) and isonicotinamide (INA) on the regrowth of *Brassica napus* calli under oxidative stress. *B. napus* callus was transferred to media containing PARP inhibitor (or controls) for one day, then to media containing the oxidative stress inducing agent acetylsalicylic acid for two days. Calli were transferred to new media and the growth over the subsequent five days was measured. They found that acetylsalicylic acid hardly inhibited callus regrowth when the media was supplemented with 3MB, suggesting that PARP inhibition protects against oxidative stress (Figure 11). In comparison to 3MB, NA and INA are weaker inhibitors and they did not protect callus regrowth to the same extent. The group did not provide information of any statistical analysis of this data set however.

This protection was also conferred in response to combined drought and heat stress in the transgenic *B. napus* hairpin AtParp2 knockdown line, but not in the azygous or wild type plants (Figure 12A). Additionally genetic knockdown of *parp1* or *parp2* reduced the level of poly (ADP-ribosyl)ation (PAR) and increased the tolerance of Arabidopsis to both drought (Figure 12B) and methyl viologen (Figure 12C). Methyl viologen acts by inhibiting photosynthesis by accepting electrons at photosystem I and adding them to oxygen generating destructive ROS (Fujii *et al.*, 1990; Asada *et*

al., 1990). Furthermore reduced PAR was also observed in the transgenic lines in response to high light (Figure 12D).

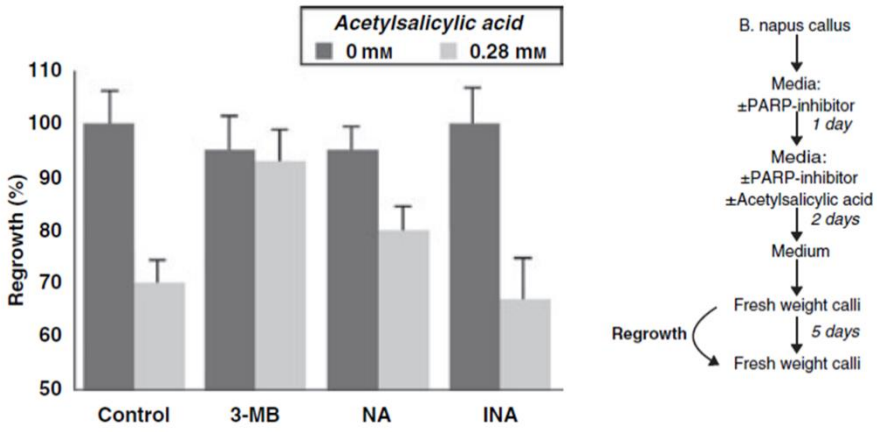

Figure 11. The effect of the PARP inhibitor 3-methoxybenzamide (3-MB), nicotinamide (NA) and isonicotinamide (INA) on the regrowth of *Brassica napus* calli. Calli were incubated for 2 d on media supplemented with 0.28 mM acetylsalicylic acid and regrowth was measured after a further 5 d. 3-MB, NA and INA were applied at 1 mM. The regrowth of control (no compound or acetylsalicylic acid treatment) was set at 100%. Error bars represent standard error (n=3). Taken from Block *et al.,* (2004).

The degradation of DNA is characteristic of both programmed and necrotic cell death the onset of which be visualised using a TUNEL assay which tags DNA breaks. PARP inhibition reduced PCD in *B. napus* hypocotyl explants following incubation with acetylsalicylic acid (Figure 13), which was consistent with the findings of Amor *et al.*, (1998).

Most stresses interfere with normal mitochondrial function through the production of harmful ROS which damage cells. The group reported that superoxide production increased by 3-8% in hpAtParp2 *B. napus* explants following treatment with acetylsalicylic acid, whereas in the wild-type explants production had increased by 167% relative to the unstressed control samples. Plants with reduced PARP activity maintained efficient mitochondrial electron transport and experienced reduced radical accumulation under stress, indicating they had lower respiration rates than wild-type plants. This was substantiated when the electron transport system in

stress-tolerant hpAtParp2 lines showed a reduced capacity to convert TTC (2,3,5-triphenyltetrazolium-chloride) to formazan in comparison to the wild-type and stress-sensitive transgenic lines (Figure 14). A TTC assay was used to indicate respiration. Although again the group did not provide evidence of any statistical analysis of the data.

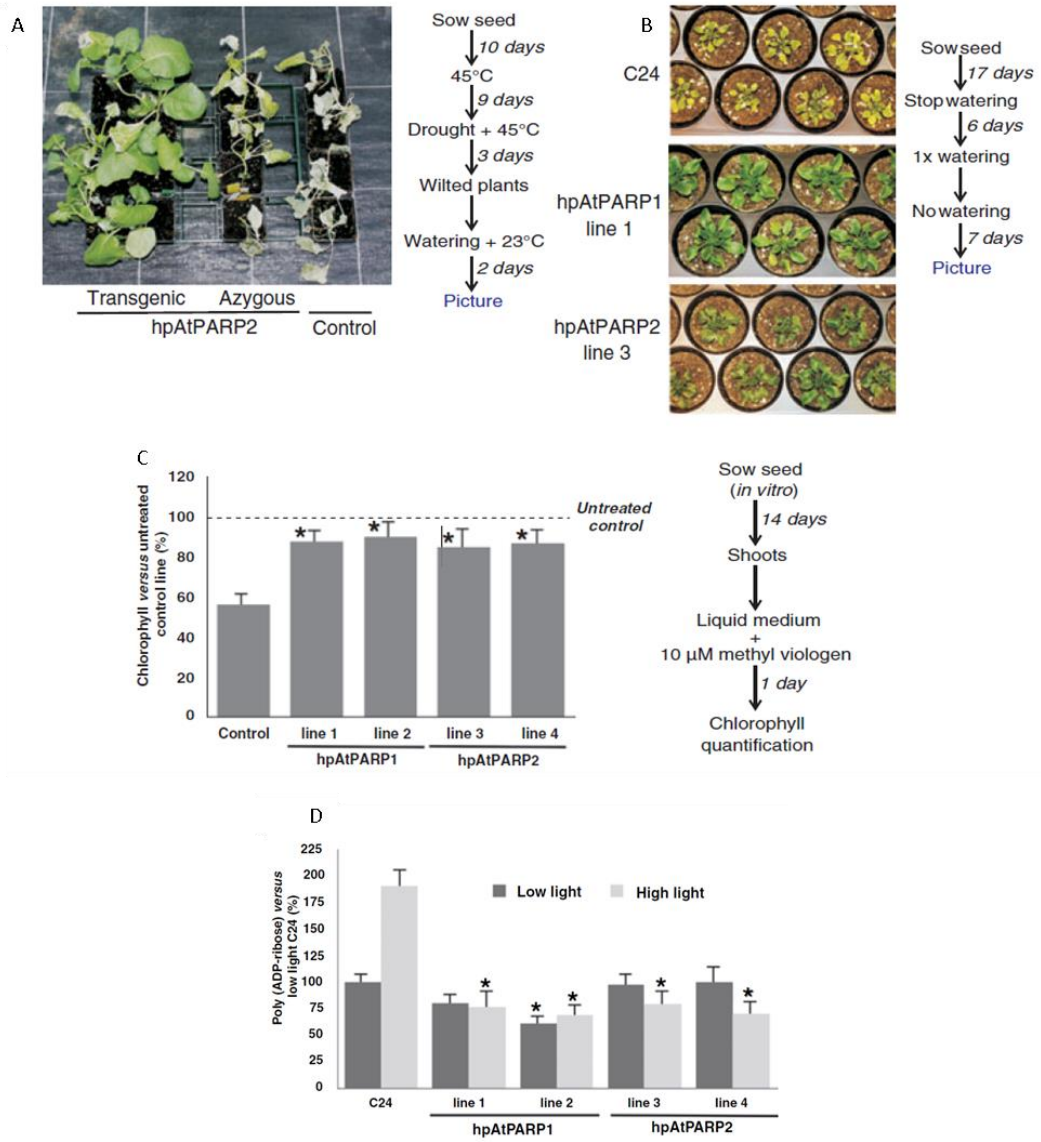

Figure 12A-D. Overexpression of *hpAtParp* constructs in *Brassica napus* and the associated stress tolerance. A: phenotypes of control, azygous and transgenic *B. napus* hpAtParp2 lines at the end of a combined heat and drought stress. B: phenotypes of Arabidopsis cv. C24 control, hpAtPARP1 and hpAtPARP2 lines at the end of a drought experiment. C: Chlorophyll content of Arabidopsis cv. C24 control, hpAtPARP1 and hpAtPARP2 lines treated for 1 d with 10 µM methyl viologen. D: The level of poly (ADP-ribosyl)ation in Arabidopsis cv. C24 control, hpAtPARP1 and hpAtPARP2 lines following high light stress. Low light = 30 µE m^{-2} s^{-1}, high light = 220 µE m^{-2} s^{-1}. Error bars represent standard error (n=3), * indicates P = 0.01. Taken from Block *et al.,* (2004).

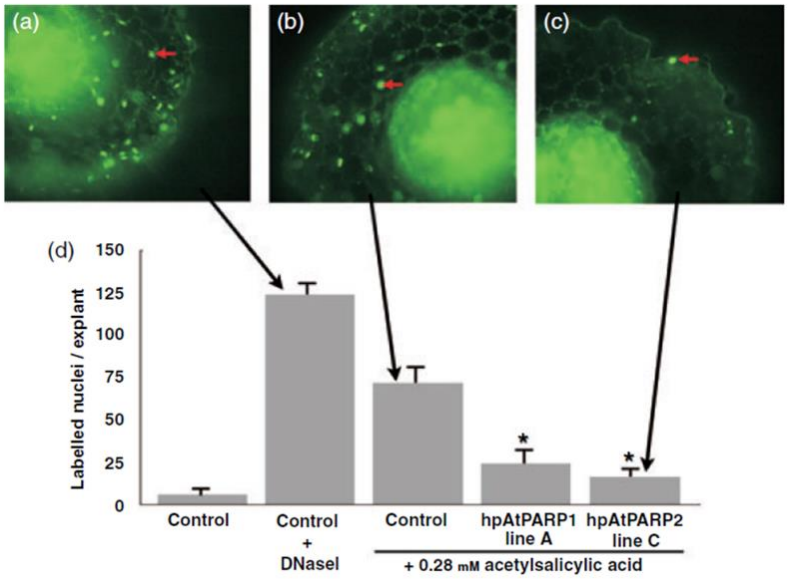

Figure 13. TUNEL assay to label DNA breaks. (a) Control plants treated for 1 h at 37°C with 40 U ml^{-1} DNase1. Explants from a non-transgenic control (b) and from hpAtPARP2 (c) lines incubated for 1 d in medium supplemented with 0.28 mM acetylsalicylic acid. The red arrows in a-c indicate labelled nuclei. D: quantification of labelled nuclei per explant. Nuclei from the cortex tissue of plants were recorded and in each experiment 50 explants per line and treatment were scored. Error bars indicate standard error (n=3), * indicates P = 0.01 and a statistically significant difference from controls. Taken from Block *et al.,* (2004).

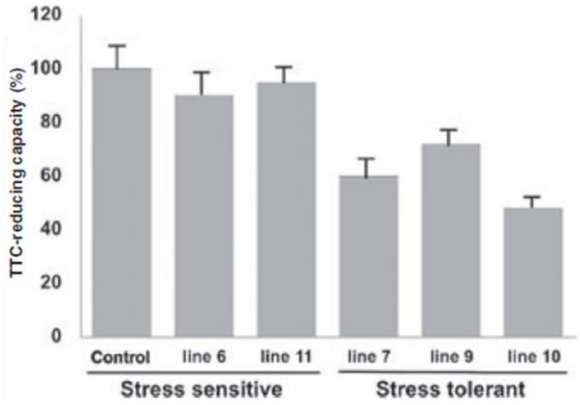

Figure 14. Mitochondrial electron transport quantified by measuring TTC (2,3,5-triphenyltetrazolium-chloride) reduction in Arabidopsis cv. Col-0 control and hpAtParp2 lines. Plants were stressed for 24 h with 220 µE m^{-2} s^{-1}. Error bars represent standard error (n=3). Taken from Block *et al.,* (2004).

Following on from the work by Block *et al.*, (2004), Vanderauwera *et al.*, (2007) reported a reduction in the accumulation of superoxide radicals in response to

oxidative stress in hpAtPARP2 Arabidopsis plants, which they attributed to more efficient scavenging.

In addition the group expanded the existing theories explaining how reduced PARP activity confers stress tolerance. They found approximately 900 transcripts which were differentially regulated in Arabidopsis in response to a high light *in vitro* stress assay, the largest functional category containing protein metabolism genes. hpAtPARP2 plants were more tolerant to high light as active repression of protein synthesis prevents proteins misfolding under stressed conditions.

They noticed that PARP deficient plants superinduced three classes of genes involved in stress protection, including flavonoid biosynthesis, starch metabolism and ABA-responsive genes. Anthocyanins are flavonoids which are well known to protect against high light stress owing to their ability to mitigate oxidative damage through light attenuation (Steyn *et al.*, 2002). Enhanced starch degradation increases the soluble sugar levels which confers low temperature tolerance (Yano *et al.*, 2005). Increased ABA levels are thought to enhance stress tolerance through the activation of a variety of stress-responsive genes. However, although ABA is understood to be required for normal development, high levels inhibit plant growth. In three years of field trials the group claimed that corn (*Zea mays*) and *B. napus* hpPARP lines had similar yields to the azygous plants grown under unstressed conditions, suggesting that PARP inhibition has potential as a crop protection strategy (Block and Metzlaff unpublished results referred to in Vanderauwera *et al.*, 2007).

Finally the group suggested a novel model for improved abiotic stress resistance in PARP deficient plants. They argued that the increased NAD^+ level seen in htAtPARP2 lines was connected to an ABA-dependent response. NAD^+ can be converted to cyclic ADP-ribose (cADPR) by ADP-ribosyl cyclase (ARC) which has been cloned and characterised in human, in rat and in *Aplysia*. However, although there are no genes with significant homologies to animal ARC present in any plant genome, several studies have demonstrated cADPR activity in plants (Hunt *et al.*, 2004). Allen *et al.*, (1995) suggested a similar role for cADPR in plants to that seen in animals after they reported calcium release from red beet vacuoles and colocalised inositol 1,4,5 triphosphate-gated calcium release. Wu *et al.*, (1997) microinjected the GUS reporter

gene fused to the promoters of the Arabidopsis ABA-inducible genes *RD29a* and *Kin*2. GUS expression increased following microinjection of cADPR suggesting cADPR affects ABA-dependent gene expression pathways. Furthermore Sánchez *et al.*, (2004) showed that increased cADPR levels induced more than one hundred ABA-responsive genes in Arabidopsis.

Vanderauwera *et al.*, (2007) failed to quantify cellular cADPR levels using an assay. However they hypothesised that under stress, hpAtPARP2 plants consume less NAD^+ and produce more cADPR as a result. This cADPR mobilises internal Ca^{2+} stores, leading to the characteristic Ca^{2+} spikes which trigger ABA biosynthesis (Xiong & Zhu, 2003). The subsequent rise of cellular ABA induces ABA-responsive transcription factors which themselves affect the expression of numerous downstream ABA- and other stress-responsive genes. Additionally ABA levels could positively regulate ADP-ribosyl cyclase activity, meaning the original signal can be amplified. Despite these demonstrations the role of cADPR in plant signalling and stress response is unclear. The effects of cADPR in mammals can be replicated in plants when cADPR is applied exogenously, but no biosynthetic pathway for cADPR in plants has been published to date so the potential contribution of cADPR in plants remains hypothetical. It is possible that a plant ARC protein which has very low homology to animal ARC exists, or that plants possess a unique cADPR synthesis pathway that is quite different from that seen in mammalian systems (Hunt *et al.*, 2004). A model for cADPR signalling is shown in Figure 15.

Vanderauwera *et al.*, expanded on the established theory that PARP deficient plants are more tolerant to abiotic stresses through enhanced energy efficiency. They showed that the stress tolerance of PARP2 deficient plants can also be explained by the preservation of NAD^+, which results in an increase in ABA levels, facilitating the induction of a range of stress-related genes. However the group did acknowledge that NAD^+ might mediate other pathways as well; and they conceded that the downregulation of PARP could also perturb the posttranslational modification of proteins involved in stress response, growth and protein turnover, among others.

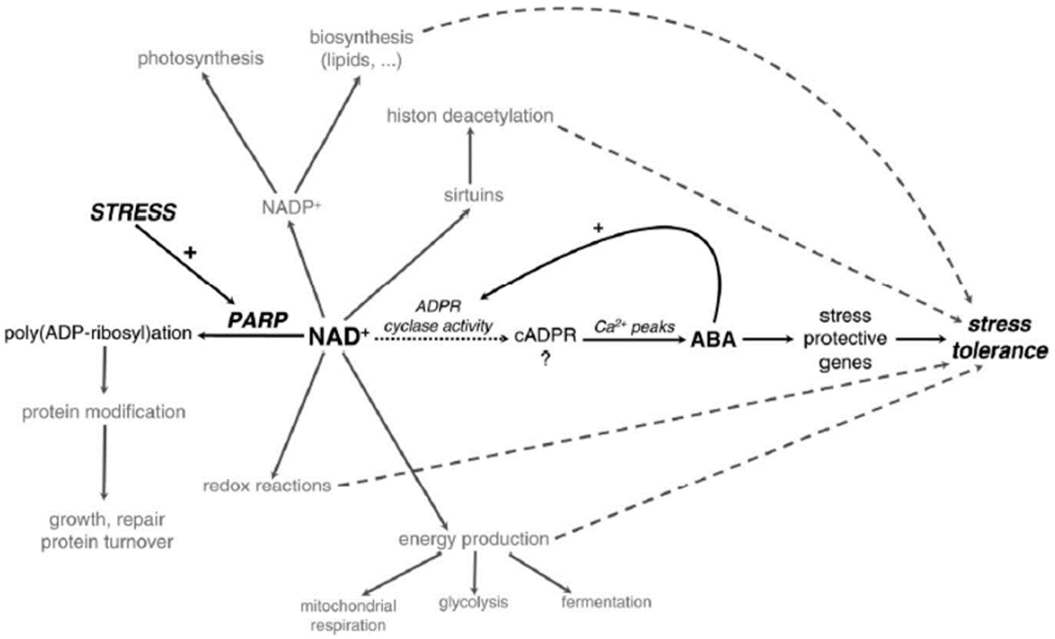

Figure 15. Model of the roles of PARP and NAD in stress response signalling. Stress increases cellular NAD^+ in hpAtPARP2 plants. ADP-ribosyl (ADPR) cyclase can convert NAD^+ to cADPR, which triggers intracellular spikes of Ca^{2+}, ABA biosynthesis and the activation of stress-responsive genes. ABA could also regulate ADPR cyclase activity providing a relay mechanism which could amplify the initial cADPR signal. Other pathways which might be involved are indicated in grey. The relative contribution of each pathway is unknown. Taken from Vanderauwera *et al.*, (2007).

The relationship between PARP activity and anthocyanin accumulation was investigated further in the work by Schulz *et al.*, (2012). Anthocyanins and other flavonoids accumulate in response to abiotic stresses such as high light, temperature extremes and nutrient deprivation. Schulz *et al.*, (2012) found that Arabidopsis plants cultured in media containing high sucrose or paraquat accumulated anthocyanins. This stress response was reduced by the addition of 3MB (Figure 16) or, to a lesser extent, by other PARP inhibitors (data not shown).

Redox profiling showed that NAD^+ increased in Arabidopsis following treatment with 3MB, as might be expected following the work by Vanderauwera *et al.*, (2007), whereas total ascorbate content decreased by more than 20% (Figure 17A-B). The accumulation of ascorbate can be beneficial under severe stress but is considered energetically wasteful at moderate stress. Both of these findings provide links between PARP activity and redox processes under stress.

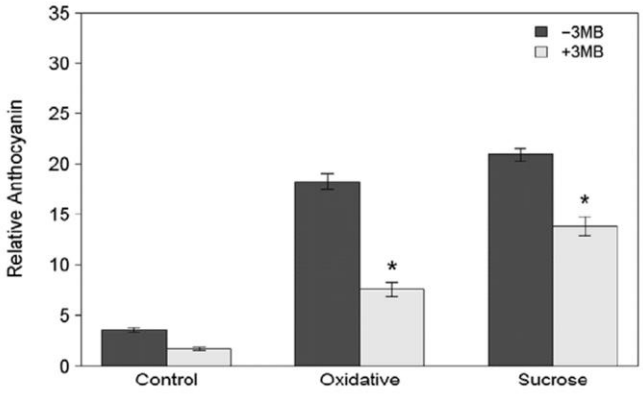

Figure 16. Relative anthocyanin contents of harvested samples. Arabidopsis Col-0 plants were grown at 22°C, 80-100 µE on MS medium either with (+3MB) or without (-3MB) the PARP inhibitor 3-methoxybenzamide and subjected to one of three conditions: control, oxidative stress (0.1 µM paraquat) or high sucrose (150 mM). Plants were harvested after 14 d. n=15 from five replicates and three independent experiments. * indicates $P < 0.05$. Taken from Schulz *et al.*, (2012).

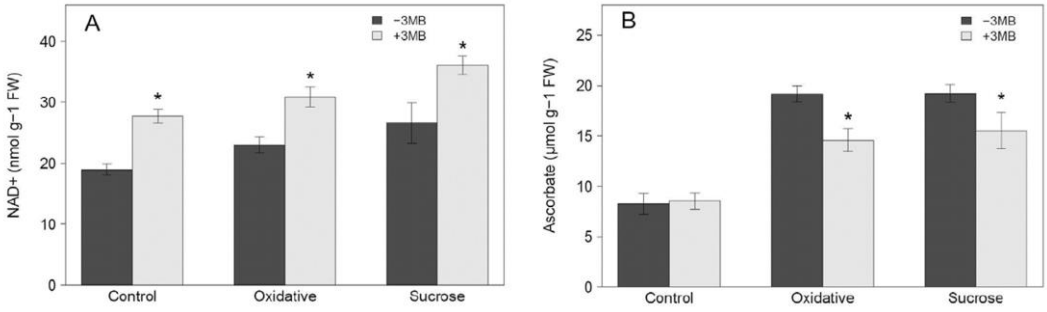

Figure 17A-B. Content of NAD+ (A) and ascorbate (B) following redox profiling. Arabidopsis Col-0 seedlings were grown as in Figure 16 and harvested after 14 d. n=6 from two independent experiments each containing six replicates. * indicates $P < 0.05$ in comparison to the plants of the same condition but without 3MB (-3MB). Taken from Schulz *et al.*, (2012).

Using chlorophyll fluorescence measurements the group were able to show that 3MB treatment had broadly positive effects on photosynthesis under both unstressed and stressed conditions (Figure 18). They observed that 3MB reduced the level of non-photochemical quenching in samples subjected to oxidative stress perhaps suggesting the PARP inhibitor allowed the plants to maintain efficient photosynthesis. Small but significant increases in the photochemical quenching parameters *q*P and ΦPSII (shown in Figure 18 as Y_II) were also recorded suggesting

3MB increased the efficiency of photosynthetic electron transport under unstressed conditions. Chlorophyll fluorescence is reviewed in more detail later.

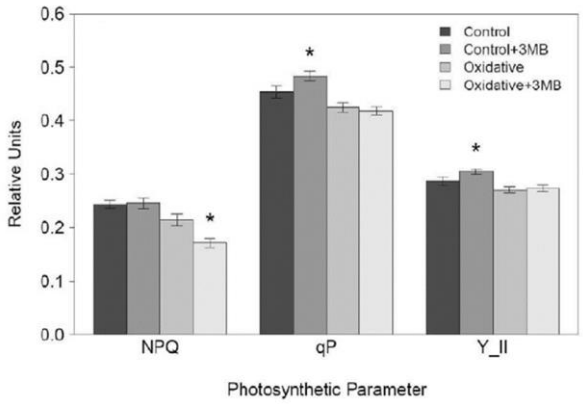

Figure 18. 3-methoxynezamide (3MB) altered Arabidopsis photosynthesis. Arabidopsis Col-0 plants were grown as in Figure 16 and analysed using PAM imaging. NPQ = non-photochemical quenching (heat dissipation); *q*P = the coefficient of photochemical quenching (the proportion of reaction centres that are open); and Y_II = the operating efficiency of photosystem II (the effective quantum yield of photosystem II). n=42 as 8-18 seedlings were analysed in four independent experiments. * indicates $P < 0.05$ between seedlings grown in the same condition but treated with or without 3MB. Taken from Schulz *et al.*, (2012).

It is known that there is a close relationship between redox balance, energy homeostasis, metabolism and photosynthesis (Kornas *et al.*, 2010). As follows, the maintenance of NAD^+ and energy homeostasis, together with enhancements in photosynthesis and growth seen in Arabidopsis following 3MB treatment, collectively support a model for stress response where PARP activity is a key regulator (Vanderauwera *et al.*, 2007). Schulz *et al.*, concluded that PARP inhibition represses the accumulation of molecules associated with defence, especially anthocyanins. Additionally they showed that PARP deficient plants were more tolerant to different stresses, such as high exogenous sucrose and paraquat. The results support the already established link between PARP activity and cellular redox state, and additionally with photosynthesis.

1.6. PARP inhibitors as crop protection agents

Since the initial work of Amor *et al.*, (1998) a more comprehensive picture of the role of PARP activity in stress response has been constructed. It is now thought that PARP inhibition confers stress tolerance through: (i) the maintenance of energy homeostasis and cellular redox metabolites; (ii) reductions in mitochondrial overrespiration, radical production, the accumulation of defence-related compounds and programmed cell death; (iii) alterations in gene expression, particularly those relating to ABA; and (iv) regulating signalling pathways, such as through the production of cADPR. Despite the progress the full role of PARP activity in plant stress response is still not fully understood.

Additionally the studies to date have their drawbacks. As suggested the genetic downregulation or knockout of PARP activity had been shown to improve plant tolerance to abiotic stress. But by 2012 chemical PARP inhibition had mainly been investigated in short-term trials, in highly artificial systems (e.g. using explants, cell cultures, hydroponics), which are not representative of the conditions crop plants experience in agricultural settings. Therefore it is not clear whether chemical PARP inhibition is a suitable strategy for improving crop stress tolerance and protecting or enhancing yield under moderate stress, which is of primary interest in the agricultural industry.

Accordingly there was a need to explore stress response and the effects of PARP inhibitors *in planta*. My project aimed to investigate this: firstly by using non-destructive techniques, so numerous measurements can be made on the same sample; secondly by applying a sub-lethal stress which is more representative of what plants face in the field; thirdly by quantifying the effects of PARP inhibitors on growth (over the entire life cycle of the plant) and yield; and finally by applying chemical inhibitors directly onto leaves, given that the genetic modification of plants has restricted application across the Europe.

1.7. Non-invasive techniques for the analysis and quantification of drought stress response

In vitro techniques in molecular biology have facilitated a great increase in our understanding of drought response in plants. However these investigations have two important limitations: firstly they use artificial conditions which are not representative of those which plants regularly experience in the environment; and secondly they involve methods which result in the destruction of samples, which can influence future measurements and may not be representative of the whole plant (Woo *et al.*, 2008; Atkinson & Urwin, 2012). As a result there is considerable interest in non-invasive imaging as a method to quantitatively assess plant function *in vivo* (Großkinsky *et al.*, 2015). Because these techniques are non-destructive multiple rounds of measurement on an individual plant are possible, meaning stress response can be studied over a longer period than is possible with more classically used invasive techniques.

Through imaging of chlorophyll fluorescence it is possible to quantify the efficiency of photosystem II photochemistry (ΦPSII) and non-photochemical energy dissipation processes (NPQ) (Maxwell & Johnson, 2000; Baker, 2008; Murchie & Lawson, 2013; Porcar-Castell *et al.*, 2014). Maximum quantum efficiency (F_v/F_m) typically measures ~ 0.83 in healthy leaves of most species and deviation from this value is often indicative of stress. Additionally, parameters relating to the rate of photosynthetic electron transport (ETR) can be measured. The derivation and measurement of these parameters is detailed in Chapter 2. It is widely accepted that photosystem II is most sensitive photosynthetic component to stress. Accordingly changes in chlorophyll fluorescence parameters can provide information about how a plant is responding to stress. In 2008 Woo *et al*., measured ΦPSII, NPQ and F_v/F_m to monitor the impact of drought stress on photosynthesis in various Arabidopsis lines. Using the technique they were able to quantify differences between the plant lines and determine which had altered drought tolerance and which had reduced photosynthetic efficiency. They concluded that F_v/F_m was a sensitive indicator of drought stress. Sperdouli & Moustakas, (2012) measured the spatio-temporal response of ΦPSII, NPQ and F_v/F_m

in response to mild, moderate and severe drought in Arabidopsis. The group were able to detect changes in photosynthetic function in response to mild drought. They concluded that their data showed that different stress intensities show spatio-temporal heterogeneity in leaves and suggested that classical single time point analyses would have been inadequate to measure this. Later in 2015 Bresson *et al.*, used F_v/F_m as a method of quantifying photosynthetic heterogeneity in water stressed Arabidopsis. Also in 2015, F_v/F_m was used to evaluate the tolerance of different grapevine genotypes to drought-cold stress by correlating it with electrolyte leakage (Su *et al.*, 2015).

Fluorescence can be combined with simultaneous gas analysis which often provides a more complete picture of how stress impacts physiology (Flexas *et al.*, 2002; Massacci *et al.*, 2008; Ashraf & Harris, 2013). By measuring gas exchange parameters it is possible to elucidate electron destination and by extension, if a plant is maintaining full photosynthetic capacity during stress or whether alterative pathways are upregulated to help dissipate excess energy. Massacci *et al.*, (2008) measured the photosynthetic response to drought onset at different irradiances in cotton. They were able to attribute the increase in ΦPSII under moderate drought stress to an increase in photorespiration. It is not possible to measure photorespiration directly using chlorophyll fluorescence alone, which demonstrates the power of the techniques when in combination.

Thermal imaging measures leaf temperature which is affected by drought stress (Merlot *et al.*, 2002; Benavente *et al.*, 2013). As plants close their stomata to conserve water, the cooling effect of transpiration is reduced and leaf temperature increases, which can be quantified using thermal imaging. Merlot *et al.*, (2002) used thermal imaging to distinguish between Arabidopsis genotypes with altered stomatal conductance. Mutants which had constitutively open stomata were easily identified because they had greater transpiration and were cooler than wild-types.

One of the most quickly obtainable measures of plant stress response is growth. An early response to the perception of stress in plants is the cessation of growth (Skirycz & Inzé, 2010; Vanková *et al.*, 2012). It is also very simple to measure as it can be done

by hand, although more often it is quantified using digital images and software programmes.

These non-invasive methods have an advantage over destructive techniques because multiple measurements can be made on the same sample, enabling stress response to be continuously quantified over a longer period. One limitation of the methods described here is that only a few (sometimes only one) samples can be measured at any one time, which limits the replication potential of experiments. The development of high-throughput phenomic platforms has alleviated this problem to some extent. These systems use automated imaging techniques (e.g. fluorescence, thermal and RGB) and robotics to measure growth, physiology and performance (Furbank & Tester, 2011; Großkinsky *et al.*, 2015). These systems are able to measure a large number of plants in any one day.

This project aimed to utilise non-invasive imaging techniques to quantify the impact of drought stress on plant physiology and growth.

1.8. Project aims

1. Use non-invasive imaging techniques to quantify the impact of drought stress on plant physiology and growth. Develop a protocol which is able to rapidly and reproducibly measure moderate drought stress response.

2. Quantify the impact of PARP inhibitors on plant photosynthesis, growth and survival under well-watered and droughted conditions.

3. Quantify the impact of PARP and PSII inhibitors on yield under well-watered and droughted conditions. Use phenomic techniques and data modelling to determine if the effects of compounds can be predicted earlier than measuring at harvest.

4. Determine the impact of PARP inhibitors on stomatal conductance and opening/closing kinetics.

Chapter 2

2. The use of non-invasive imaging to quantify plant drought response

2.1. Introduction

In vitro techniques in molecular biology have facilitated an increase in our understanding of drought response in plants. However these investigations have two important limitations: (1) they use artificial conditions which may not be representative of those which plants experience in the environment and (2) they involve methods which result in the destruction of samples, which can influence repeat measurements and may not be representative of the whole plant (Woo et al. 2008). As a result there is interest in developing non-invasive imaging to quantitatively assess plant function *in vivo* (Li *et al.*, 2014; Humplík *et al.*, 2015). Because these techniques are non-destructive, multiple measurements can be made on an individual plant and stress response can be studied over a longer period than is possible using invasive techniques.

Chlorophyll fluorescence imaging has become the most powerful and popular technique for the rapid, quantitative assessment of photosynthetic efficiency and fluorescence data is now common in studies analysing plant stress response (Maxwell & Johnson, 2000; Baker, 2008; Murchie & Lawson, 2013; Porcar-Castell *et al.*, 2014). The underlying principles of chlorophyll fluorescence are that light incident on chlorophyll molecules can have one of three fates: (1) it can be used to drive electron transport and photosynthesis (photochemistry); (2) it can be re-emitted in heat dissipation processes; or (3) it can be re-emitted as light, termed chlorophyll fluorescence. These processes occur in competition with each other such that any increase in the efficiency of one will result in a decrease in the efficiency of the other two. Consequently, it is possible to measure changes in the efficiency of photochemistry and heat dissipation by measuring the fluorescence emission. When photosynthesis is perturbed by stress a decline in photochemistry is accompanied by increases in heat dissipation and chlorophyll fluorescence.

Figure 19 shows a typical fluorescence trace from which coefficients can be defined. Measurement begins when the measuring beam (MB) is switched on and a minimal fluorescence signal (F_0) is generated. The application of a saturating flash (SP) transiently closes all of the reaction centres and gives rise to a value of dark-adapted

maximum fluorescence (F_m), which would be obtained in the absence of any photochemical quenching. If then actinic light (AL) is applied, which is strong enough to drive photosynthesis, saturating flashes (SP) will generate light-adapted maximum fluorescence values (F_m'). F_t denotes the steady-state fluorescence value immediately prior to an SP. If the AL is then switched off the fluorescence emission will decrease over time back to F_0, a process that can be accelerated by the application of far-red light.

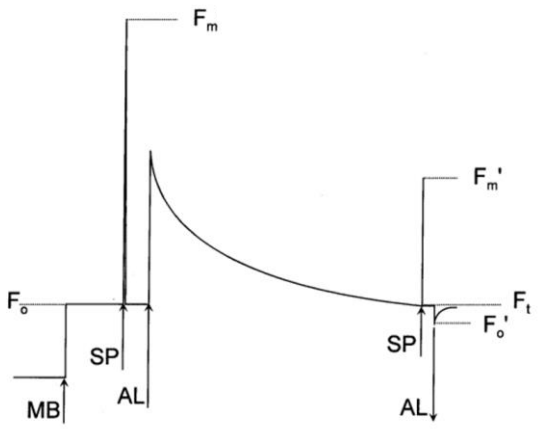

Figure 19. An example chlorophyll fluorescence trace. A measuring light (MB) is switched on giving the minimum fluorescence level (F_0). Saturating flashes (SP) can be applied to determine the dark-adapted maximum fluorescence (F_m). Actinic irradiance (AL) is then applied to drive photochemistry and saturating flashes can be applied periodically to determine the maximum fluorescence (F_m') in the light. F_t describes the level of fluorescence immediately before the application of a SP. If the AL is turned off the fluorescence level decrease to a light-adapted minimum (F_0'). F_0 will be achieved in time or through the application of far-red light. A prime (') notation denotes light-adapted. ↑ represents the application of light and ↓ denote the withdrawal of light at that time point. Taken from Maxwell & Johnson, (2000).

More complex parameters which are informative of plant physiology and health can be derived from these basic fluorescence kinetics parameters (Table 2; Maxwell & Johnson, 2000; Baker, 2008; Murchie & Lawson, 2013). Perhaps the most commonly used to date is F_v/F_m which is a measure of the maximum quantum yield of photosystem II, or the efficiency if all of the reaction centres were open. F_v/F_m must be recorded following a period of dark-adaption so that all of the photosystem II

reaction centres are open and F_0 can be accurately determined. Healthy leaves of most plants have values of around 0.83, which may decline if a plant experiences stress or photoinhibition, meaning F_v/F_m can be a sensitive indicator of photosynthetic performance (Calatayud *et al.*, 2006; Woo *et al.*, 2008; Sperdouli & Moustakas, 2012).

Water deficit induces stomatal closure which results in a reduction of the internal concentration of CO_2 (Zivcak *et al.*, 2013). As a consequence, an imbalance between the electron requirement for CO_2 fixation and the rate of electron generation by photochemistry may arise over time, leading to the over-excitation of the reaction centres, damage to the photosynthetic machinery of photosystem II, and a decline in F_v/F_m (Bresson *et al*. 2015). As the duration or severity of drought increases F_v/F_m values may decrease more dramatically and the plant may lose viability (Woo *et al*. 2008).

A widely used photochemical quenching parameter is ΦPSII which measures the proportion of light absorbed by the chlorophyll molecules of photosystem II that drives photochemistry. ΦPSII is related to the rate of linear electron transport and photosynthesis. In fact, under laboratory conditions a strong linear relationship exists between electron transport rate and carbon fixation, although this relationship can and does break down if a plant experiences stress (Maxwell & Johnson, 2000; Baker, 2008).

F_v/F_m and ΦPSII provide information about the proportion of absorbed light which is used in photochemistry. Conversely, non-photochemical quenching (NPQ) describes the evolutionary photoprotective mechanisms of heat dissipation in the light harvesting complexes of photosystem II (Perez-Bueno et al. 2008). To calculate NPQ and assess the proportion of absorbed light that is dissipated as heat, it is necessary for samples to be dark-adapted (Baker, 2008). The period of dark-adaption should be long enough to allow for the accurate determination of a reference value of F_m, where the efficiency of photochemical quenching is at a maximum and NPQ is at a minimum. NPQ is calculated by relating the change in F_m to the final F_m value. Broadly, NPQ will increase if a plant experiences stress either as a result of the protective responses or as a direct result of the damage itself. NPQ can be split into

at least three components according to the time it takes each to relax. The most quickly relaxing component (over a time scale of minutes) is termed high energy-state quenching or *q*E, which describes the formation of a proton gradient (ΔpH) across the thylakoid membrane as protons move into the lumen (Quick & Horton, 1984; Ruban, 2016). This results in the activation of the xanthophyll cycle and the deepoxidation of violaxanthin to zeaxanthin. Additionally the protein PsbS becomes protonated changing it to its quenching state. The exact mechanisms of the quenching resulting from these conversions are unknown, although it is suggested that zeaxanthin and protonated PsbS may induce heat dissipation by causing a conformational change in the photosystem II antennae, converting it to a quenching state (Kereïche *et al.*, 2010; Ruban, 2016), or by interacting with the photosystem II supercomplexes to create quenching sites (Xu *et al.*, 2015). A second process which also relaxes over a time period of minutes is termed state transitions or *q*T. *q*T describes the migration of light harvesting complexes from photosystem II to photosystem I under the governance of the plastoquinone pool (Roach & Krieger-Liszkay, 2014). This process rebalances the energy between the photosystems when photosystem II becomes over-excited relative to photosystem I. The third component *q*I relaxes over a time period of hours and is considered to be largely the result of photoinhibition; either from extended exposure to light (over the course of a day) or due to stress, both of which lead to a downregulation of the reaction centres of photosystem II.

F_v/F_m, ΦPSII and NPQ can provide a comprehensive assessment of the state of photosystem II. It can quantify the extent to which photosystem II is using absorbed light and the extent to which it is being damaged by excess light (Maxwell and Johnson 2000). Because electron transfer through photosystem II is indicative of the overall rate of photosynthesis this information can be used to assess photosynthetic performance further. Additionally because photosystem II is considered to be the most vulnerable part of the photosynthetic apparatus to light-induced damage, changes to photosynthetic parameters which measure its performance are likely amongst the first manifestations of stress in a leaf (Takahashi & Badger, 2011). As outlined above, one of the first physiological responses of a plant to drought stress

is to close its stomata to conserve water. In time stomatal limitation will restrict the supply of CO_2 for fixation; reducing the activity of the Calvin cycle enzymes, decreasing the consumption of ATP and NADPH, and leading to the over-reduction of the electron transport chain (Zivcak *et al.*, 2013; Yamori, 2016). If electron transport rates are maintained damage to the photosynthetic machinery can result. Consequently a plant may downregulate linear electron transport by reducing ATP synthase conductivity (Kramer *et al.*, 2004*a*) or by limiting the electron capacity through the cytochrome b_6f complex (Foyer *et al.*, 2012). This downregulation can manifest as a reduction in ΦPSII. If a plant cannot use the energy it absorbs to drive photochemistry it must dissipate it as heat to avoid damage, so normally a reduction in ΦPSII is accompanied by an increase NPQ (Horton *et al.*, 2008). In general, any increase in the efficiency of a protective mechanism should decrease ΦPSII because such a mechanism competes with photochemistry for the light a plant absorbs (Genty *et al.*, 1989; Chaves *et al.*, 2009).

Photosynthetic parameters can be measured under different conditions. For the purposes of this work two will be described, photosynthetic induction and steady-state. Photosynthetic induction describes the processes that occur when actinic light is applied to a dark-adapted sample. Following the application of light the photosynthetic reaction centres close and fluorescence increases (Maxwell & Johnson, 2000; Baker, 2008; Murchie & Lawson, 2013; Porcar-Castell *et al.*, 2014). The quenching of this fluorescence arises from a combination of stress-sensitive processes. Firstly, electron transport begins as an electron is passed from the chlorophyll reaction centre to a downstream acceptor and subsequently to further downstream acceptors. This will result in an increase in ΦPSII. Electron transport generates the ΔpH gradient which is necessary for the generation of heat dissipation processes and is responsible for the initial rise in NPQ in dark-adapted samples. Key metabolites (e.g. RuBP) are recruited and enzymes necessary for the Calvin cycle are activated (e.g. Rubisco activase, Rubisco). Stomata open an order of magnitude slower than photosynthetic events but increased conductance will allow CO_2 to diffuse in for fixation (Lawson *et al.*, 2012). These reactions increase at different rates until steady-state is achieved. At steady-state the underlying reactions described

proceed at constant rates. Because photosynthetic induction is more dynamic, parameters measured during this period can be more susceptible to stress than at steady-state. However steady-state measurements are more easily explained, so measuring under either condition has its own advantages and disadvantages. The majority of studies using chlorophyll fluorescence quote measurements of parameters under steady-state conditions.

Although it is itself a powerful technique it has been suggested that the most elegant applications of chlorophyll fluorescence use the technique in combination with others to gain a more complete picture of plant stress response. One example is the simultaneous measurement of gas exchange and chlorophyll fluorescence (Massacci *et al.*, 2008; Zivcak *et al.*, 2013). ΦPSII can be converted to estimate linear electron transport rate which is related to photosynthetic carbon assimilation. However as alluded to earlier, the relationship which exists between electron transport and CO_2 assimilation can break down under stress, largely due to the activity of processes such as photorespiration, the Mehler reaction and nitrogen metabolism, which compete with photochemistry for electrons (Maxwell & Johnson, 2000; Baker, 2008). These processes make it impossible to accurately determine CO_2 fixation by chlorophyll fluorescence alone, however this can be achieved when fluorescence and gas exchange are measured simultaneously. Measurements of CO_2 assimilation and photosynthetic parameters (such as ΦPSII) can be made simultaneously using an infrared gas analyser (IRGA), which allows the contribution of competing processes to be estimated. This technique provides a more robust assessment of how drought stress affects physiology, as fluorescence alone does not reveal where the electrons generated by photosynthetic electron transport are partitioned to. Additionally IRGAs measure stomatal conductance allowing the impact of drought on ΦPSII and other parameters to be explained.

Thermal imaging can complement chlorophyll fluorescence imaging. When water is in plentiful supply a large proportion of stomata will be open (in daylight) and the resulting transpiration of water from the internal tissue surfaces has an evaporative cooling effect on the leaf. During drought stress a plant closes its stomata to prevent water loss and this may manifest as an increase in leaf temperature which can be

measured using thermal imaging (Merlot *et al.*, 2002; Benavente *et al.*, 2013). In this way leaf temperature can serve as a proxy for stomatal response and drought-induced reductions in stomatal conductance can explain ΦPSII changes.

In the longer-term, plants will arrest growth during water shortage and partition assimilates into the maintenance of existing tissues. Growth reduction occurs soon after the onset of drought stress and is independent of photosynthesis and carbon status, indicating that growth retardation is not a secondary effect of stress (Skirycz & Inzé, 2010). From an agricultural perspective although growth reductions will enhance survival rate in response to severe stress, during more moderate stress episodes where survival is not at risk it can be counter-productive and cause yield losses. Water stress is believed to reduce plant growth by reducing cell number and cell size, as shown in Arabidopsis and sunflower, which are largely believed to be under hormonal control. Although the exact roles of each remain unclear ABA, ethylene, gibberellins and DELLA proteins have been shown to play prominent roles in growth regulation under stress (Achard *et al.*, 2017; Navarro *et al.*, 2017). Because of the ease in which measurements can be made, growth is often a useful parameter in stress studies.

This chapter describes the development of protocols used to quantify physiological and physical responses to drought in *Arabidopsis thaliana*, *Brassica napus* and *Triticum aestivum* using non-invasive imaging techniques. Arabidopsis was selected as it is a model species with a short life cycle and there are available genetic resources. *B. napus* is a dicot related to Arabidopsis and is an economically important crop species, as is *T. aestivum*.

2.1.1. Aims and objectives

- Develop a reproducible regime for applying and measuring the progression of drought stress in *Arabidopsis thaliana*.

- Use non-invasive techniques such as chlorophyll fluorescence, thermal and digital imaging and gas exchange to quantify the impact of drought on physiology and growth, and determine early-onset parameters which are indicative of stress.
- Determine the impact of drought on Arabidopsis seed yield.
- Using the Arabidopsis drought and imaging protocols, define similar ones for the economically important crop species *Brassica napus* and *Triticum aestivum*.
- Define protocols that can be used in future work to assess the impact of existing and novel PARP inhibitors on plant physiology and growth.

2.2. Materials and Methods

2.2.1. Plant material and growth conditions

Seeds of *Arabidopsis thaliana* ecotype Columbia (Col-0) were cold stratified in dH_2O at 4 °C for 4 days and transferred onto individual pots (6 cm diameter; LBS Horticulture; UK). Seedlings germinated and grew over 14 days (unless stated) before measurements began (14 days after sowing). *Brassica napus* (Temple; Elsoms; UK) and *Triticum aestivum* (Paragon; Cope Seeds and Grain; UK) seeds were germinated on wet filter paper in Petri dishes in darkness for 4 days. Seedlings were transplanted into individual pots (10 x 10 x 10 cm; LBS Horticulture; UK) and grown for 14 days before measurements were taken (18 days after sowing). All plants were grown in a peat based soil containing a 3:1 mix of M3 compost (Levington; UK) and sand. Unless stated germination and growth occurred in a controlled environment chamber with an irradiance of 150 µmol m^{-2} s^{-1} during a 10/14 hour day/night photoperiod at 22 °C with a relative humidity of 40%. When in the growth chamber plants were moved daily to minimise the impact of light gradients.

2.2.2. Drought treatment

All plants were watered daily throughout germination and the 14 day growth period. Water was withheld from droughted plants on the day after the 14 day growth period, which was defined as day 0. Well-watered plants received daily watering throughout. Drought severity was quantified by calculating the % soil water content where saturated pot = 100% and oven-dried soil = 0%.

2.2.3. Chlorophyll fluorescence imaging

Chlorophyll fluorescence was measured using an Imaging-PAM fluorometer and ImagingWin software (Heinz-Walz GmbH; Germany). Samples were positioned at a

working distance of 8.5 cm to the LED-array illumination unit IMAG-MAX/L and the photon flux density (PAR) was defined at this height.

Individual experiments are described later but in all cases fluorescence parameters were calculated using the following generic protocol. A full list of parameters and abbreviations used in this chapter are described in Table 2. Preliminary experiments measuring the response of F_v/F_m to different lengths of dark adaption indicated that 5 min was sufficient to obtain maximum values and this was adopted in all of the following experiments. Following dark adaption a weak measuring light recorded the minimum fluorescence level (F_0) and a saturating pulse recorded the maximum level (F_m), from which F_v/F_m was calculated. The actinic light was then switched on and as plants went through photosynthetic induction subsequent saturating pulses measured the maximum fluorescence yield in the light (F_m'). This, combined with the fluorescence yield immediately before the flash (F'), allowed the calculation of parameters related to photosynthetic electron transport (ΦPSII and qP) and non-photochemical quenching (NPQ and qN). Absorptivity was measured by subsequent illumination of the sample with red then near-infrared light.

For the fluorescence experiments in 2.3.1, imaging began 18 days after sowing when water was withheld from droughted plants (day 0) and then at regular intervals. F_v/F_m was measured following dark adaption and then parameters were recorded during 20 min induction at one of three irradiances: low (100 µmol PAR m^{-2} s^{-1}), medium (200 µmol PAR m^{-2} s^{-1}) or high (400 µmol PAR m^{-2} s^{-1}). These irradiances were determined by a preliminary light saturation profile experiment. To assess steady-state photosynthesis plants were illuminated sequentially with low, medium and then high light for varying times (Figure 20).

For the fluorescence experiments in 2.3.2, 2.3.5 and 2.3.8, measurements began 14 days after sowing (day 0). F_v/F_m was recorded following dark adaption and induction was measured at high light (400 µmol PAR m^{-2} s^{-1}) for 20 min (Figure 20). Steady-state parameters were averages of values taken between 18.5 and 20 min. Prior to dark adaption a measurement of absorptivity was recorded for each plant. In all cases measurements were taken at the earliest one hour after the growth chamber lights were switched on and ceased one hour prior to the lights turning off. For parameters,

values were averages of those from within an area of interest applied individually to each sample. False colour images were extracted from PIM files through ImagingWin (Walz, 2017).

Table 2. Calculation of fluorescence parameters and some abbreviations used in this chapter.

Basic parameters derived from fluorescence kinetics			
F_0	Minimum fluorescence level under very low light (PSII reaction centres are open)		
F_m	Dark-adapted maximum fluorescence level during a saturating pulse (PSII reaction centres are transiently closed)		
F_m'	Light-adapted maximum fluorescence level under actinic light shortly after a saturating pulse		
F'	The fluorescence level immediately before a saturating pulse under actinic light		
F	Average current fluorescence yield (from values 3 s following saturating pulse)		
PAR	Photosynthetically active radiation		
0.5*	Efficiency factor (assumes half of the incident irradiation is absorbed by PSII)		
Parameters derived from basic fluorescence parameters		**Calculation**	**References**
F_v/F_m	Maximum quantum yield of PSII (all reaction centres are open)	$(F_m - F_0)/F_m$	(Maxwell & Johnson, 2000; Baker, 2008; Murchie & Lawson, 2013; Porcar-Castell *et al.*, 2014; Ruban, 2016)
ΦPSII	Operating efficiency of PSII in the light	$(F_m' - F')/F_m'$	
NPQ	Non-photochemical quenching	$(F_m-F_m')/F_m'$	
qL	Coefficient of photochemical quenching (Lake model of antenna pigment organisation)	$(F_m' - F)/(F_m' - F_0')$ x F_0'/F	(Kramer *et al.*, 2004*a*)
F_0'	Minimal fluorescence yield of light-adapted sample, lowered with respect to F_0 by NPQ	$F_0' = F_0/(F_v/F_m + F_0/F_m')$	(Baker, 2008)
ETR	Electron transport rate	ΦPSII x 0.5* x PAR x Abs	
Abs	Absorptivity	1 – Red/NIR reflection	
ΦNO (used in Chapter 3)	Quantum yield of non-regulated energy dissipation	1/(NPQ + 1 + qL $(F_m/F_0$ -1)	(Kramer *et al.*, 2004*a*)

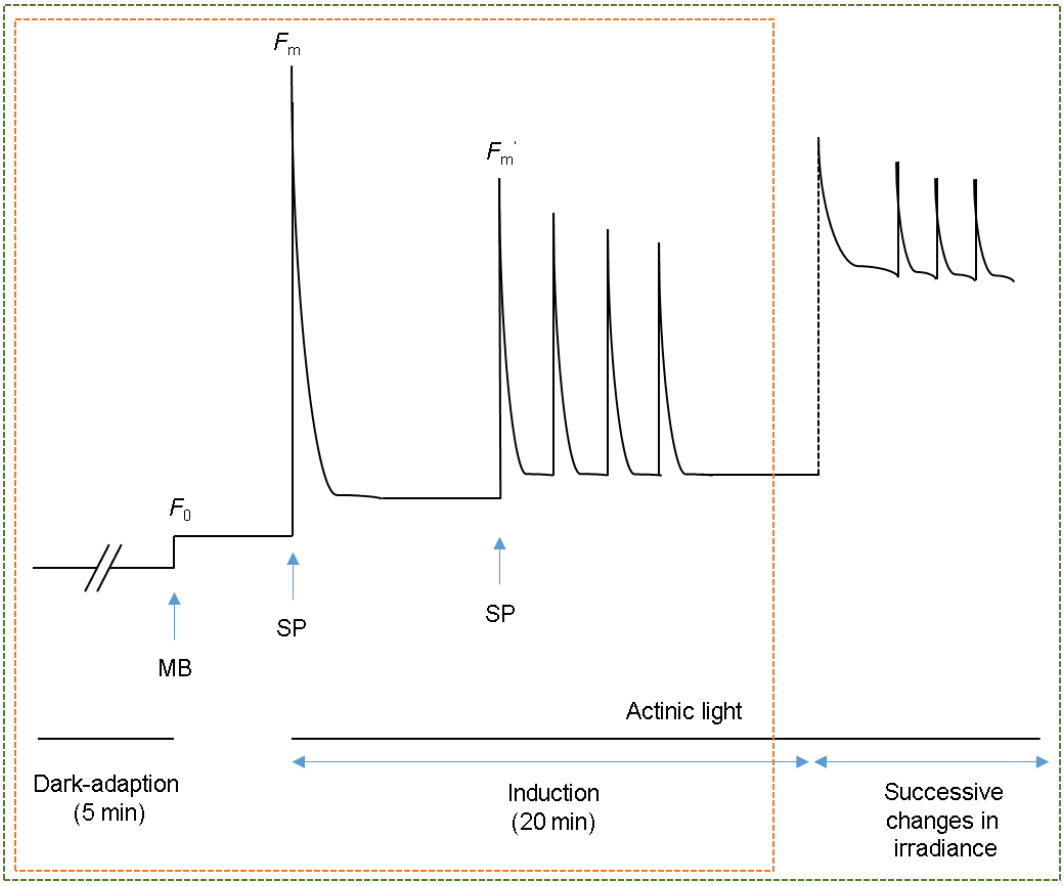

Figure 20. A schematic fluorescence trace as would typically be produced following the protocols used in this chapter. In 2.2.2, 2.3.5 and 2.3.8, plants were dark-adapted for 5 min before 20 min induction (represented by the orange box). In 2.3.1, plants were additionally illuminated at 100, 200 then 400 µmol PAR m^{-2} s^{-1} for different time periods (green box). MB = measuring beam, SP = saturating pulse. Fluorescence parameters are described in Table 2.

2.2.4. Thermal imaging

Measurements of leaf temperature in *A. thaliana* and *T. aestivum* were made using an SC660 thermal camera and analysed using FLIR Tools software (FLIR Systems; USA). The measurements began 14 and 18 days after sowing in Arabidopsis and *T. aestivum* respectively, and were taken at intervals. In all cases imaging took place in the climate chamber where plants were growing and samples were given 30 min to acclimatise after the camera was positioned before measuring started. A fan positioned to one side blew air across the surface of the plants to disturb the

boundary layer. For analysis, four areas of interest from each plant were selected and the average of those values gave one replicate.

2.2.5. Growth, yield and viability analyses

Arabidopsis leaf area and rosette diameter were measured using imageJ software (ImageJ; USA) on digital images (Canon EOS REBEL T1i/EOS 500D; Japan). For yield calculations the aerial tissue and all seed were harvested when the plants were mature and the last siliques on the inflorescence had dried and were ready to dehisce. Seed were dried for > 4 weeks in airtight containers with silica beads. The aerial tissue and total seed yield per plant were weighed. 100 seeds from each plant were counted and weighed to calculate individual seed weight. To assess if drought reduced seed viability, > 50 seeds from each plant were sown and % germination was measured 7 days later.

The height of *B. napus* and *T. aestivum* plants from the base of the plant at the soil surface to the highest point of the highest leaf was measured using a ruler. The number of emerged leaves (excluding cotyledons) was scored visually.

2.2.6. Leaf gas exchange measurements

Gas exchange was measured using a LI-6400-40 gas analyser with a leaf chamber fluorometer (Licor; USA). Measurements took place 15 days after withholding water from droughted plants (day 15; 33 days after sowing) on the top most expanded true leaf, which was leaf 3 or 4 in all cases. The parameters net assimilation, stomatal conductance and transpiration were recorded simultaneously with the fluorescence parameters F_v/F_m and ΦPSII. Following 5 min dark adaption data were collected during 7 min induction at high light with 400 µmol mol^{-1} CO_2, 22 °C leaf temperature and ~ 50% relative humidity.

2.2.7. Statistical analyses

Minitab was used to perform Student t-tests to assess for significance between treatments (Minitab 17; Minitab, Inc; USA). GraphPad Prism 7 software was used to construct graphs and charts (GraphPad Software, Inc: USA).

2.3. Results

2.3.1. The impact of drought on photosynthetic parameters in *Arabidopsis thaliana*

Drought has multiple physiological and developmental impacts on plants. Initial experiments were performed to identify how physiological parameters, measured using chlorophyll fluorescence imaging, altered as *A. thaliana* plants experienced drought stress. The aim of this experiment was to identify parameters that altered at different stages of drought imposition. Arabidopsis plants were sown and grown for 18 days in individual pots containing a 3:1 mixture of a peat-based compost and sand, after which time water was withheld (day 0). Control (well-watered) plants continued to receive daily watering throughout the experiment. The severity of drought stress was determined by calculating the % soil water content (with water-saturated soil = 100% and oven-dried soil = 0%). A preliminary experiment using the chlorophyll fluorometer was used to define a light saturation curve for well-watered Arabidopsis plants. Plants were exposed to increasing irradiances and steady-state values of ØPSII were measured and used to calculate the electron transport rate (ETR). Photosynthetic rate increased with irradiance becoming saturated at a PAR of 400 µmol m^{-2} s^{-1} (Figure 21). Three irradiances were defined as low (100 µmol PAR m^{-2} s^{-1}), medium (200 µmol PAR m^{-2} s^{-1}) and high (400 µmol PAR m^{-2} s^{-1}).

Figure 22 shows the development of drought as the experiment proceeded. Whilst well-watered control plants had soil water contents of 96-100% throughout the experiment, the soil water content fell exponentially in drought treatments reaching values of ~ 20% 8 days after water withdrawal and close to 0% after 15 days. Pictures of plants 7 and 15 days after water withholding are shown in Figure 23A and 23B respectively. After 7 days all plants appeared green and turgid although well-watered plants were larger, with a mean leaf rosette area of 6.3 cm^2 in comparison to 4.2 cm^2 for droughted plants ($P < 0.05$, Students t-test). After 15 days well-watered plants had grown whilst droughted plants had become severely desiccated and shrivelled. In well-watered control plants values of F_v/F_m remained constant at 0.75-0.78 (Figure

22). Similar values were seen in droughted plants except for the very last time point when values dropped sharply to 0 when the soil water content was < 12%.

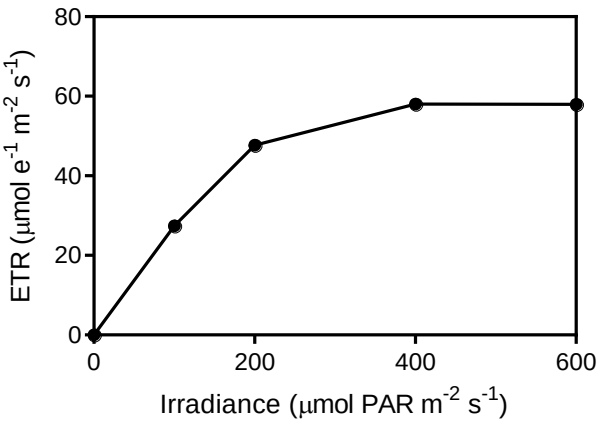

Figure 21. The response of the rate of electron transport (ETR) in Arabidopsis control plants to increasing light irradiance. Values are the mean (n=4) ± SE.

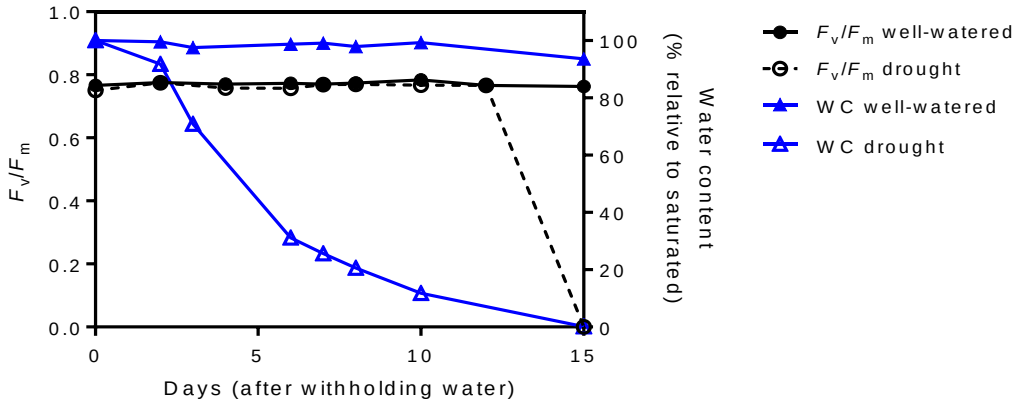

Figure 22. Changes in soil water content (WC; triangles) in well-watered (closed symbols) and droughted (open symbols) treatments. The photosynthetic parameter F_v/F_m (circles) was measured at intervals after withholding water (day 0). Values are the mean (n=3) ± SE.

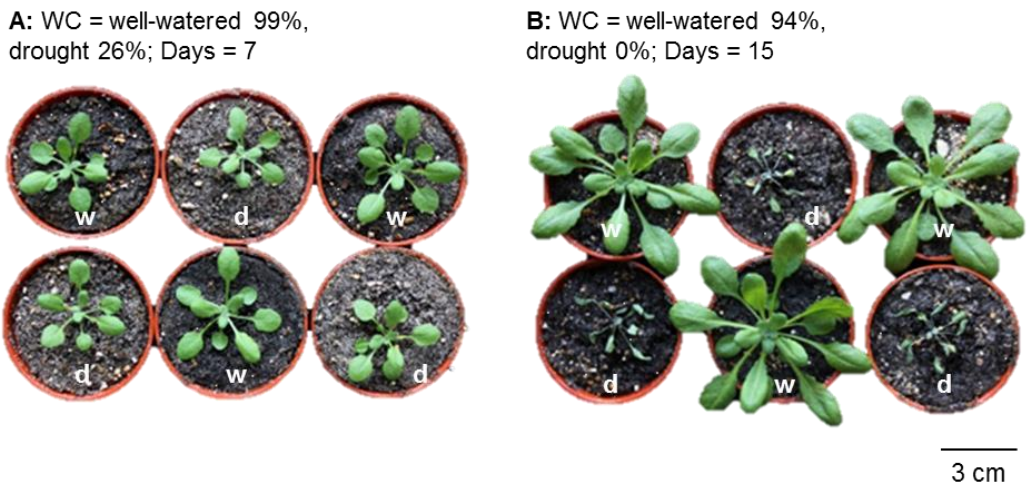

Figure 23A-B. Pictures of Arabidopsis plants taken after (A) 7 d and (B) 15 d. w = well-watered, d = drought. In the droughted treatments the soil water content (WC) had decreased to 26% after 7 d and 0% after 15 d.

To determine the impact of drought on chlorophyll fluorescence parameters, plants were dark adapted for 5 min, F_v/F_m was measured and then plants were illuminated with high (400), medium (200) or low (100 µmol m^{-2} s^{-1}) light for 20 min to allow plants to go through photosynthetic induction. Once steady-state was attained samples were irradiated sequentially at low, then medium, then high light.

The rate of ΦPSII induction did not alter significantly in well-watered control plants throughout the experiment (Figure 24A-F). Although the steady-state values were strongly affected by irradiance, the initial rapid rise in ΦPSII was achieved 3-4 min post-illumination. Induction was slower in droughted plants although similar stead-state values were eventually achieved. This slowing of induction was evident 6 days after water withholding and marked from 8 days onwards when soil water content was ~ 20%. The slowing of induction was most evident at higher irradiances and no differences were seen at 100 µmol PAR m^{-2} s^{-1}. During the initial rapid rise of ΦPSII, NPQ increased and then declined in all treatments (Figure 25A-F). Similar steady-state values were attained. The NPQ measurements mirrored those of ΦPSII – a slowed ΦPSII induction was accompanied by a longer period of elevated NPQ. When plants underwent a light transition between two irradiances there were no differences in ΦPSII or NPQ kinetics, indicating that kinetic differences were only apparent after a period of dark-adaptation rather than simply a change in irradiance (Figure 24A-F; Figure 25A-F).

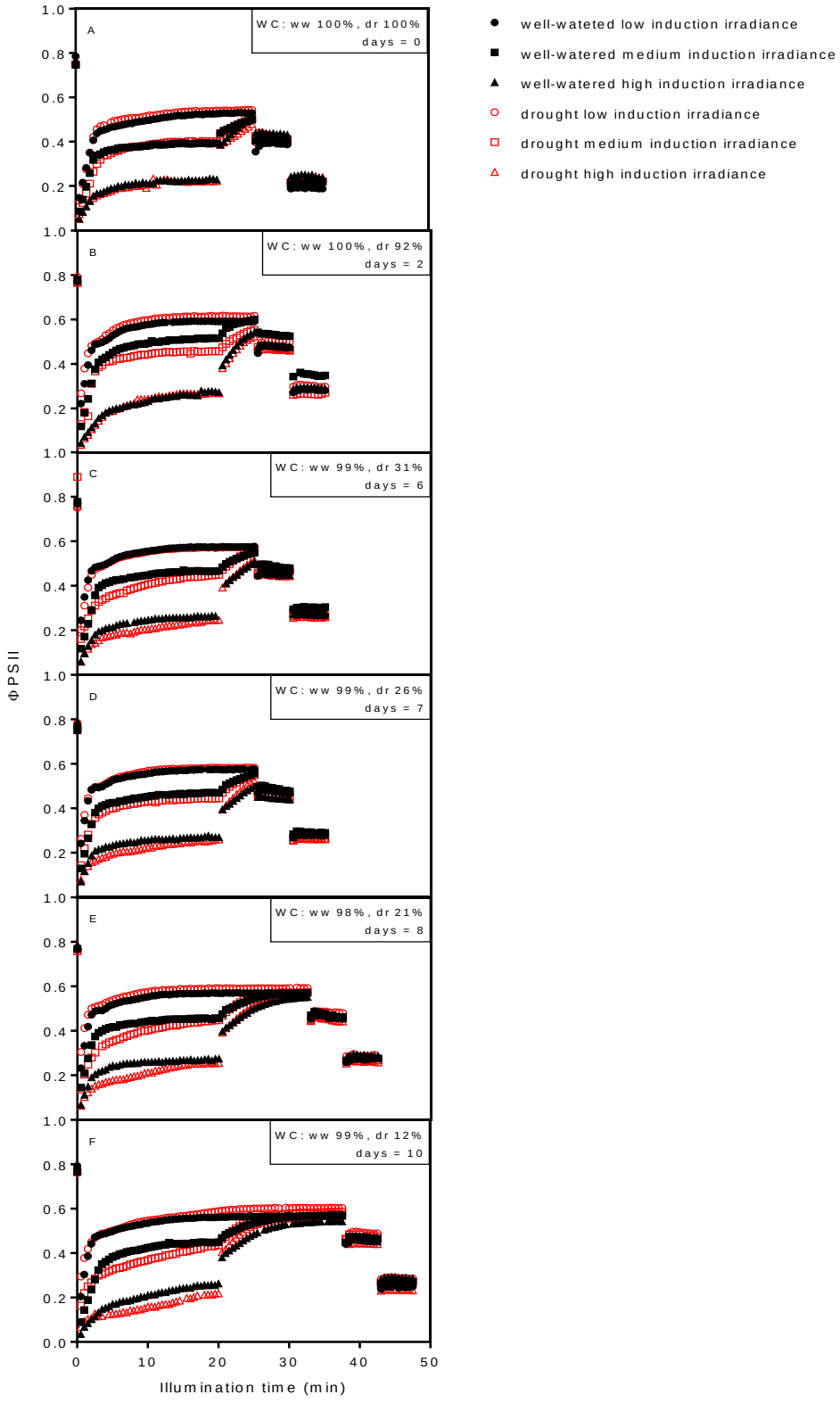

Figure 24A-F. ΦPSII in well-watered (black shapes) and droughted (red shapes) Arabidopsis when induction was measured at low (circles), medium (squares) or high (triangles) light. WC = soil water content, ww = well-watered, dr = drought. Measurements were made at intervals after withholding water from droughted plants (day 0). n=1

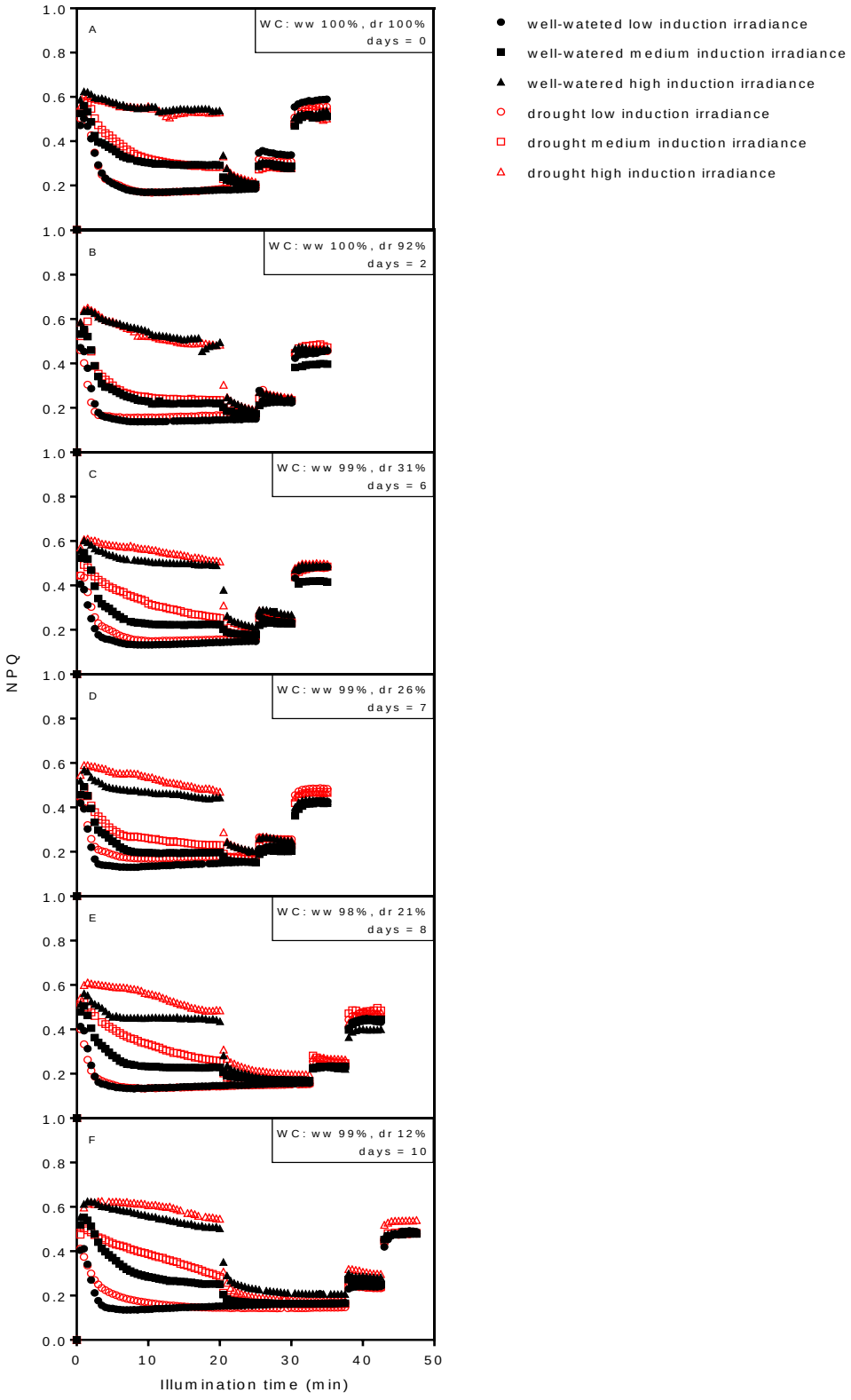

Figure 25A-F. NPQ in well-watered (black shapes) and droughted (red shapes) Arabidopsis when induction was measured at low (circles), medium (squares) or high (triangles) light. WC = soil water content, ww = well-watered, dr = drought. Measurements were made at intervals after withholding water from droughted plants (day 0). n=1.

2.3.2. Are the changes in the rates of induction of ΦPSII and NPQ reproducible?

The above experiment indicated that drought-induced changes in the rate of induction of ΦPSII and NPQ when measured at high irradiance. Replication was limited because each sample took > 40 min to measure. To increase replication only a subset of the conditions were chosen for the following experiment. Plants sown onto individual pots germinated and grew for 14 days before withholding water (day 0 = 14 days after sowing). Induction was measured in 4 replicates under high light (400 μmol m^{-2} s^{-1}) at intervals.

Although differences in ΦPSII between treatments were observable earlier, they were most marked after 8 days of water withholding when the soil water content was ~ 20% in droughted plants (Figure 26A-D). On day 8 ΦPSII was significantly lower in droughted plants between 2.5-12.5 min of induction ($P < 0.05$). Both well-watered and drought treatments achieved similar steady-state values throughout the experiment. The increase in ΦPSII following the application of light to dark-adapted samples had a fast and a slow phase. ΦPSII increased quickly between 0-5 min of induction and then more slowly thereafter. Drought slowed the increase between 0-5 min. Changes in NPQ mirrored those seen in ΦPSII and on day 8 NPQ was significantly elevated in droughted plants whereas it declined more quickly in well-watered control plants ($P < 0.05$; Figure 27A-D).

Drought resulted in reproducible changes in induction kinetics when soil water content had declined to ~ 20% and although these changes could be seen at some earlier time points, they were not as marked. ΦPSII after 5 min of induction appeared to be a parameter that reproducibly responded early to drought (Figure 28A). Steady-state measurements of ΦPSII and F_v/F_m were not affected by drought over the same time period (Figure 28B-C). These results indicate that the underlying processes of photosynthetic induction were sensitive to water withholding, but mild to moderate drought did not reduce plants maximum potential efficiency (F_v/F_m).

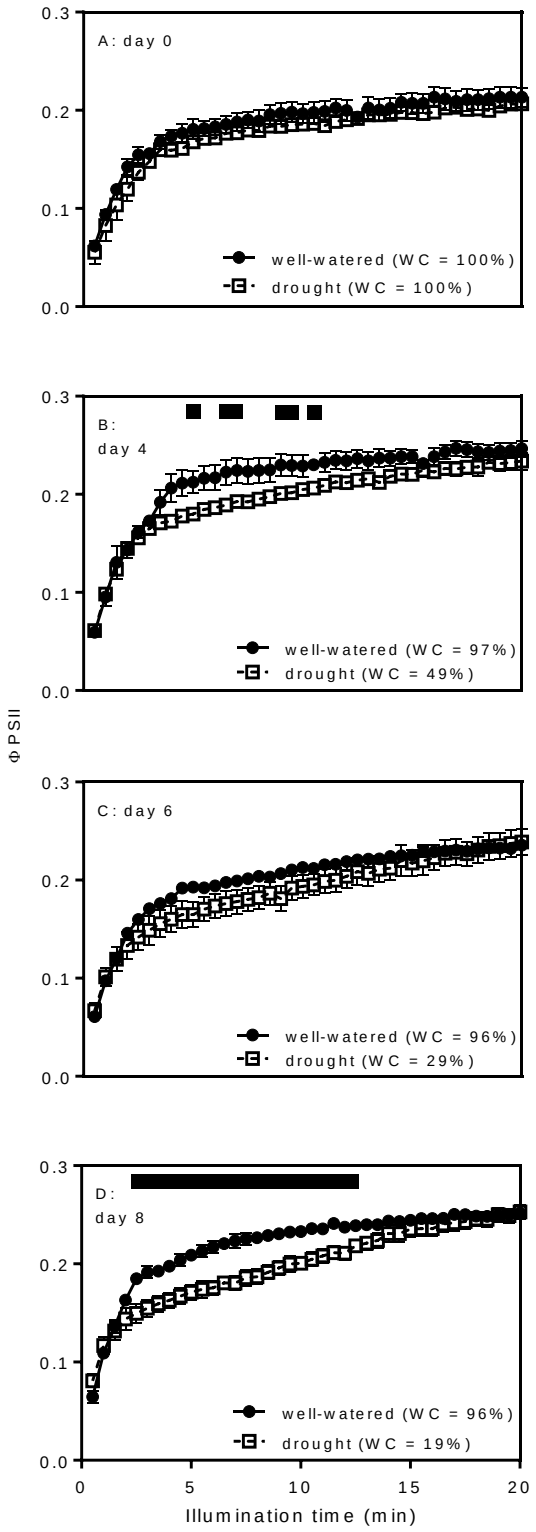

Figure 26A-D. ΦPSII in well-watered (closed symbols) and droughted (open symbols) plants during high light induction. Water was withheld from droughted plants on day 0 and soil water content (WC) is listed at intervals. Black squares/bars indicate values which are significantly different between treatments, $P < 0.05$, Students t-test. Data are means (n=4) ± SE.

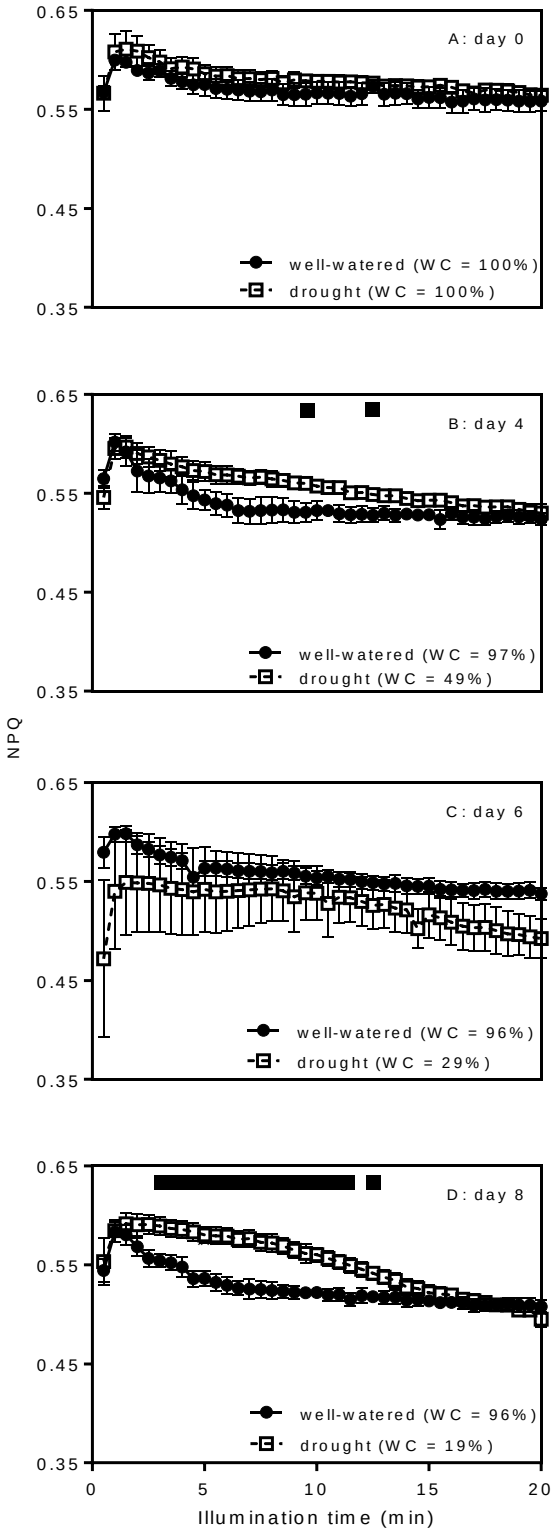

Figure 27A-D. NPQ in well-watered (closed symbols) and droughted (open symbols) plants during high light induction. Water was withheld from droughted plants on day 0 and soil water content (WC) is listed at intervals. Black squares/bars indicate values which are significantly different between treatments, $P < 0.05$, Students t-test. Data are means (n=4) ± SE.

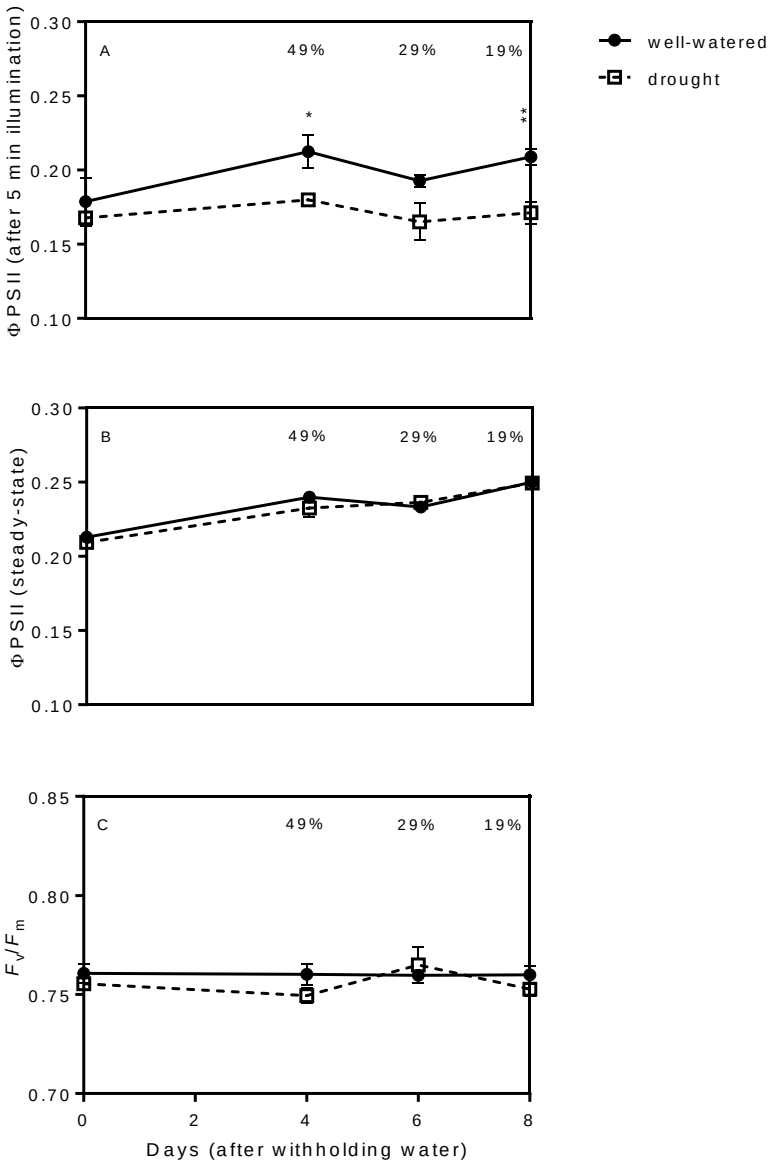

Figure 28A-C. ΦPSII after (A) 5 min of high light induction and (B) at steady-state, and (C) F_v/F_m in well-watered (closed symbols) and droughted (open symbols) plants. F_v/F_m was measured using a saturated flash following dark adaption. Steady-state ΦPSII values are averages of those taken between 18.5-20 min of illumination. Water was withheld from droughted plants on day 0 and soil water contents are listed at intervals. * indicates $P < 0.05$, ** indicates $P < 0.005$, Students t-test. Values are the mean (n=4) ± SE.

Drought stress can cause significant heterogeneity in leaves which can make comparisons between unstressed and stressed samples difficult (Sperdouli & Moustakas, 2012; Bresson *et al.*, 2015). Figure 29A-B indicates that the samples were homogenous as the patterns of change in ΦPSII and NPQ during induction were

similar in both treatments, although they occurred at different rates. The samples shown in Figure 29A-B were representative.

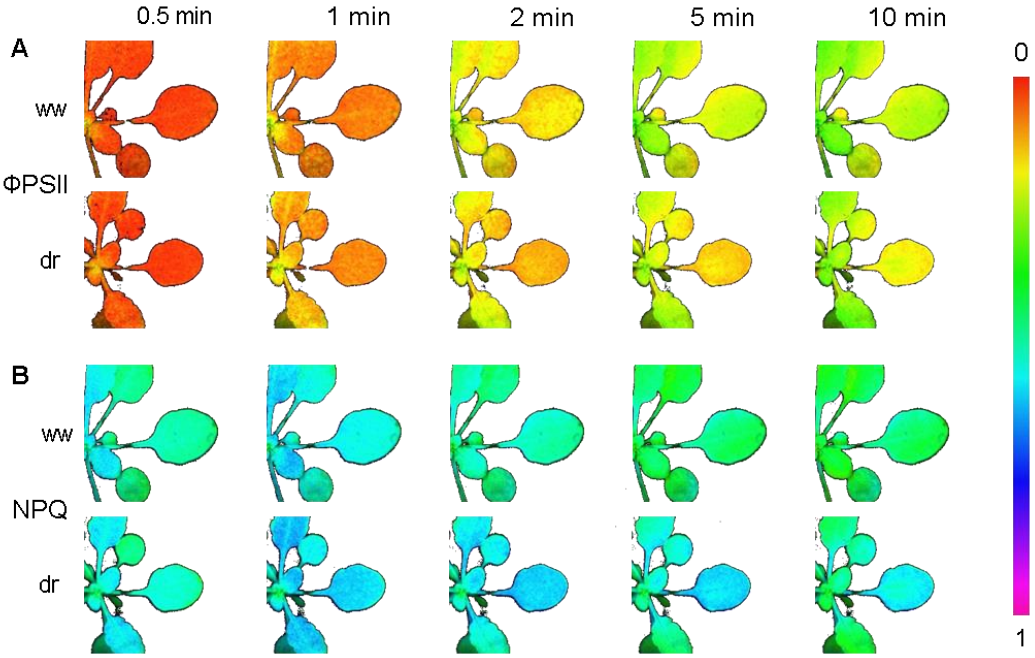

Figure 29A-B. False colour images of (A) ΦPSII and (B) NPQ during high light induction at the time points indicated. ww = well-watered, dr = drought. Soil water content was 96% in the well-watered plants and 19% in droughted plants. Values are extracted from the images using the false colour scale (right-hand side) which runs from 0 (red) to 1 (purple).

2.3.3. The impact of drought on leaf temperature in *Arabidopsis thaliana*

As an adaptive response to water shortage plants will close their stomata to conserve water. This can reduce the extent of the cooling effect of transpiration and lead to leaf temperature increases. Leaves of all plants were of similar temperatures at the beginning of the experiment (Figure 30A). When soil water content was ~ 29% thermal imaging revealed that droughted leaves were 0.3 °C warmer than well-watered leaves (Figure 30B). All plants increased in temperature 2 days later however droughted leaves were still 0.3 °C warmer on average (Figure 30C). At no time point was the difference in mean leaf temperature of well-watered samples significantly different from droughted plants.

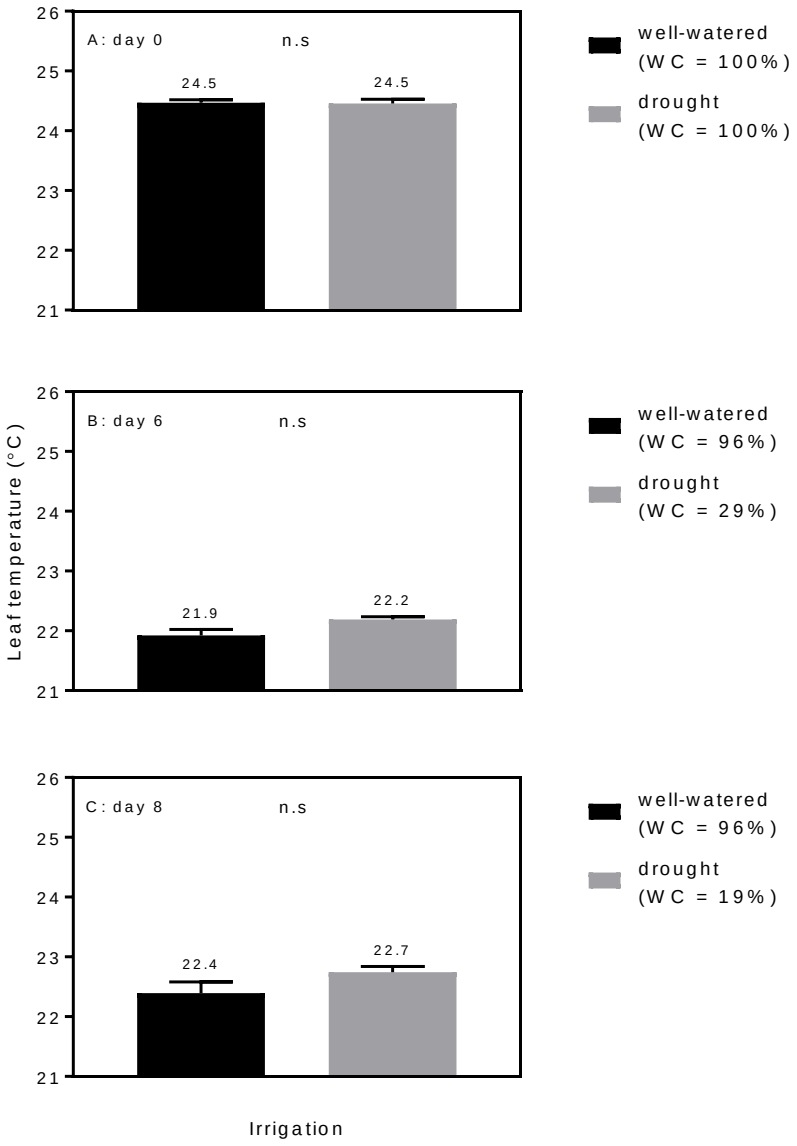

Figure 30A-C. Changes in leaf temperature measured at intervals. Water was withheld from droughted plants on day 0. WC = soil water content. n.s = non-significant, Students t-test. Values are the mean (n=3) ± SE.

2.3.4. The impact of drought on growth and yield in *Arabidopsis thaliana*

When suffering water scarcity plants will halt growth which, if sustained, can irreversibly reduce yield. Plant diameter was measured to investigate the impact of drought on growth. To allow yield parameters to be quantified, droughted plants were rewatered 12 days after water withholding (

Figure 31A) and daily from then on until inflorescences developed. For yield measurements all aerial plant parts and the total seed for each plant were harvested

and dried before analysis. To test if drought had any effect on seed viability > 50 seeds from each plant were sown and % germination was measured after 7 days.

The diameters of all plants increased with time throughout the experiment (

Figure 31B). For the first 9 days well-watered and droughted plants were of comparable size, but at the time of rewatering droughted plants were 1.3 cm smaller than the well-watered samples ($P < 0.005$, Student's t-test). On the day of rewatering (day 12) well-watered plants had a significantly higher relative growth rate, although the reverse was true from day 16 onwards (

Figure 31C). Drought did not lead to yield penalty suggesting there was enough time for plant growth to recover before yield set or that plant size is not a determinant of yield over this range. After harvest there were no significant differences in aerial dry weight (Figure 32A), seed yield (Figure 32B) or seed weight (Figure 32C) between treatments. Similarly drought did not significantly reduce the seed viability (Figure 32D).

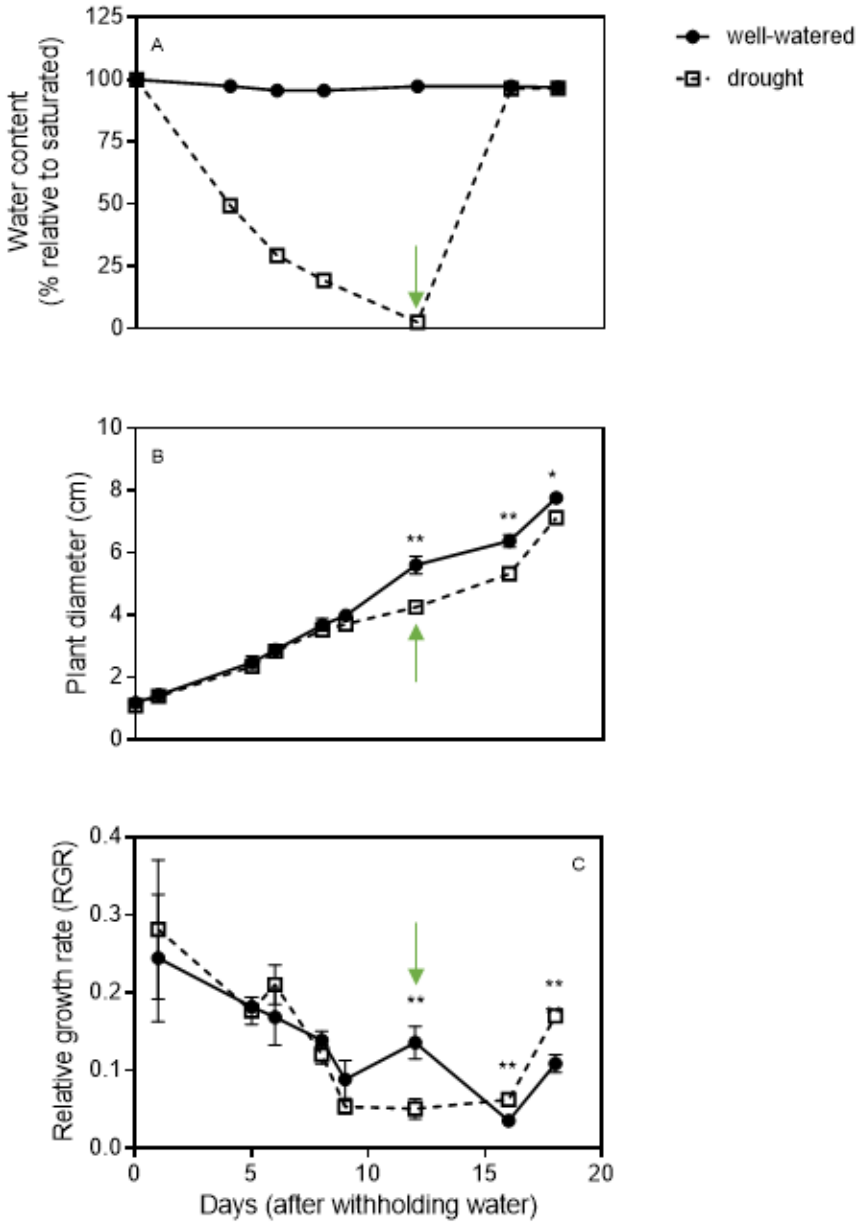

Figure 31A-C. Changes in (A) soil water content, (B) plant diameter and (C) relative growth rate in well-watered (closed symbols) and droughted (open symbols) treatments. Water was withheld from droughted plants on day 0 until they were rewatered on day 12 (green arrows), and daily from then on. ** denotes $P < 0.005$, * denotes $P < 0.05$, Students t-test. Values are the mean (n=4) ± SE.

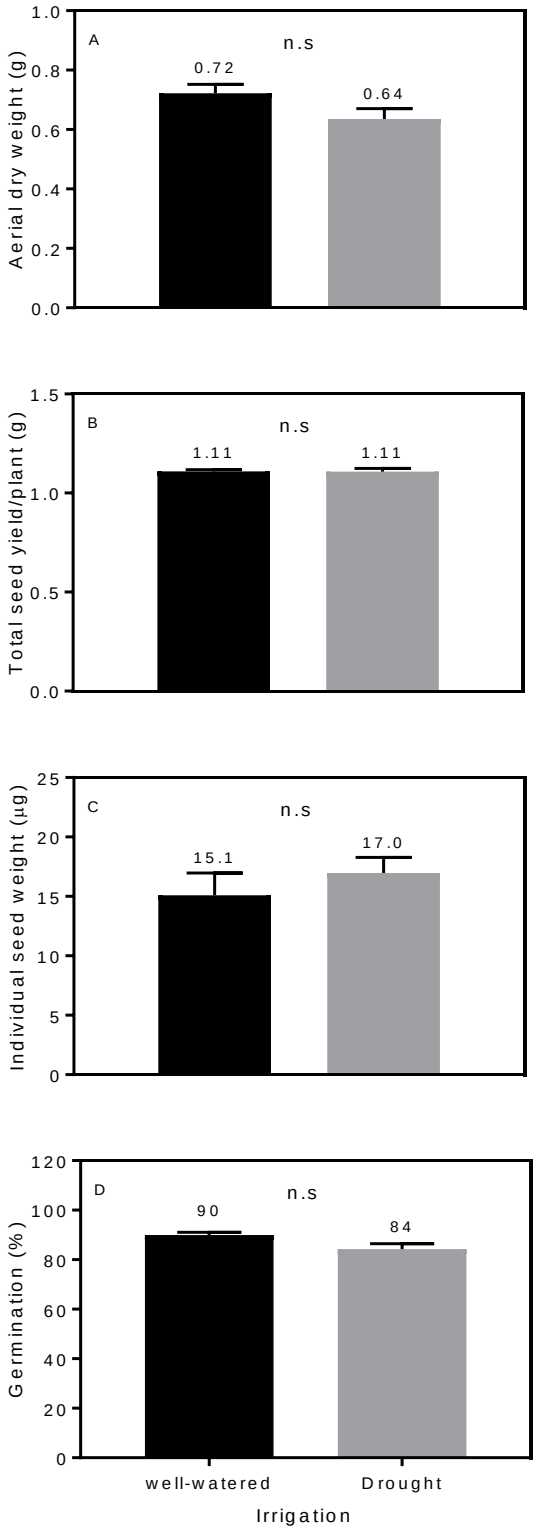

Figure 32A-D. Post-harvest measurements of (A) aerial dry weight, (B) total seed yield/plant and (C) individual seed weight, and (D) % germination. Aerial plant parts and seed were desiccated before weighing. > 50 seeds were sown from each plant and % germination was scored after 7 days. n.s = non-significant, Students t-test. Values are the mean (n=4) ± SE.

2.3.5. Drought-induced changes in induction kinetics and growth in *Brassica napus*

In Arabidopsis drought caused changes in photosynthetic induction kinetics at 20% soil water content and in plant growth at < 5%. The aim of the following experiment was to investigate if these findings occurred in the related dicot *Brassica napus*. Plants were sown and grown for 18 days in individual pots containing a 3:1 mix of a peat based compost and sand, after which water was withheld from droughted plants (day 0). Well-watered plants were watered daily throughout and drought severity was quantified as previously. Photosynthetic induction parameters at high light and F_v/F_m were measured on the same leaf of each plant throughout. Growth was assessed at intervals by measuring plant height and leaf number.

Figure 33 shows how drought progressed over the course of 20 days of water withholding. Whilst soil water content remained > 98% in well-watered treatments, it declined exponentially in droughted plants measuring ~ 17% after 15 days of withholding water and < 5% after 20 days. F_v/F_m declined gradually in well-watered plants from 0.78 on day 0 to 0.69 after 20 days as a result of leaf ageing (Figure 33). In contrast F_v/F_m was between 0.75-0.77 in droughted plants during the first 15 days of water withholding, meaning on days 12 and 15 it was significantly higher than the well-watered treatment ($P < 0.05$). In droughted plants F_v/F_m declined abruptly after 18 days to 0 by 20 days.

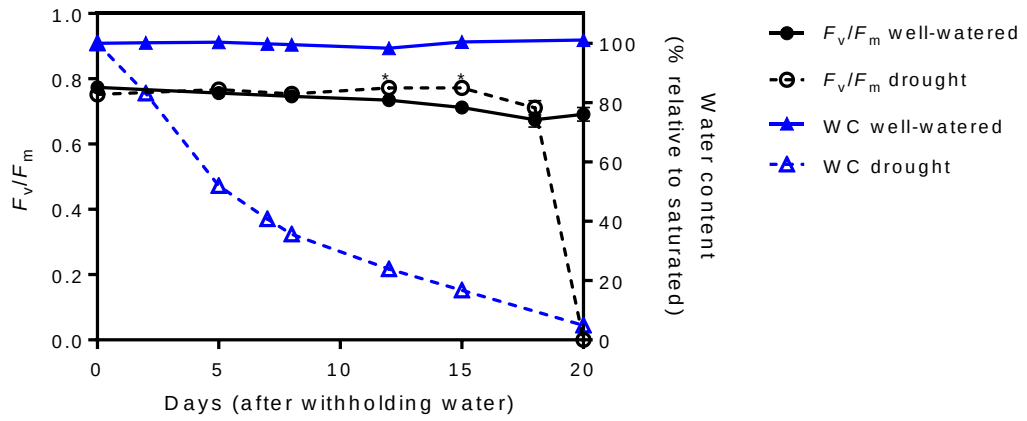

Figure 33. Changes in soil water content (WC; triangles) in well-watered (closed symbols) and droughted (open symbols) treatments. F_v/F_m (circles) was quantified at intervals after withholding water from droughted plants (day 0). * indicates P < 0.05, Students t-test. Values are the mean (n=4) ± SE.

In well-watered plants the initial rapid rise in ΦPSII induction was complete after ~ 3 min, before ΦPSII plateaued and steady-state was achieved (Figure 34A-F). This pattern was typically observed at all measuring points. In droughted plants from 8 days onwards there was a biphasic induction of ΦPSII, whereby an initial rapid rise was followed by a second slower rise. In all plants steady-state was achieved after ~ 15 minutes. After 18 days of withholding water ΦPSII remained low throughout induction in droughted plants. Significantly elevated NPQ was observed in droughted samples 5 days after water was withheld and this persisted until 20 days (Figure 35A-F). NPQ levels decreased slightly over the course of the experiment in well-watered plants as leaves developed and aged.

As with Arabidopsis, drought-induced changes in ΦPSII induction were seen in *B. napus* when the soil water content was ~ 20%, although the kinetics were different (Figure 26A-F; Figure 34A-F). In contrast to Arabidopsis however, steady-state ΦPSII was perturbed in *B. napus* when the soil water content was 50% and thereafter (Figure 26A-F; Figure 34A-F). Additionally NPQ was elevated in *B. napus* during induction and at steady-state after soil water content declined to ~ 36% and below (Figure 35C-F).

Figure 36 shows there was little heterogeneity in leaves between treatments, although the F_v/F_m image highlights light blue/green areas where the well-watered leaf had begun to senesce as it aged. As development had been delayed in the droughted leaf there was no evidence of the effects of senescence processes. The samples in Figure 36 were representative.

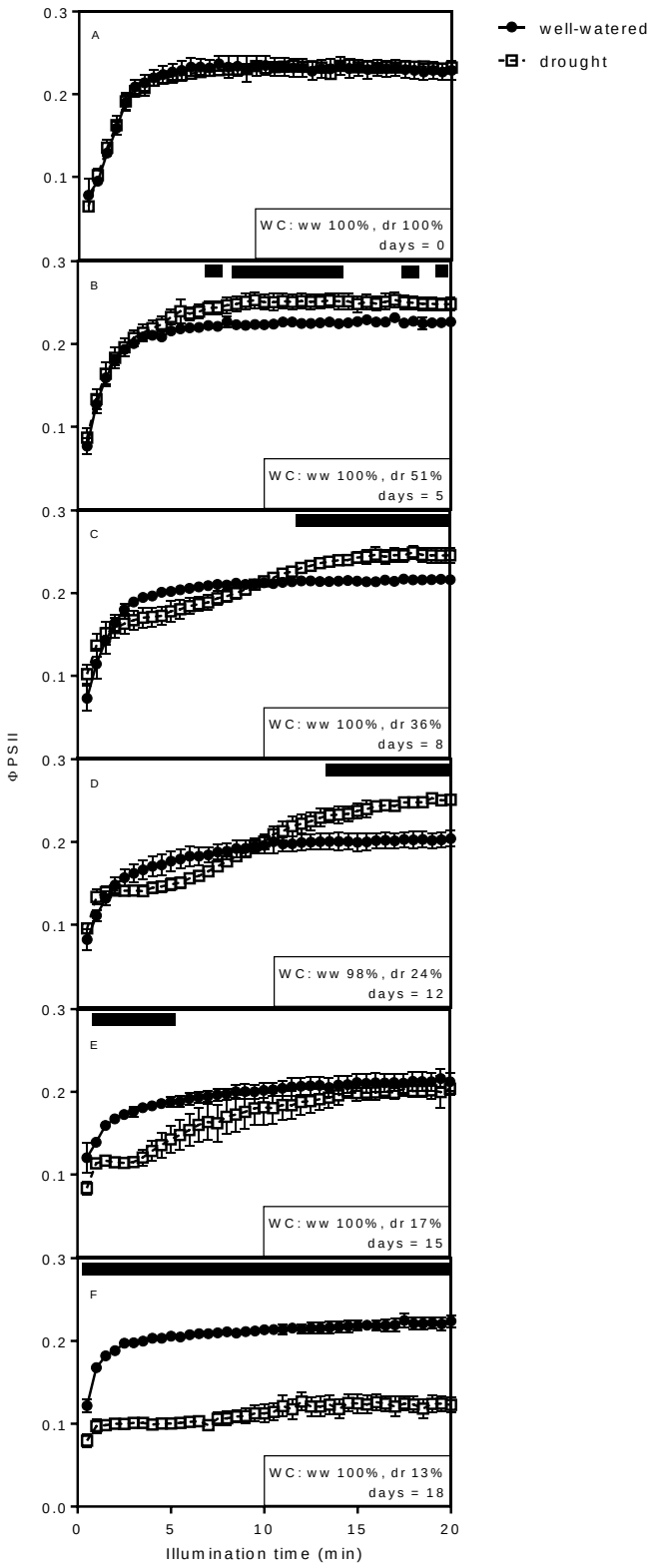

Figure 34A-F. ΦPSII in well-watered (closed symbols) and droughted (open symbols) *B. napus* plants during high light induction. Water was withheld from droughted plants on day 0 and soil water content (WC) is listed at intervals. Black squares/bars indicate values which are significantly different between treatments, $P < 0.05$, Students t-test. Data are the mean (n=4) ± SE.

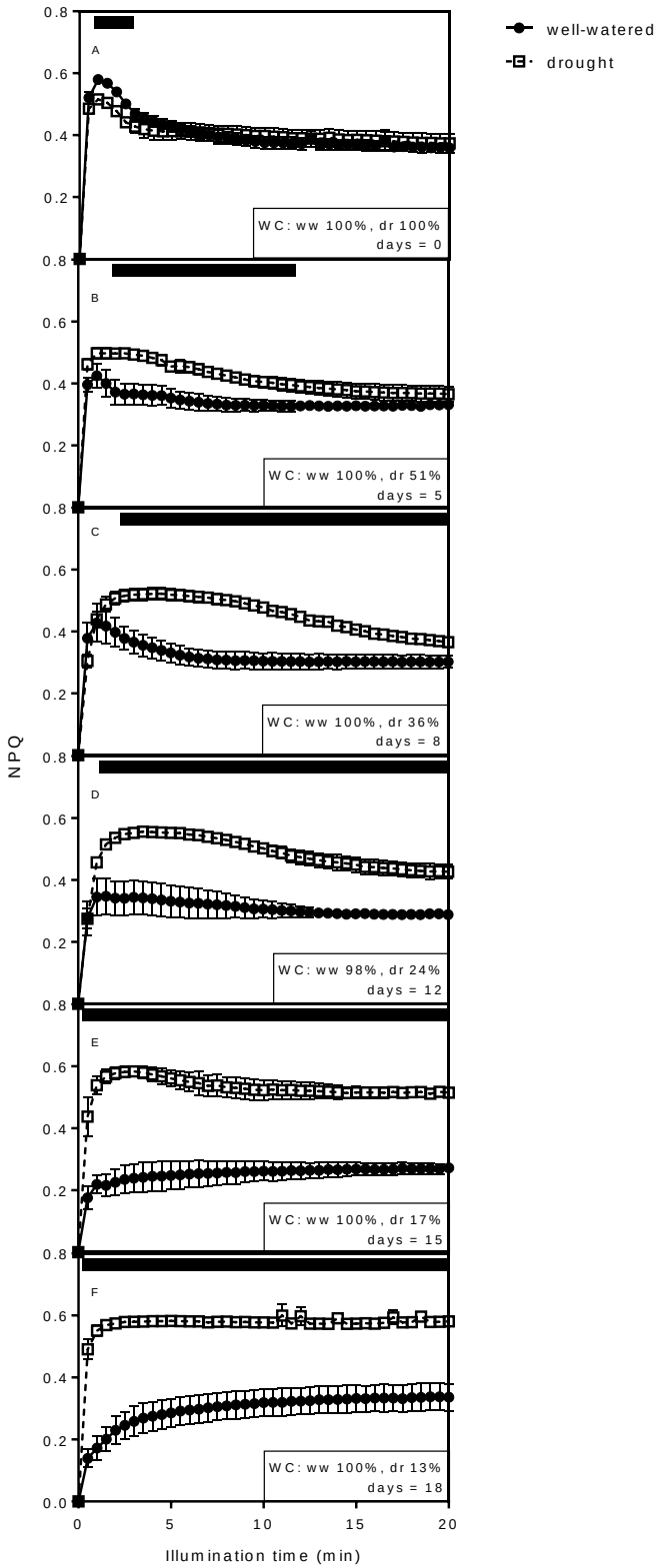

Figure 35A-F. NPQ in well-watered (closed symbols) and droughted (open symbols) *B. napus* plants during high light induction. Water was withheld from droughted plants on day 0 and soil water content (WC) is listed at intervals. Black bars indicate values which are significantly different between treatments, $P < 0.05$, Students t-test. Data are the mean (n=4) ± SE.

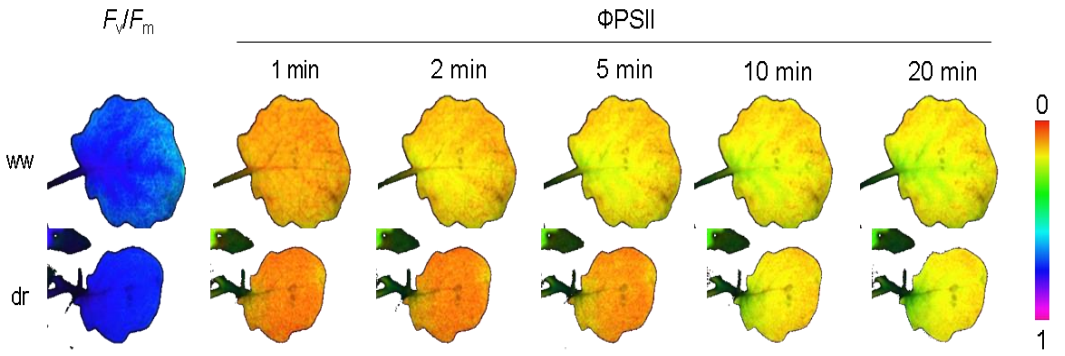

Figure 36. False colour images of F_v/F_m and ΦPSII during high light induction at the indicated time points. ww = well-watered, dr = drought. At the time of imaging soil water content was 100% and 17% in well-watered and droughted plants respectively. Values are extracted from the images using the false colour scale (right-hand side) which runs from 0 (red) to 1 (purple).

2.3.6. The impact of drought on growth in *B. napus*

Well-watered plants grew taller at each time point relative to the previous most throughout, as did droughted plants until 15 days after water withholding, when they began to wilt (Figure 37A). On day 18 droughted plants were 5.1 cm shorter ($P < 0.005$), however no significant differences were observed before this point. Similarly, leaf number increased in all plants throughout and values were similar between treatments until the final measurements on day 18, when droughted plants had fewer leaves ($P < 0.005$; Figure 37B). Relative growth rate was significantly slower in droughted plants from day 12 onwards (Figure 37C).

The results so far indicated that induction kinetics were altered in Arabidopsis and *B. napus* when the soil water content was ~ 20% (Figure 26D and Figure 27D; Figure 34E and Figure 35E). Growth rate was perturbed at a similar time but this did not manifest in measures of size until soil water content was < 10% (

Figure 31B-C; Figure 37A-C).

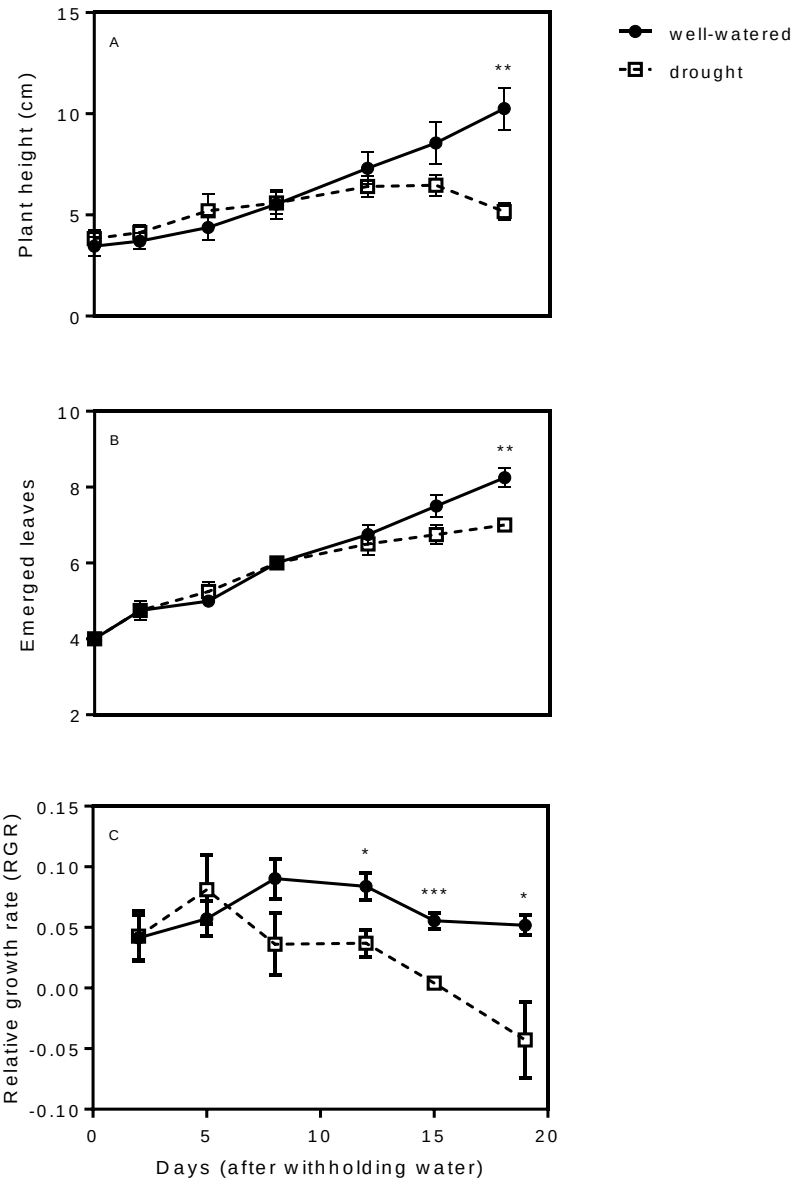

Figure 37A-C. Changes in (A) plant height, (B) the number of emerged leaves and (C) relative growth rate in well-watered (closed symbols) and droughted (open symbols) plants. Water was withheld from droughted plants on day 0. Treatments were tested for significance between each other using Students t-test. * denotes $P < 0.05$, ** denotes $P < 0.005$ and *** denotes $P < 0.0005$. Values are the mean (n=4) ± SE.

2.3.7. Low stomatal conductance limited the rate of induction of ΦPSII in droughted *B. napus*

Drought reduced the rate of ΦPSII during induction in Arabidopsis and *B. napus*. Photosynthetic induction is a complex process consisting of a number of underlying

reactions. Although chlorophyll fluorescence is a sophisticated analysis tool it cannot resolve all of the components of induction. The aim of this experiment was to use simultaneous gas exchange and fluorescence to investigate why drought reduced the rate of ΦPSII induction. *B. napus* plants were grown as previously described and measurements were made when soil water content was ~ 18%, 15 days after withholding water from droughted plants. High light induction was measured for 7 min following 5 min dark adaption. There was no significant difference in F_v/F_m between treatments (Figure 38).

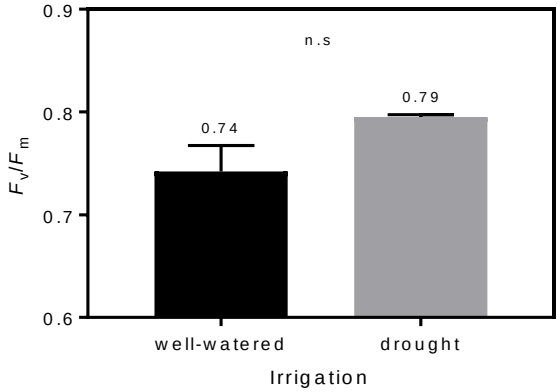

Figure 38. F_v/F_m measurements, made 15 days after water was withheld from droughted plants when soil water content was ~ 18%. n.s = non-significant, Students t-test. Values are the mean (n=6) ± SE.

Figure 39A-B shows that drought reduced the rate of ΦPSII and carbon assimilation (*A*) during induction. There was a strong relationship between ΦPSII and *A* which was linear under drought stress, but this did not hold true under well-watered conditions (Figure 40). Figure 39C shows that stomata remained open in well-watered plants after dark-adaption. Reduced stomatal conductance was correlated with lower ΦPSII and *A* during induction in droughted plants. Low conductance limits the supply of CO_2 for the Calvin cycle which leads to a downregulation of ΦPSII. Stomatal limitation concurrently reduced the rate of transpiration in the drought treatment (Figure 39D).

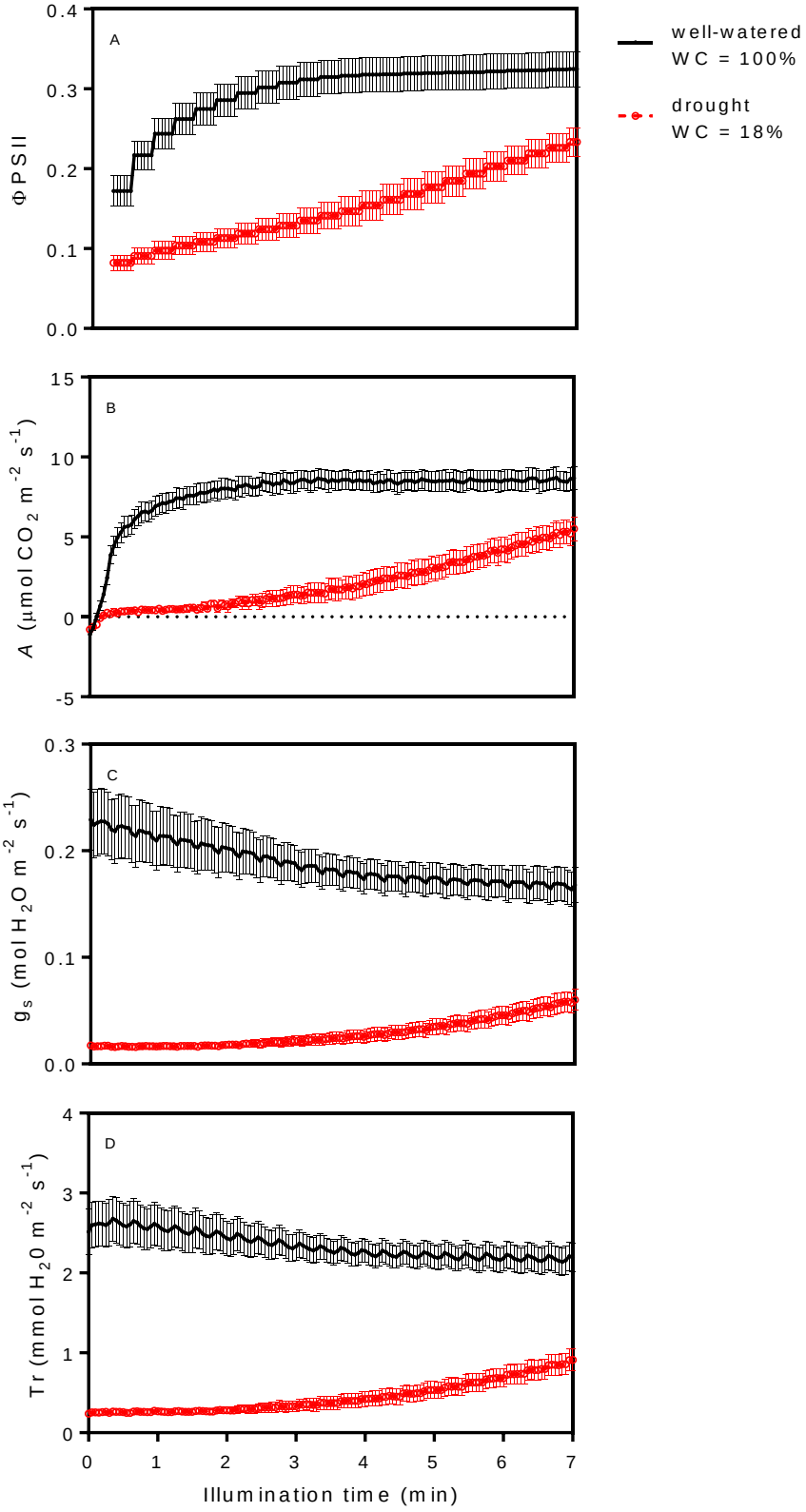

Figure 39A-D. (A) ΦPSII; (B) carbon assimilation rate, *A*; (C) stomatal conductance g_s; and (D) transpiration rate, Tr; in well-watered (black symbols) and droughted (red symbols) plants during high light induction. WC = soil water content. Values are the mean (n=6) ± SE.

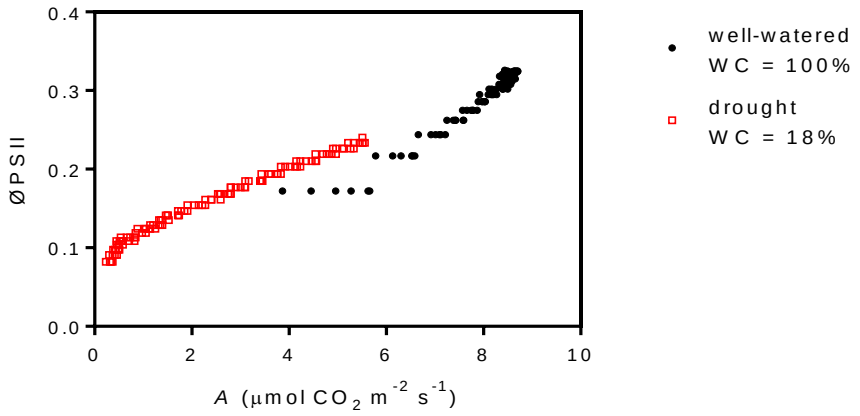

Figure 40. Relationship between carbon assimilation rate (*A*) and ΦPSII in well-watered (black symbols) and droughted (red symbols) plants. WC = soil water content.

2.3.8. Are the drought-induced changes in induction kinetics and growth seen in the dicots reproducible in the monocot *Triticum aestivum*?

Drought caused reproducible changes in physiology and growth in Arabidopsis and *B. napus,* the onset of which coincided with specific soil water content levels. The aim of this experiment was to investigate if drought had similar impacts on the monocot *Triticum aestivum.* Plants were sown onto a 3:1 mix of a peat based compost and sand for 18 days in individual pots before water was withheld from droughted plants (day 0). Well-watered plants received water daily. High light induction parameters and F_v/F_m were quantified on the same leaf and thermal imaging was conducted at intervals throughout. Growth was monitored by measuring plant height and leaf number.

Figure 41 shows the progression of drought over the course of the experiment. Soil water content was > 98% in well-watered plants throughout, whereas it declined in droughted samples to ~ 7% after 15 days of withholding water, and ~ 1% after 18 days. F_v/F_m remained stable between 0.76 and 0.8 in all plants except at the final time point when it declined to 0.66 in droughted samples. In contrast to *B. napus*, F_v/F_m in *T. aestivum* remained stable at very low soil water content (Figure 33; Figure 41).

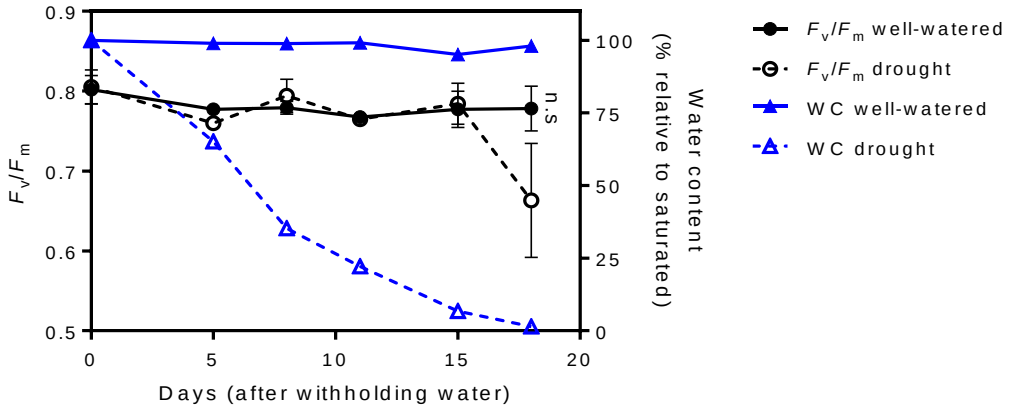

Figure 41. Changes in soil water content (WC; triangles) in well-watered (closed symbols) and droughted (open symbols) treatments. The photosynthetic parameter F_v/F_m (circles) was measured at intervals after withholding water (day 0). n.s = non-significant, Students t-test. Values are the mean (n=5) ± SE.

The initial rapid rise in ΦPSII induction was significantly slower when soil water content was ~ 22% in droughted plants, 11 days after water withholding (Figure 42A-F). This change was more marked after 15 days and the kinetics appeared biphasic. Treatments had similar steady-state values at most time points except days 8 and 18, when ΦPSII was higher and lower in droughted plants respectively. Plants were still photosynthesising when the soil water content was ~ 1%.

Droughted leaves of *T. aestivum* were warmer throughout the experiment, however no statistically significant differences between treatments were observed at any time point (Figure 43A-C).

Well-watered plants grew throughout the experiment (Figure 44A). By day 15 droughted plants had stopped growing although tissues appeared green and turgid (Figure 44A; Figure 45). At no point were any statistically significant differences in height between treatments observed (Figure 44A). Relative growth rate was significantly higher in droughted plants on day 8 ($P < 0.05$) and slower on day 18 ($P < 0.05$), although similar rates were observed in both treatments at all other time points (Figure 44B).

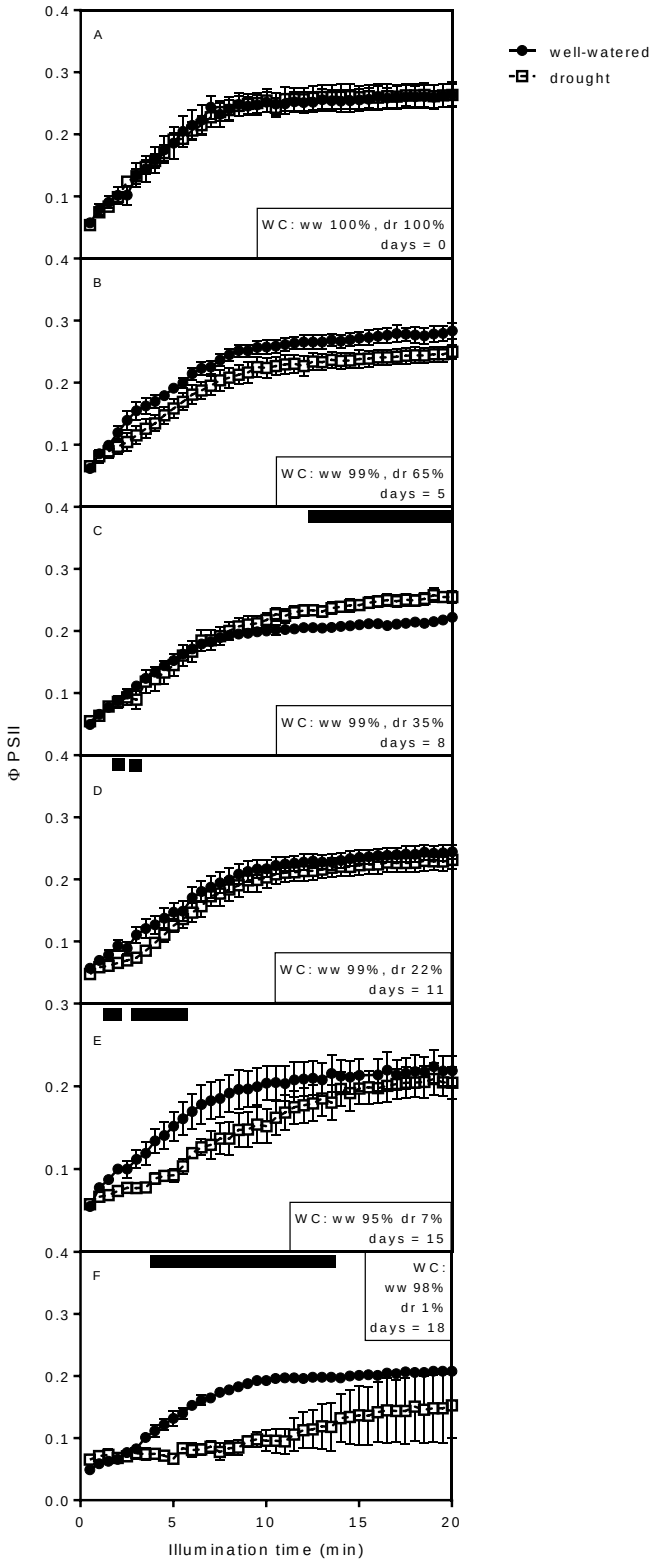

Figure 42A-F. ΦPSII in well-watered (closed symbols) and droughted (open symbols) *T. aestivum* plants during high light induction. Water was withheld from droughted plants on day 0 and soil water content (WC) is listed at intervals. Black squares/bars indicate values which are significantly different between treatments, $P < 0.05$, Students t-test. Data are the mean (n=5) ± SE.

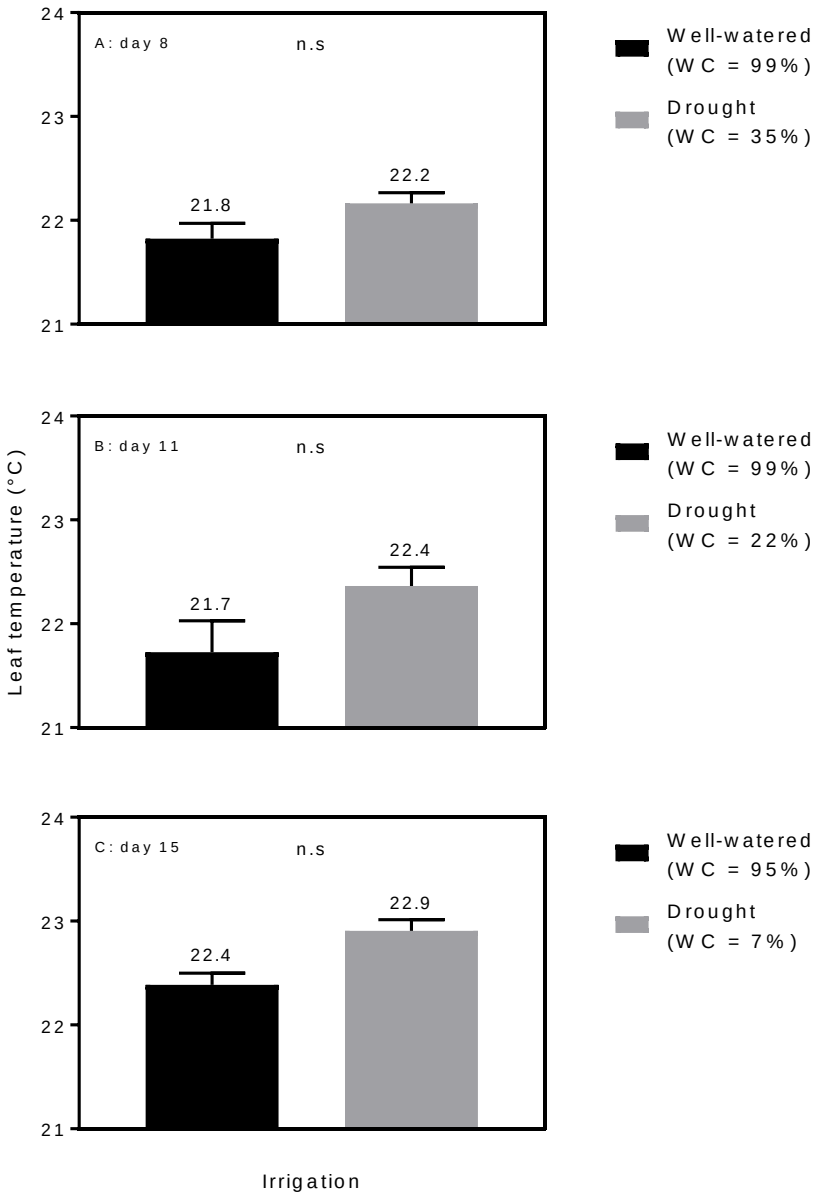

Figure 43A-C. Leaf temperatures measured at intervals after withholding water from droughted plants on day 0. WC = soil water content. n.s = non-significant, Students t-test. Values are the mean (n=4) ± SE

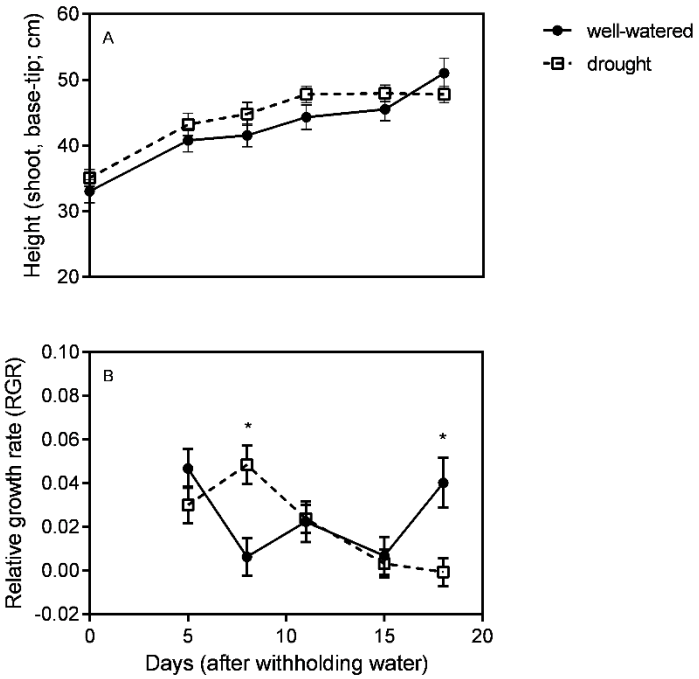

Figure 44A-B. Changes in (A) plant height and (B) relative growth rate in well-watered (closed symbols) and droughted (open symbols) *T. aestivum* plants. Water was withheld from droughted plants on day 0. * indicates $P < 0.05$, Students t-test. Values are the mean (n=5) ± SE.

Figure 45. Pictures of well-watered (ww) and droughted (dr) *T. aestivum* taken 15 d after withholding water. WC = soil water content.

2.4. Discussion

Drought has numerous effects on plant biochemistry, physiology and growth. Non-invasive imaging techniques provide ways to rapidly assess *in vivo* plant response to drought stress. Ecophysiological stress studies have classically used the fluorescence parameter F_v/F_m as a method of assessing plant health (Woo *et al.*, 2008; Jansen *et al.*, 2009; Sperdouli & Moustakas, 2012; Bresson *et al.*, 2015). Unstressed leaves of most species typically measure ~ 0.83, which usually declines to ~ 0.79 during the photoperiod and deviation from this range can be indicative of stress, a consequence of leaf ageing processes, or both (Maxwell & Johnson, 2000; Baker, 2008). In order to determine F_v/F_m accurately it is necessary to dark-adapt the plant which can significantly add to the sampling time. Experiments in this work have shown that changes in F_v/F_m were characteristically late-onset and only occurred after prolonged stress. Typically F_v/F_m declined rapidly to 0 when soil water content was below 10% (Figure 22; Figure 33; Figure 41). This is not uncommon and several studies have reported that F_v/F_m declined a matter of hours before plants lost viability. Woo *et al.*, (2008) showed that in Arabidopsis (Col-0) plants subjected to drought, a decline from ~ 0.8 to ~ 0.7 occurred after 14 d of drought, which was followed by a decline to ~ 0.15 over the course of the following 48 hours. None of these plants recovered after rewatering. Therefore F_v/F_m is a good indicator of plant health and any deviation to lower values are indicative of a decline in viability. However, it is not sensitive enough to indicate that a plant is suffering mild or moderate stress.

Plants undergo photosynthetic induction when they are transferred from darkness into light. Dark-light transition triggers stomatal opening, photosynthetic electron transport and the formation of ΔpH gradients, and the recruitment and activation of enzymes involved in the Calvin cycle (Maxwell & Johnson, 2000; Baker, 2008; Murchie & Lawson, 2013). These underlying processes are dynamic, complex and difficult to interpret. Drought reproducibly altered ΦPSII and NPQ during induction in independent experiments when soil water content was ~ 20% in Arabidopsis and *B. napus,* and ~ 7% in *T. aestivum*. Drought reduced ΦPSII during the first 10 min of high light induction in Arabidopsis, and over the first 5 in *B. napus* (Figure 24A-F;

Figure 26A-D; Figure 34A-F) and *T. aestivum* (Figure 42A-F). Initial fluorescence protocols, which measured the response of parameters to drought and took ~ 50 min to complete, were shortened in subsequent experiments and these protocols highlighted a reproducible indicator of drought stress. Values of ΦPSII after 5 min of induction highlighted significant differences between treatments in all three species (Figure 26D; Figure 28A; Figure 34E; Figure 42E). At the soil water contents quoted the increase of ΦPSII over the first 1 min of induction was unaffected by drought. The activation of electron transport and the development of a transthylakoid ΔpH responsible for this initial rate of increase in ΦPSII are only perturbed by severe drought (Murchie & Lawson, 2013). The comparable F_v/F_m values of well-watered and droughted samples at these time points further suggest that drought had not significantly damaged the photosynthetic machinery (Figure 22; Figure 33; Figure 41). The second rise in ΦPSII thereafter is determined by stomatal opening and enzyme and metabolite recruitment, which respond an order of magnitude slower. Mild to moderate drought stress can reduce stomatal conductance, NADPH production and RuBP regeneration, which will reduce the rate of ΦPSII increase during the next phase of induction. In all species declines in ΦPSII during induction were concurrent with sustained periods of elevated NPQ which suggests plants were regulating the dissipation of excess energy (Figure 25A-F; Figure 27A-D; Figure 35A-F). The high lumen pH generated by electron transport promotes the conversion of violaxanthin to zeaxanthin in the xanthophyll cycle and the protonation of the NPQ regulator PsbS, leading to increased NPQ (Kereïche *et al.*, 2010; Xu *et al.*, 2015; Ruban, 2016). The ΔpH gradient relaxes slowly so these processes can persist resulting in sustained elevated NPQ during stress. After ~ 20 min of induction plants reached steady-state where the rates of the underlying reactions proceed at constant rates. Steady-state parameters are often quoted in the literature because they are easy to interpret, but they are not as sensitive to drought as induction measures and take longer to obtain. At steady-state ΦPSII and NPQ were largely uninformative until terminal drought (Figure 24A-F; Figure 25A-F; Figure 26A-D; Figure 27A-D; Figure 34A-F; Figure 35A-F; Figure 42A-F). At the high irradiance (400 µmol m^{-2} s^{-1}) defined in preliminary light saturation experiments (Figure 21), photosynthesis was driven to an extent which highlighted drought-induced changes in induction parameters (Figure 24A-F; Figure

25A-F). These differences were not visible or less marked at the lower irradiances as stressed plants were still able to partition the reduced incident light into photochemistry.

Drought can cause significant heterogeneity in leaves although there was no evidence of this in either Arabidopsis or *B. napus* when the soil water content was ~ 20% (Figure 29A-B; Figure 36) (Sperdouli & Moustakas, 2012; Bresson *et al.*, 2015). However the F_v/F_m image revealed signs of age related senescence in the well-watered *B. napus* plant which was not evident in the droughted sample (Figure 36). This delay in the senescence pathway explains why F_v/F_m was significantly higher in droughted plants on days 12 and 15 (Figure 33).

Measuring simultaneous fluorescence and gas exchange is a powerful technique because it can explain how drought is perturbing induction parameters (Maxwell & Johnson, 2000; Baker, 2008; Murchie & Lawson, 2013). Chlorophyll fluorescence alone cannot quantify stomatal response or assimilation rates (and by extension the activity of alternative electron sinks), whereas it can when used in combination with gas exchange. When soil water content had declined to ~ 18% in *B. napus*, ΦPSII was characteristically reduced over a 7 min high light induction (Figure 39A), which slowed the rate of carbon assimilation (Figure 39B). Analysis revealed that drought dramatically reduced stomatal conductance and that stomata were slow to respond to light (Figure 39C). Stomata began to open in droughted plants after ~ 4-5 min of induction and this coincided with an increase in the rate of assimilation. In contrast, 5 min of dark-adaption was not long enough for stomata to close in well-watered plants and this delayed response enabled rapid induction. Stomatal closure will be revisited in Chapter 5. Stomata regulate the diffusion of CO_2 from the atmosphere into the leaves and to the sites of carboxylation (Baker, 2008). Leaves close their stomata to conserve water during drought stress in response to ABA translocation from the roots (Pinheiro & Chaves, 2011; Bauer *et al.*, 2017). Low stomatal conductance results in CO_2 limitation at Rubisco, which limits the rate of assimilation during induction and reduces the requirement for ATP and NADPH for the Calvin cycle (Chaves, 2002; Flexas & Medrano, 2002; Lawlor, 2002). This can cause reductions in linear electron transport and ΦPSII, and increases in heat dissipation

and alternative electron sinks (Baker, 2008). CO_2 limitation can result in the over-reduction of the electron transport chain and the generation of ROS including superoxide, hydrogen peroxide and hydroxyl radicals at photosystem I (Mahajan & Tuteja, 2005). ROS need to be scavenged before they damage the plant. These ROS can act as second messengers in redox signal transduction pathways and are implicated in hormonal mediated events (Foyer & Noctor, 2003). For example, hydrogen peroxide induces stomatal closure and the induction of heat shock proteins (Karpinska *et al.*, 2000). It has been shown in Arabidopsis that the application of ABA to guard cells induced hydrogen peroxide production and stomatal closure (Desikan *et al.*, 2004).

Another consequence of low stomatal conductance is a reduction in the cooling effect of transpiration and leaves of droughted Arabidopsis and *T. aestivum* plants became significantly warmer than well-watered samples as drought progressed, although these differences were non-significant in all cases (Figure 30A-C; Figure 43A-C) (Merlot *et al.*, 2002; Benavente *et al.*, 2013). The warming was observed at 29% and 7% soil water content in Arabidopsis and *T. aestivum* respectively, most likely because Arabidopsis has a rosette growth formation with leaves which have large surface area to volume ratios. Leaves of *T. aestivum* are long, thin and can orientate to change the amount of light they absorb. This means that per unit area, proportionally more light will be incident on Arabidopsis leaves making droughted plants warmer at higher soil water contents in comparison to *T. aestivum*. Additionally, crop plants such as *T. aestivum* are optimised for electron transport and carbon assimilation so they have a greater capacity to use absorbed light in photochemistry, reducing the requirement for heat dissipation processes and transpiration. Thermal imaging is used to measure leaf temperature and probe stomatal conductance (Merlot *et al.*, 2002). Abiotic stress often leads to a reduction in transpiration from the leaf. However thermal imaging can prove difficult due to a number of technical limitations (Li *et al.*, 2014). For example, thermal imaging is influenced by objects surrounding the sample and its environment. Because of the flat growing form of Arabidopsis, leaves are in contact with the soil below which can affect their temperature. Additionally, because *T. aestivum* grows vertically leaves

have to be clamped in for measuring which can cause damage. Furthermore, because of the three-dimensional morphology of wheat, the orientation of the leaves to the light source and the camera angle must be considered in data analysis (Jones *et al.*, 2009).

Drought-induced cessation of growth is an early response to water shortage which is largely under hormonal control (Mahajan & Tuteja, 2005). Drought significantly reduced plant diameter and slowed relative growth rate in Arabidopsis when soil water content had declined to ~ 3% (

Figure 31B-C). However relative growth rate recovered following rewatering (

Figure 31C). In droughted *B. napus* at ~ 24% soil water content relative growth rate was significantly slower in comparison to well-watered plants and it remained slower thereafter (Figure 37C). Plant height and the number of emerged leaves were not significantly affected by drought until soil water content had declined to ~ 5% (Figure 37A-B). Finally, no significant differences in plant height were observed between *T. aestivum* treatments throughout the experiment, although relative growth rate was significantly slower in droughted plants after 18 days of water withholding when the soil water content was ~ 1% (Figure 44A-B). When experiencing moderate water scarcity plants will partition resources away from growth and into acclimation responses in order to maintain cellular integrity, such as the synthesis of osmolytes (e.g. glycine betaine) and protective proteins (e.g. late embryogenesis abundant proteins) (Zhu, 2002; Chaves & Oliveira, 2004). Providing the drought does not cause terminal damage, viable parts of the plant will resume growth upon rewatering. To investigate the effect of a moderate drought on Arabidopsis yield, plants were recovered and seed was harvested. Drought had no significant impact on the aerial dry weight, seed yield, seed weight or viability (Figure 32A-D). This indicates that either the drought was not severe enough to irreversibly reduce yield and that plants had enough time to recover between rewatering and harvest, or that growth does not determine yield. However seed yield in Arabidopsis has been shown to be under genetic and hormonal control, which are both influenced by growth and stress (Van Daele *et al.*, 2012). Seed size is a consequence of the growth of zygotic tissues and the seed coat, processes which are genetically controlled and have several specific

regulators (Sun *et al.*, 2010). Any stress that results in the modification of the expression of these regulators may affect seed size. Seed number, which can be negatively correlated with size, has been shown to be dependent on inflorescence architecture (Alonso-Blanco *et al.*, 1999). Arabidopsis mutants which had an increased number of branches and siliques also had higher seed numbers (Choe *et al.*, 2001). Measurements of yield are complicated in Arabidopsis by the indeterminate nature of the inflorescence meaning comparisons between plants of different treatments can be difficult due to the large potential variation within treatments (Benlloch *et al.*, 2007).

With regard to experimental design, and with the application of hindsight, the arbitrary selection of > 90% soil water content for the well-watered condition should be revised in any future work. Such high soil water content could result in waterlogging and in plants experiencing anoxia, which would mean two stressed conditions were compared. Future approaches should evaluate this potential problem.

This work aimed to use non-invasive imaging techniques to identify early-onset, reproducible indicators of drought stress. In all of three species tested, ΦPSII after 5 min of high induction became significantly lower in droughted plants. The reduction in ΦPSII coincided with soil water content, appearing at ~ 20% in the dicot species and at ~ 7% in *T. aestivum*. This rapidly-obtainable indicator has a sampling time of 10 min which facilitated high replication. This is in contrast to steady-state photosynthetic measurements which either took longer to generate, were uninformative, or both. Leaf temperature was also indicative of drought stress but these measurements take longer to acquire and can be fraught with technical difficulties. Growth rate was reduced by drought before any effect on growth appeared in the phenotype. Although growth parameters are relatively easy to determine they do not provide any information on the underlying physiology of drought. In summary, a short 10 min fluorescence protocol is sensitive enough to detect drought-induced perturbations to physiology when soil water content declines to species-specific thresholds.

Chapter 3

3. The impact of PARP inhibitors on photosynthesis and growth

3.1. Introduction

Among other activities poly (ADP-ribose) polymerases (PARPs) recognise and bind to breaks in DNA and have therefore been implicated in plant abiotic stress response (Briggs & Bent, 2011; Schulz *et al.*, 2012). Stress-induced upregulation of the synthesis and activity of this enzyme group leads to a number of cellular consequences that are considered undesirable in an agricultural context. For example, PARP activity leads to metabolite depletion (e.g. ATP and NAD^+), mitochondrial overrespiration and changes in stress-responsive gene expression. All of these processes reduce the resources available for growth and ultimately, yield. It was hypothesised that a reduction of stress-induced PARP activity would mean plants were better able to maintain energy homeostasis and growth under stress (Block *et al.*, 2004). Accordingly, research into methods which reduce or inhibit the production and activity of PARPs has increased over the last two decades.

Several studies have reported the successful downregulation or inhibition of PARP activity using genetic or chemical methods. Chemical PARP inhibition has an advantage over genetic approaches given the current preventative legislation that exists across the European continent. PARP inhibitor compounds target the conserved enzymatic active site thus overcoming the functional redundancy encountered in studies using genetic knock-out and knock-down technologies due to the presence of multiple *PARP* genes (Briggs & Bent, 2011). Although a substantial body of literature exists on the use of PARP inhibitors in animals, there have been relatively few publications detailing the effects in plants. Table 3 lists four studies in which three compounds have shown PARP inhibition activity in plants.

Results from these studies have built a consensus on how PARP inhibition enhances stress tolerance and maintains growth under stress. Amor *et al.*, (1998) showed that the extent of H_20_2-induced cell death was reduced in soybean cultures supplemented with PARP inhibitor. They also suggested that PARPs directed cellular response depending on the severity of the incident stress. If following mild stress the damage can be repaired, PARPs will initiate recovery and DNA repair processes. However if the damage is too severe PARPs will initiate cell death.

Table 3. Studies investigating chemical PARP inhibition in plants. 3AB = 3-aminobenzamide, 3MB = 3-methoxybezamide, Nic = nicotinamide, INA = iso-nicotinamide.

PARP inhibitor(s)	**Species**	**Observed effect(s)**	**Reference**
3AB, Nic	*Glycine max*	PARP inhibition reduced oxidative stress-induced cell death in soybean culture cells.	(Amor *et al.*, 1998)
3MB, Nic, INA	*Brassica napus*	Callus regrowth was hardly inhibited by oxidative stress when media was supplemented with 3MB. Nic and INA are weaker inhibitors and had less of a protective effect.	(Block *et al.*, 2004)
3MB	Arabidopsis	Chemical PARP inhibition improved plant growth in response to a variety of abiotic stressors.	(Schulz *et al.*, 2012)
3MB	Arabidopsis	PARP inhibition enhanced growth under unstressed conditions by increasing cell number.	(Schulz *et al.*, 2014)

Block *et al.*, (2004) suggested that plants with reduced poly (ADP-ribosyl)ation were tolerant to multiple abiotic stresses because they were able to maintain cellular energy homeostasis. They postulated that reduced consumption of ATP and NAD^+ avoided excessive mitochondrial respiration and associated ROS generation, increasing energy-use efficiency. The depletion of cellular ATP can trigger the formation of mitochondrial permeability pores through which cell death initiators are released, along with mitochondrial ATPase which exacerbates the initial depletion signal. ROS can damage mitochondria directly and the presence of permeability pores disrupts the electron transport chain and energy generation. It is the combination of high energy consumption and low ATP generation that promotes cell death. The group showed that pharmacological PARP inhibition reduced stress-induced energy consumption, enabled plants to recover from stress injury and reduced the onset of cell death processes. They concluded by suggesting that treatments which reduce PARP activity and maintain energy-use efficiency could be a valuable approach to enhance crop stress tolerance.

More recently in 2012 Schulz *et al.*, showed that chemical PARP inhibition increased growth under unstressed conditions and during short- and long-term stress events. Similarly to Block *et al.*, (2004), they found that in comparison to untreated plants, PARP inhibitor treatment led to increased NAD^+ content and increased ΦPSII (operating efficiency of photosystem II) and *q*P (proportion of absorbed light used in photochemical quenching), supporting a close link between PARP activity and photosynthesis hypothesised by Arena *et al.*, (2011). However, this hypothesis needs to be treated with caution because the increases in ΦPSII and *q*P were recorded from control (unstressed) plants treated with PARP inhibitor, not recorded from plants under the stressed condition. They also reported that oxidative stressed plants treated with PARP inhibitor had significantly lower NPQ, although this may not be a desirable response as will be discussed later. The group concluded by proposing PARPs are central regulators of photosynthesis, energy and redox homeostasis, and metabolism.

In 2014 Schulz *et al.*, showed that PARP inhibitor application enhanced the growth of hydroponically grown Arabidopsis plants under non-stressed conditions. They reported that 3MB treated plants had significantly higher fresh weight and shoot and root biomass (Figure 46A-D). They suggested the increased growth was a consequence of increased cell number resulting from a shortening of the cell cycle and more cell division. As a technical consideration hydroponic systems are prone to contamination and hypoxia so may not always represent unstressed conditions (Conn *et al.*, 2013; Alatorre-Cobos *et al.*, 2014). They concluded that PARP activity regulates the cell cycle, gene expression, redox and energy homeostasis, and primary and secondary metabolism. The group went on to say that PARPs are a prominent player in growth regulation prompting the suggestion that the enzymes are a target for the biotechnological modulation of plant growth.

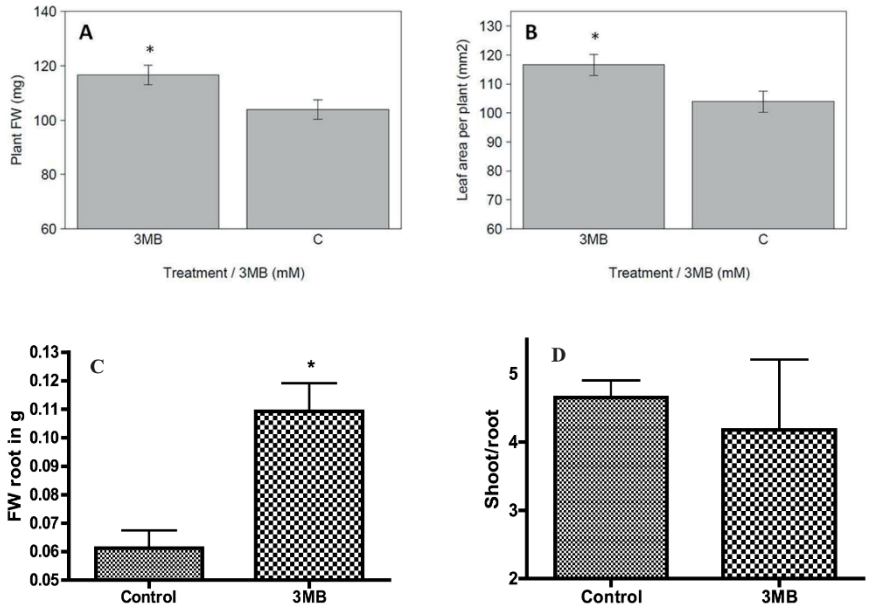

Figure 46. (A) Fresh weight, (B) shoot and (C) root biomass, and (D) the shoot/root ratio of hydroponically grown Arabidopsis plants treated with either 3-methoxybenzamide (0.2 mM 3MB) or DMSO (125 µL, control). Measurements for (A) were made after 26 days of growth. For (B), (C) and (D) plants were harvested after 30 days. * denotes statistically significant difference between control and treated plants ($P < 0.05$). Values are the mean (n=18) ± SE. Taken from Schulz *et al*., (2014)

Plants have evolved to survive in natural ecosystems and not in agricultural environments. Growth inhibition during severe stress will enhance a plants chances of survival but during periods of mild or moderate stress this response will limit a plants yield potential, which is undesirable in a crop context (Skirycz & Inzé, 2010). From an agricultural perspective agents that improve growth under drought stress have potential in crop protection strategies. In this manner PARP inhibitors provide a potential route to enhancing growth and yield under stress.

The studies discussed here are not without their limitations however. For example, in all of the experiments detailed in Table 3 chemical inhibitors were applied to cultured cell suspensions or growth media. Neither of these conditions are representative of how a crop plant might react to stress in the field and so claims of the potential for enhanced crop growth and yield are without sufficient foundation. Additionally, the techniques used in some of these studies were destructive, so stress response and inhibitor impact can only be quantified at one time point per sample. Subsequently there was a requirement to study the effects of PARP inhibitor

application *in planta*. Work in this chapter used the chlorophyll fluorescence imaging and growth analysis protocols developed in the previous chapter to quantify the impacts of drought stress and inhibitor application. Furthermore, recent advances in novel synthesis methods have led to the design and engineering of a new suite of inhibitors which are thought to be more plant specific than the classically used compounds, although many of them are yet to be tested *in planta* (Briggs & Bent, 2011). This work used a novel PARP inhibitor 2TBC as well as the classically used 3-methoxybenzamide (3MB; Figure 47).

3.1.1. Aims and objectives

- Apply a drought to *A. thaliana* and *B. napus* and monitor the progression by measuring pot weight as a proxy for soil water content.
- Assess the impact of the PARP inhibitors 2TBC and 3MB:
    - Determine if PARP inhibitor application increased survival in response to severe drought.
    - Use the chlorophyll fluorescence protocols defined in the previous chapter to quantify the impact of drought and inhibitor treatment on photosynthesis.
    - Measure parameters such as relative growth rate, rate of leaf emergence, rosette area and leaf number to quantify the effects of the stress and the compounds on growth and development.
    - Quantify the impact of a sub-lethal drought and PARP inhibitors on seed yield in Arabidopsis.

3.2. Materials and Methods

3.2.1. Plant material

Seeds of *Arabidopsis thaliana* ecotype Columbia (Col-0) were cold stratified for 4 days and grown in individual pots (6 cm diameter; LBS Horticulture; UK) for 14 days before measurements began (14 days after sowing). *Brassica napus* (Temple; Elsoms; UK) seeds were germinated over 4 days on wet filter paper in Petri dishes and transplanted into individual pots (10 x 10 x 10cm; LBS Horticulture; UK) and grown for 14 days before measurements started (18 days after sowing). All plants were grown in a peat based soil containing a 3:1 mix of M3 compost (Levington; UK) and sand. Germination and growth occurred in a controlled environment chamber with an irradiance of 150 µmol m^{-2} s^{-1} during a 10/14 hour day/night photoperiod at 22 °C with a relative humidity of 40%. When in the growth chamber plants were moved daily to minimise the effects of light gradients.

3.2.2. Drought treatment

All plants were watered daily throughout germination and growth. Following the indicated periods of growth, water was withheld from droughted plants and this time point was defined as day 0. Well-watered plants received water every 2 days. Drought severity was quantified by calculating the % soil water content where saturated pot = 100% and oven-dried soil = 0%.

3.2.3. Compound selection and application

Two PARP inhibitors were selected including 2TBC which had shown positive results in preliminary field trials conducted by the industrial partner Bayer Crop Science who supplied the compound. Additionally, the established PARP inhibitor 3-methoxybenzamide (3MB; Figure 47) was used for comparison (Sigma; USA). Stock solutions of 2TBC were prepared by dissolving 0.032 g in 3.6 ml acetone and 400 µl

dimethyl sulfoxide (DMSO). The resulting solution was added to 394 ml of deionised water and 2 ml of the adjuvant rapeseed oil methyl-ester (MERO; Bayer Crop Science; Germany), giving a solution with a final concentration of 364 µM 2TBC. Acetone and DMSO were supplied by Sigma (USA). Stock solutions of 3MB were prepared by dissolving 0.055 g in 9 µl acetone and 1 µl DMSO. This solution was added to 975 ml of deionised water and 5.5 ml MERO, giving a solution with a final 3MB concentration of 364 µM. In both cases stock solutions were diluted to give solutions of lower concentrations where necessary. Compounds were sprayed to run-off once using handheld sprayers (LBS Horticulture; UK). Mock treatments were performed which contained the solvents used to dissolve 2TBC or 3MB but no inhibitor. Untreated plants were unsprayed.

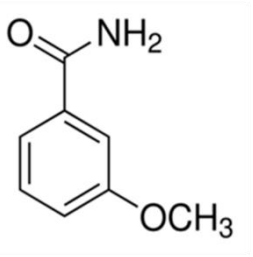

Figure 47. Chemical structure of 3-methoxybenzamide (3MB). The structure of 2TBC cannot be provided.

3.2.4. Chlorophyll fluorescence imaging

Chlorophyll fluorescence imaging was carried out using the equipment and technical considerations outlined in Chapter 2.2.3, although a shorter protocol was used. Plants were dark adapted for 5 min before an F_v/F_m measurement was recorded and induction parameters were measured for 5 min at high actinic light (400 µmol PAR m^{-2} s^{-1}). F_v/F_m, ΦPSII and NPQ were measured along with ΦNO, which describes the quantum yield of non-regulated energy dissipation.

3.2.5. Leaf gas exchange measurements

Gas exchange was measured using a LI-6400-40 gas analyser with a leaf chamber fluorometer (Licor; USA). Measurements took place 15 days after withholding water (day 15; 33 days after sowing) on the top-most expanded true leaf, which was leaf three or four in all cases. The parameters ΦPSII, stomatal conductance and net assimilation were recorded. Following 5 min dark adaption data were collected during 18 min induction at high light with 400 µmol mol^{-1} CO_2, 22 °C leaf temperature and ~ 50% relative humidity.

3.2.6. Growth and yield analyses

For analyses of Arabidopsis, rosette area was measured using digital images (Canon EOS REBEL T1i/EOS 500D; Japan) and imageJ software (ImageJ; USA). Relative growth rate was calculated, RGR = $(size_{time2} - size_{time1}) \div (time_2 - time_1)$. For yield calculations seed were harvested when the plants were mature and the last siliques on the inflorescence had dried and were ready to dehisce. Seed were harvested and dried for > 4 weeks in airtight containers with silica beads before weighing. The height of *B. napus* plants, from the soil surface to the highest point of the highest leaf, was measured using a ruler. The number of emerged leaves for both species was counted and did not include cotyledons.

3.2.7. Statistical analyses

Minitab was used to perform statistical analyses such as Student t-tests and one-way ANOVAs. Data were tested for equal variance. For ANOVAs Tukey's or Dunnet's multiple comparisons tests were used when variances were equal and Games-Howell was used when variances were unequal (Minitab, Inc; USA). GraphPad Prism 7 software was used to construct graphs and charts (GraphPad Software, Inc; USA).

3.3. Results

3.3.1. The impact of PARP inhibitors on photosynthesis and growth in *Arabidopsis thaliana*

Studies have demonstrated that chemical PARP inhibition enhances *in vitro* plant growth under stress, but relatively little work has investigated the effects on photosynthesis. The following experiments aimed to use the protocols defined in Chapter 2 to assess the effects of PARP inhibitors on physiology and growth, rapidly and reproducibly. In the following experiments Arabidopsis plants were sown and grown for 14 days in individual pots after which water was withheld from droughted plants (day 0 = 14 days after sowing). Well-watered plants were watered every 2 days throughout. Drought progression was determined by calculating soil water content as in Chapter 2.

A preliminary experiment was performed to assess plant survival in response to critical drought stress and PARP inhibitor application. Water was withheld for 15 days before droughted plants were rewatered and F_v/F_m was measured 7 days later to assess viability. To determine the impact of a PARP inhibitor, 2TBC was applied to run-off when the soil water content had declined to ~ 35%, 6 days after water withholding. Plants were treated with either 36.4 µM or 364 µM 2TBC to assess the impact of different inhibitor concentrations. Mock treatments were performed using solutions which contained the solvents used to dissolve 2TBC but no inhibitor. Untreated plants were unsprayed. Figure 48 shows images of plants 7 days post-rewatering and Table 2 **Error! Reference source not found.** lists average F_v/F_m values of surviving plants. All well-watered plants survived although spraying with 364 µM 2TBC reduced growth. All unsprayed droughted plants failed to recover after rewatering (F_v/F_m = 0). In contrast, spraying increased survival with 50% of the mock treatment (F_v/F_m = 0.8) and 100% of the 364 µM 2TBC treatment surviving (F_v/F_m = 0.79). These findings indicated that 2TBC application enhanced survival under stress but led to a growth penalty under well-watered conditions.

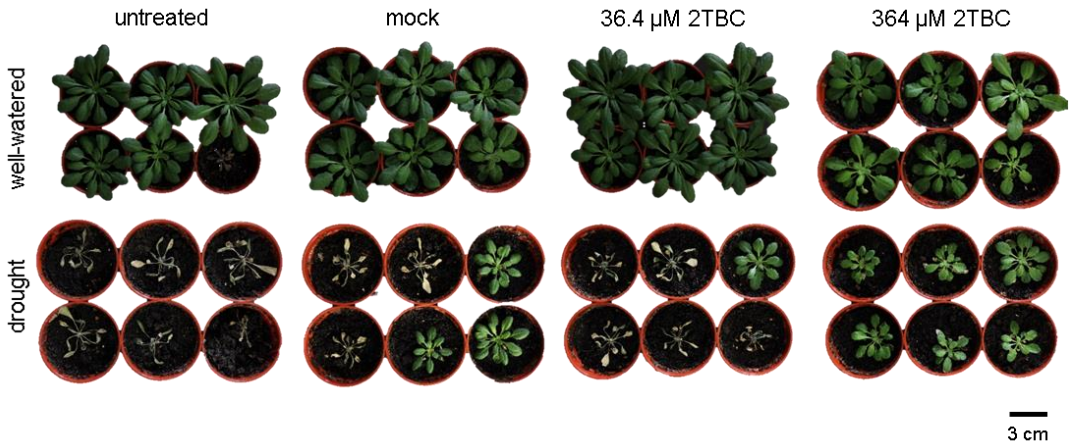

Figure 48. Pictures of Arabidopsis taken 7 days after droughted plants were rewatered following 15 days of water withholding. Treatments were applied to run-off after 6 days of withholding water.

Table 2. % survival of plants 7 days after rewatering of droughted plants following 15 days of water withholding. Percentages are of six replicates per treatment. F_v/F_m values are averages of surviving plants only ($F_v/F_m > 0$).

Treatment → / **↓ Irrigation**		Untreated	Mock	36.4 µM 2TBC	364 µM 2TBC
Well-watered	Survival (%)	100	100	100	100
	Ave. F_v/F_m	0.80	0.81	0.81	0.82
Drought	Survival (%)	0	50	17	100
	Ave. F_v/F_m	-	0.80	0.81	0.79

The aim of the following experiment was to investigate how PARP inhibitor application affected physiology and growth, particularly under drought conditions. Data from Chapter 2 indicated that significant drought-induced changes in photosynthetic induction kinetics were reproducibly observed during the first 2-5 min of illumination in Arabidopsis and *B. napus*. To increase replication fluorescence protocols were shortened to 5 min dark-adaption followed by 5 min high light (400 µmol m^{-2} s^{-1}) induction. Water was withheld from droughted plants 14 days after sowing (day 0). Plants were untreated or sprayed to run-off with either mock solution, 36.4 µM 2TBC or 364 µM 2TBC, 6 days after water withholding when soil

water content had declined to ~ 35% in droughted samples. To assess the impact of 2TBC application photosynthetic parameters were measured at intervals. To investigate if 2TBC affected growth either under drought or during recovery, droughted plants were rewatered after 15 days and growth parameters were measured throughout.

Figure 49 shows how drought developed as the experiment proceeded. Whereas soil water content was > 80% in all well-watered plants throughout, it declined exponentially in droughted samples to ~ 20% after 8 days of water withholding and < 5% after 15 days. Droughted plants were rewatered on day 15 and thereafter until the experiment's conclusion. Interestingly, relative to untreated plants the soil water content values of mock treated and 36.4 µM and 364 µM 2TBC treated plants were significantly higher on day 8 ($P < 0.05$, one-way ANOVA with Dunnett's multiple comparisons test) (Figure 49; Figure 50A-D). This might indicate that the application solutions were supplying additional water to plants.

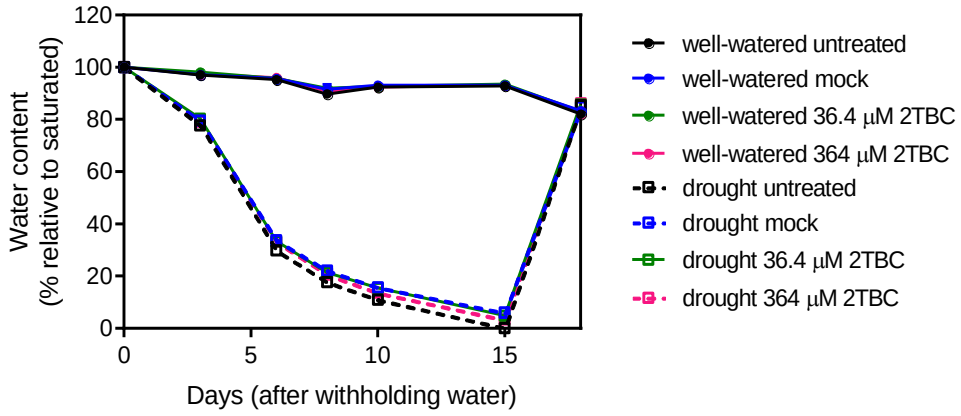

Figure 49. Changes in soil water content in well-watered (closed symbols) and droughted (open symbols) treatments. Water was withheld from droughted plants on day 0 and samples were rewatered after 15 days (green arrow). Values are the mean (n=4) ± SE.

The initial rapid rise in ΦPSII was complete in well-watered plants after ~ 3 min (Figure 50A-D). Drought reduced the rate of ΦPSII induction when soil water content declined to ~ 20%. There was no additional impact of treatment with mock solution or 36.4 µM 2TBC in either well-watered or droughted plants, however spraying with

364 µM 2TBC significantly reduced ΦPSII and exacerbated the impact of drought (Figure 50A-D; Figure 53A). NPQ mirrored ΦPSII such that drought induced a sustained period of elevated NPQ, except in the 2TBC treated plants which had low NPQ throughout (Figure 51A-D; Figure 53B). Low values of ΦPSII and NPQ were accompanied by relatively high values of ΦNO in 364 µM 2TBC treated plants in comparison to plants of all other treatments (Figure 52A-D; Figure 53C). Additionally, this treatment reduced F_v/F_m to 0.58 and 0.39 in well-watered and droughted plants respectively, suggesting that this concentration of PARP inhibitor was potentially damaging (Figure 53D). The effects of chemical treatments on leaf tissue are shown in Figure 54. Whereas the untreated and mock treated plants appeared healthy, those treated with 2TBC had chlorotic spots.

Well-watered plants of all treatments were of a similar size at each time point, except those sprayed with 364 µM 2TBC which were significantly smaller after 10 days and thereafter ($P < 0.05$, one-way ANOVA with Tukey's multiple comparisons test; Figure 55A-D). In comparison to well-watered samples, rosette area was significantly smaller in the droughted plants after ~ 10 days of water withholding but there was no additional effect of any chemical treatment. On average droughted plants had fewer leaves than well-watered plants after 15 days but no significant differences were observed prior to this (Figure 56A-D). Treatment did not significantly impact leaf number until day 15 when well-watered and droughted plants sprayed with 364 µM 2TBC had fewer leaves than the corresponding unsprayed samples. In contrast to the considerable changes in physiology observed after 8 days in plants treated with the higher concentration of 2TBC, measurements of area and leaf number did not differ until some time after. In comparison to untreated plants treatment with 364 µM 2TBC significantly reduced relative growth rate ($P < 0.05$, one-way ANOVA with Dunnett's multiple comparisons test; Figure 57A). In well-watered plants the reduction was observed between days 8 and 10, whereas in droughted samples it was from day 10 onwards. No other treatment had a significant impact on relative growth rate. Significant reductions in the rate of leaf emergence for 364 µM 2TBC treated well-watered plants were observed from day 10 onwards and in droughted

plants on day 22 ($P < 0.05$, one-way ANOVA with Dunnett's multiple comparisons test; Figure 57B).

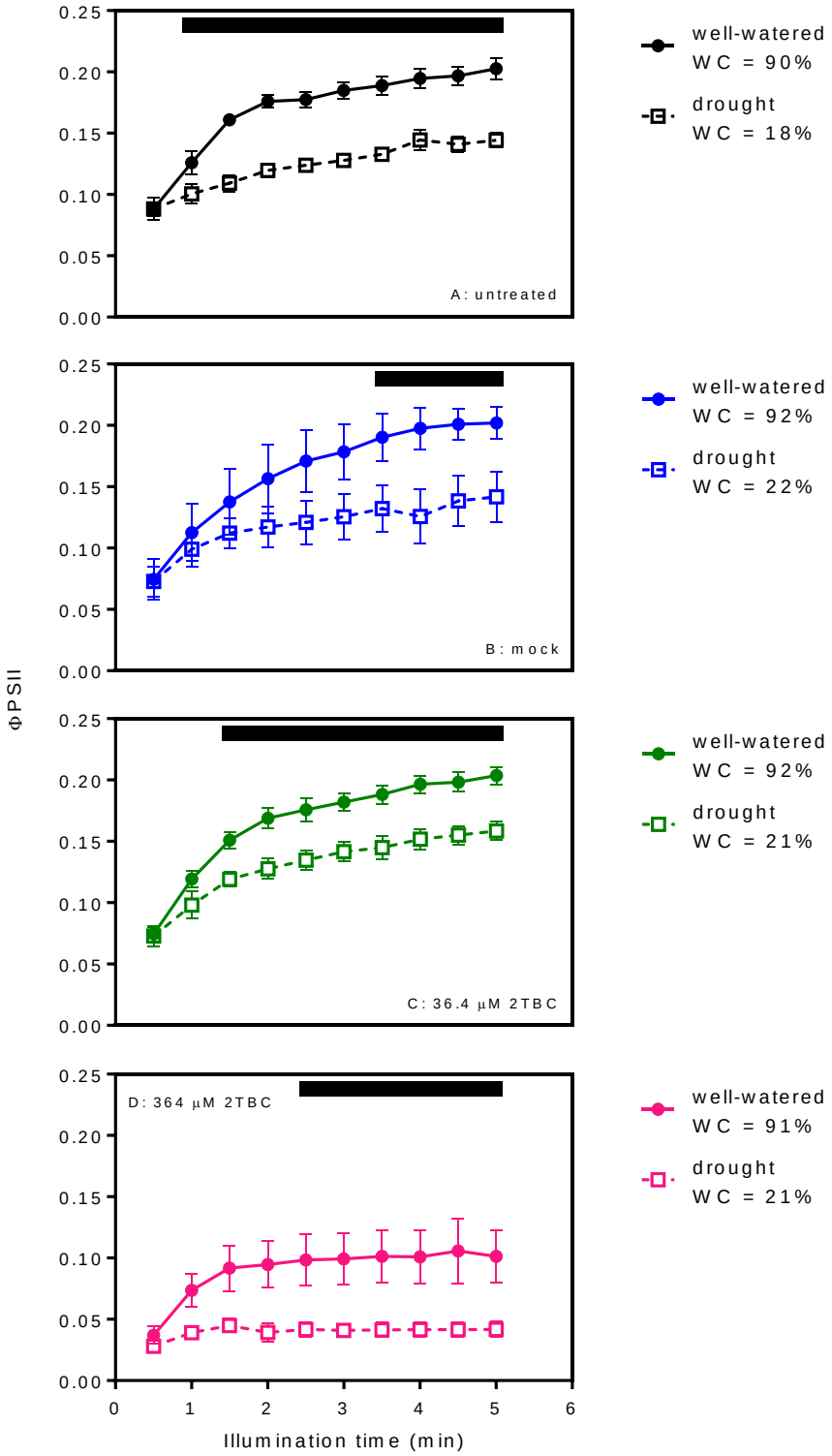

Figure 50A-D. Induction ΦPSII in well-watered (closed symbols) and droughted (open symbols) plants colour coded by treatment (A-D). Measurements were made 8 days after water withholding. WC = soil water content. Black blocks indicate significance between well-watered and droughted data points, $P < 0.05$, Students t-test. Data are means (n=4) ± SE.

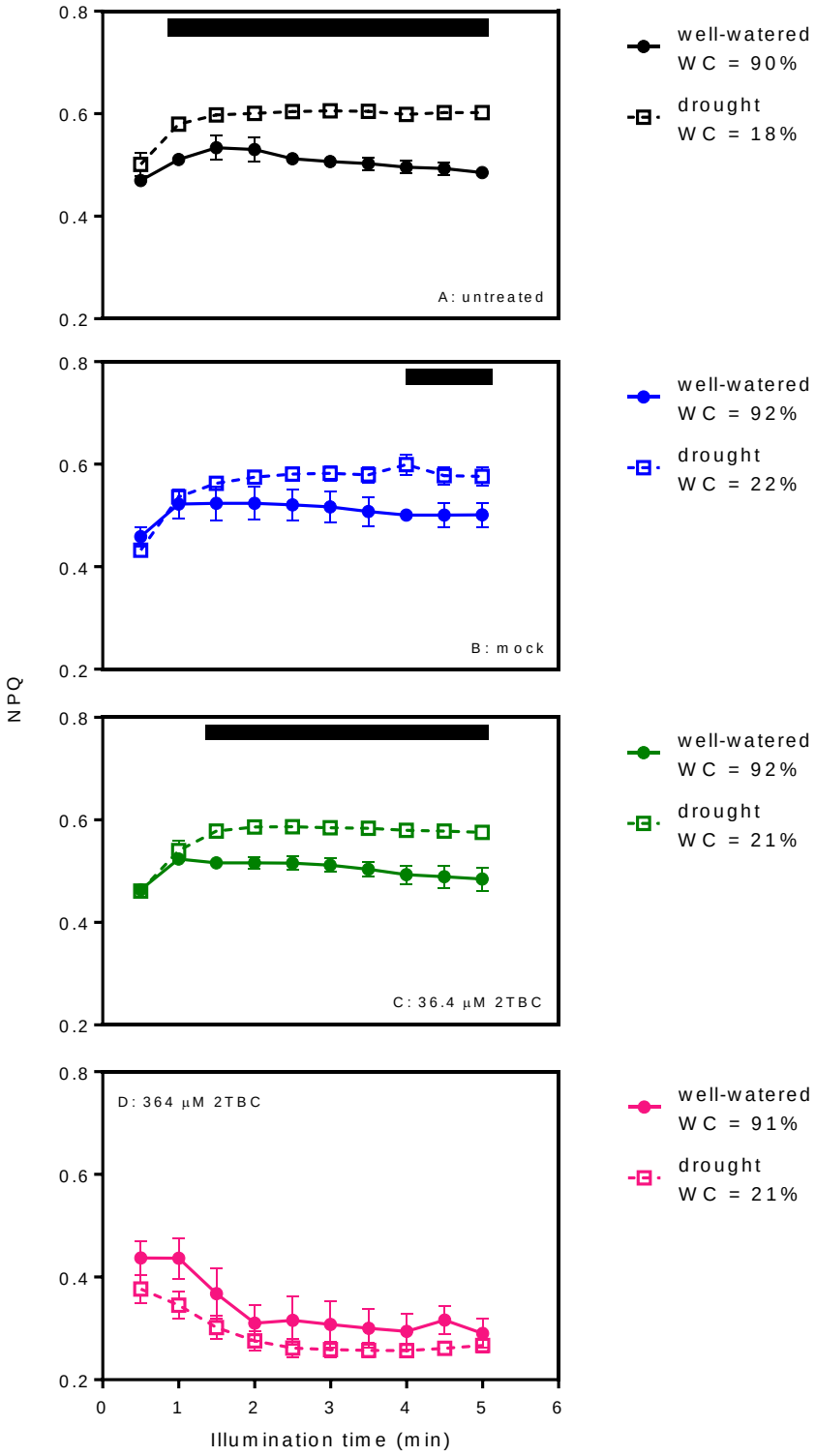

Figure 51A-D. Complementary NPQ data to Figure 50A-D in well-watered (closed symbols) and droughted (open symbols) plants colour coded by treatment (A-D). WC = soil water content. Black blocks indicate significance between well-watered and droughted data points, $P < 0.05$, Students t-test. Data are means (n=4) ± SE.

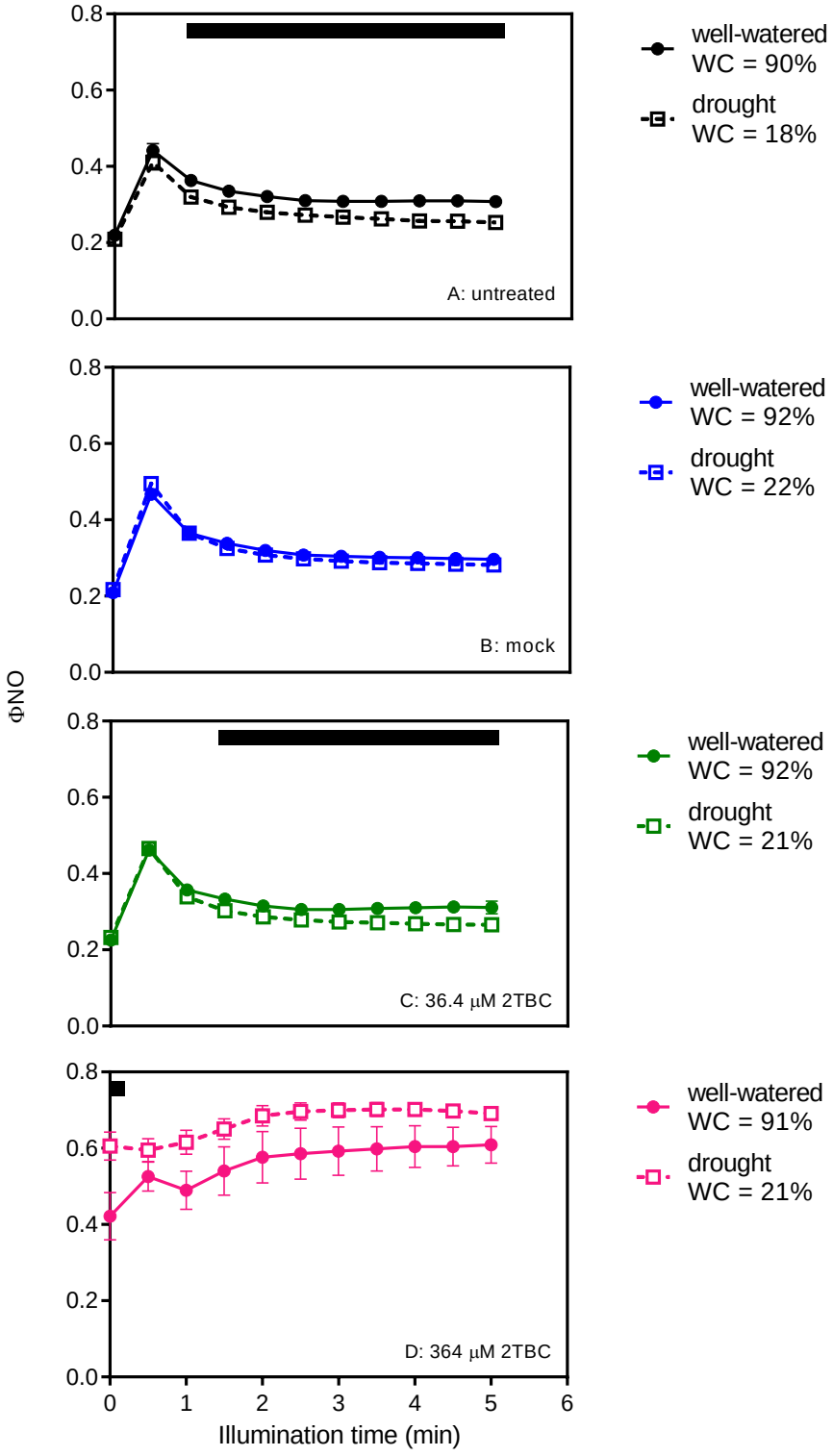

Figure 52A-D. Complementary ΦNO data to Figure 50A-D and Figure 51A-D. Well-watered (closed symbols) and droughted (open symbols) data are colour coded by treatment (A-D). Black blocks indicate significance between well-watered and droughted data points, $P < 0.05$, Students t-test. Data are means (n=4) ± SE.

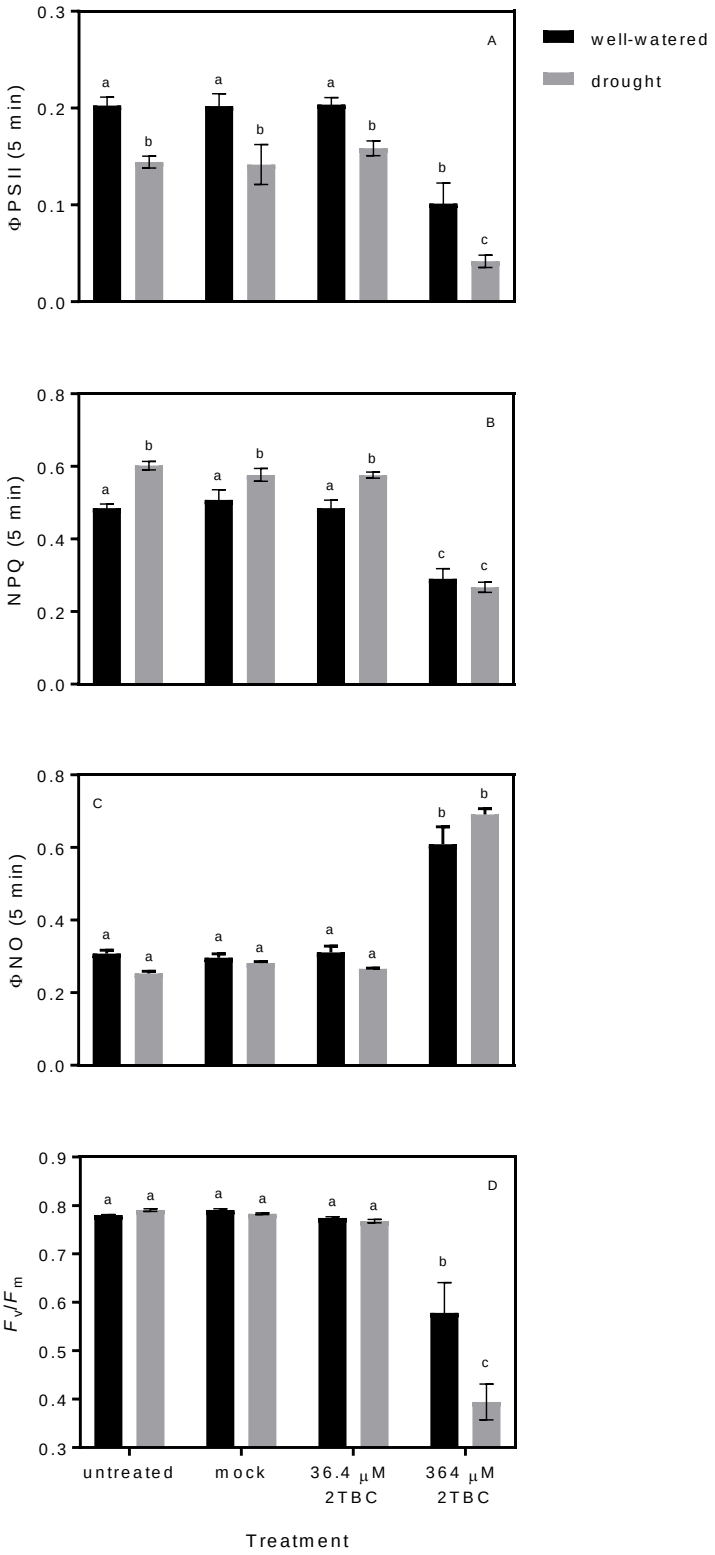

Figure 53A-D. (A) ΦPSII, (B) NPQ, (C) ΦNO measured after 5 min of induction, and (D) F_v/F_m measured 8 days after withholding water from droughted plants. Different letters indicate statistically significant differences, $P < 0.05$, one-way ANOVA with Tukey's multiple comparisons test. Values are the mean (n=4) ± SE.

Figure 54. Pictures of the effects of 2TBC taken 2 days after treatment. Untreated plants were unsprayed, mock solution contained solvents and adjuvant but no inhibitor, 2TBC = mock solution + PARP inhibitor. Images were representative.

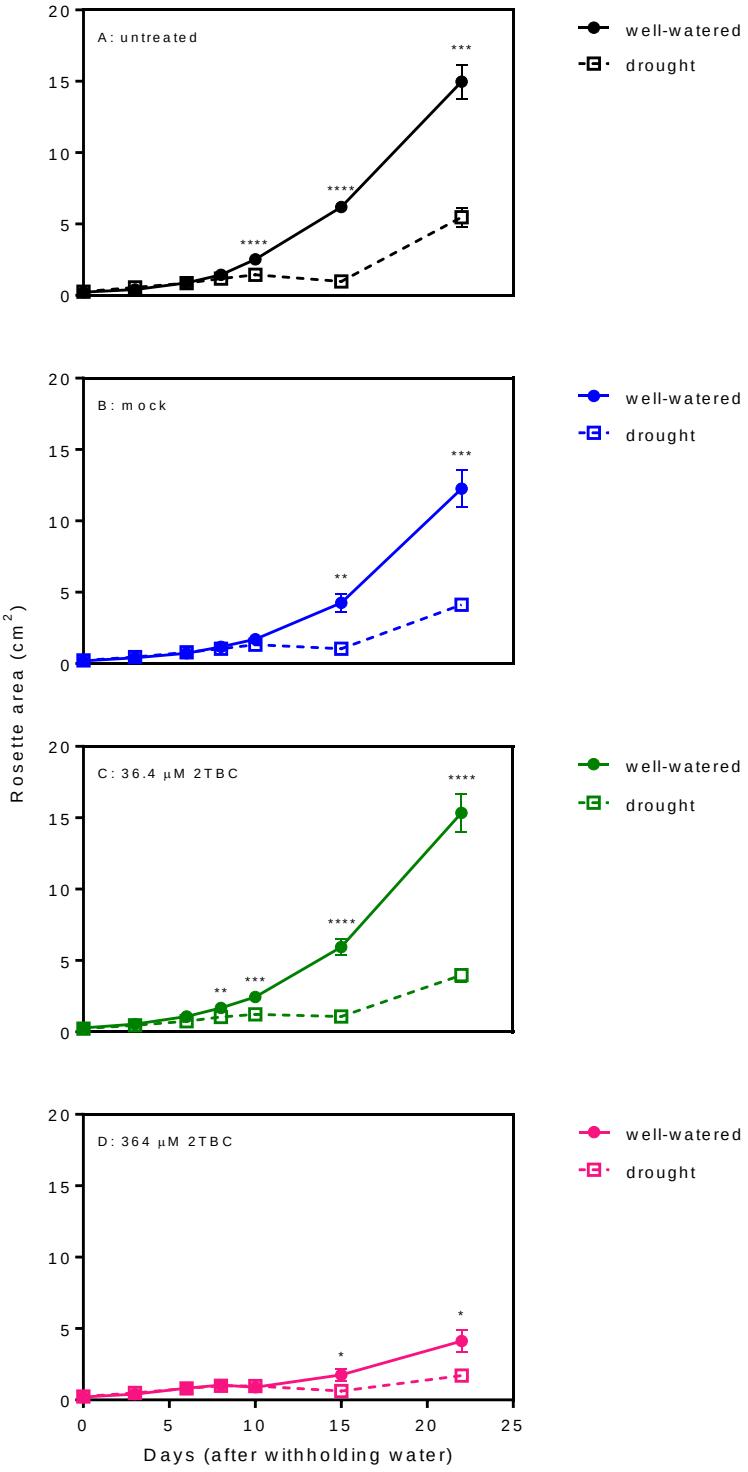

Figure 55A-D. Changes in rosette area in well-watered (closed symbols) and droughted (open symbols) plants colour coded by treatment (A-D). Water was withheld from droughted plants on day 0 until they were rewatered after 15 days. * = P < 0.05, ** = P < 0.005, *** = P < 0.0005, **** = P < 0.0001, denotes significance between well-watered and droughted plants of the same treatment, Students t-test. Values are the mean (n=6) ± SE.

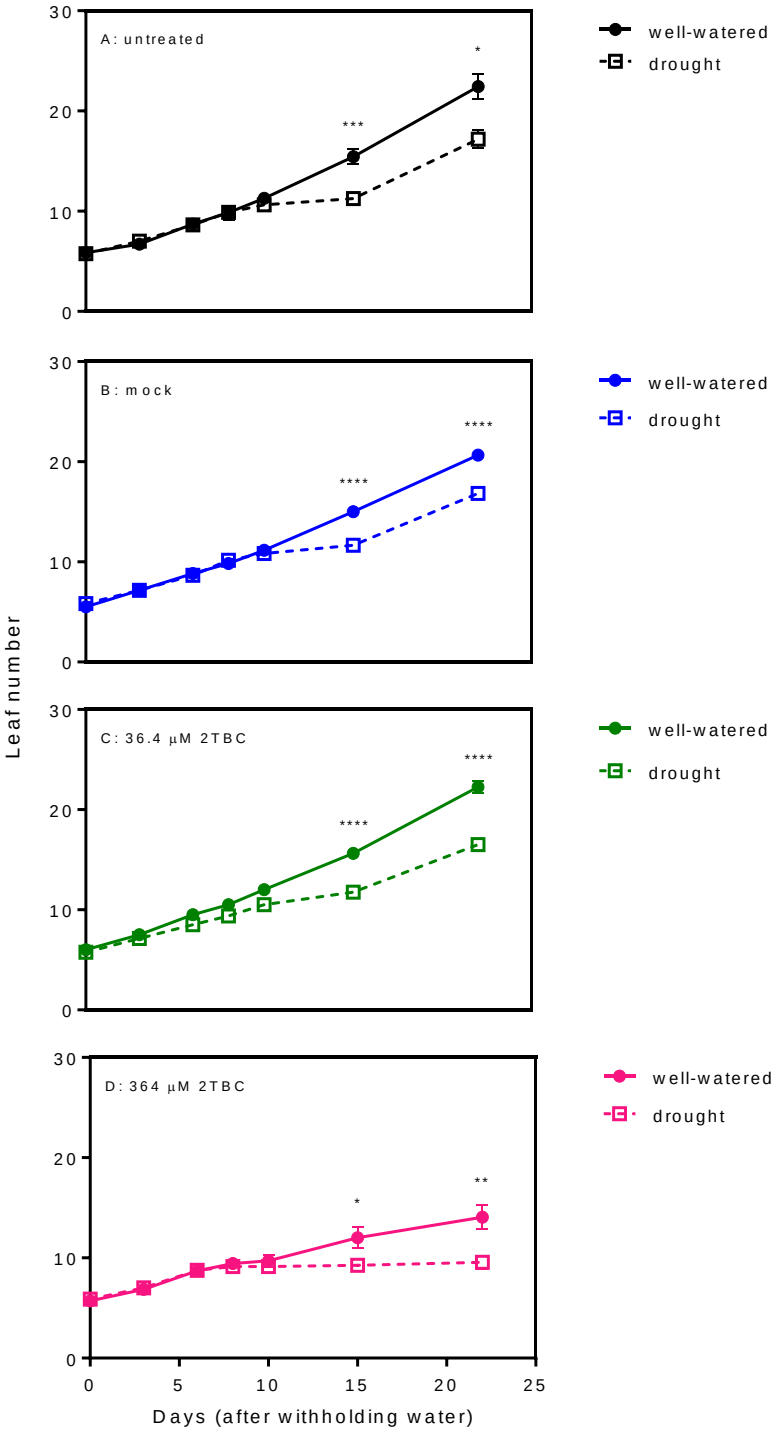

Figure 56A-D. Changes in leaf number in well-watered (closed symbols) and droughted (open symbols) plants colour coded by treatment (A-D). Water was withheld from droughted plants on day 0 until they were rewatered after 15 days. * = P < 0.05, ** = P < 0.005, *** = P < 0.0005, **** = P < 0.0001 denotes significance between well-watered and droughted plants of the same treatment, Students t-test. Values are the mean (n=6) ± SE.

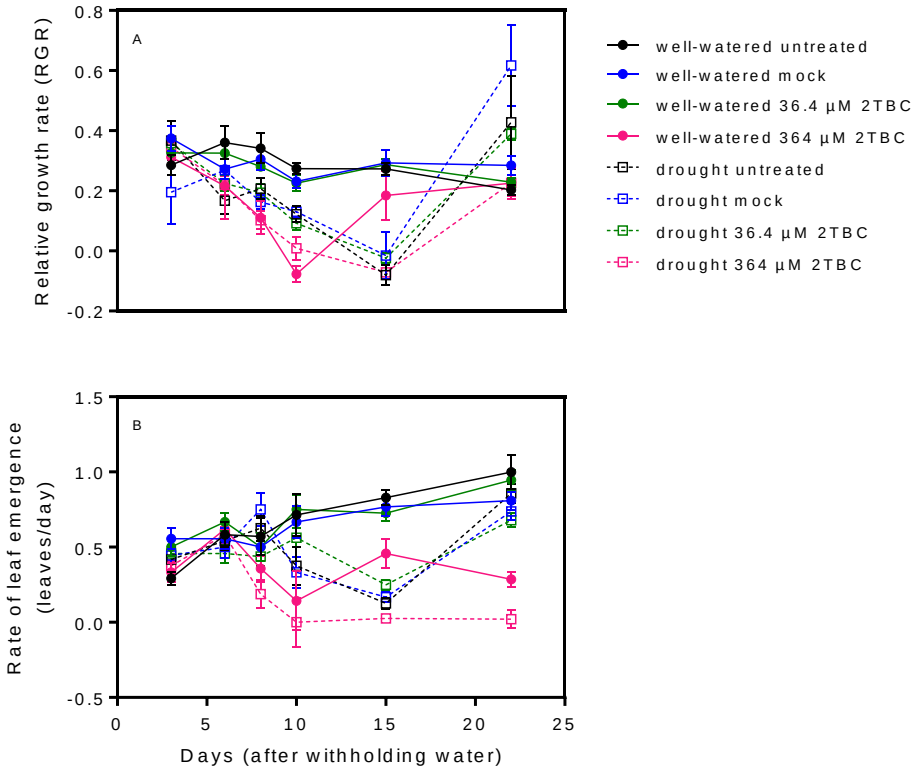

Figure 57A-B. Changes in (A) relative growth rate and (B) rate of leaf emergence in well-watered (closed symbols) and droughted (open symbols) plants colour coded by treatment. Water was withheld from droughted plants on day 0 until they were rewatered after 15 days. Values are the mean (n=6) ± SE.

3.3.2. Determining an effective concentration of 2TBC which protects against drought and does not damage tissue in *A. thaliana*

The previous results suggested that the higher concentration of inhibitor was adversely affecting physiology and growth. A dose response experiment was conducted with the aim of establishing a more suitable working concentration of 2TBC which protected against drought but did not damage leaf tissue. For this experiment, plants were sown and grown as described in 3.3.1 and water was withheld from droughted plants for 15 days before they were rewatered and survival was measured. In addition to untreated samples, mock solution and five concentrations of 2TBC were applied to run-off 6 days after water withholding. Growth was measured at intervals throughout.

Droughted plants were rewatered after 15 days and all plants were then imaged after an additional 7 days to assess viability (Figure 58). All well-watered plants were alive but higher inhibitor concentrations caused growth reductions and leaf yellowing. Those treated with 18.2 or 91 µM 2TBC suffered the mildest growth penalty relative to the untreated samples. All untreated and mock treated droughted plants lost viability and did not recover after rewatering. Those sprayed with either 182 µM or 273 µM 2TBC had a 60% survival rate, although only 20% of the plants treated with 364 µM survived which was a considerably lower percentage than previously observed (Figure 48; Figure 58). In contrast to previous results no concentration of 2TBC conferred 100% survival following rewatering (Figure 48; Figure 58).

Figure 59A-B shows the changes in relative growth rate of plants during the first 12 days of the experiment. Statistical analysis using a one-way ANOVA with Dunnett's multiple comparisons test found no significant difference between any plants prior to the day of application (day 6). By day 10 all plants treated with 182, 273 or 364 µM 2TBC had significantly slower relative growth rates compared to the untreated plants of the same irrigation regime. This remained the case for well-watered plants on day 12. By contrast, there was no difference between untreated and treated droughted plants on day 12 as growth had ceased and samples had begun to desiccate.

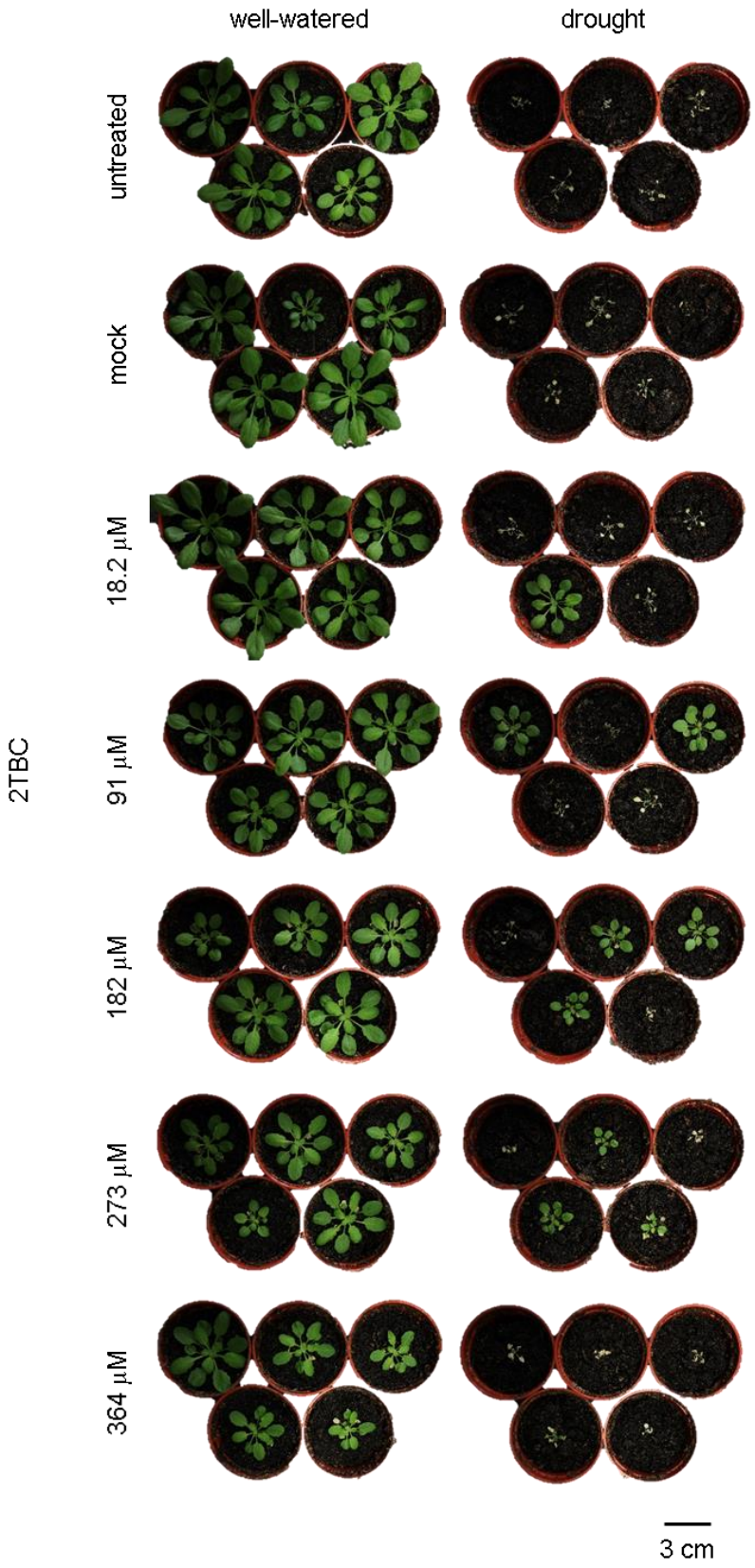

Figure 58. Pictures of plants following a 2TBC dose response. Water was withheld from droughted plants for 15 days before recovery and pictures were taken 7 days after rewatering. Treatments were applied to run-off after 6 days of withholding water.

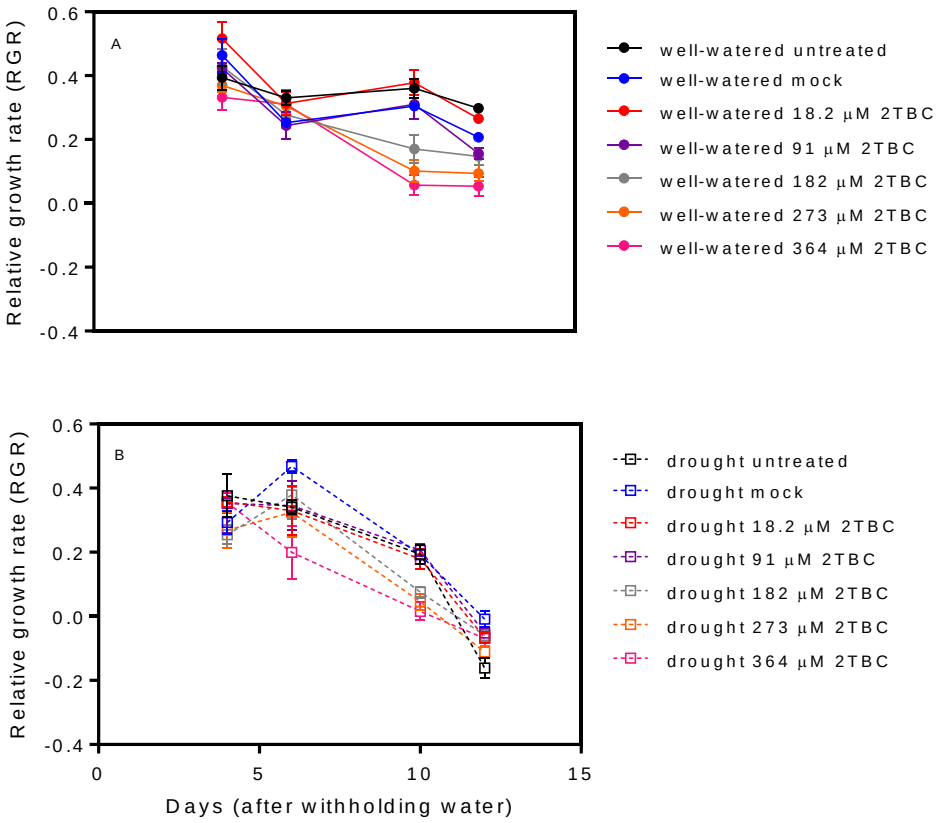

Figure 59A-B. Relative growth rate in (A) well-watered (closed symbols) and (B) droughted (open symbols) plants colour coded by treatment. Water was withheld from droughted plants on day 0. Values are the mean (n=5) ± SE.

The application of 2TBC reproducibly enhanced survival to terminal drought in comparison to untreated samples but there were growth penalties associated with high inhibitor concentrations. For further analysis, 91 µM and 182 µM 2TBC were selected because they increased survival by 60% in comparison to the untreated plants and the growth penalty was less severe than higher concentrations. For the following experiment plants were sown, grown and droughted as described in 3.3.1 and physiological parameters were measured during high light induction when soil water content was ~ 20%. Chemicals were sprayed to run-off at ~ 35% soil water content.

Values of ΦPSII after 5 min of induction were similar for all well-watered plants (Figure 60; Figure 61A). Drought led to a reduction in ΦPSII during induction but there was no additional impact of chemical treatment. NPQ was not significantly changed

as a result of compound application (Figure 61B). There were no significant changes in ΦNO or F_v/F_m in response to drought or chemical treatment, except in droughted samples treated with 91 µM 2TBC where F_v/F_m was reduced (Figure 61C-D).

In comparison to untreated samples, plants sprayed with 91 µM or 182 µM 2TBC had significantly smaller areas after 10 days of water withholding ($P < 0.05$, one-way ANOVA with Dunnett's multiple comparisons test; Figure 62A). Treatment with either concentration of 2TBC led to significantly slower relative growth rates in well-watered plants by day 10 (Figure 62B). No significant differences were observed between well-watered samples before day 10 or between droughted treatments at any point.

All plants were imaged 2 days after spraying to capture the visual impacts of chemical treatment (Figure 63). Untreated and mock treated plants were green and healthy whereas 2TBC treatment led to leaf rolling, yellowing and necrosis. Well-watered and droughted samples were similarly affected by inhibitor treatment suggesting that the 2TBC application solutions were harmful in the concentrations tested.

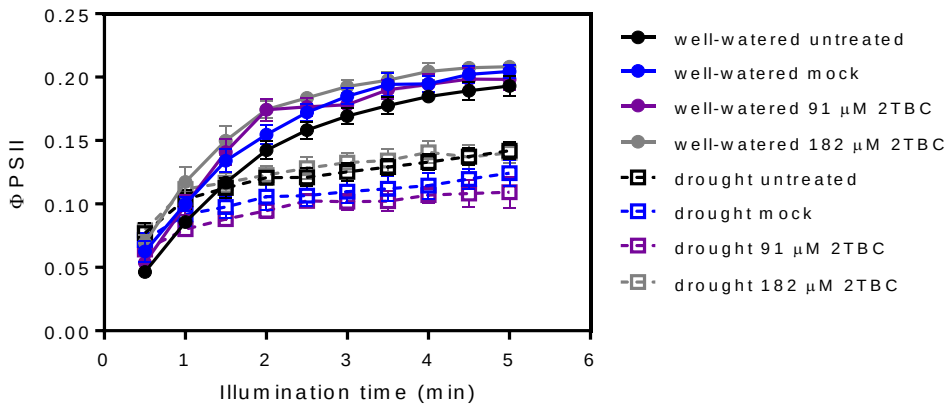

Figure 60. ΦPSII in well-watered (closed symbols) and droughted (open symbols) plants colour coded by treatment. Measurements were taken when soil water content of droughted treatments were ~ 18%. Values are the mean (n=4) ± SE.

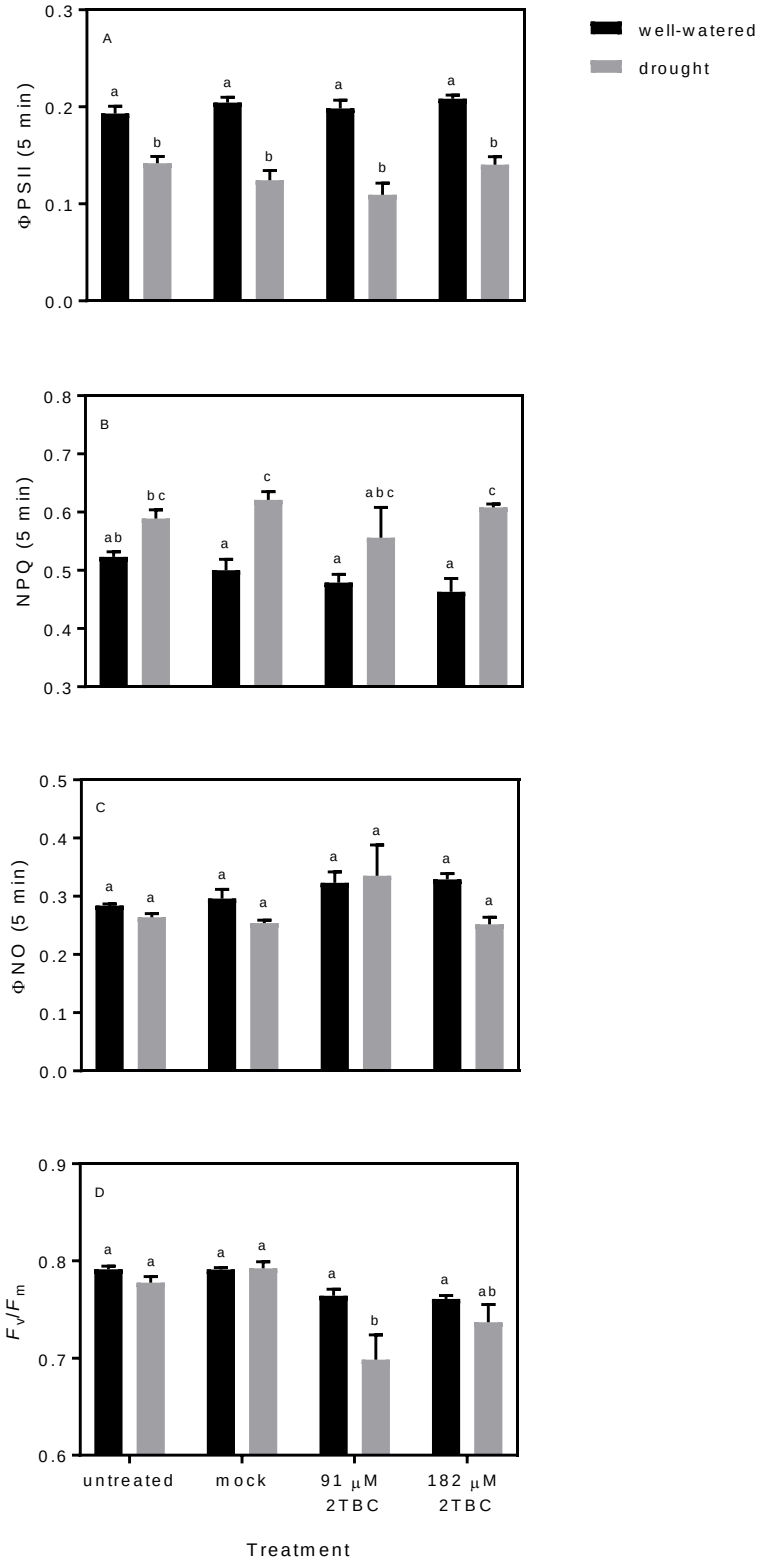

Figure 61A-D. (A) ΦPSII, (B) NPQ and (C) ΦNO measured after 5 min of induction, and (D) F_v/F_m measured 8 days after withholding water from droughted plants. Different letters indicate statistically significant differences, $P < 0.05$, one-way ANOVA with Tukey's multiple comparisons test. Values are the mean (n=4) ± SE.

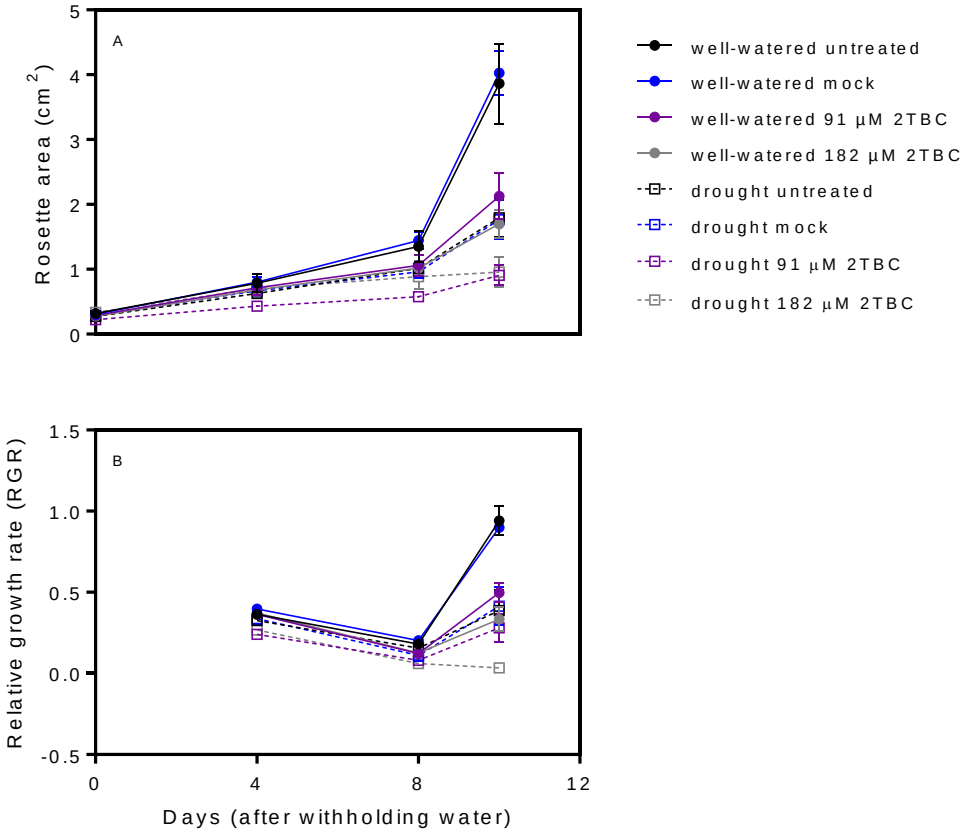

Figure 62A-B. Changes in (A) rosette area and (B) relative growth rate in well-watered (closed symbols) and droughted (open symbols) plants colour coded by treatment. Water was withheld from droughted plants on day 0. Values are the mean (n=4) ± SE.

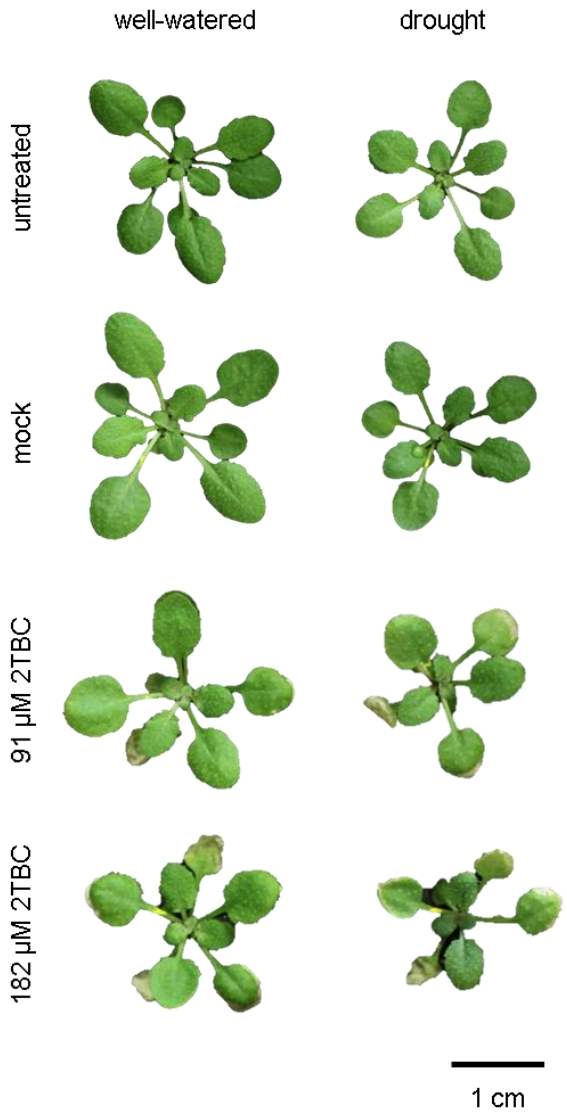

Figure 63. Pictures of the effects of 2TBC taken 2 days after treatment. Untreated plants were unsprayed, mock solution contained solvents and adjuvant but no inhibitor, 2TBC = mock solution + PARP inhibitor. Samples were representative.

3.3.3. The impact of 2TBC on seed yield in *A. thaliana*

Sustained inhibition of growth can cause yield loss. Application of 2TBC reproducibly reduced growth and resulted in tissue damage which could limit yield potential. To assess if 2TBC had any effect on Arabidopsis yield seed was harvested when siliques were ripe. Water was initially withheld from droughted plants 14 days after sowing, for 15 days, until they were rewatered and watered every 2 days subsequently until inflorescence. Plants were treated with 91 µM 2TBC which was selected because of its comparatively mild impact on growth and visual health. The compound was applied to run-off when soil water content had declined to ~ 35% in droughted plants,

6 days after water withholding. Seed from each plant was harvested and dried in airtight containers supplemented with silica beads for > 1 month before weighing.

Following rewatering, only 37.5% of untreated and mock treated plants survived whereas 100% of those treated with 91 µM 2TBC remained viable. Well-watered untreated and mock sprayed plants yielded similar amounts of seed however those treated with inhibitor produced significantly less (Figure 64A; Table 4). Drought had a significant negative impact on seed yield however there was no additional effect of chemical application. Relative to untreated and mock sprayed droughted plants, the larger total seed yield from the 2TBC treated plants was due to more plants surviving the drought period and not as a result of individual plants producing more seed (Figure 64B).

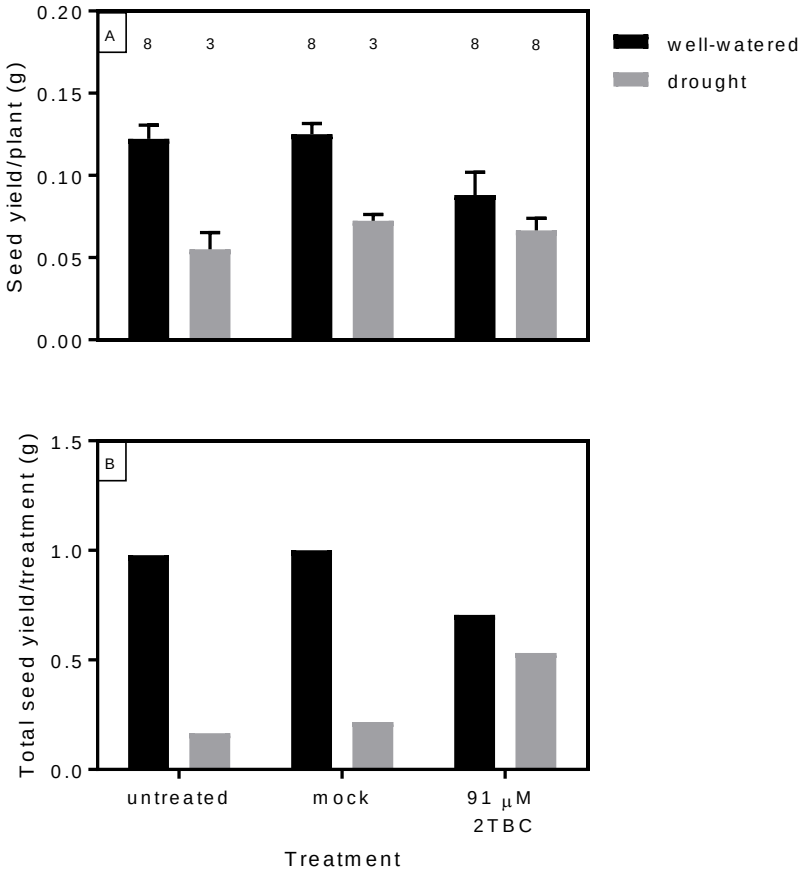

Figure 64A-B. (A) Average seed yield/plant and (B) total seed yield of all plants of each treatment. Plants were droughted for 15 days before rewatering. The numbers above the bars in (A) indicate how many out of 8 replicates of each treatment survived following rewatering. Seed were desiccated before weighing. Statistical results for (A) are shown in Table 4. Values in (A) are the mean (n= the number above each bar) ± SE. Values in (B) are total amounts.

Table 4. Statistical results from the general linear model with interaction term for average seed yield/plant shown in Figure 64A.

Source	DF	Adj SS	Adj MS	F-Value	P-Value
irrigation	1	0.017126	0.017126	26.43	0.000
treatment	2	0.002674	0.001337	2.06	0.144
irrigation*treatment	2	0.003283	0.001641	2.53	0.095
Error	32	0.020732	0.000648		
Total	37	0.047032			

3.3.4. The effect of the PARP inhibitor 3-methoxybenzamide on physiology and growth of *A. thaliana*

The aim of the following experiment was to assess if the impacts of 2TBC on Arabidopsis physiology and growth were common to other PARP inhibitors. Plants were sown and grown for 14 days in individual pots after which water was withheld from droughted plants (day 0 = 14 days after sowing). Well-watered plants received water every 2 days throughout. Treated plants were sprayed to run-off with either mock solution, or 36.4 µM or 364 µM of the PARP inhibitor 3-methoxybenzamide (3MB) - the same concentrations initially tested with 2TBC. Compounds were applied when the soil water content had declined to ~ 35% in droughted plants, 6 days after withholding water. To examine the effect of 3MB on survival to severe stress, droughted plants were rewatered after 15 days of water withholding. Photosynthetic parameters, relative growth rate and the rate of leaf emergence were measured at intervals.

Drought reduced the rate of ΦPSII induction after soil water content had declined to ~ 20%, ~ 8 days after water withholding. At this time point there were no significant differences in soil water content between the different droughted treatments. ΦPSII during induction was similar for all well-watered plants and there was no significant impact of any treatment on values measured 5 min after the onset of illumination (Figure 65A; Figure 66A). All droughted plants had similar ΦPSII values throughout induction also and although induction appeared faster in 364 µM treated samples, this change was non-significant. Corresponding NPQ values also indicated the impact of drought which resulted in significantly elevated NPQ after 5 min, except in 364 µM treated plants where there was no difference between well-watered and droughted plants (Figure 65B; Figure 66B). Figure 65C and Figure 66C show that all plants had similar ΦNO values throughout induction. Additionally, all plants recorded F_v/F_m values between 0.77-0.79 at this time point (Figure 66D).

Drought significantly reduced relative growth rate and the rate of leaf emergence after 15 days of water withholding although both of these parameters recovered in surviving plants following rewatering. Relative to untreated plants there was no

significant impact of 3MB application on relative growth rate or the rate of leaf emergence throughout in either well-watered or droughted plants (Figure 67A-D). Additionally, there was no visual damage resulting from 3MB treatment suggesting the application solution was less damaging than the 2TBC solution (Figure 68). Post-rewatering, 50% of the untreated droughted plants survived (Figure 69). Treatment with mock solution or either concentration of 3MB conferred an enhanced survival rate of 83%. Following rewatering all droughted plants grew at similar rates and there were no significant differences in rosette area or leaf number between treatments, indicating 3MB treatment did not hinder recovery (Figure 67C-D; Figure 70A-B). All well-watered plants had comparable rosette areas and leaf numbers at the end of the experiment (Figure 70A-B).

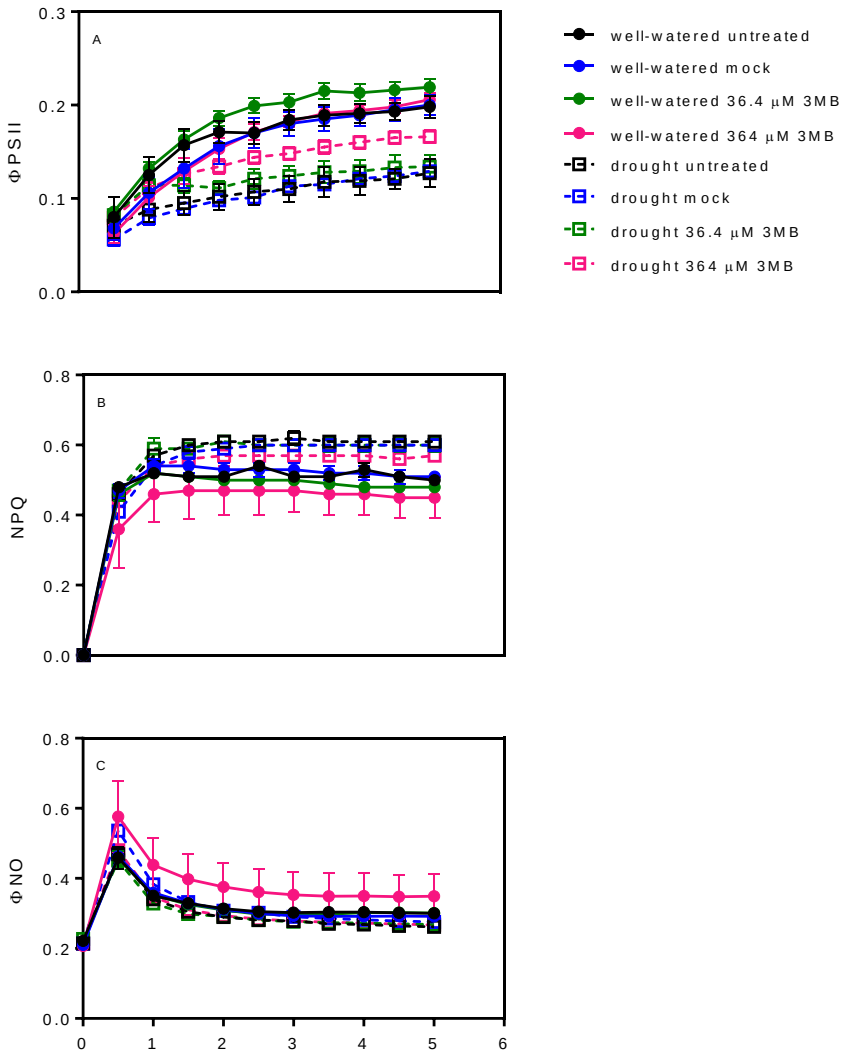

Figure 65A-C. (A) ΦPSII, (B) NPQ and (C) ΦNO in well-watered (closed symbols) and droughted (open symbols) plants colour coded by treatment. These measurements were made under the same conditions as those in Figures 50-52 A-D. Measurements were taken when soil water content was ~ 20% in droughted plants. Values are the mean (n=4) ± SE.

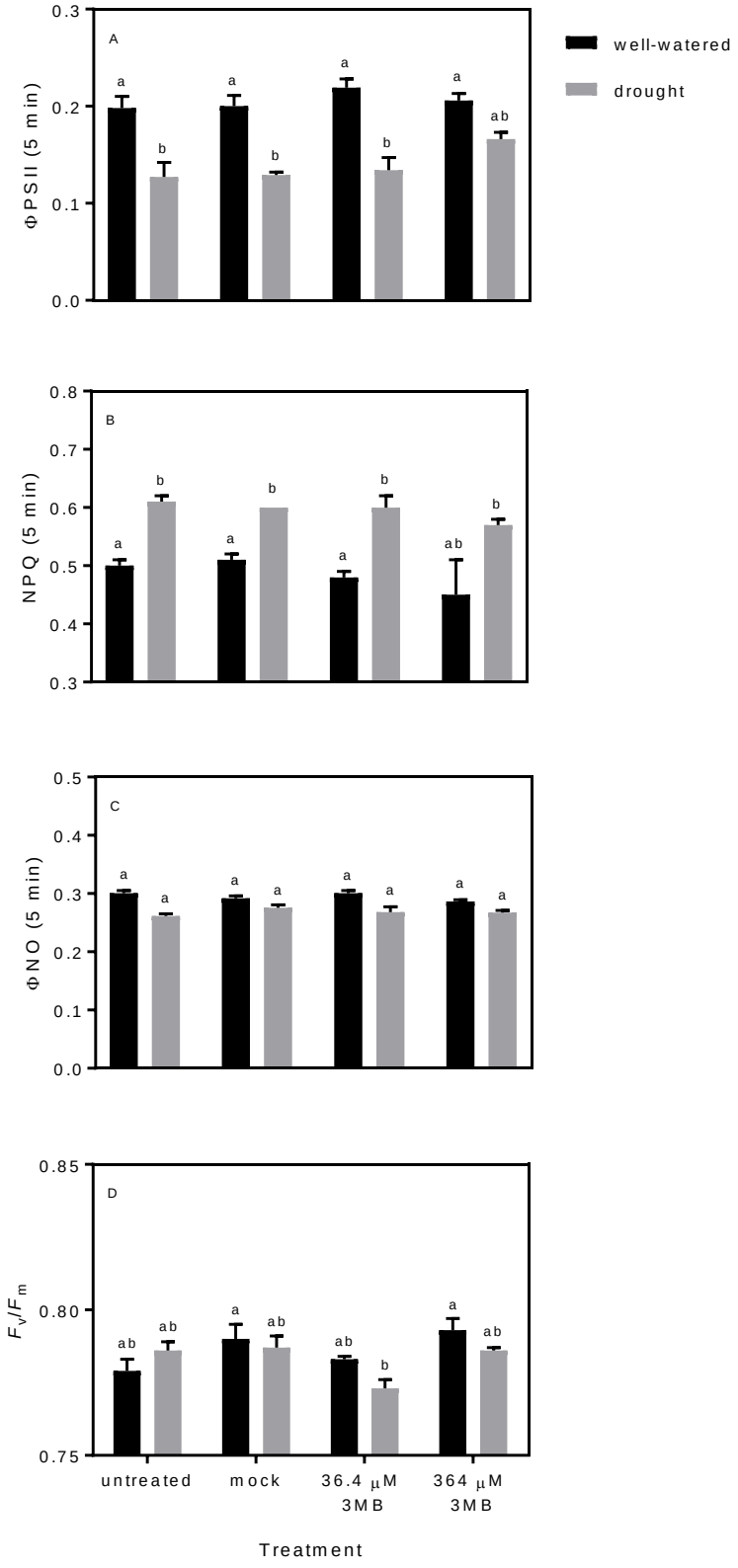

Figure 66A-D. (A) ΦPSII, (B) NPQ and (C) ΦNO measured after 5 min of induction, and (D) F_v/F_m measured 8 days after withholding water from droughted plants. Different letters indicate statistically significant differences, P < 0.05, one-way ANOVA with Tukey's multiple comparisons test. Values are the mean (n=4) ± SE.

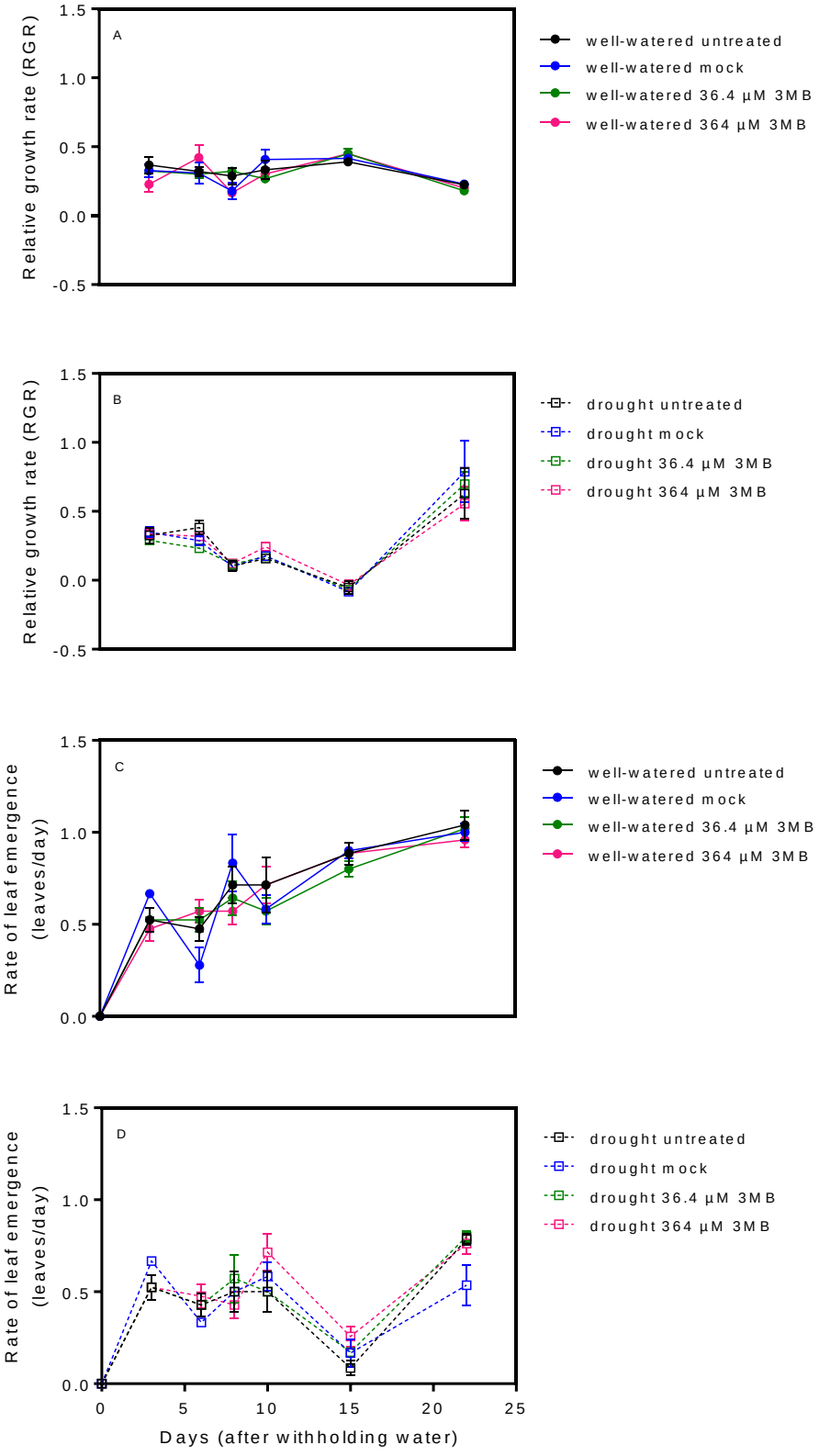

Figure 67A-D. Changes in (A & B) relative growth rate (RGR) and (C & D) leaf emergence in well-watered (closed symbols) and droughted (open symbols) plants colour coded by treatment. Water was withheld from droughted plants on day 0 until they were rewatered after 15 days. Values are the mean (n=6) ± SE.

Figure 68. Pictures of the effects of 3MB taken 2 days after treatment. Untreated plants were unsprayed, mock solution contained solvents and adjuvant but no inhibitor, 3MB = PARP inhibitor. Samples are representative.

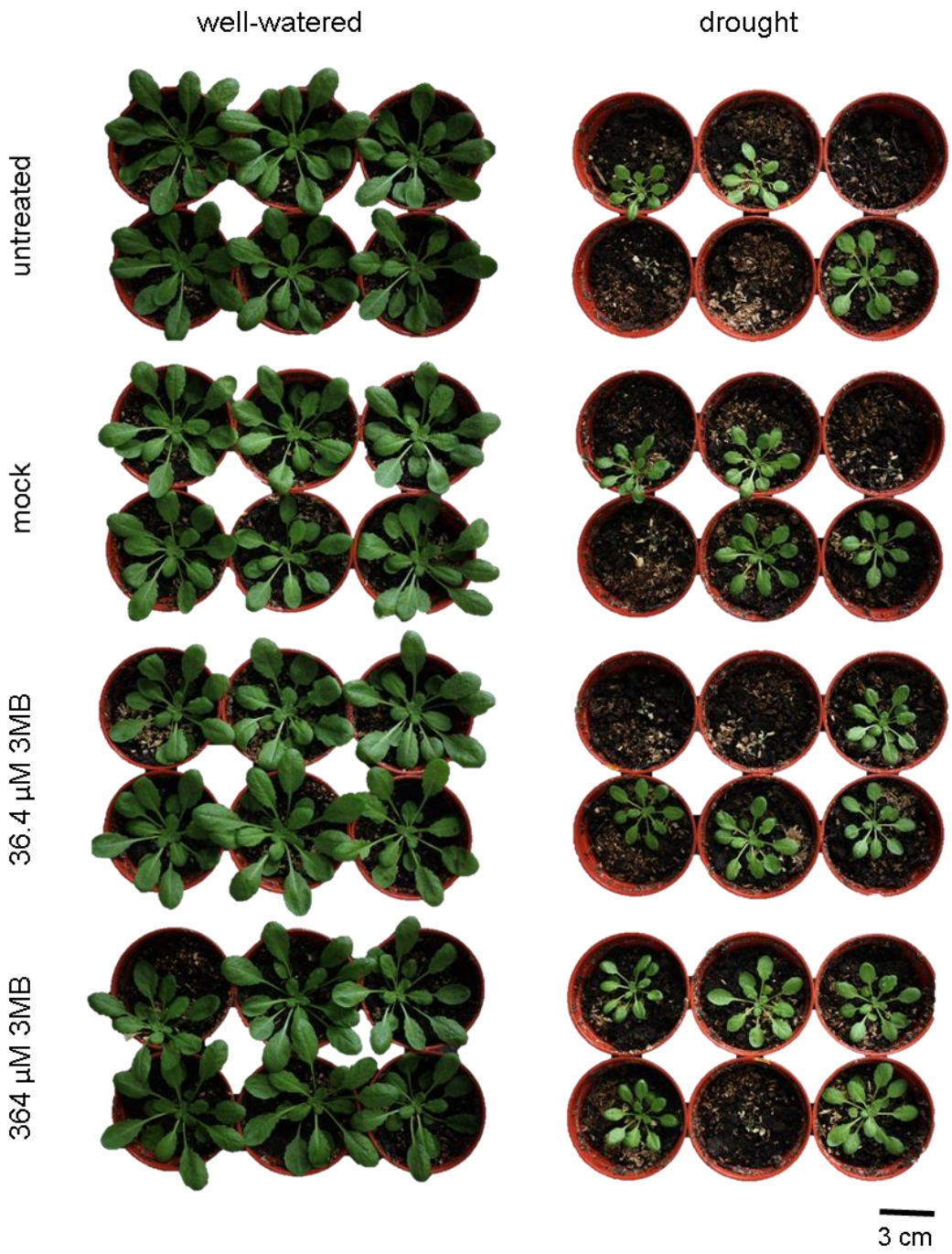

Figure 69. Pictures of Arabidopsis taken 7 days after droughted plants were rewatered following 15 days of water withholding. Treatments were applied to run-off after 6 days of withholding water.

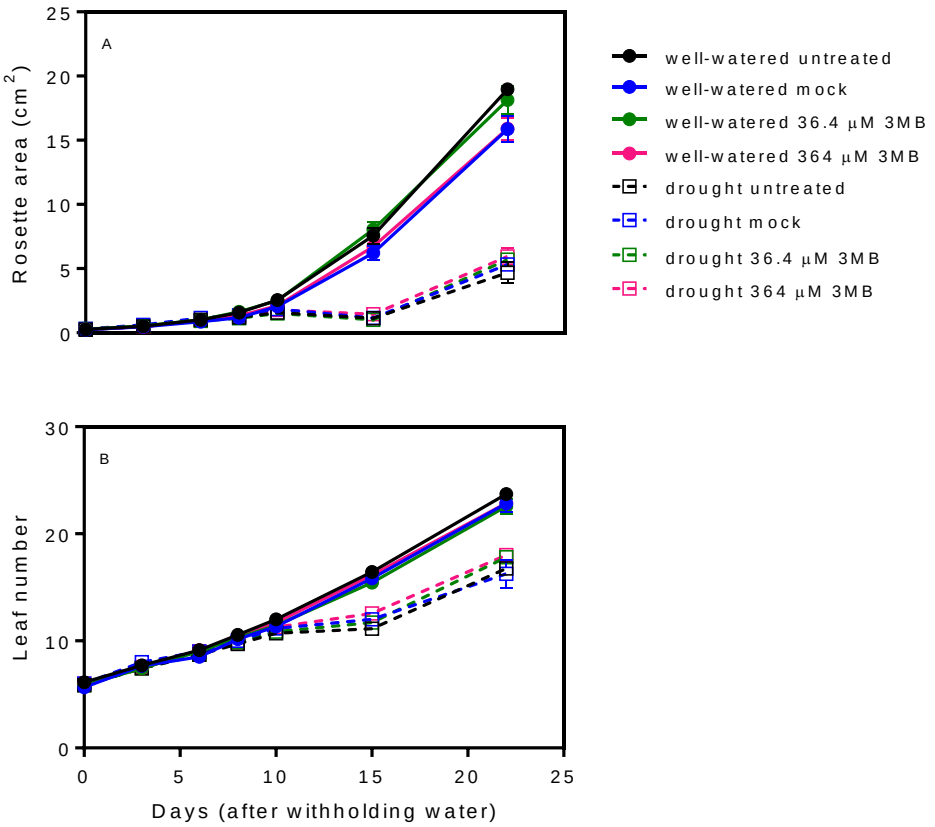

Figure 70A-B. Changes in (A) rosette area and (B) leaf number in well-watered (closed symbols) and droughted (open symbols) plants colour coded by treatment. Water was withheld from droughted plants on day 0 until they were rewatered after 15 days. Values are the mean (n=6) ± SE.

3.3.5. The impact of 2TBC on photosynthesis and growth in *Brassica napus*

To assess the impact of 2TBC application on *B. napus,* plants were sown and grown for 18 days in individual pots before water was withheld from droughted plants (day 0). Treatments were applied to run-off when soil water content measured ~ 35%, 8 days after water withholding. Figure 71 shows images of the plants 2 d after treatment. During high light photosynthetic induction, relative growth rate (height) and leaf number were measured at intervals.

Photosynthetic parameters were measured when soil water content declined to ~ 20% in droughted samples. At this time point there were no significant differences in soil water content between any of the droughted treatments. Values of ΦPSII

measured after 5 min of induction were comparable in all plants except in droughted samples sprayed with 2TBC (Figure 72A). Corresponding NPQ values shown in Figure 72B indicate that treatment with 364 µM 2TBC significantly reduced the ability of plants to generate NPQ. Elevated ΦNO in these plants supports this further (Figure 72C). Additionally, F_v/F_m values were > 0.7 in all plants except in droughted plants sprayed with 364 µM 2TBC where it was reduced to ~ 0.5 (Figure 72D). These results further suggest that 2TBC was either preventing plants generating a proton gradient for NPQ or damaging the plants reducing their ability to regulate energy conversion to photochemistry or heat.

Figure 71 shows characteristic leaf rolling and chlorosis in 2TBC sprayed plants which was particularly evident at 364 µM and under drought conditions. Untreated and mock treated plants appeared green and healthy. There was no significant difference in relative growth rate or leaf number between the treatments (Figure 71; Figure 73A-B).

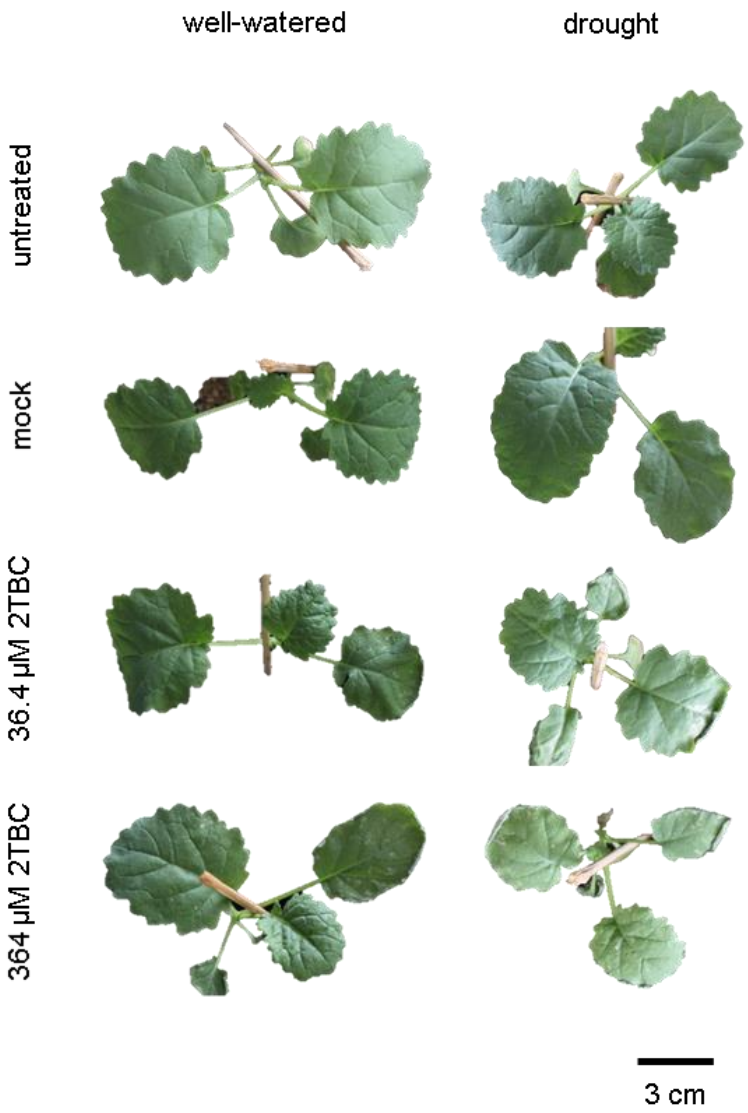

Figure 71. Pictures of the effects of 2TBC taken 2 days after treatment. Untreated plants were unsprayed, mock solution contained solvents and adjuvant but no inhibitor, and 2TBC = PARP inhibitor. Samples were representative.

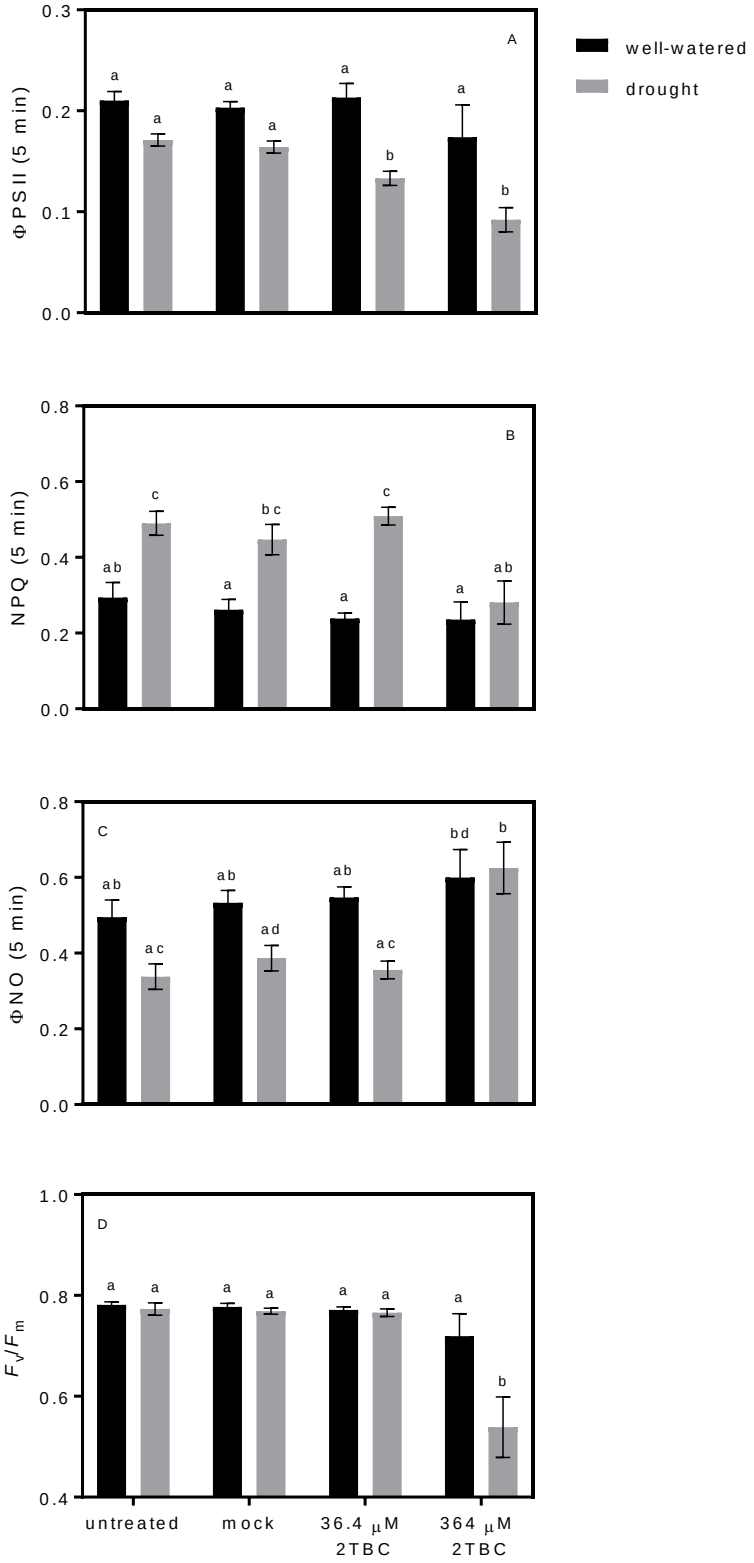

Figure 72A-D. (A) ΦPSII, (B) NPQ and (C) ΦNO measured after 5 min of induction, and (D) F_v/F_m measured 15 days after withholding water from droughted plants. Different letters indicate statistically significant differences, $P < 0.05$, one-way ANOVA with Tukey's multiple comparisons test. Values are the mean (n=4) ± SE.

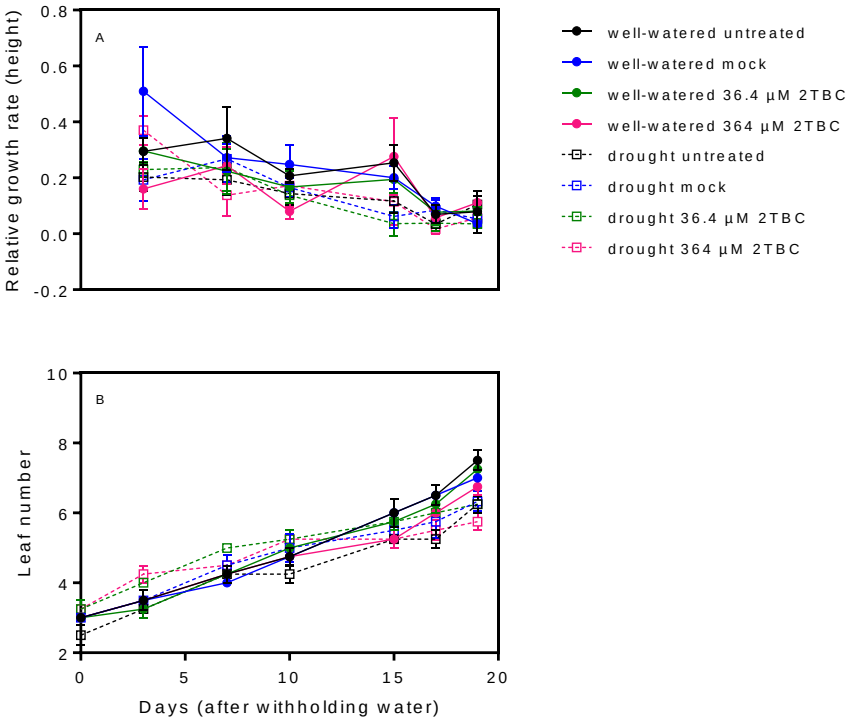

Figure 73A-B. Changes in (A) Relative growth rate and (B) leaf number in well-watered (closed symbols) and droughted (open symbols) plants, colour coded by treatment. Water was withheld from droughted plants on day 0. Values are the mean (n=4) ± SE.

To examine the effect of 2TBC in more detail gas exchange parameters were measured after *B. napus* plants were droughted for 15 days and soil water content had declined to ~ 18%. Plants treated with 364 µM 2TBC were sprayed to run-off after 8 days. Parameters were measured over an extended 18 min induction period because stomatal conductance and carbon assimilation respond to light more slowly than ΦPSII. ΦPSII increased quickly in well-watered plants and steady-state was attained after ~ 10 min (Figure 74A). Both droughted plants went through induction more slowly. Relative to untreated plants, the application of 364 µM 2TBC reduced ΦPSII throughout induction. Following dark-adaption, stomatal conductance was higher in well-watered plants suggesting that the dark period was not long enough for stomata to respond fully (Figure 74B). Stomata began to open after ~ 5 min induction in droughted plants and there was not much difference between the untreated and 2TBC treated plants. The initial rapid rise of carbon

assimilation was comparable between well-watered plants of both treatments although it plateaued in 2TBC sprayed plants more quickly (Figure 74C). In contrast, assimilation was much slower in droughted plants during the first 10 min of illumination after which it began to rise. After 18 min of illumination values of assimilation were higher for the untreated plant in comparison to the 2TBC treated sample. These results suggest that there were costs associated with both drought and inhibitor application.

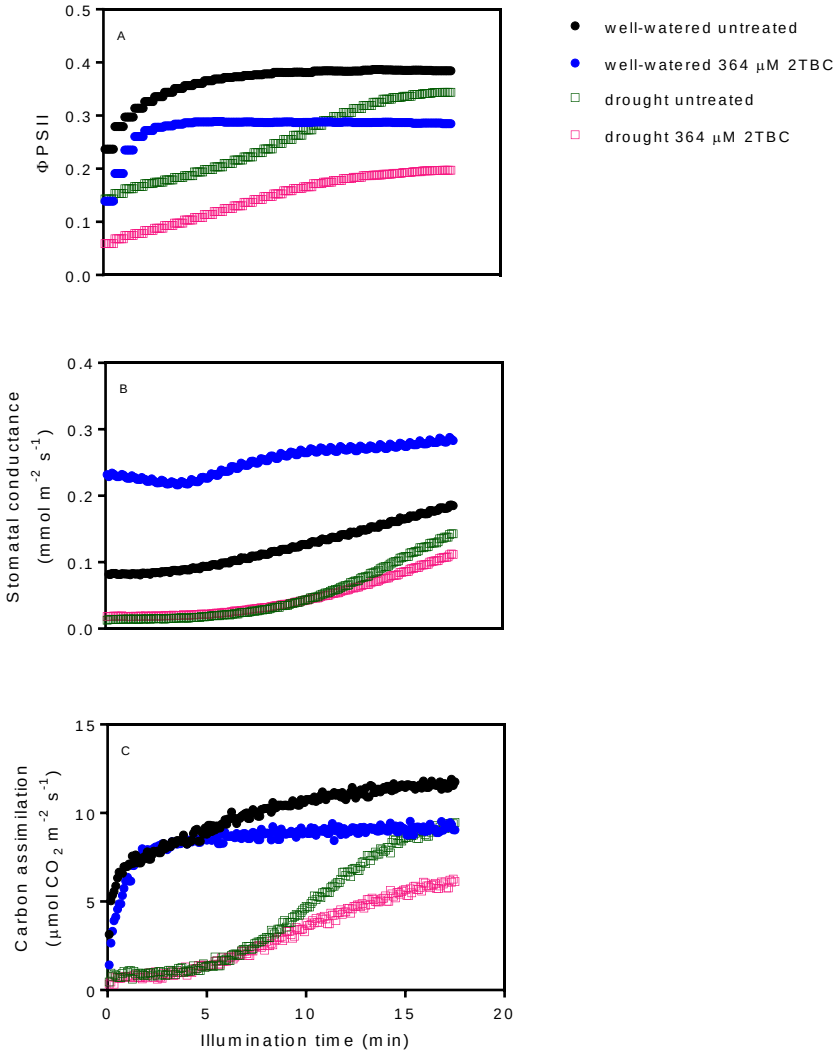

Figure 74A-C. (A) ΦPSII, (B) stomatal conductance and (C) carbon assimilation during high light induction in *B. napus*, colour coded by treatment. 2TBC was applied to plants to run-off at ~ 35 %, 8 days after withholding water from droughted plants. At the time of measuring the soil water content in droughted samples was ~ 17%. n=1.

3.4. Discussion

Several studies have reported that PARP inhibition enhanced stress tolerance and promoted growth (Block *et al.*, 2004; Schulz *et al.*, 2012, 2014). In the majority of cases these studies involved *in vitro* seedling assays or genetic manipulation. The aim of these experiments was to investigate the effects of PARP inhibitors on physiology, growth and yield *in planta*. Two compounds with known PARP inhibition activity were selected, 2TBC and 3MB (3-methoxybenzamide).

PARP inhibitors reproducibly enhanced survival to severe drought stress. Relative to untreated and mock treated plants the application of 2TBC and 3MB increased survival after rewatering (Figure 48; Figure 58; Figure 69). It has been suggested previously that PARP inhibition increases survival by maintaining energy homeostasis, reducing excessive mitochondrial overrespiration and associated ROS production and preventing cell-death initiating processes (Block *et al.*, 2004; Vanderauwera *et al.*, 2007; Schulz *et al.*, 2012). Survival typically increased with higher concentrations of 2TBC although this was not the case for 364 µM 2TBC treated plants in the dose response assay in Figure 58 which did not survive. This contradicted results in Figure 48 where this concentration of 2TBC led to 100% survival. Because run-off is an observational amount, imprecision can result in different amounts of compound being applied to plants across independent experiments. The plants in Figure 58, may have received a higher dosage than those in Figure 48 which might have had a toxic effect and reduced survival. Additionally, because viability is lost within 24 hours, that is to say that a droughted plant has an F_v/F_m value within a range considered healthy but then dies within 24 hours, it is possible to rewater plants after the same period of drought (e.g. after 15 days), but at different times of day and get different survival rates between independent experiments. Alternatively plants could simply lose water slightly differently. Occasionally mock treatment enhanced survival of droughted plants. In addition to the solvents acetone and DMSO, the mock solution contained the adjuvant methylated rape seed oil (MERO; Access, 2015). The function of an adjuvant is to reduce the surface tension of water molecules, thereby reducing the droplet size and

increasing the coverage of an agrochemical across the leaf surface (Janků *et al*., 2012). This helps increase the penetration of the product into the plant. The spray mixes of the mock solution and those containing 2TBC were largely water based. Spraying plants to run-off with these mixes inevitably led to application of water which would have been partly responsible for the enhanced survival observed in these treatments. There is further evidence of this in the physiological analysis following this survival experiment in which untreated droughted plants had significantly lower soil water contents (~ 18%) than treated plants (> 21%; Figure 50A-D). An alternative explanation is that the spraying of a chemical treatment (including mock treatment) induced stomatal closure as an adaptive plant response to foreign substances. Stomatal closure induced by spray application would have been beneficial to plants experiencing drought stress and may have prolonged survival due to water conservation (Chaves, 2002). Increased survival following inhibitor application prompted a more detailed investigation into the impact of 2TBC and 3MB on induction physiology and growth.

The results in Chapter 2 indicated that ΦPSII and NPQ were significantly perturbed by drought during the first 2-5 min of high-light induction. These changes coincided with a decline in the soil water content to ~ 20% in both Arabidopsis and *B. napus*. To facilitate an increase in replication the fluorescence protocols used in this work included 5 min dark-adaption and 5 min high-light illumination, enabling multiple compounds and concentrations to be measured in one day. Plants were measured when soil water content was ~ 20% so multiple experiments could be conducted simultaneously. Schulz *et al.*, (2012) reported that treatment with the PARP inhibitor 3MB significantly enhanced ΦPSII in Arabidopsis under non-stressed conditions, although there was no significant impact under oxidative stress. However, because several studies have reported growth preservation or stimulation in PARP inhibited plants under stress it was hypothesised that treated plants would have higher ΦPSII values than untreated samples under drought conditions. Theoretically this could lead to increased carbon assimilation and growth. Instead, application of 364 µM 2TBC led to a significant reduction of ΦPSII in both Arabidopsis and *B. napus* (Figure 50A-D; Figure 53A; Figure 72A). Lower concentrations such as 36.4, 91 and 182 µM

2TBC did not significantly alter ΦPSII in Arabidopsis (Figure 60; Figure 61A). Although in droughted *B. napus* plants sprayed with 36.4 μM 2TBC, ΦPSII decreased relative to untreated and mock treated plants (Figure 72A). As the two processes are in competition with each other NPQ usually increases as ΦPSII decreases. However, both ΦPSII and NPQ were reduced in all Arabidopsis and droughted *B. napus* plants sprayed with 364 μM 2TBC (Figure 50D; Figure 51D; Figure 53A-B; Figure 72A-B). These plants also measured high levels of non-regulated energy dissipation (ΦNO). The calculation of ΦNO relies on the accurate determination of *q*L, which is an estimation of the degree of openness of the PSII reaction centres (RCs) (Kramer *et al.*, 2004*a*). *q*L assumes that a large number of PSII RCs are embedded in a matrix of antennae and all open RCs compete for excitons in the pigment bed. This is in contrast to an alternative calculation of the proportion of open RCs, *q*P, which assumes each RC has its own antenna. The reality is described most accurately by an intermediate between *q*L and *q*P, although it is now widely accepted that the arrangement postulated by *q*P is not possible and *q*L provides a far closer approximation (Kramer *et al.*, 2004*a*). So, high values of ΦNO indicate that the regulated heat dissipation processes are operating inefficiently. For example, the Arabidopsis *npq4* mutant which lacks the NPQ regulating protein PsbS has low NPQ and high ΦNO (Dong *et al.*, 2015). There are two potential explanations for the presence of high ΦNO. Firstly, it is possible that the concentration of inhibitor in the 364 μM application mix was damaging to plant tissue whereas lower concentrations were not. This effect would have been exacerbated because both Arabidopsis and *B. napus* have flat leaves meaning excess application solution could have been retained on the leaf surface instead of draining away. This is supported by the decline in F_v/F_m observed in plants of this treatment in the days following application (Figure 53D; Figure 72D). Additionally treatment with higher concentrations of 2TBC led to chlorotic and necrotic spots forming on leaves which were not visible on mock treated plants, suggesting they were as a result of the inhibitor and not due to the substances in the mock solution (Figure 54; Figure 63; Figure 71). Secondly, reduced NPQ could be due to an uncoupling effect caused by high concentrations of 2TBC. An uncoupling agent prevents the build-up of the proton gradient required for the generation of NPQ and absorbed energy is instead dissipated through non-regulated

processes, explaining the increase in ΦNO (Arnon & Tang, 1985; Dean & Miskiewicz, 2003; Goss *et al.*, 2008). Additionally, by removing the ΔpH gradient a constraint on electron transport is lifted so uncouplers usually increase electron transport and elevate ΦPSII. However, significantly elevated ΦPSII was not observed in inhibitor treated plants at any of the concentrations used in this work. Given that the lower concentrations of 2TBC had little or no significant impact on photosynthetic parameters, it is most likely that the 364 μM 2TBC spray application was causing damage to the plants. Declining F_v/F_m values and presence of chlorotic and necrotic spots support this hypothesis.

In the previous chapter gas exchange analysis indicated that the drought-induced changes in induction ΦPSII resulted from a stomatal closure. To investigate the impact of 2TBC on stomatal response a similar gas analysis was performed (Figure 74A-C). Application of 2TBC reduced ΦPSII and carbon assimilation relative to untreated plants. Under droughted conditions this was likely a result of slowed stomatal opening in response to light, however the well-watered plant sprayed with 2TBC had higher stomatal conductance following dark-adaption and throughout induction in comparison to the untreated plant. A protective agrochemical might serve to make crops more responsive to the stresses they face. Application of an anti-transpirant during water scarcity would likely enhance a plants chances of survival by promoting water conservation. PARPs have been linked to ABA stress-responsive gene expression (Schulz *et al.*, 2012). Additionally Vanderauwera *et al.*, (2007) showed that plants with reduced PARP activity had elevated ABA levels under both unstressed and high-light stress conditions. The extent of ABA-induced stomatal closure could be increased by PARP inhibitor application, which would be a beneficial response for plants experiencing water-deficit and could explain the increased survival to critical drought in this work. In droughted samples the amount of CO_2 available for carbon assimilation could have been reduced as a consequence of stomatal closure reducing the amount of assimilates available for growth. This could lead to the downregulation of photosynthetic electron transport and decreases in ΦPSII, particularly at the near-saturating irradiance used during induction experiments here. Additionally, ABA is required for normal plant growth but high

concentrations can inhibit growth processes which could explain why PARP inhibited plants grew less well than untreated and mock treated plants (Xiong & Zhu, 2003; Vanderauwera *et al.*, 2007).

2TBC reduced seed yield in Arabidopsis under well-watered conditions but led to an overall increase in yield from droughted plants as more plants survived the stress condition (Figure 64A-B). In this experiment drought had a significant impact on average seed yield per plant which was in contrast to the results in Chapter 2, indicating the stress was more severe in this chapter. Measurements of seed yield in Arabidopsis were made difficult because of the indeterminate nature of the inflorescence and because not all of the processes affecting yield are fully understood (Van Daele *et al.*, 2012). Additionally, if a crop is stressed to the extent that it is hours away from losing viability the quality of the product will be reduced to such an extent that it will likely be discarded. Compounds which improve yield because more plants survive critical stress but which also damage under non-stressed conditions are still unlikely to be industrially desirable, even if the onset of drought can be predicted to a certain extent. A trade-off arises between the costs and benefits associated with chemical treatment. In areas such as the mid-west of the USA or in Australia where drought regularly recurs and lasts for extended periods, the negative effects of protective compounds under non-stressed conditions would be accordingly less marked.

Compounds which protect against the negative impacts of stress and allow plants to maintain photosynthesis and growth have potential application in crop protection strategies (Armstrong & Clough, 2009). Several studies have suggested that successful PARP inhibition conferred tolerance to a broad range of abiotic stressors *in vitro* (Block *et al.*, 2004; Schulz *et al.*, 2012). One of the aims of this work was to investigate the impact of PARP inhibitors when applied to whole plants in soil. PARP inhibitors protected plants against critical drought stress and enhanced survival. The hypothesis that the compounds might enable plants to maintain photosynthesis was not substantiated and the results suggested the reverse was true. The ΦPSII changes were perhaps linked to reduced stomatal conductance which generated a new hypothesis that PARP inhibitors were acting as anti-transpirants, increasing the

extent of stomatal closure. Further investigation into the effects of PARP inhibitors on stomatal conductance and photosynthesis in response to drought will be presented in a later chapter. Conversely, 2TBC treated plants which showed visual signs of damage had reduced values of F_v/F_m and grew more slowly than untreated plants. It is possible that these growth changes occurred because of elevated ABA levels. However the results from mock and 3MB treated plants indicated that the higher concentrations of 2TBC were most likely damaging. The work in the following chapters expands on the experiments here. It was necessary to investigate the impact of PARP inhibitors in a long-term stress study and quantify final yield. More work needed to be done to investigate how PARP inhibitors were changing plant physiology.

In summary:

- PARP inhibitor application reproducibly enhanced survival in response to critical drought stress, particularly at higher concentrations.
- PARP inhibitor application had negative impacts on photosynthesis and growth, particularly at higher concentrations.

Chapter 4

4. Modelling the impact of PARP and PSII inhibitors on yield

4.1. Introduction

Drought is an important environmental stressor of plants which limits the productivity of crops worldwide (Fisher *et al.*, 2016). Drought commonly occurs in major wheat growing areas such as the USA and Australia and affects plants on the molecular, biochemical, physiological and morphological levels (Boyer, 1982; Boyer & Westgate, 2004). Plants have evolved to survive in natural ecosystems rather than crop environments and can over-respond to moderate stresses. Many plant responses to abiotic stresses such as drought are considered inappropriate in an agricultural context because they are energetically wasteful, often occur at the expense of growth and can reduce the amount of assimilates diverted to yield. One such example is the stress-induced upregulation of production and activity of poly (ADP)-ribose polymerases (PARPs), which are known to deplete cellular energy metabolite stores (Block *et al*., 2004; Briggs & Bent, 2011). Studies have suggested that downregulation of PARP activity during stress could maintain energy stores and growth and yield could be enhanced as a result. Because of the current legislative restriction across the European continent, attention has turned to developing chemical PARP inhibitors which have potential application in crop protection strategies. To date several compounds have shown PARP inhibition efficacy in plants although the majority of compounds have been selected from work in mammalian biology (Briggs & Bent, 2011). Development of new banks of structurally related compounds which are more specific to plant PARPs is well underway.

Classical phenotyping methods to measure drought stress response are time-consuming, labour-intensive and often destructive, meaning repeat measurements on the same plant are not possible (Fisher *et al.*, 2016). These techniques are able to assess physiology and growth at one time point only, so it is not always possible to extrapolate and predict the long-term effects on future performance (i.e. yield). In contrast, dynamic phenotyping techniques with automated watering and imaging systems are non-invasive and can quantify plant growth and development in response to various stresses over the course of a plants life cycle (Großkinsky *et al*.,

2015; Rahaman *et al*., 2015). Accordingly these phenomic technologies have received considerable research attention and funding in recent years. These techniques are particularly applicable to small compound research because the long-term effects of arrays of compounds can be studied *in planta*. That said, long-term stress studies which quantify the impact of compounds on growth and final yield inevitably take a long time to complete, even if the normal progression through life-cycle stages can be accelerated through the precise control of environmental conditions. Therefore any method that can accurately predict the impact a compound will have on final yield earlier than measuring at harvest would be extremely useful in agro-chemical research.

Grain number and grain weight are the key components of yield in wheat (Griffiths *et al.*, 2015). Grain number is believed to be the result of growth from flag leaf emergence to flowering whereas grain weight is the product of growth post-anthesis (flowering). The impact of abiotic stress at different stages of reproductive development on yield components in wheat is shown schematically in Figure 75. Grain number is said to be the most vulnerable component of yield to abiotic stress, particularly during pollen development (Dolferus *et al*., 2011). From an evolutionary point of view it is better for a stressed plant to produce a small number of large seeds by sacrificing tillers and florets in order to ensure fecundity. In a crop context this strategy is likely to reduce potential grain number and yield. However, the underlying determinants of grain number under abiotic stress are poorly understood, making it difficult to develop methods to increase this yield component (Dolferus *et al*., 2011).

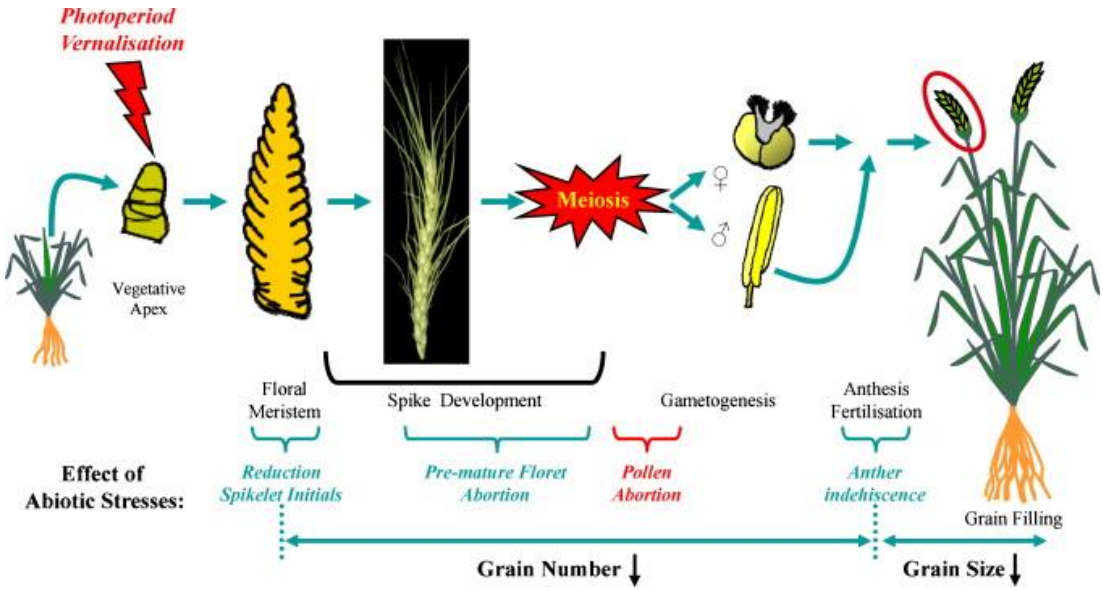

Figure 75. Overview of the reproductive stages in wheat and the impact of abiotic stress on reproductive development. Taken from Dolferus *et al*., (2011).

There is some debate about the nature of the relationship between grain size and weight, if indeed there is one at all. Several studies have reported a negative correlation between grain number and grain weight (Kuchel *et al*., 2007; McIntyre *et al*., 2010; Dorostkar *et al*., 2015). A common challenge in science is to decipher if a relationship between two variables is a correlation or a cause and effect. To that end there is contention between grain number and wheat yield. The question remains: is high grain number empirically correlated with high yield because the two are the product of the same underlying processes; or does high grain number cause high yield? The former position is argued by Sinclair & Jamieson, (2006) who suggest both grain number and yield are a consequence of carbon and nitrogen assimilation. The alternative causal argument is made by Fischer, (2008) who claims that grain number is itself the primary determinant of yield. If the Sinclair and Jamieson hypothesis is correct, PARP inhibitors should maximise a plants ability to assimilate resources as the expression and activity wasteful stress response pathways are reduced. Additionally any compounds which extend the period in which plants can mobilise assimilates for grain filling by delaying senescence pathways (as in the stay-green effect) would be beneficial (Lopes & Reynolds, 2012). If Fischer is correct, the timing of application of potentially protective compounds would have to be targeted within

the growth period believed to be critical for the determination of grain number. Furthermore the timing of developmental transitions, such as that between vegetative and reproductive growth, is known to be critical for biomass accumulation in cereals (Camargo *et al.*, 2016).

The work in this chapter used the phenomic facilities at Bayer Crop Science in Frankfurt, Germany to quantify the impact of PARP inhibitors and structurally related compounds (PSII inhibitors) on plant growth and yield, under drought stress. Modelling techniques were explored to determine if the impact of the stress and compound application on final yield could be predicted earlier.

4.1.1. Aims

- To determine the impact of PARP and PSII inhibitors on wheat yield under well-watered and water-stressed conditions.
- To determine the impact of time of application of these inhibitors on yield.
- To determine if phenomic approaches could predict final yield at earlier development stages.
- Use modelling techniques to determine if growth can be predictive of final yield.

4.1.2. Objectives

- Use defined irrigation regimes to apply drought to *T. aestivum*.
- Quantify the impacts of drought and inhibitor application on growth and yield at harvest.
- Spray the compounds at three stages of development to assess the impact of application time on growth and yield.
- Use continuous, non-invasive RGB imaging to capture pixel data for each plant over the entire life cycle. Using these data, extract useful parameters which quantify the impacts of drought and inhibitor application on plant growth and health.

- To determine if models of plant growth can be used to predict yield at harvest.

4.2. Materials and methods

4.2.1. Plant material and germination conditions

Summer wheat (*Triticum aestivum*; AC Harvest; Canada) seeds were germinated over 7-10 days in 15 cm, 3 L capacity pots containing a 2 cm layer of sand on top of soil. Every 100 g of soil contained 12 mg of phosphorous, 41 mg of potassium and 15 mg of magnesium (LUFA NORD-WEST; Germany). White pots were used to reduce heat uptake as root temperature is known to be important for biomass development in cereals. Pots were watered every 2 days and stored in a greenhouse with 350 µmol PAR m^{-2} s^{-1} on a 12 hour/12 hour day/night cycle, at 16 °C/12 °C temperatures and ~ 60% relative humidity during light hours. Once germination was complete (BBCH 9/12) plants were transferred to the climate chamber for the duration of the experiment.

4.2.2. Climate chamber conditions

The climate profile was designed to simulate the March to September life cycle of AC Harvest over a reduced period of 90-100 days. All environmental conditions were controlled according to a regime designed to closely replicate the conditions that summer wheat would normally experience in the field. Minimising environmental fluctuations reduced the time from emergence to harvest. The acceleration of growth and development under controlled conditions meant that an ordinary month in the field could be simulated in 14 days in the chamber. The regime was derived from a climate model based on 50 years of recorded weather data, from 50 stations in summer wheat growing areas worldwide, and was tailored to plant variety and soil type. Maximum irradiance was 350 µmol PAR m^{-2} s^{-1} measured at belt height. The climate profile is detailed in Table 1 in the Appendix.

4.2.3. Watering regimes and drought application

In the climate chamber plants were watered using automatic pumps (Watson-Marlow; UK). Well-watered and droughted plants received 200 ml and 120 ml of water respectively, at defined time points listed in Table 5. The well-watered regime delivered just under the maximum capacity for water of the pots which was 250 ml. The drought irrigation regime was designed to apply water deficit over the course of the life cycle. Pots were closed at the bottom with a layer of impermeable paper and placed in trays to prevent water escape. Pots were weighed at intervals throughout.

Table 5. Details of the watering intervals. This is shown graphically in Figure 79A-B. dat = days after transfer.

Watering time points (days after transfer)	Comments
0	Only small amounts of water required during early stages of life cycle
10	
20	
25	Reduced the watering intervals
32	
40	
Then every 3 days until 82 (final watering)	After 40 dat root uptake significantly increases so watering frequency was adjusted accordingly

4.2.4. Pot randomisation

A randomisation protocol was programmed which repositioned 10 pots every 6 hours to minimise the impact of light, temperature and humidity gradients. Ensuring homogenous conditions is necessary when comparing different treatments in long-term stress experiments. Plants were transferred into the chamber in blocks arranged by treatment. The randomisation protocol moved plants from different rows which resulted in complete disorder of the original layout in 14 days (Figure 76).

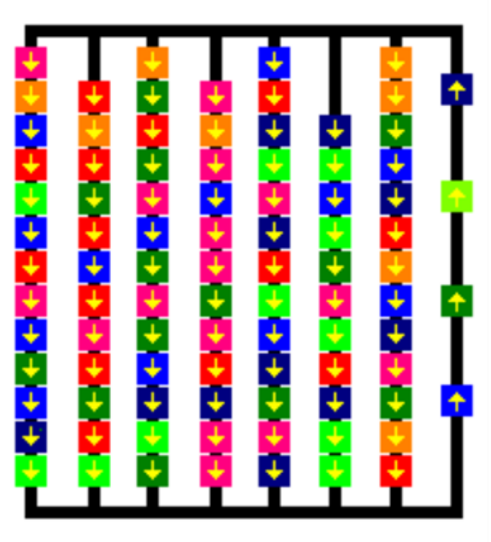

Figure 76. A schematic of the pot randomisation protocol applied in this trial which moved plants from different rows. Robotics moved 10 pots every 6 hours to a new position. This schematic represents a general protocol applied in many trials invoving phenotyping platforms of this kind, it is not an explicit description of the randomisation protocol applied in this chapter.

4.2.5. The BBCH scale

The BBCH (abbreviated from Biologische Bundesanstalt, Bundessortenamt und Chemische Industrie) scale is a uniform coding system of the phenological growth stages of all monocotyledonous species including wheat (Federal Biological Research Centre for Agriculture and Forestry, 2001). The wheat life cycle is divided into ten principal growth stages, which are each subdivided into multiple secondary growth stages. The scale follows a two digit coding system which runs from 00 to 99, with the first digit corresponding to the principal growth stage and the second digit corresponding to the secondary growth stage. Each two digit code describes a phenological stage of development which is phenotypically distinct from any other two digit code. A summary of the scale is shown in

Table 6 with a more detailed description in Table 2 in the Appendix. The BBCH scale was used in this work to identify compound application times (discussed below).

Table 6. The principal growth stages of the BBCH scale for the description of phenological growth stages of cereals including wheat. Adapted from Federal Biological Research Centre for Agriculture and Forestry, (2001). A more complete description inclusive of the secondary growth stages is shown in Table 2 in the Appendix.

BBCH scale: cereals (including wheat; *Triticum aestivum*)	
Principal growth stage	**Description**
0	Germination
1	Leaf development
2	Tillering
3	Stem elongation
4	Booting
5	Inflorescence emergence/heading
6	Flowering/anthesis
7	Development of fruit
8	Ripening
9	Senescence

4.2.6. Compound selection and application

The compounds used in this experiment are listed in Table 7 but the exact chemical structures cannot be released. All compounds were supplied by Bayer Crop Science (Germany). Compounds 1 and 2 have known PARP inhibition activity and compounds 3 and 4 have known PSII inhibition activity. All compounds are structurally related benzimidazoles. Compounds were mixed with an adjuvant named genapol (genapol XM 060; Iso-tridecyl alcohol ethoxylate methyl ether with 6 polyoxyethylene; Clariant; Switzerland), which stabilises emulsions by increasing kinetic stability. This means that the size of the droplets in the emulsion remain more stable over time. For application 17.68 mg of wettable powder (WP05) of each compound was dissolved in 30 ml dH_20 containing 0.1% genapol. Bayer use a standard formulation (e.g. wettable powder) for test compounds in which the amount of active ingredient is given by the formulation code (WP05 = 5% active ingredient + 95% formulation

powder). To achieve delivery of 10 g ha^{-1} of active ingredient, 0.6 ml of each solution containing compound was applied to each plant. Additionally, mock treatments were performed using solutions of dH_20 with 0.1% genapol but no inhibitors. Compounds were applied using handheld sprayers (Carl Roth; Germany). Untreated plants were unsprayed.

Table 7. A list of the compounds used in this experiment. Compounds were assigned a referred name for referral in this work.

Bayer substance code (BCS-)	**Assigned name**	**Compound class**	**Activity**
CO80755	Compound 1	PARP inhibitor	Confirmed *in vitro* PARP inhibition activity
CK52259	Compound 2		
AF22791	Compound 3	PSII inhibitor	Confirmed strong PSII inhibition and weak PARP inhibition activity *in vitro*
CN85321	Compound 4		Confirmed weak PSII inhibition and no recorded PARP inhibition activity *in vitro*

Compounds were applied at one of three application points which were defined by phenological growth stage and identified using the BBCH scale. Applications were scheduled at: (1) leaf development/early tillering (BBCH 13/21, early application); (2) late tillering/early stem elongation (BBCH 29/32, mid-point application); and (3) heading (BBCH 50/55, late application). Each application time point was an independent treatment such that any plant was sprayed only once. Each treatment had 11 replicates except the untreated which had 10, totalling 350 plants. A summary of the setup is shown in Table 8.

Table 8. Experimental setup by irrigation, application stage and treatment. Replicate numbers for each treatment are shown in brackets. dat = days after transfer.

Application stage information ↓	**Well-watered (200 ml H_2O)**	**Drought (120 ml H_2O)**
N/A	Untreated (10)	Untreated (10)
Early application BBCH 13/21 (leaf development/early tillering) 16 dat	Genapol (11) Comp 1 (11) Comp 2 (11) Comp 3 (11) Comp 4 (11)	Genapol (11) Comp 1 (11) Comp 2 (11) Comp 3 (11) Comp 4 (11)
Mid-point application BBCH 29/32 (late tillering/early stem elongation) 37 dat	Genapol (11) Comp 1 (11) Comp 2 (11) Comp 3 (11) Comp 4 (11)	Genapol (11) Comp 1 (11) Comp 2 (11) Comp 3 (11) Comp 4 (11)
Late application BBCH 50/55 (heading) 50 dat	Genapol (11) Comp 1 (11) Comp 2 (11) Comp 3 (11) Comp 4 (11)	Genapol (11) Comp 1 (11) Comp 2 (11) Comp 3 (11) Comp 4 (11)
Total plants: 350		

4.2.7. Imaging acquisition and analysis

Images were captured using a LemnaTec 3D Scanalyzer system (LemnaTec GmbH; Germany). Plants were scheduled to be photographed every day for the duration of the experiment although technical faults occasionally interrupted this plan. Two 1280 x 960 images were recorded each time at two rotations (0 °, side-view 1; 90 ° side-view 2) and analysed using LemnaBase software (LemnaTec GmbH; Germany). The average pixel number from the two side-view images was used to calculate plant object sum area, which can be plotted over time to construct growth curves. Additionally the area of interest (i.e. plant) in each image is divided into five colour classes and each pixel is related to one of these classes using the principle of nearest neighbourhood classification: dark green, green, medium bright green, bright green and chlorosis/necrosis (Altman, 1992). Tissue health was assessed by measuring the ratio of pixels in the four green (healthy) classes to those in the one yellow (chlorosis/necrosis) class.

4.2.8. Quantification of yield parameters

Plants were harvested 99 dat when they had died and the seed were dry (BBCH 99). Ears were classified as primary, secondary, tertiary or quaternary according to height where ears of the different classification did not overlap (Figure 77). Grain number and weight per ear were measured for each plant. Thousand kernel (grain) weight (TKW) was quantified for each plant = (total grain weight/total grain number) x 1000. The coating of the harvested seed was removed prior to weighing. All weighing was complete within 7 days of harvest to reduce any differences that might occur as a result of extended storage.

4.2.9. Data modelling and statistical analysis

RStudio was used to perform statistical analysis on the data set (RStudio, Inc; USA). Preliminary analysis suggested the data were not normally distributed and had unequal variances between well-watered and droughted samples ($P = 4.581 \times 10^{-10}$; Bartlett test of homogeneity of variances). Further tests revealed the variances within treatments were unequal also (well-watered, P = 0.00028; drought, P = 0.04391). Unless stated data were analysed using Kruskal-Wallis Tests with Dunn's Test of Multiple Comparisons and Benjamini-Hochberg procedure for false discovery.

Graphs and figures were constructed using GraphPad Prism 7 (GraphPad Software, Inc; USA) and the ggplot plotting package in RStudio (Wickham, 2009). Generalised additive models (GAMs) were fitted on raw and log transformed object sum area and green:yellow ratio data using the gam package in RStudio. The number of knots in the model was adjusted to alter the degree of flexibility and improve the fit. Goodness of fit was then measured by the coefficient variance score (termed GCV) which decreased as the fit improved. A correlation term was added using the GAM mixture (gamm) function to correct for the autocorrelation problem associated with GAMs. Individual fits were manually inspected and are shown in the Appendix along with the R scripts for the model. Because the GAMs predicted values it allowed missing data points and discontinuities to be determined also. Maximum values of object sum area were extracted from GAM fitted data. Figure 78 shows an outline of the decision making processes in the data analysis.

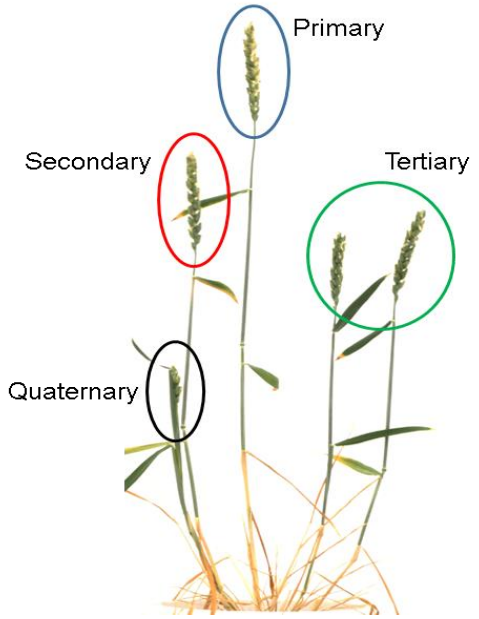

Figure 77. Diagrammatic representation of the classification of ears. Primary, secondary, tertiary and quaternary ears were classified according to height. Ears that were non-overlapping when stems were held upright were of a different category.

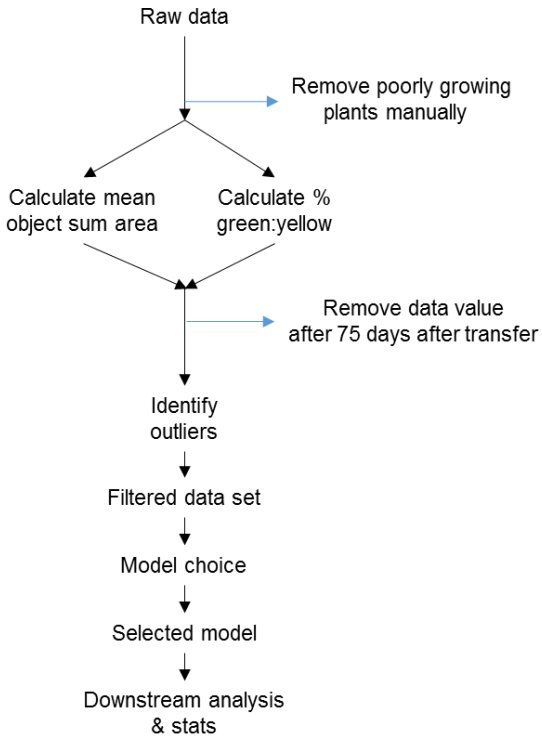

Figure 78. Schematic representation of the process of data collection, processing and analysis.

4.3. Results

4.3.1. The impact of drought and inhibitor application on the growth and yield of *T. aestivum*

Following transfer into the climate chamber plants were subjected to one of two watering regimes. At each watering time point well-watered and droughted plants received 200 ml and 120 ml of water respectively. Figure 79A-B shows sample data of the impact of the two watering regimes on pot weight over the course of the experiment. After ~ 40 days all plants were using all of the water they received before the next scheduled application. Figure 79C shows how the total amount of water added to plants of both regimes changed over time. The drought regime applied 40% less water than the well-watered regime, meaning that by the final application 82 dat the well-watered and droughted plants had received 4000 ml and 2400 ml of water in total respectively. The impact of drought was evident in the phenotype ~ 35 dat (BBCH 29/32) (Figure 80A-B). Drought restricted growth and plants generally produced less tillers and ears than well-watered samples. Compounds were applied at three time points: BBCH 13/21 (early), BBCH 29/32 (mid-point) or BBCH 50/55 (late) (Table 8). Figure 81 shows example pictures of plants at each application point.

Plants were harvested 99 dat (BBCH 99) and the number of ears, number of grains and grain weight were measured. Wheat plants produce a number of ears which reflects growth from the start of tillering to flag leaf emergence (BBCH 20/37-39). All plants produced one primary ear although drought caused a significant reduction in total ear number and the number of secondary and tertiary ears produced (Figure 82A-C). However there was no additional impact of compounds at any application point and all treatments recorded comparable values of total and secondary ear numbers (Figure 83A-B; Figure 84A-B). Tertiary ear numbers are not shown because the majority of droughted treatments had < 3 replicates, including the untreated plants. Only one droughted plant produced a quaternary ear.

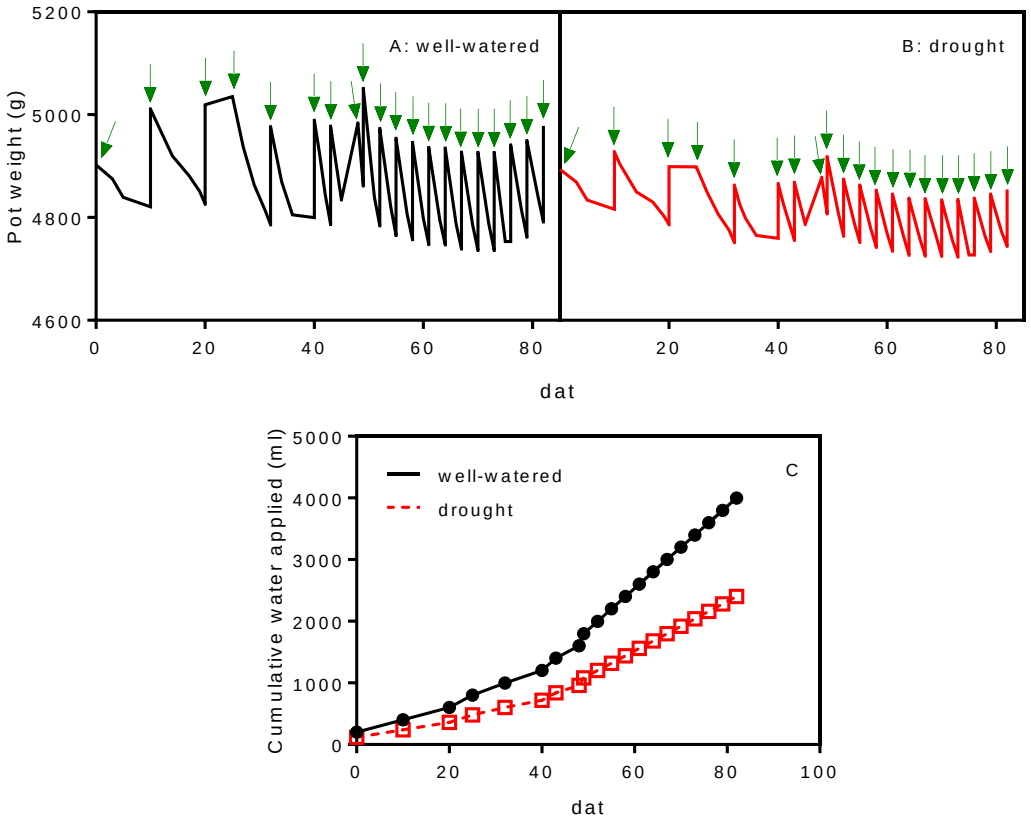

Figure 79A-C. Changes in pot weight of (A) well-watered (black line) and (B) droughted (red line) plants, and (C) cumulative water added over the course of the experiment. Watering time points are indicated by the green arrows. The sample data shown are from untreated plants only. dat = days after transfer. Values are the mean (n=10).

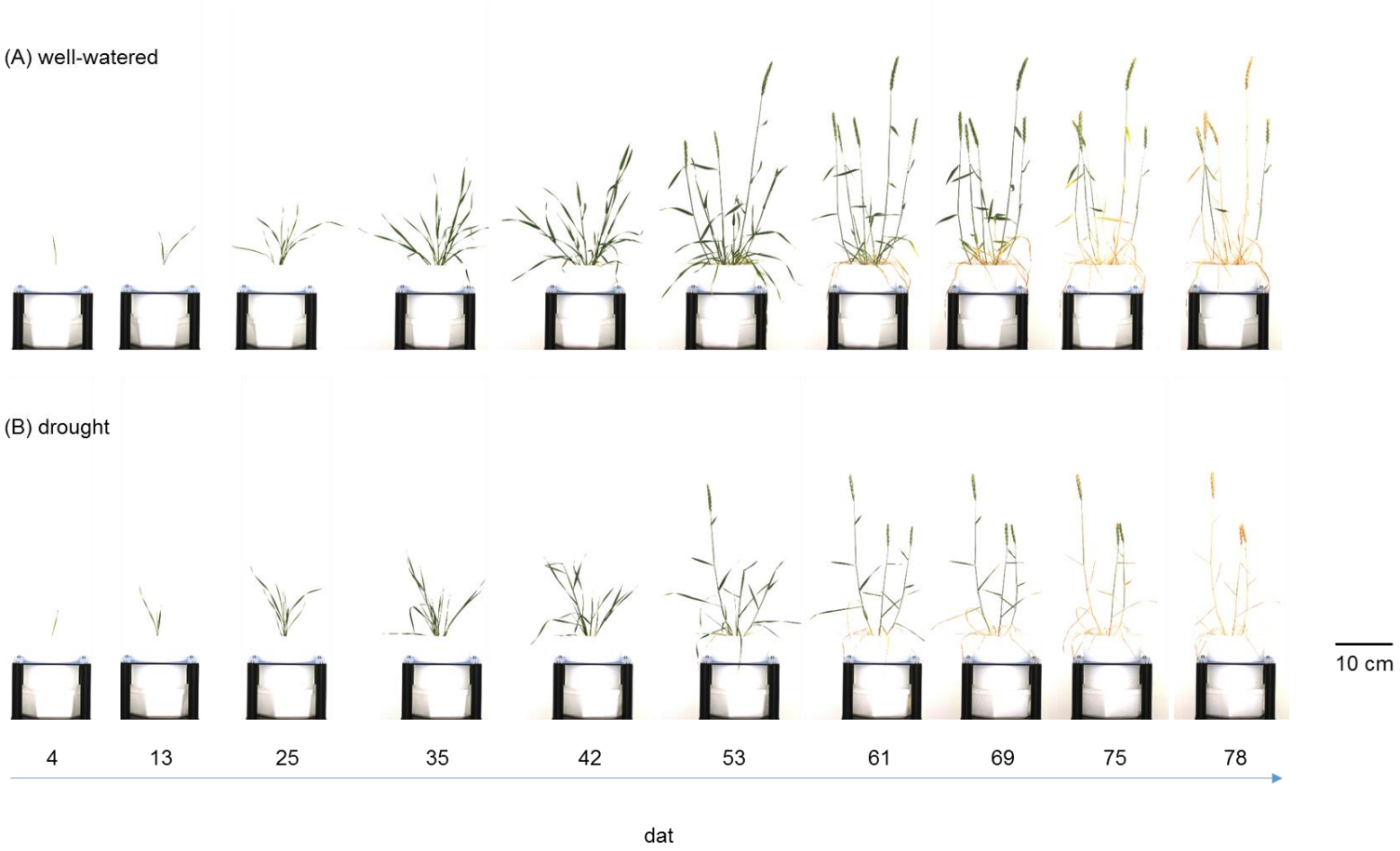

Figure 80A-B. Example pictures of (A) well-watered and (B) droughted plant growth over the course of the experiment. Both of these plants were untreated. dat = days after transfer.

Figure 81. Example pictures of plants at the three application time points. The principal growth stages are labelled.

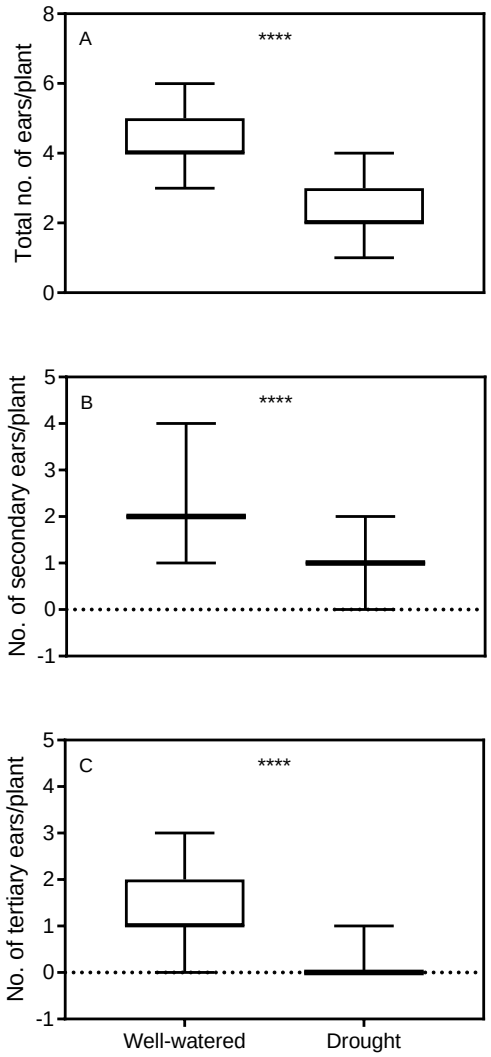

Figure 82A-C. The average (A) total number of ears, (B) number of secondary ears and (C) the number of tertiary ears of all well-watered and droughted plants. These data are averages of plants of all treatments of each irrigation regime. **** denotes $P < 0.0001$, Student's t-test, $n > 150 \pm SE$.

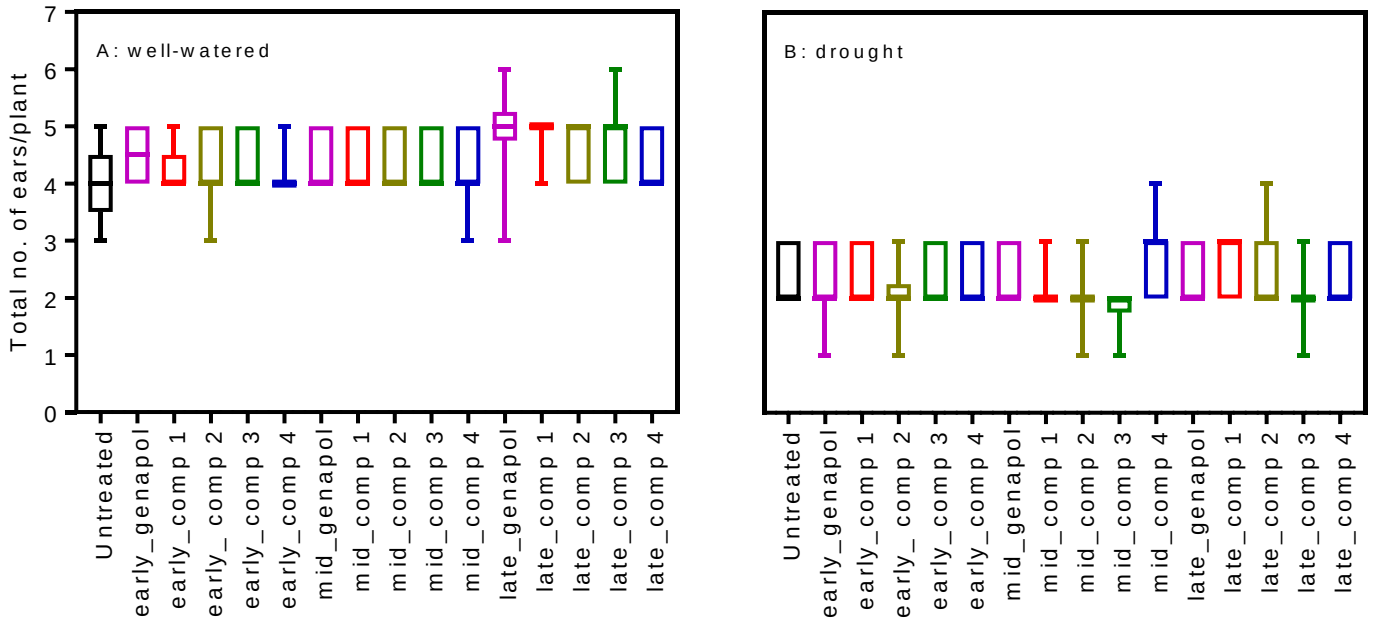

Figure 83A-B. Total number of ears per plant under (A) well-watered and (B) droughted conditions. The box plots are colour coded by treatment and arranged according to application time: early, mid (mid-point) or late. (n=8-11).

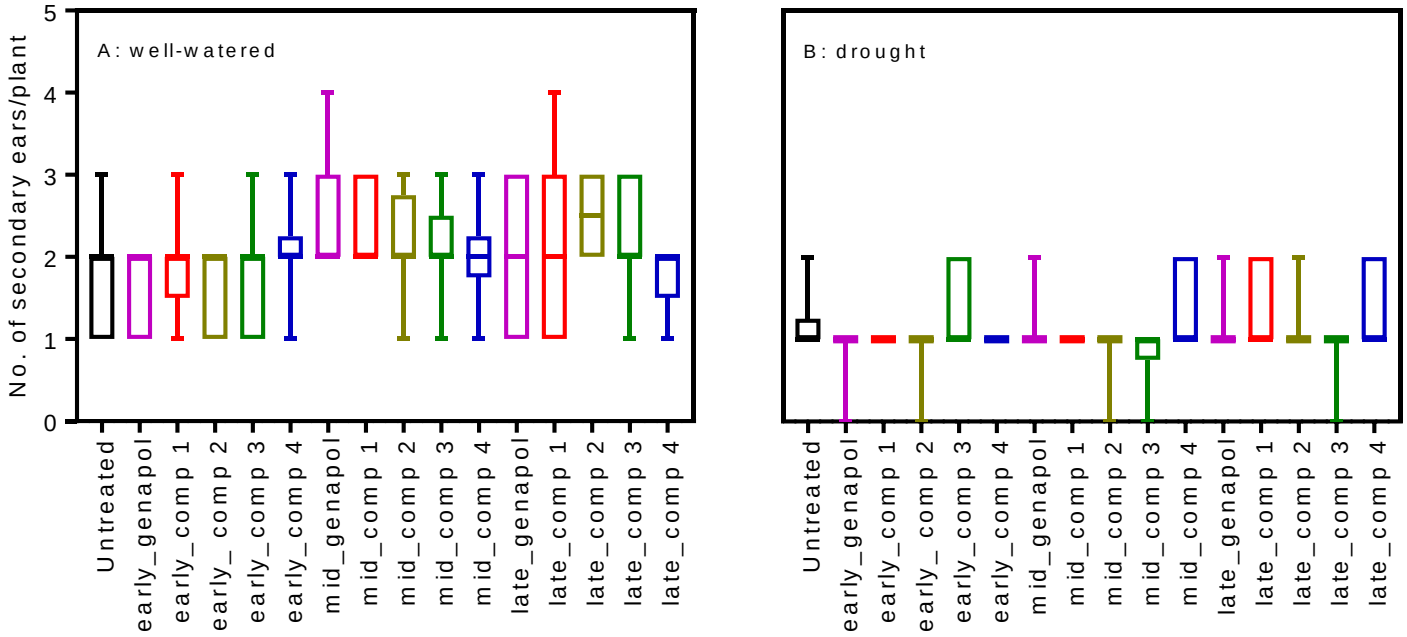

Figure 84A-B. Average number of secondary ears per plant under (A) well-watered and (B) droughted conditions. The box plots are colour coded by treatment and arranged according to application time: early, mid (mid-point) or late. (n=8-11).

Grain number per ear is reflective of growth from flag leaf emergence to flowering (BBCH 37-39/59). Although chemical treatment and application time did not influence the number of ears, it is possible that the compounds had subtle effects and therefore it was necessary to assess different yield components in greater detail. Ordinarily, plants which produce more ears will set more grain than plants with fewer ears unless part of, or the entire ear is aborted (i.e. due to stress). Indeed well-watered plants produced 128 grains per plant on average, more than double the 61 grains produced by droughted samples (Figure 85A-B). At the mid-point application plants sprayed with compound 2 produced significantly less grain than those treated with genapol or compound 4. Similarly treatment with compound 3 reduced grain number relative to compound 4. No treatment significantly altered grain number relative to untreated plants of the same irrigation regime. The difference in grain number was largely caused by variations in the grain yield of secondary and tertiary ears. The average primary ear yield was similar for all plants with well-watered and droughted plants producing 39 and 32 grains respectively (Figure 86A-B). In contrast the secondary ears of well-watered plants yielded ~ 2.5 times more grain than droughted plants ($P < 0.0001$) (Figure 87A-B). However there was no significant impact of either chemical treatment or application time on primary, secondary or tertiary grain number (Figure 86A-B; Figure 87A-B). Only two untreated droughted plants produced tertiary ears but there was no significant difference between those treatments which had ≥ 3 replicates. The average number of grain per ear for each plant was calculated but of all the treatments only drought had a significant impact ($P < 0.0001$) (Figure 88A-B).

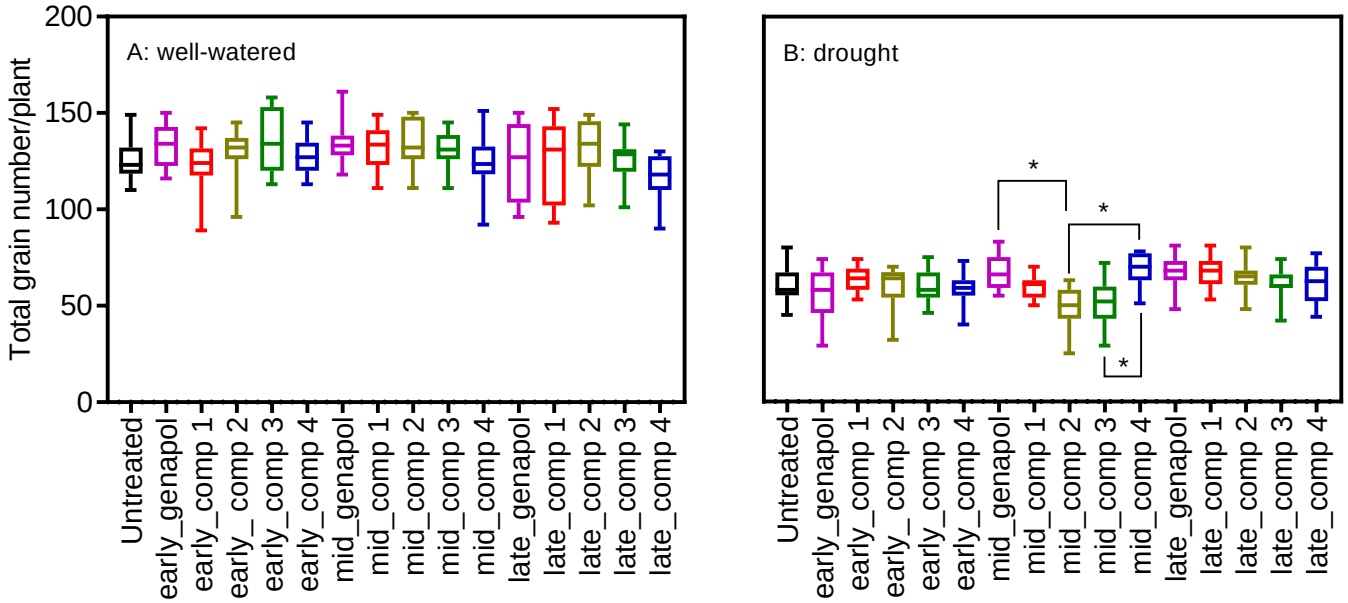

Figure 85A-B. Average total grain number of (A) well-watered and (B) droughted plants. The box plots are colour coded by treatment and arranged according to application time: early, mid (mid-point) or late. * = P < 0.05, Dunn test for multiple comparisons. (n=8-11).

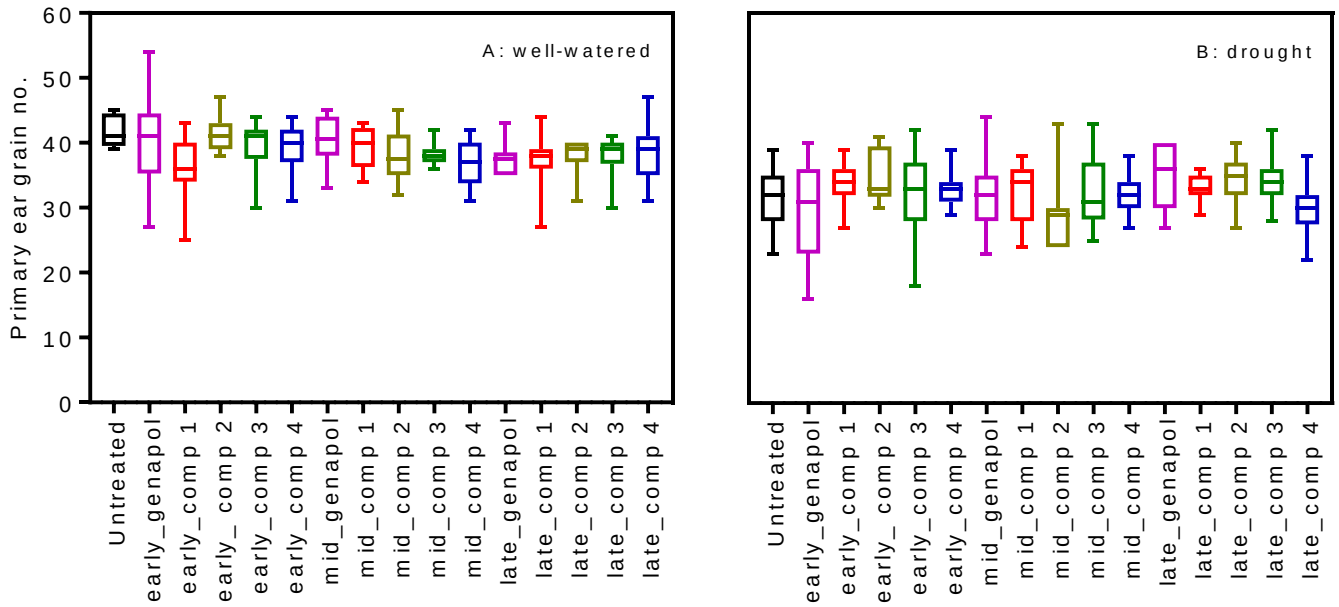

Figure 86A-B. Average grain number from the primary ear of (A) well-watered and (B) droughted plants. The box plots are colour coded by treatment and arranged according to application time: early, mid (mid-point) or late. (n=8-11).

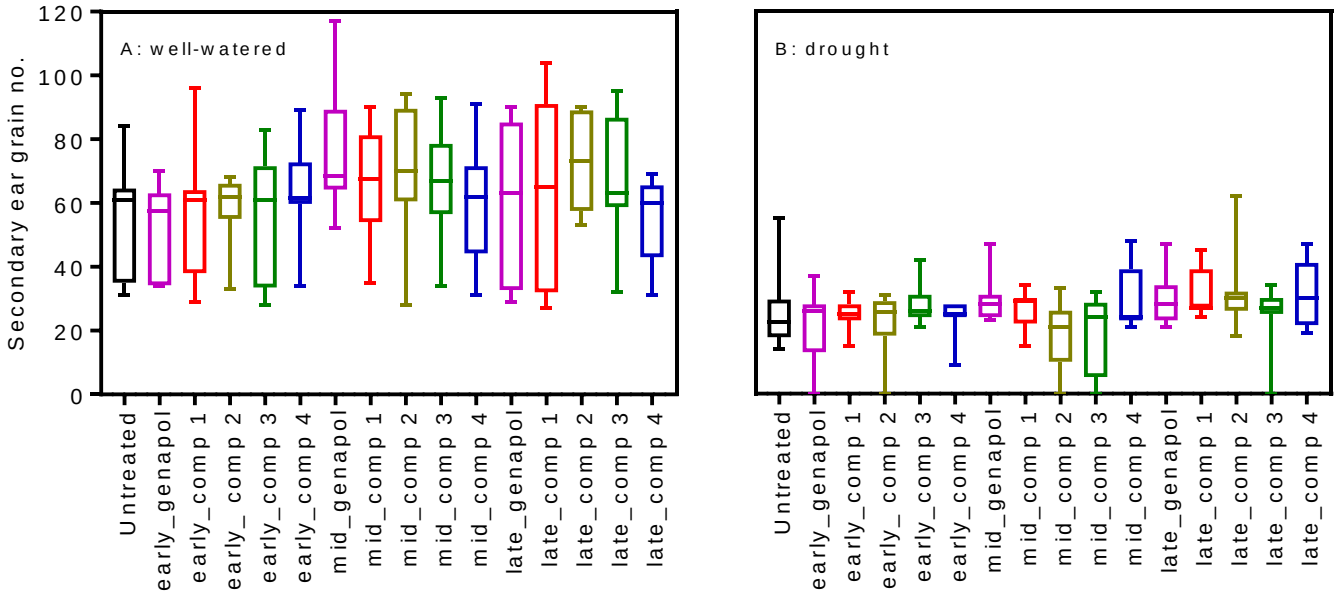

Figure 87A-B. Average grain number from the secondary ears of (A) well-watered and (B) droughted plants. The box plots are colour coded by treatment and arranged according to application time: early, mid (mid-point) or late. (n=8-11).

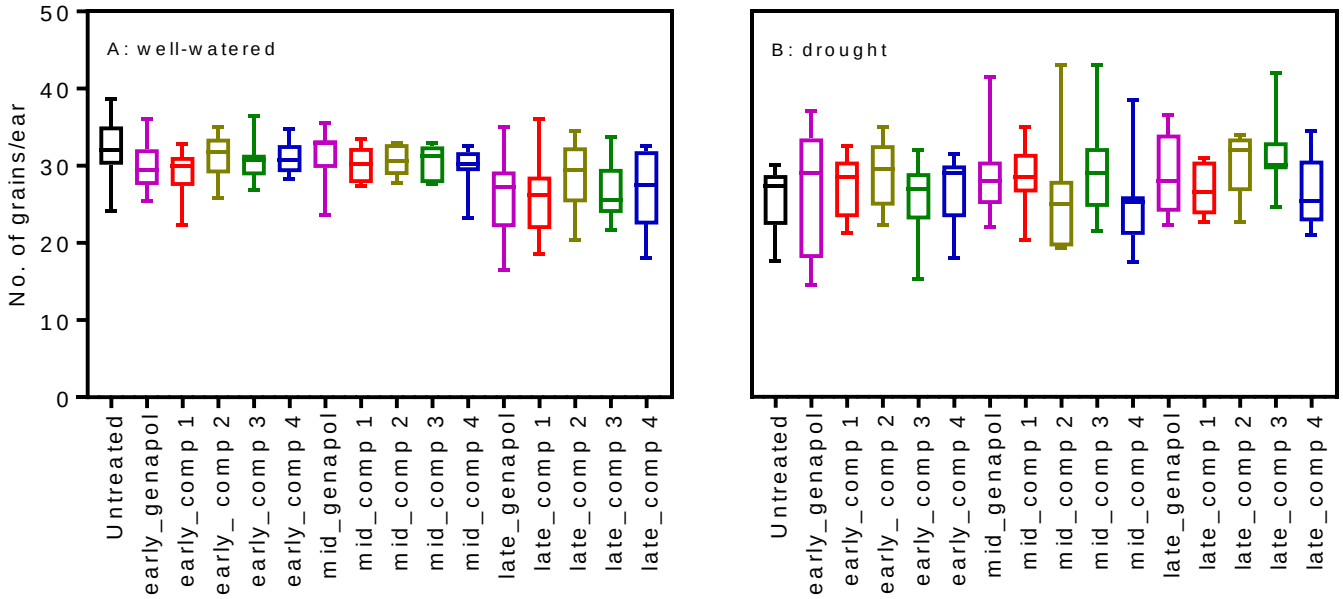

Figure 88A-B. Average number of grains per ear of (A) well-watered and (B) droughted plants. The box plots are colour coded by treatment and arranged according to application time: early, mid (mid-point) or late. (n=8-11).

Individual weight per grain reflects growth after flowering (BBCH 60/69). Thousand kernel (grain) weight (TKW) was calculated for each plant by dividing the total grain weight by the total grain number and multiplying by 1000. Under well-watered conditions spraying at the early time point did not affect TKW (Figure 89A). In contrast, mid-point treatment with compound 2, 3 or 4 led to significant reductions in TKW in comparison to untreated plants. Similarly, so did spraying with genapol or compounds 1 or 2 at the late application point. At this time point treatment with compound 4 enhanced TKW relative to genapol and compound 1. Under droughted conditions compounds and application time had less impact (Figure 89B). Only treatment with compound 2 at the mid-point application led to a significant reduction in TKW relative to untreated plants. These results suggest that chemical treatments were not significantly affecting grain number but some were impacting grain weight.

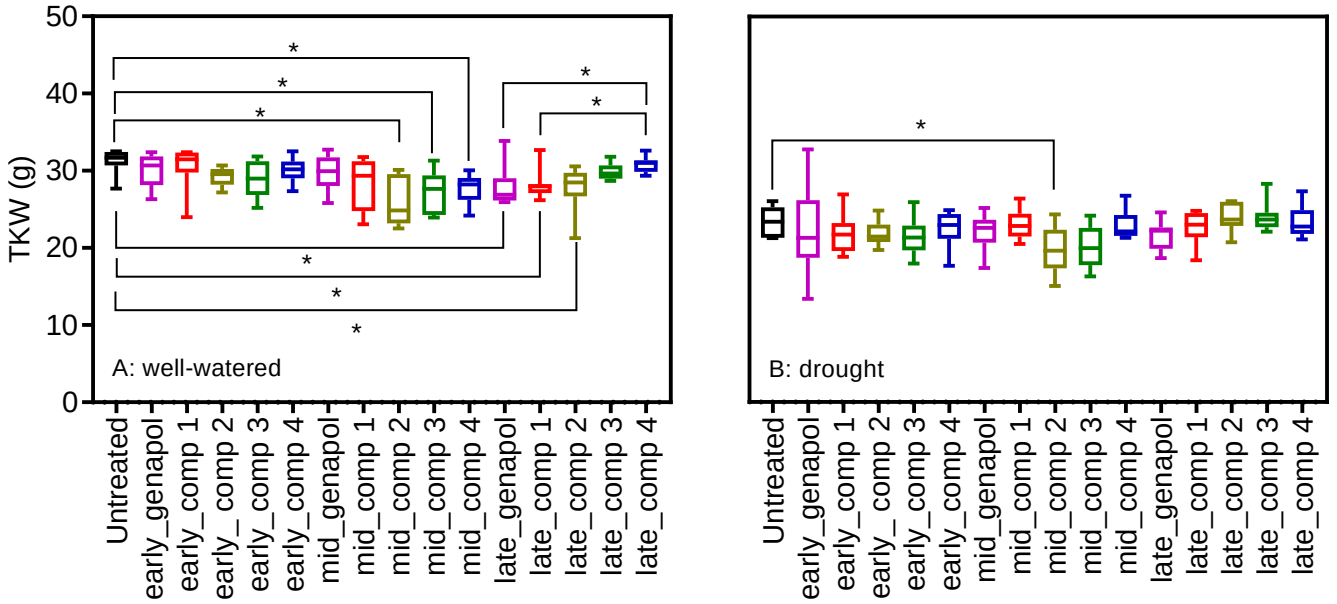

Figure 89A-B. Thousand kernel (grain) weight (TKW) of (A) well-watered and (B) droughted plants. The box plots are colour coded by treatment and arranged according to application time: early, mid (mid-point) or late. * = $P < 0.05$, Dunn test for multiple comparisons (n=8-11).

4.3.2. Parameters can be extracted from imaging data to measure growth and remove outliers

RGB images of plants were taken daily throughout the experiment although some days were missed due to technical faults. Imaging captured two side-view pictures of each plant arranged at 90 ° relative to each other (Figure 90A-B). The images contain pixel data which quantify object sum area (OSA). The average OSA from the two side-view images can be calculated and plotted over to time to measure growth. Figure 91 shows how plants grew over the course of the experiment. There was a significant impact of drought on OSA which became apparent after ~ 30 days after transfer (of plants into the chamber, dat) and was marked from ~ 40 days onwards. The ratio of green to yellow pixels in the image data quantifies the degree of senescence and is indicative of plant development and stress. Figure 92 shows how the green:yellow ratio changed over time. In well-watered plants the green:yellow ratio increased to a maximum ~ 50 dat and then declined as parts of the plants began to senesce. In droughted plants the maximum value was reached earlier, typically ~ 30 dat, after which the curves plateaued and then declined after ~ 50 dat. Relative to the untreated plants compound application generally resulted in increased variation within treatments.

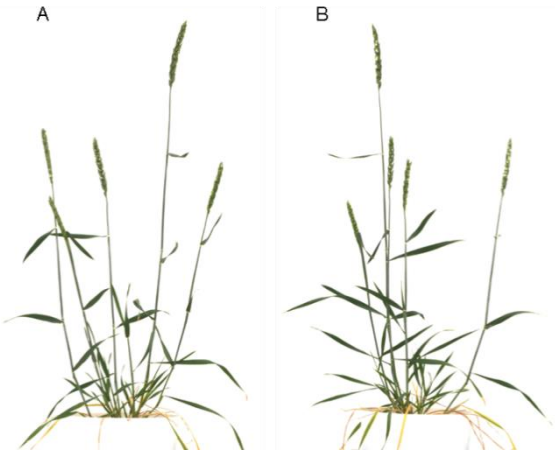

Figure 90A-B. Sample images from (A) side-view 1 and (B) side-view 2 which are 90 ° to each other.

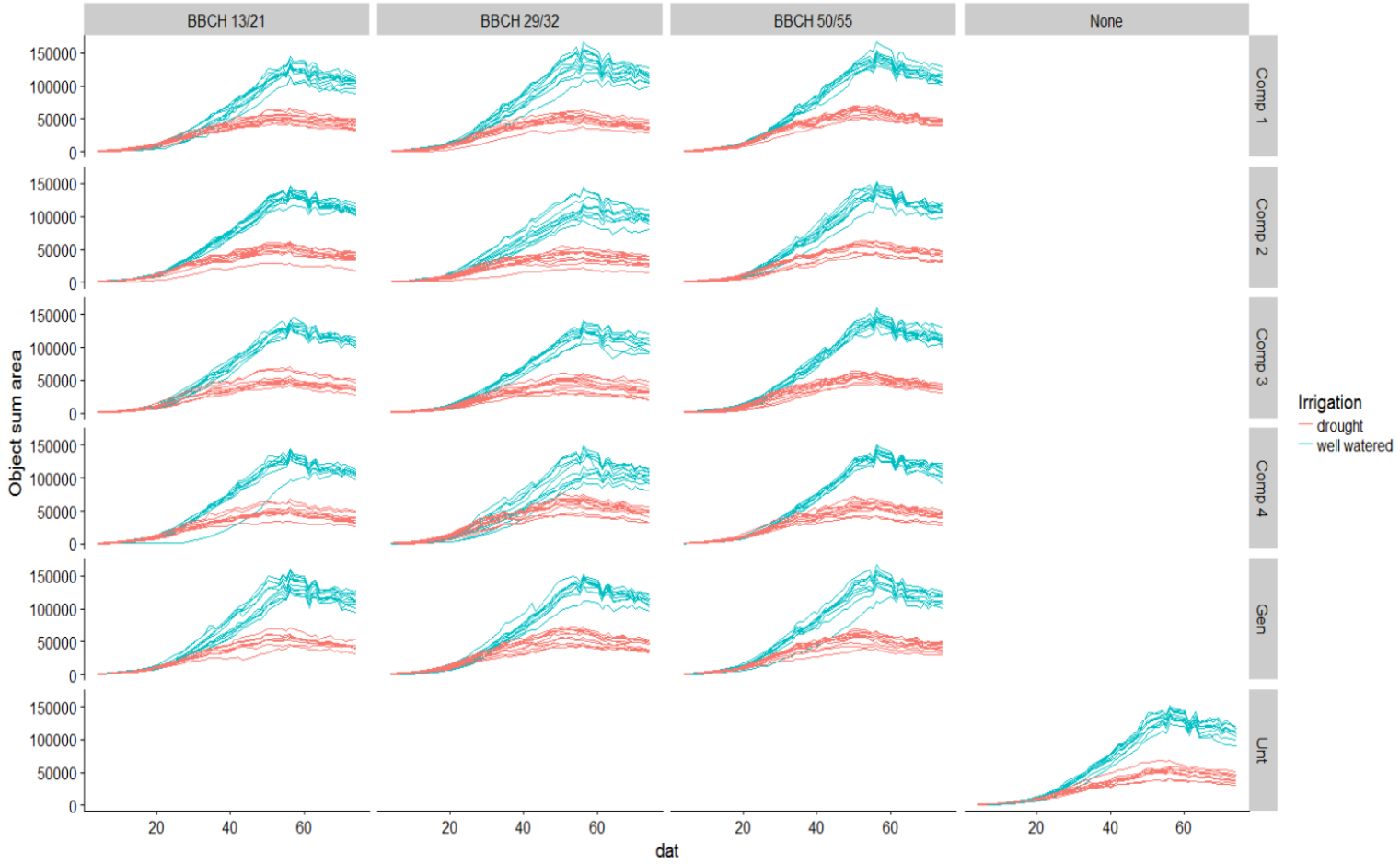

Figure 91. Growth of plants over the course of the experiment extracted from pixel data which contains values of object sum area. Data are arranged by application time and treatment and colour coded by irrigation. Unt = untreated, Gen = genapol, Comp 1-4 = compounds 1-4, dat = days after transfer.

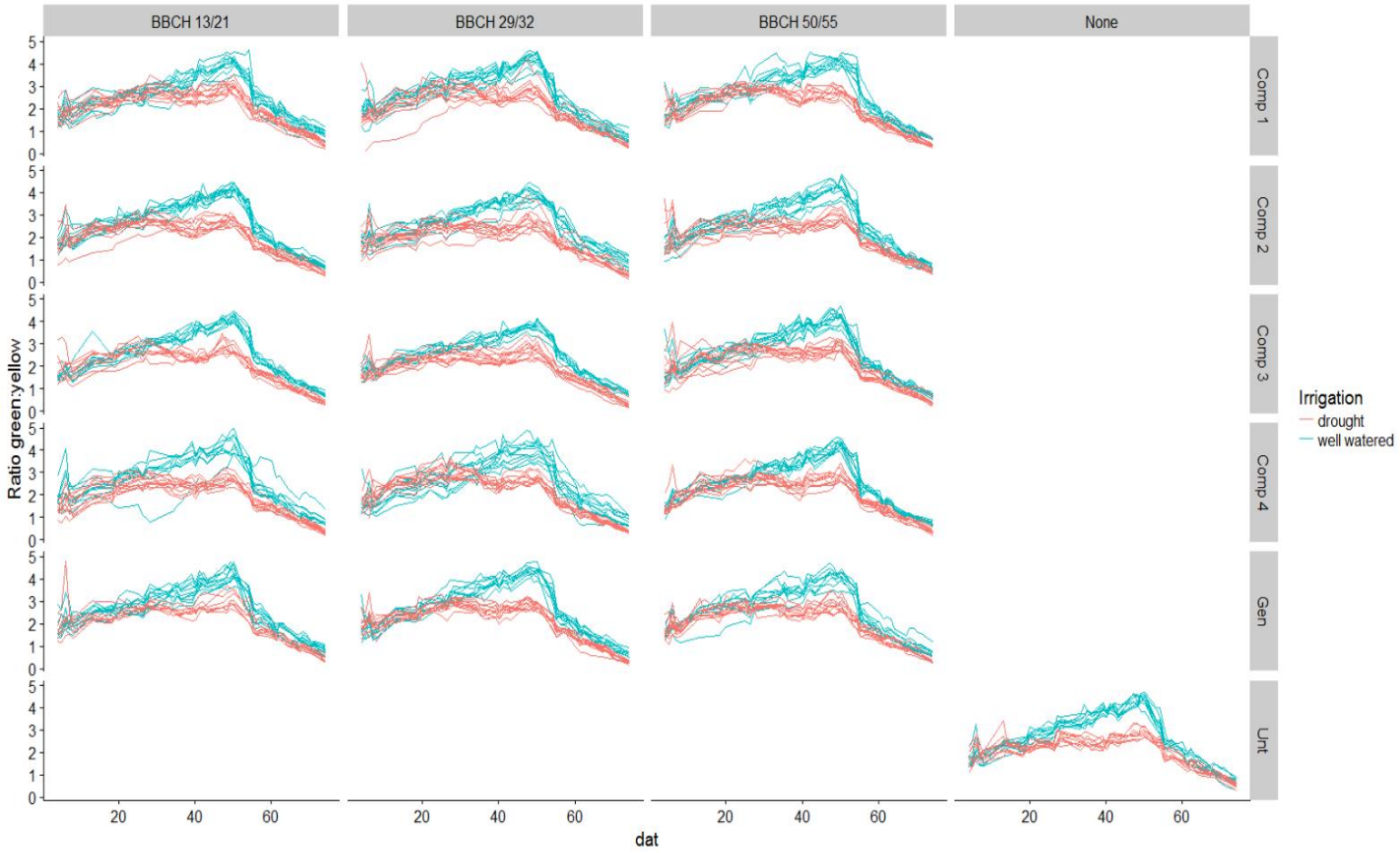

Figure 92. Changes in the green:yellow ratio over the course of the experiment extracted from colour class pixel data. Data are arranged by application time and treatment and colour coded by irrigation. Unt = untreated, Gen = genapol, Comp 1-4 = compounds 1-4, dat = days after transfer.

Three plants which failed to establish were easily identified and removed manually early in the trial. The OSA and green:yellow ratio curves indicated that the data set contained further outliers which were removed from the data set by applying an exclusion principle to the data (Figure 91; Figure 92). Plants were flagged for removal if their OSA or green:yellow ratio was more than two standard deviations away from the average values of that treatment. This degree of deviation from the treatment mean had to be observed before a compound was applied. This ensured that changes in OSA or green:yellow ratio that might have resulted from chemical treatment did not result in a plant been omitted from the data set, whilst genuine outliers which had failed to grow were removed. Six plants were identified for removal based on this principle, including the plant shown in Figure 93 which was treated with genapol at the late application point.

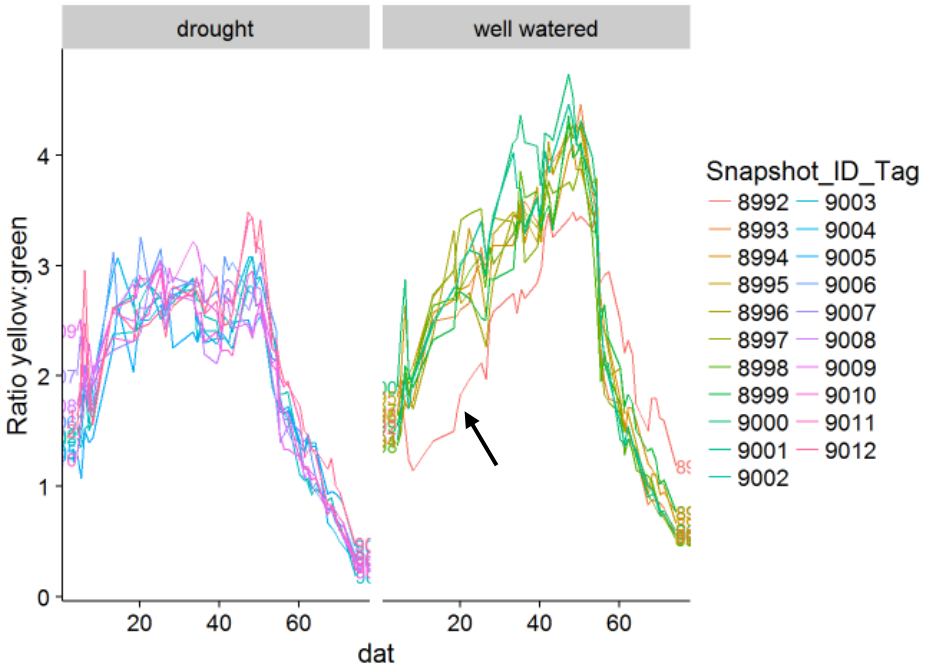

Figure 93. Green:yellow ratio of plants sprayed with genapol at the late application point over the course of the experiment. The arrow indicates an outlying replicate which was removed from the data set. dat = days after transfer.

4.3.3. Data processing and model selection

Modelling data allows more sophisticated analysis and the extraction of useful parameters in a more statistically robust manner than is possible to achieve with empirical methods. A classically used logistic growth model, which has a rise to a maximum, is unsuitable for this data set because of the decline in OSA observed towards the end of the experiment. The raw data were quite noisy and there was a considerable increase in variation over time so the data were log transformed before model fitting. Figure 94A-B shows raw and log transformed OSA data for the plants treated with compound 2 at the mid-point application. This sub-set of data is used in the following figures and tables to illustrate the model fitting process.

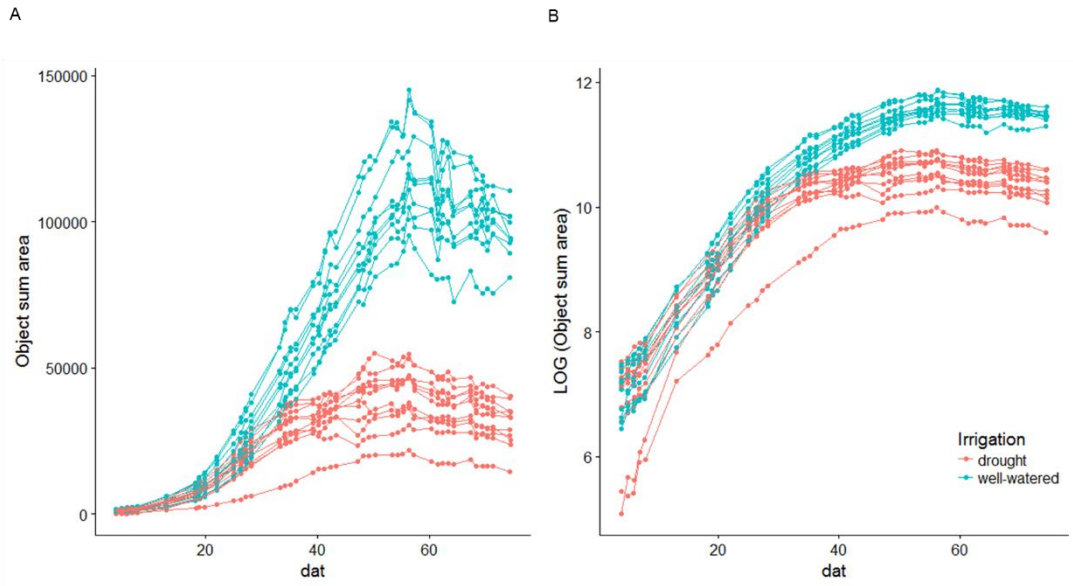

Figure 94A-B. Sample (A) raw and (B) log transformed object sum area data for well-watered (blue) and droughted (red) plants treated with compound 2 at the mid-point application.

A suitable model should be able to reduce the noise in the data but be flexible enough to capture the small changes in growth or green:yellow ratio that might occur following chemical treatment. A generalised additive model (GAM) was fitted to log transformed object sum area data using gam function in RStudio. GAMs have an

intrinsic smoothing function which fits knots at data points to smooth fits between different polynomial curves. Increasing the number of knots adjusts the degree of flexibility in the fit allowing subtle inflection points, such as those that might result following chemical application, to be detected in a way that is not possible using a polynomial model. Goodness of fit is quantified by the coefficient variance score (GCV) which decreases as the fit improves and vice versa. Figure 95 shows GAMs with different number of knots fitted to sample log transformed OSA data. Table 9 confirms that that increasing the knots from 3 to 7 improved the fit as the GCV decreased. Increasing to 8 knots resulted in a GCV increase indicating 7 knots was optimal for this data set. To confirm the suitability of the model the GAM was plotted to the raw OSA data. Figure 96A-B shows how the subtle inflections in the curve were picked up when more knots were added to the model. There was no observable pattern in the residuals of the raw OSA data with fitted GAM with 7 knots further confirming the suitability of the model (Figure 97). Additionally, a correlation term was added using the GAM mixture (gamm) function which corrected for the autocorrelation problem associated with the model. GAMs assume that residuals are identically and independently distributed. This is not logically fulfilled with time series values which are highly correlated with past values, meaning the errors in the model are correlated also, and a correction is required. The model was applied to OSA curves for each plant and all of the individual fits were manually inspected and are shown in the Appendix.

Several imaging time points were missed due to technical faults which led to discontinuities in the data. The GAM was used to predict OSA values at all time points and generate a continuous data set with a resolution of 1 day. The maximum value of OSA for each replicate can be extracted from the resulting data as shown in Figure 98. Maximum OSA quantifies the impacts of irrigation regime, treatment and application time on the growth potential of the plants. Additionally, measuring the time taken for plants to achieve maximum OSA can be informative as drought and chemical treatment may alter growth rate and development.

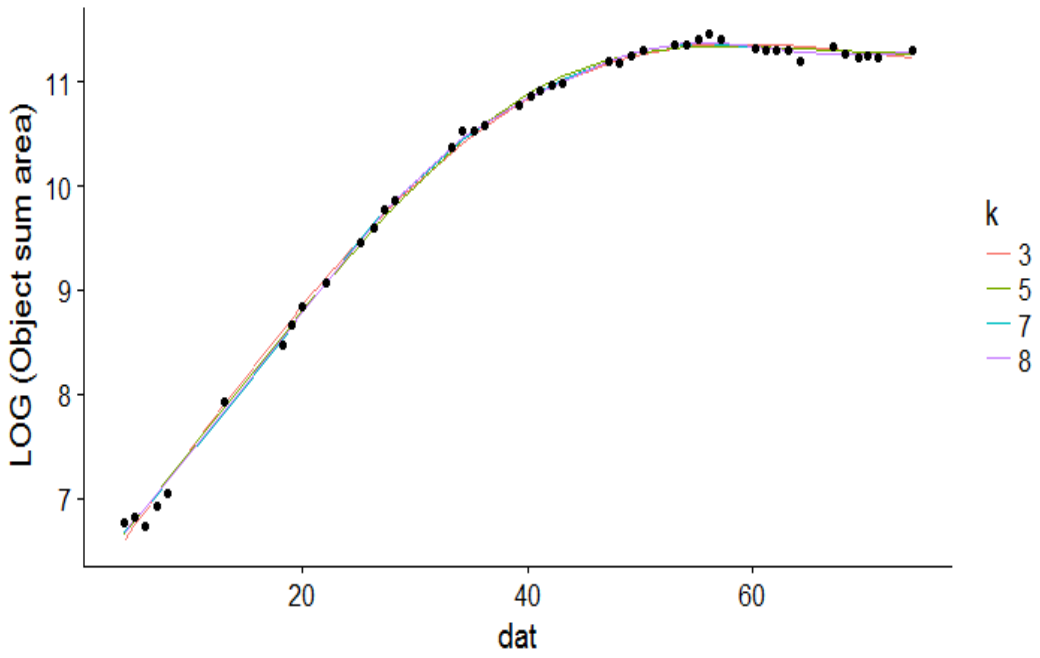

Figure 95. GAM with different number of knots (k) fitted to log transformed sample OSA data for plants treated with compound 2 at the mid-point application. The optimum k = 7 (see GCV in Table 9). dat = days after transfer.

Table 9. Coefficient variance score (GCV) of a GAM fitted with different number of knots to sample growth data from Figure 95.

Knots (k)	GCV
3	0.008204183
5	0.003644337
7	0.003376329
8	0.003462966

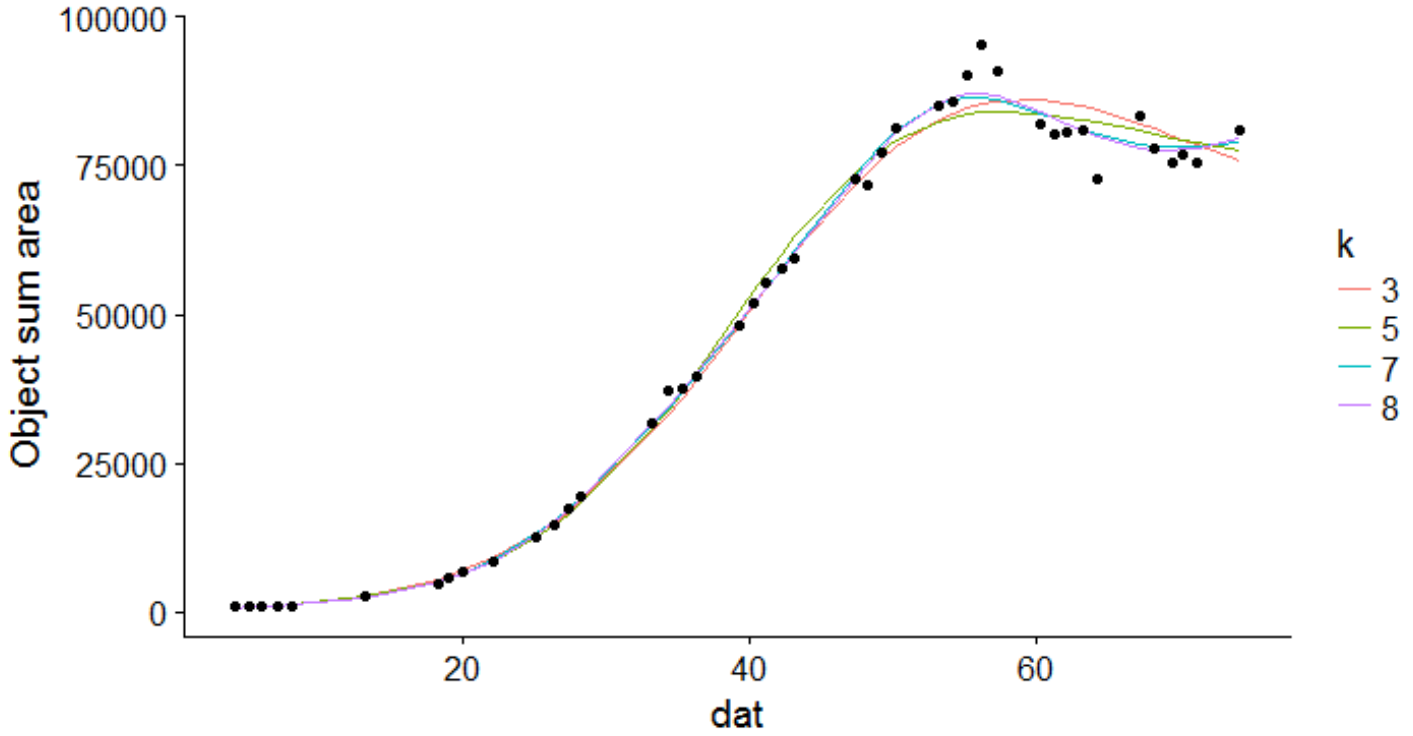

Figure 96. Corresponding raw OSA data to Figure 95 with GAM fitted. Increasing the knots (k) from 3 to 7 improved the fit of the model to the data. Increasing to k = 8 did not improve the fit. dat = days after transfer.

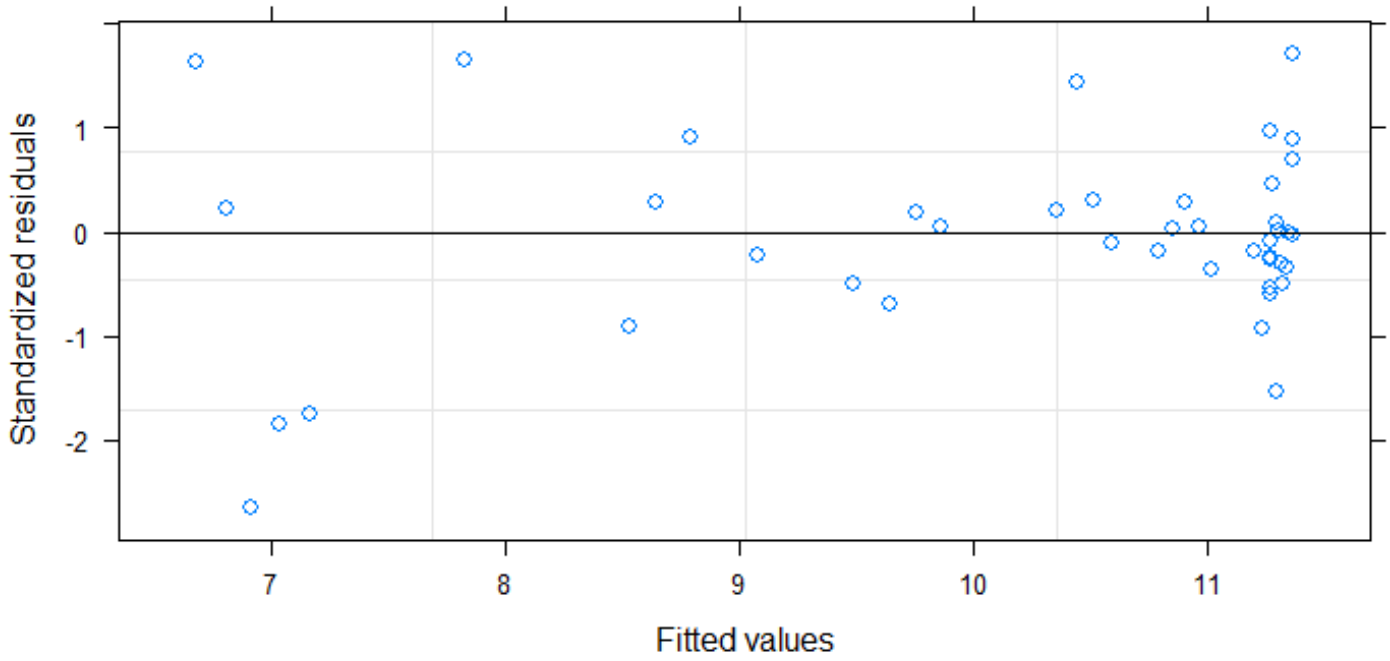

Figure 97. Residuals of the data with fitted GAM with k = 7 shown in Figure 96.

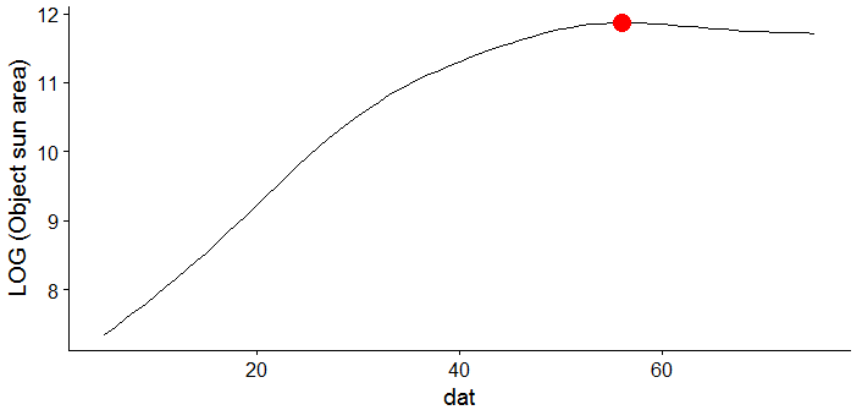

Figure 98. The extraction of maximum OSA (red dot) from the GAM (k = 7) fitted to log transformed OSA sample data. dat = days after transfer.

Figure 99 shows the impact of application time and compound treatment on maximum OSA under both well-watered and droughted conditions. Drought had the largest impact on maximum OSA with well-watered and droughted samples averaging 11.8 (± 0.1 S.D.) and 10.9 (± 0.2 S.D.) respectively ($P < 0.0001$). When applied at the early time point compound treatment did not alter maximum OSA and plants of all treatments of the same irrigation regime had similar values. However, spraying at the mid-point application led to increased variation within and between treatments. Under well-watered conditions treatment with compound 2 reduced maximum OSA relative to the untreated. By comparison, plants treated with compound 1 or 4 had significantly larger maximum OSAs than those sprayed with compound 2 or 3. There was no impact of compound treatment at the early application under droughted conditions either. There was increased variation among the mid-point treatments. Compounds 2 and 3 had smaller maximum OSAs than the plants treated with either compound 4 or genapol. Compounds had no impact at the late application under either irrigation regime which is not surprising given the proximity of application time to plants achieving maximum OSA.

Figure 100 shows the average time it took plants of each treatment to reach maximum OSA. Of all of the treatments drought once again had the greatest impact. Well-watered and droughted plants achieved maximum OSA in ~ 57.3 (± 1.6 S.D) and ~ 53.7 (± 2.2 S.D) days respectively ($P < 0.0001$). This is most likely because drought is

known to accelerate the rate of progression through life cycle stages. Relative to untreated plants of the same irrigation regime, chemical treatment did not significantly change the time taken to reach maximum OSA at any application point, except droughted plants sprayed with genapol at the mid-point application which reached maximum OSA ~ 3.6 days earlier than the untreated.

4.3.4. Maximum OSA was predictive of yield at the mid-point application

Relative to untreated plants chemical treatment at either the early or late application point had little impact on maximum OSA (Figure 99). This holds true for both irrigation regimes. Yield was similarly unaltered by chemical treatment at either of these application points (Figure 101). However, treatment at the mid-point application resulted in changes in maximum OSA under both well-watered and droughted conditions. Interestingly these changes appeared to predict the effect of a compound on yield. For example, under droughted conditions, spraying compound 2 or 3 led to slight reductions in maximum OSA relative to untreated plants. The reverse was true for plants sprayed with compound 4 or genapol, with compound one having little effect. At harvest, plants sprayed with compound 2 or 3 had significantly lower yields than untreated plants. Those treated with compound 4 or genapol had marginally greater yields although these differences were not significantly different to untreated plants. Compound 1 had comparatively little effect. The slight reductions in maximum OSA observed in well-watered plants treated with compound 2, 3 or 4 translated into marginal yield decreases relative to untreated plants, although these differences were not statistically significant. Table 10 summarises the impact of mid-point chemical treatment on maximum OSA and final yield relative to untreated plants. At this application time point maximum OSA was predictive of yield at harvest. In the majority of cases maximum OSA was achieved at least 39 days before plants were harvested and yield was measured. The ability to reliably predict the impact of a compound on yield this far in advance is desirable to the agro-chemical industry.

4.3.5. Under droughted conditions there was a relationship between maximum OSA and yield

Maximum OSA had been predictive of yield at the mid-point application suggesting there was a relationship between the two. Under droughted conditions there was a strong linear relationship between maximum OSA and yield at all application points, however this did not necessarily hold true under droughted conditions as the data were more scattered (Figure 102). The average data in Figure 103 suggest that under droughted conditions, the intensity of the stress was driving growth and yield, particularly in the mid-point treated plants. Although there was a similar pattern under well-watered conditions, it was not as strong indicating that other factors may have been influencing growth and yield.

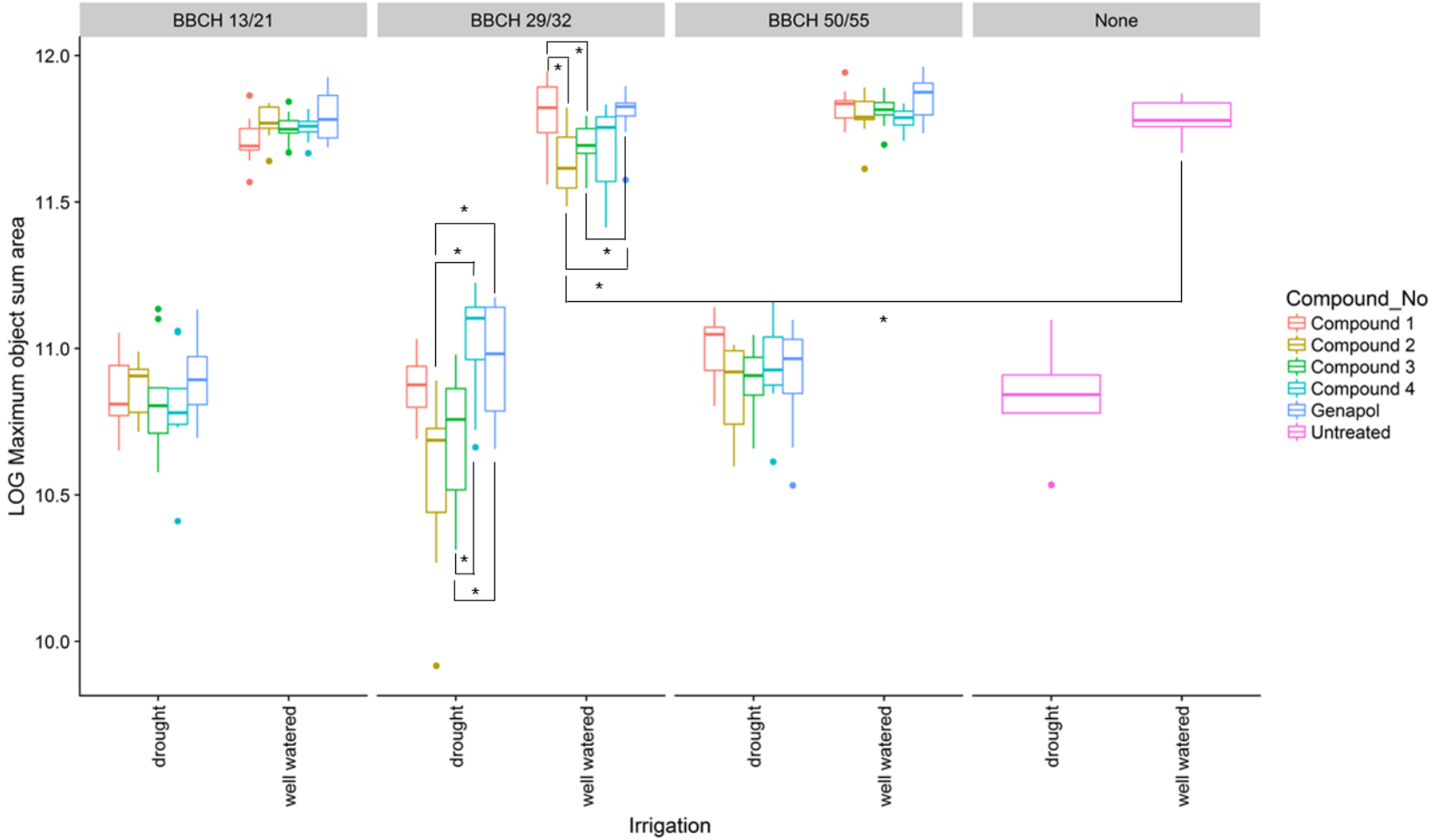

Figure 99. Average LOG maximum OSA for each treatment. The box plots are colour coded by treatment and arranged according to application time: early (BBCH 13/21), mid-point (BBCH 29/32) or late (BBCH 50/55). * = $P < 0.05$, Dunn test for multiple comparisons. (n=8-11).

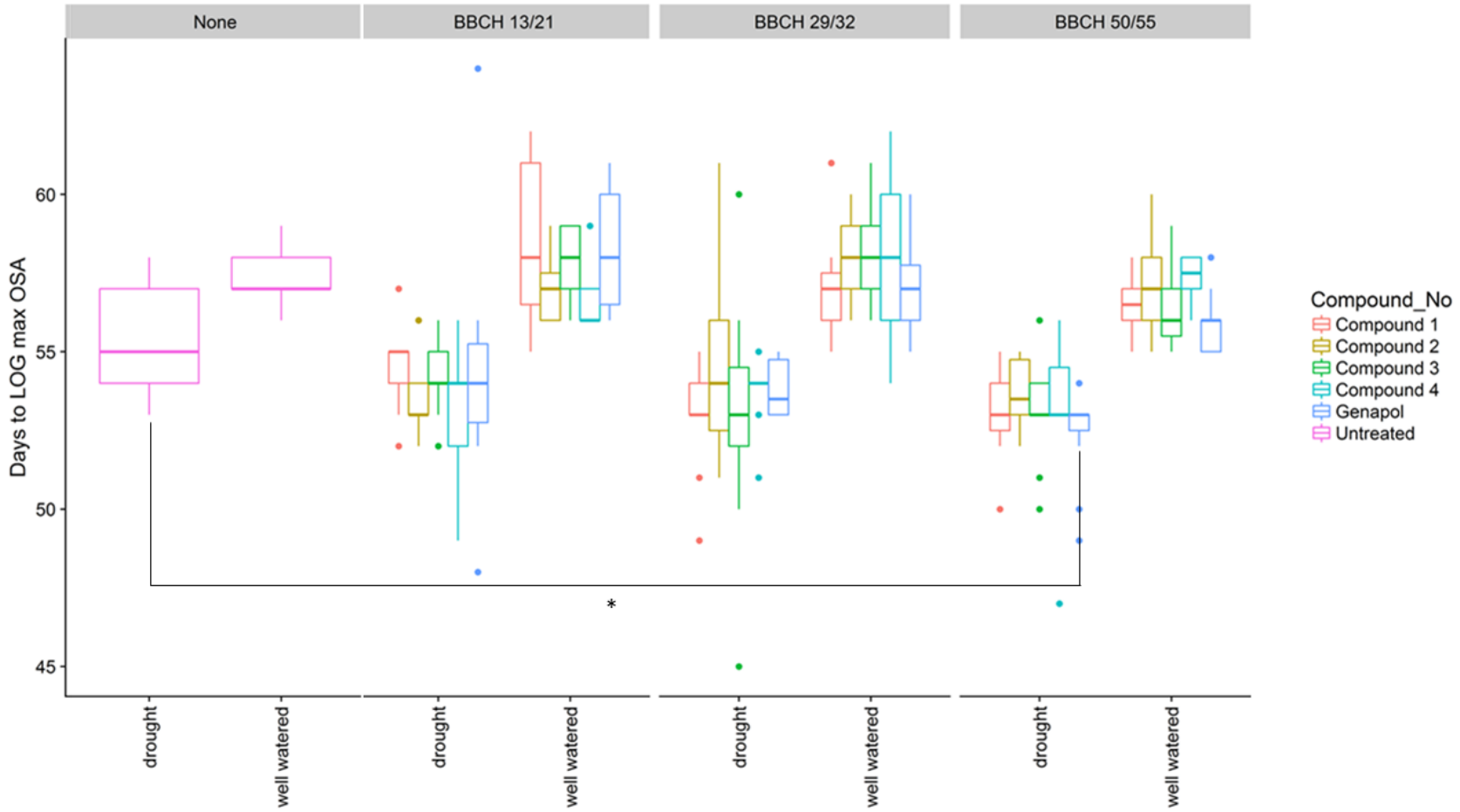

Figure 100. Average time taken to reach LOG maximum OSA. The box plots are colour coded by treatment and arranged according to application time: early (BBCH 13/21), mid-point (BBCH 29/32) or late (BBCH 50/55). * = $P < 0.05$, Dunn test for multiple comparisons. (n=8-11).

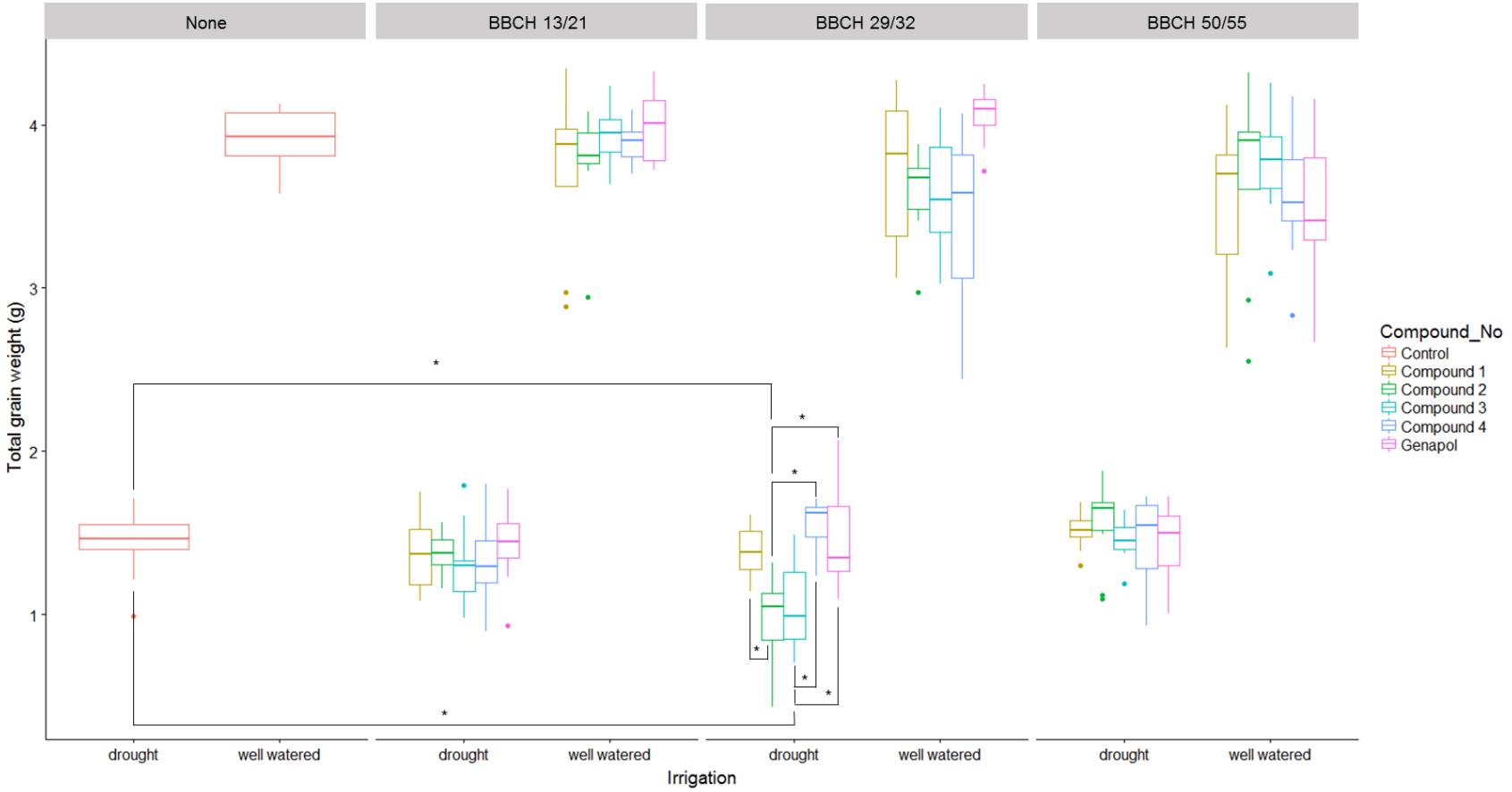

Figure 101. Yield measured by total grain weight. The box plots are colour coded by treatment and arranged according to application time: early (BBCH 13/21), mid-point (BBCH 29/32) or late (BBCH 50/55). * = $P < 0.05$, Dunn test for multiple comparisons. (n=8-11).

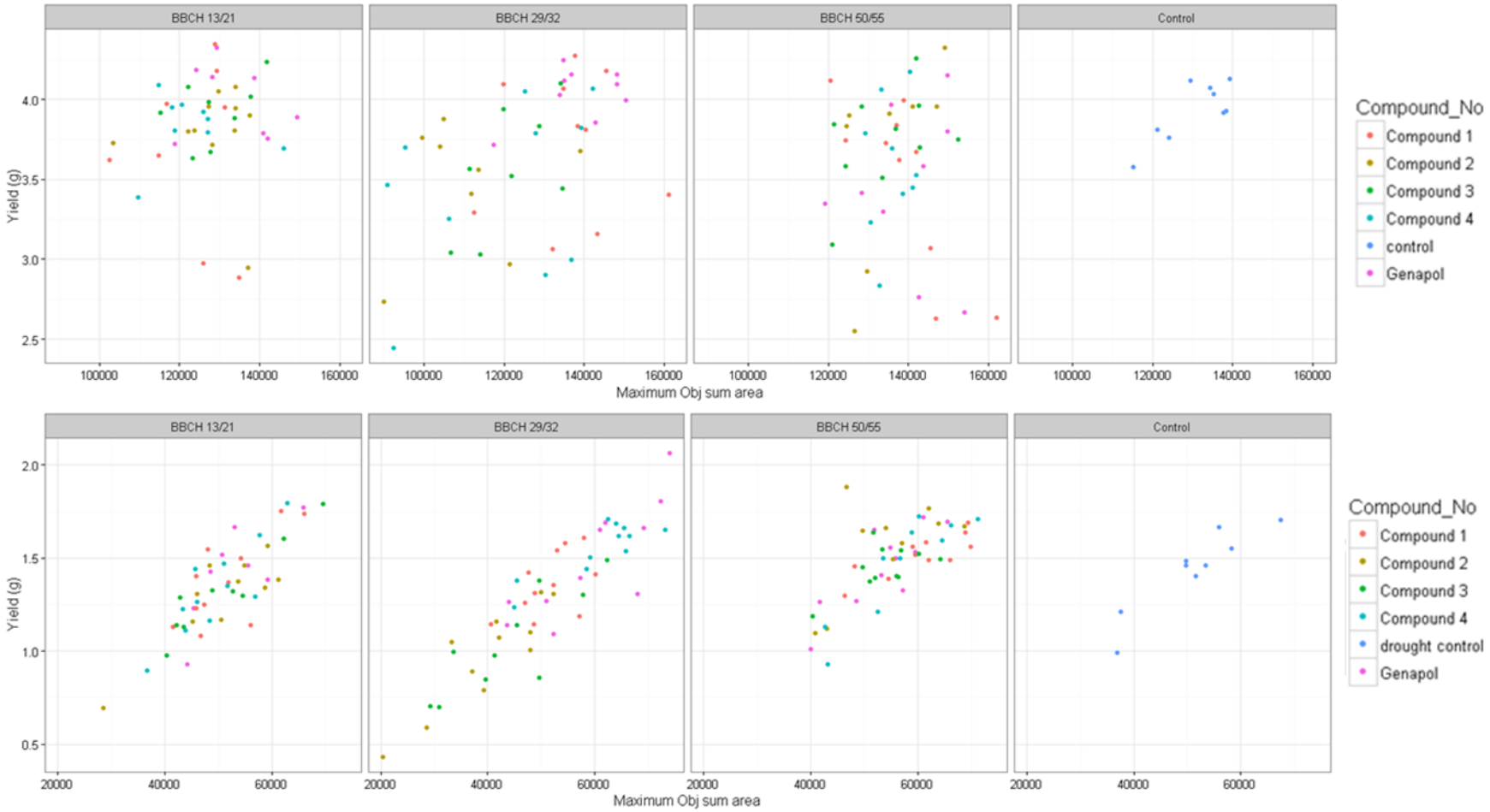

Figure 102. The relationship between maximum OSA and yield (total grain weight) in well-watered (top panel) and droughted (bottom panel) plants. The plots are arranged according to application stage: early (BBCH 13/21), mid-point (BBCH 29/32) and late (BBCH 50/55). Untreated control data are shown separately. (n=8-11).

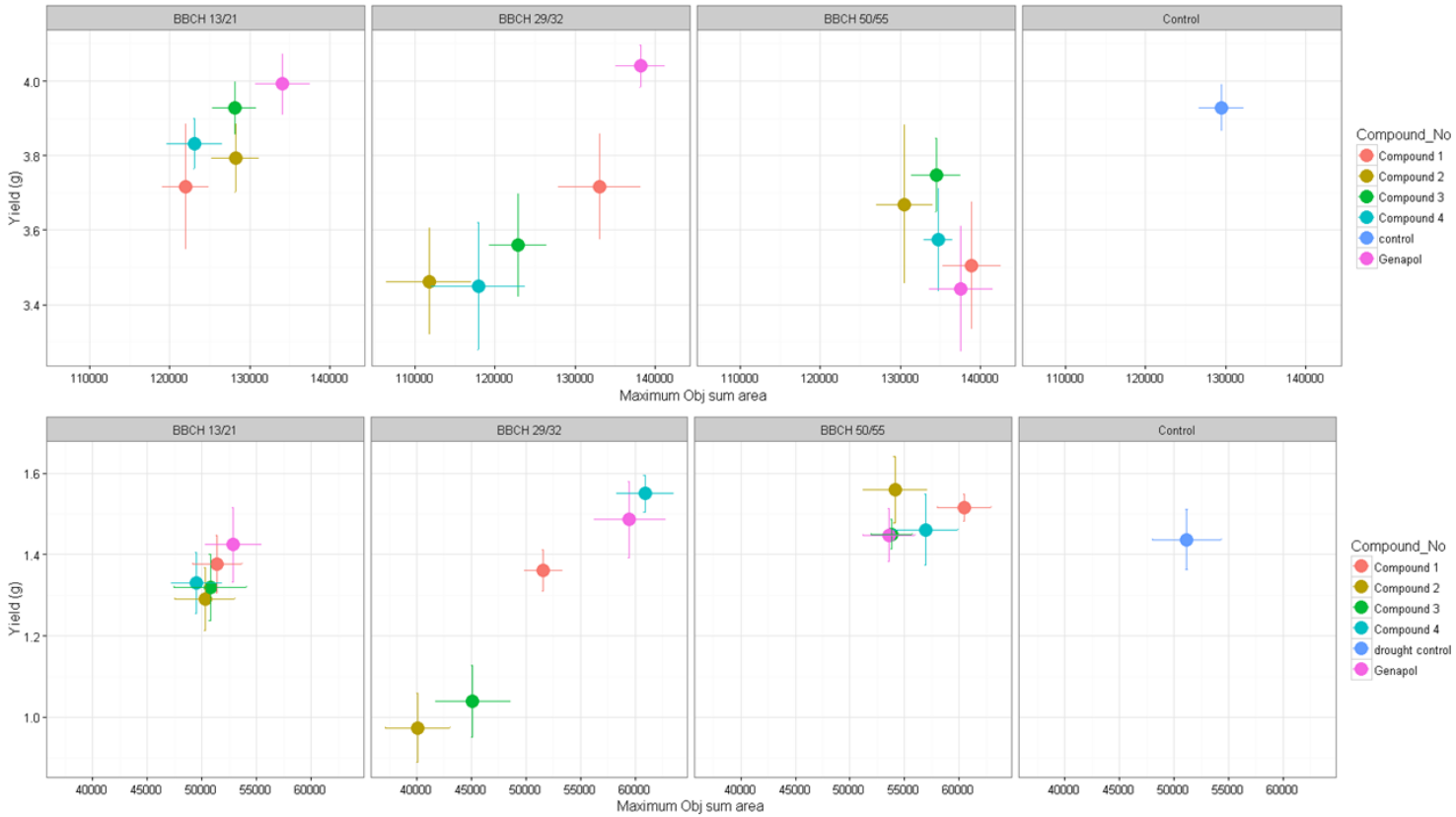

Figure 103. The relationship between maximum OSA and yield (total grain weight) in well-watered (top panel) and droughted (bottom panel) plants. The plots are arranged according to application stage: early (BBCH 13/21), mid-point (BBCH 29/32) and late (BBCH 50/55). Untreated control data are shown separately. Values are the mean (n=8-11) ± SD.

Table 10. Relationship between LOG maximum OSA and yield (average total grain weight per plant, g). Plants were treated at the mid-point application point (BBCH 29/32). The impact of treatment on LOG max OSA and yield is quantified as % relative to the untreated plants of the same irrigation regime. Yield data were tested for significance against the untreated plants of the same irrigation regime using a Kruksal-Wallis test with Dunn test for multiple comparisons (P values are listed). Values are the mean (n=8-11) ± SE.

Irrigation	Treatment (applied at mid-point)	LOG Max OSA (± SE)	% relative to untreated	Yield (g) (± SE)	% relative to untreated	P value
Well-watered	Untreated	11.787 (0.021)	N/A	3.928 (0.062)	N/A	N/A
	Genapol	11.797 (0.028)	0.1	3.985 (0.074)	1.5	0.569
	Comp 1	11.799 (0.037)	0.1	3.717 (0.143)	-5.4	0.564
	Comp 2	11.638 (0.04)	-1.3	3.463 (0.143)	-11.8	0.201
	Comp 3	11.688 (0.029)	-0.8	3.53 (0.12)	-10.1	0.271
	Comp 4	11.676 (0.045)	-0.9	3.449 (0.171)	-12.2	0.212
Drought	Untreated	10.822 (0.059)	N/A	1.412 (0.07)	N/A	N/A
	Genapol	10.956 (0.062)	1.2	1.486 (0.093)	5.2	0.976
	Comp 1	10.871 (0.032)	0.5	1.361 (0.051)	-3.7	0.748
	Comp 2	10.562 (0.086)	-2.4	0.974 (0.084)	-31	0.012
	Comp 3	10.688 (0.071)	-1.2	1.039 (0.088)	-26.5	0.035
	Comp 4	11.023 (0.055)	1.9	1.55 (0.044)	9.8	0.562

4.3.6. Could the impacts of compounds be predicted earlier using the GAM?

The impacts of compounds applied at the mid-point application were visible at the time of measuring maximum OSA which is a product of plant growth up to that point. The GAM fitted to the LOG OSA data was used to investigate if the changes in growth induced by compound application could be observed earlier. Growth was normalised to the day of compound application and displayed for the 5 days prior to treatment and the following 30 days. Untreated and treated plants displayed different growth kinetics, so for the purposes of modelling genapol was used as the reference control as all plants sprayed with a compound were also treated with genapol. Compound 4 led to growth stimulation under both irrigation regimes which was visible ~ 10 days after application (Figure 104). Relative to genapol the remaining compounds reduced growth, which was visible after a similar amount of time. Except in the case of compound 1, these growth changes were reflected in the values of maximum OSA meaning that the impacts of compounds could be predicted ~ 6-14 days before maximum OSA was attained (Figure 99).

From an industrial perspective it is desirable to be able to predict the quantitative impacts of compounds on yield in as shorter time as possible from the start of the experiment. The model was used to determine if the early application point highlighted growth changes in the same way as the mid-point. Figure 105 shows that there were no observable growth changes in the days following the early application, perhaps because the plants had a relatively large relative growth rate at this point and the compounds had a proportionally smaller effect by comparison. However, the effects of compound application were predicted using a GAM fitted to growth data much earlier than was possible by measuring final yield parameters.

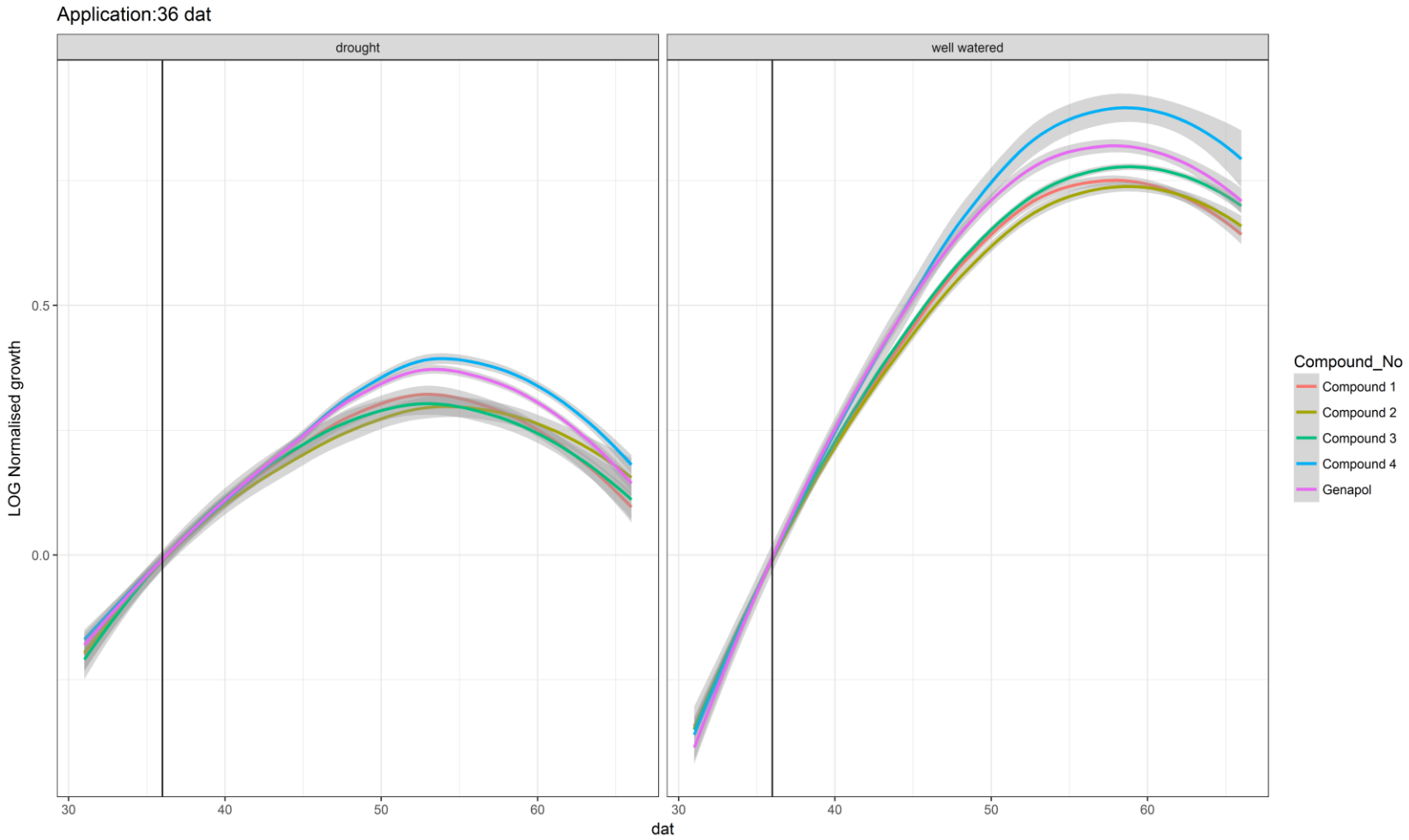

Figure 104. LOG OSA normalised to the mid-point day of application 36 days after transfer (dat). Data shown for the 5 days prior to application and the following 30 days. (n=8-11).

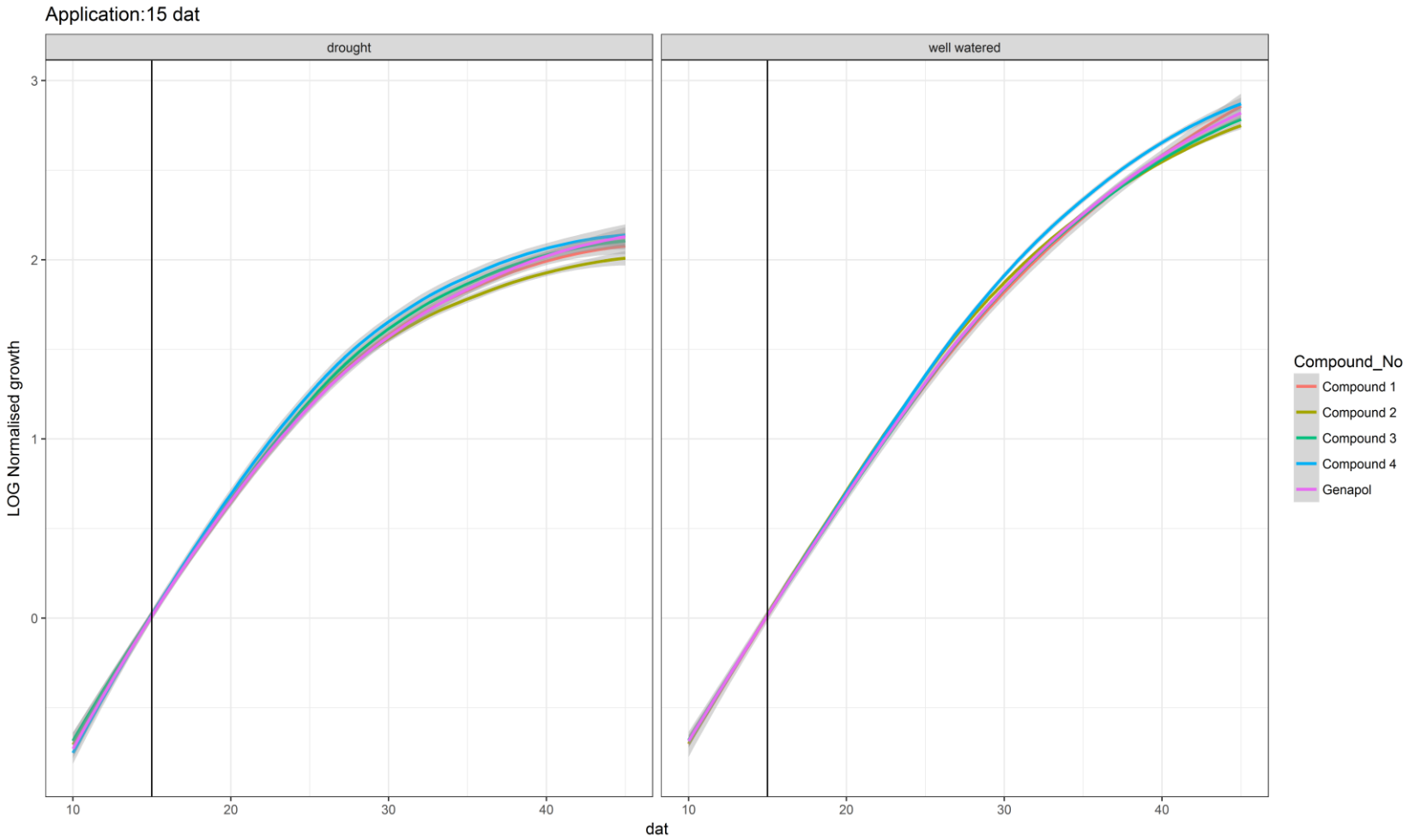

Figure 105. LOG OSA normalised to the early application day of treatment 15 days after transfer (dat). Data shown for the 5 days prior to application and the following 30 days. (n=8-11).

4.3.7. There was no apparent stay-green effect resulting from chemical treatment

When sprayed at the late application point (50 dat) some treatments slightly enhanced maximum OSA and yield under droughted conditions (Figure 99; Figure 103). Because of the proximity of the application point to the realisation of maximum OSA, it was probable that there was not enough time for potential growth changes to take effect and be measured, so it was not sensible to use growth data to assess the impact of compounds at this stage. Instead, the GAM was fitted to % green pixel data to investigate the onset of senescence and examine if PARP inhibitors conferred a stay-green response which would allow plants to keep photosynthesizing during grain filling. Values of % green ~ 13 days after application were assessed for significant differences between treatments. No significant stay-green effect resulting from any chemical treatment was observed and % green pixels declined at a similar rate in all plants (Figure 106). Interestingly, under well-watered conditions most treatments led to slight yield reduction indicating a cost/benefit trade-off to application (Figure 101).

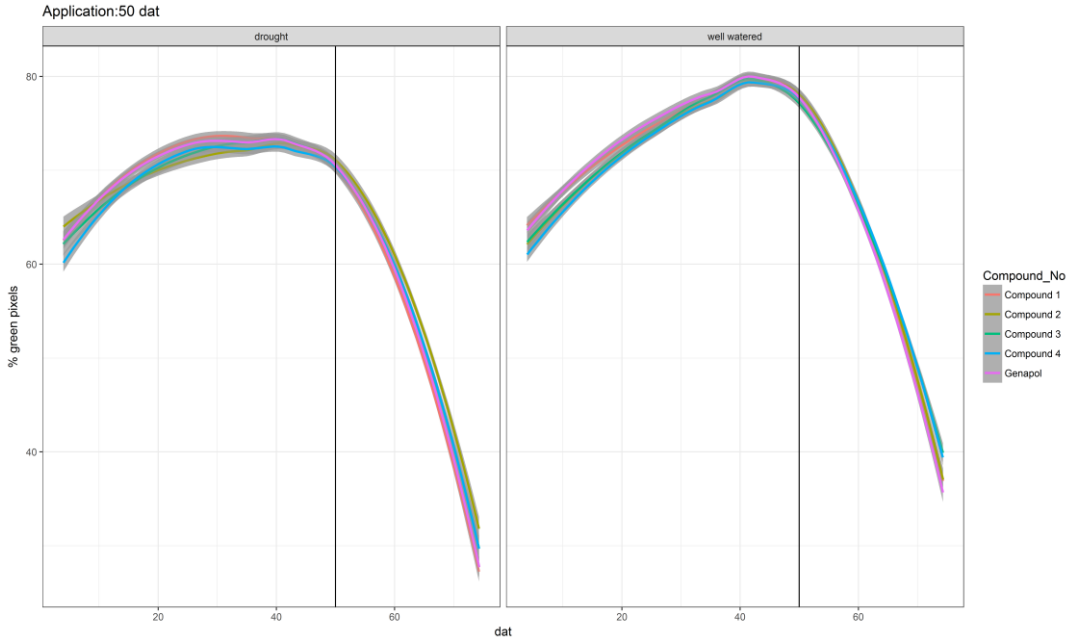

Figure 106. LOG % green pixels normalised to the late application day of treatment 50 days after transfer (dat). Data shown for the 45 days prior to application and the following 25 days. (n=8-11).

4.4. Discussion

Enhanced growth during the vegetative period of cereal crops has been said to contribute to increased yield because more assimilate is available for translocation into the grain during grain filling (Asseng & van Herwaarden, 2003; Yang & Zhang, 2006). Several studies have suggested that PARP-deficiency preserves or enhances growth under unstressed and stressed conditions. Accordingly PARP inhibition has been suggested as a potential route to increasing crop yield, particularly in stressed environments (Vanderauwera *et al.*, 2007). However, the majority of studies of PARP inhibition in plants have been *in vitro* or have involved relatively short-term assays (or both), neither of which are conditions which represent those a crop plant might experience in the field. Relatively little work published quantified the yield of PARP-deficient plants. Unpublished results by Block and Metzlaff in Vanderauwera *et al*., (2007) claim that PARP-deficient *B. napus* plants showed unaltered yield under unstressed conditions, but had ~ 40-60% yield increase relative to wild-type plants upon exposure to drought. However, these studies used RNAi technology and from a commercial perspective, such a genetic approach is out of the question across the European continent for the foreseeable future. Consequently, there was a need to investigate the impact of chemical PARP inhibitors on crop yield which this work aimed to achieve.

The impact of PARP and PSII inhibitors on the growth and yield of *T. aestivum* in response to drought was studied using a phenomic approach including non-invasive, automated imaging and watering. Continuous RGB imaging during the whole life cycle of the plants was used to quantify growth. A generalised additive model (GAM) was fitted to the growth data and used to predict values. The impact of drought was evident in the growth data around 30 days after the plants were transferred into the climate chamber, indicating the onset was relatively early in the life cycle (Figure 91; Figure 94A). The effect was visible in the phenotype at BBCH 29/32, around 35 days after transfer (Figure 80A-B). The GAM was used to extract values of maximum OSA which was reached earlier in droughted plants, likely because stress is known to accelerate development (Figure 98; Figure 100) (Wan *et al*., 2008; Farooq *et al*., 2014).

Because maximum OSA is a product of the growth prior to its measurement, all droughted plants had significantly lower values than well-watered plants, further demonstrating the early-onset, severe nature of the stress (Figure 99). It would be useful to use the water data from the trial to determine how plants were using the applied water.

Drought had a severe adverse effect on yield relative to well-watered plants (Figure 101). Grain number and grain weight are the primary determinants of yield in wheat (Griffiths *et al.*, 2015). Grain number is determined by growth from flag leaf emergence to flowering (BBCH 37-39/59) and grain weight reflects growth after flowering (BBCH 60/69) (AHDB, 2015). However, a pre-determinant of both of these components is the number of ears per plant, which is reflective of growth from tillering to flag leaf emergence (BBCH 20/37-39). The results suggest that the most significant impact of drought was on the number of ears per plant (Figure 82A-C; Figure 83A-B). This affirms the evidence that drought had an early adverse impact and suggests that the intensity of the stress was perhaps too severe, and was initiated too quickly. The negative impact of drought on total grain number per plant was a result of plants producing fewer ears. Obviously a plant with a lower number of ears has a reduced capacity for total grain number and, by extension, total grain weight per plant. However, the average number of grains per ear was only slightly reduced in droughted plants (Figure 88A-B). This suggests that the stress was limiting ear number. Plants produced the amount of ears to support the grain they could fill under stress. This is consistent with the view of Sinclair & Jamieson, (2005) who suggest that grain number is a consequence of resource accumulation rather than a yield determinant. In this way the number of grains is reflective of the condition of a plant and its ability to accumulate resources throughout the vegetative stage. Because of the severity of the drought, growth was perturbed early and the number of ears per plant was restricted. Additionally, resource accumulation would have been limited in these plants. This, in addition to stress pre- and post-anthesis, would have reduced the grain filling potential of droughted plants and reduced yield (Pheloung & Siddique, 1991; Schnyder, 1993; Yang & Zhang, 2006; Dolferus *et al*., 2011). Additionally, the accumulation of ABA during drought stress can accelerate

senesce and reduce the length of the grain filling period (Yang & Zhang, 2006). It has been shown that there is often an inverse correlation between grain number and size (Cristina *et al*., 2016; Abdipour *et al*., 2016). These results do not necessarily support this relationship. Well-watered plants produced more grain and had higher values of TKW than droughted plants. However, care should be taken when interpreting this relationship because of the severity of the stress.

No PARP or PSII inhibitor led to significantly enhanced yield at harvest under either irrigation regime (Figure 101). Out of the 30 treatments, 2 led to significant decreases in yield relative to their respective control – one PARP and one PSII inhibitor. The majority of the impacts of these two compounds classes on yield were small and, except in a few cases, invariably negative. This indicated that there was a cost associated with application which is consistent with the results in Chapter 3. Under some conditions there appeared to be a slight (but non-significant) benefit to the application of genapol. It is perhaps not surprising for PSII inhibitors to reduce yield given that they inhibit electron transport downstream of photosystem II, preventing the conversion of absorbed light to electrochemical energy, and result in the build-up highly reactive oxidative species which damage the photosynthetic machinery and affect cellular integrity (Fuerst & Norman, 1991; Murata *et al*., 2007). The understanding of the negative impact of PARP inhibition is less clear however.

The intention of this experiment was to determine if inhibitors could protect yield under stress at particularly vulnerable life cycle stages, around stem elongation and anthesis (Dolferus *et al*., 2011). In order to achieve this compound application was split between three time points. It was hypothesised that, by directing the application time to the phenological stages of development which are moist susceptible to stress, a protective compound might preserve yield under drought. The early application point was selected to investigate if the compounds made plants more tolerant to early-onset drought by augmenting stress response (as discussed in Block *et al*., 2004). However, no significant impacts on yield were observed for any treatment at this time point perhaps indicating that the effect of the compound had worn off (Figure 101). The two later points were selected because they are known to be sensitive to drought stress (Dolferus *et al*., 2011). At the mid-point application

plants sprayed with some compounds had significantly increased yields in comparison to other compounds, but not relative to the untreated plants. Relative to untreated samples, only significant reductions were measured.

Under droughted conditions there was some evidence that maximum OSA and yield were enhanced by the application of PARP and PSII inhibitors at the late time point. It was hypothesised that the compounds might have a stay-green effect whereby they delayed senescence, allowing plants to continue photosynthesising during the grain filling period, resulting in larger values of maximum OSA and yield (Christopher *et al*., 2016; Rebetzke *et al*., 2016). In contrast, several studies suggest that delayed senesce may have an adverse impact on yield because of poor re-mobilisation of stored assimilates, a process which requires the initiation of senescence (Mi *et al*., 2002; Gong *et al*., 2005; Yang & Zhang, 2006). The GAM predicted the decline of % green area and, by extension, the onset of senescence. In particular, whole-plant senescence at the end of the life cycle was measured, as opposed to the normal death of tissue throughout during development. No significant stay-green effect was observed as a result of compound application (Figure 106).

Given the intensity of the stress, it is likely that potentially smaller impacts of compounds might have been masked. Furthermore because of the limited replication (10) of the untreated samples, it is possible that these plants performed better than would usually be expected, which would skew the results. On reflection, the experimental setup was perhaps unsuitable for investigating the impact of application time.

As stated earlier, growth was quantified throughout the experiment and maximum OSA was quantified using the GAM. A key finding of this work is that there was a strong linear relationship between maximum OSA and yield (total grain weight) at the mid-point application, particularly under droughted conditions (Figure 102; Figure 103). This did not necessarily hold true under well-watered conditions although there was some evidence of a weaker relationship. Because maximum OSA is determined by growth beforehand this suggested that the intensity of the stress was driving growth and yield. Under well-watered conditions other factors may have been more crucial in affecting growth and yield, such as sink strength (Reynolds *et al*., 2005;

Miralles & Slafer, 2007). The relationship between maximum OSA and yield under droughted conditions meant that it was possible to predict the impact a compound would have on yield by measuring maximum OSA, which was achieved > 45 days earlier than measuring yield at harvest. Further to this, using the GAM it was possible to detect the growth changes resulting from compound application ~ 10 days after spraying, which shortened the time by an additional 9 days (Figure 104). This is of significant potential application in agro-chemistry as it dramatically shortens the time required to get an accurate measure of the impact of a compound *in planta*. The data modelling can be applied to any compound type (e.g. herbicides, defence primers).

The work in this chapter aimed to quantify the impact of PARP and PSII inhibitors on yield. Studies of PARP inhibition in particular have primarily been *in vitro*, short-term and have utilised genetic techniques (or a combination of all three). It was therefore necessary to determine the impact of inhibitors on whole-plants, in soil. Although no favourable impacts were recorded, by modelling growth data it was possible to predict the impact of compounds on final yield much earlier than measuring yield itself. This ability was dependent on drought stressed conditions at BBCH 29/32. This key finding is of great potential commercial application.

In summary:

- PARP and PSII inhibitors had generally negative impacts on growth and yield in *T. aestivum*.
- There was a strong linear relationship between growth and yield, observed most markedly under the stressed condition, which allowed the effects of compounds on yield to be predicted earlier than measuring at harvest.

Chapter 5

5. The impact of PARP deficiency on photosynthesis and gas exchange

5.1. Introduction

Chemical PARP inhibitor application reproducibly enhanced survival in response to severe drought in multiple independent experiments described in Chapter 3, suggesting that the compounds were of benefit to plants under stress. An initial hypothesis was that stress reduces electron transport rate and that PARP deficiency might alleviate the stress, reducing the negative impacts on photosynthesis. This hypothesis was formed because of the increased survival observed in Chapter 3 and as several studies suggested that PARP-deficient plants had enhanced growth relative to controls (Block *et al*., 2004; Schulz *et al*., 2012, 2014). Enhanced growth in PARP-deficient plants might be a consequence of increased carbon assimilation and altered photochemical efficiency, which may manifest in changes in ΦPSII. Additionally, Schulz *et al*., (2012) reported small but significant increases in ΦPSII and *q*P whilst NPQ was reduced in unstressed plants treated with the PARP inhibitor 3MB (Figure 107). That said, 3MB did not significantly alter ΦPSII or *q*P in plants subjected to oxidative stress.

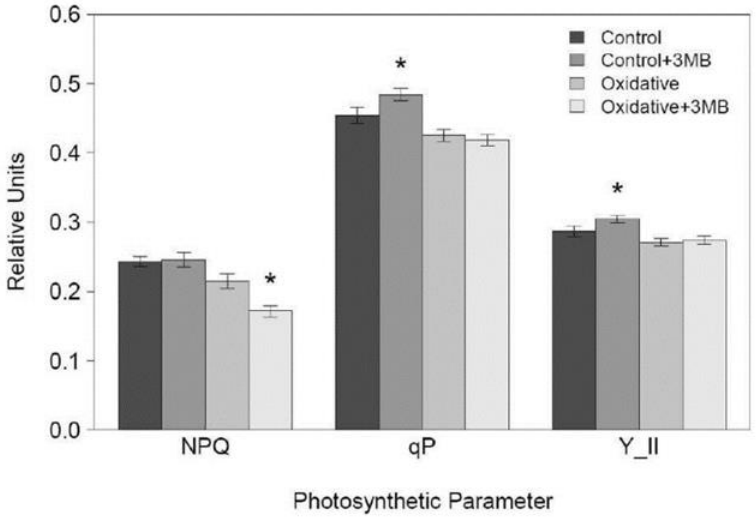

Figure 107. NPQ, *q*P and ΦPSII (Y_II) measured in Arabidopsis plants subjected to control and oxidative stress (0.1 µM paraquat) conditions. MS media was supplemented with the PARP inhibitor 3MB (+ 3MB) in the indicated samples. * denotes significant difference ($P < 0.05$) between seedlings grown in the same condition but treated with 3MB or without 3MB. Taken from Schulz *et al*., (2012).

In this thesis the application of the PARP inhibitor 2TBC consistently reduced values of ΦPSII during photosynthetic induction. Low values of ΦPSII were often concurrent with low NPQ, reduced F_v/F_m and high ΦNO values, particularly at high inhibitor concentrations, suggesting that 2TBC was damaging the plants. Further to this, in the work by Schultz *et al*., (2012) shown in Figure 107, NPQ decreased significantly whilst ΦPSII remained unchanged in plants treated with 3MB and exposed to oxidative stress. The inhibitor exacerbated the impact of the stress perhaps indicating it caused damage and led to an impaired ability to regulate energy dissipation.

There are a few potential explanations for the differences in the findings of the work in Chapter 3 and those in Schultz *et al*., (2012). Firstly, whereas Schulz *et al*., measured steady-state photosynthesis, the parameters in Chapter 3 were measured during photosynthetic induction. As work in Chapter 2 showed, a plant experiencing a moderate drought could have the same steady-state ΦPSII values as a well-watered plant. At steady-state all of the underlying reactions are proceeding at constant rates. As explained in 2.1, induction is a more dynamic process with a number of underlying reactions which are easily perturbed by stress or chemical treatment (Murchie & Lawson, 2013*b*). Hence, it was during induction when the differences in ΦPSII (and other parameters) between non-stressed and moderately drought stressed plants were most marked. It could be the case that the negative impacts of a harmful compound on ΦPSII are visible during induction, as was the case with 2TBC in Chapter 3 in this work, but masked at steady-state, as in the case of 3MB in Schultz *et al*., (2012) (Figure 107). Secondly, different inhibitors (and concentrations thereof) were used in the two works. In Chapter 3 2TBC application had negative impacts on photosynthetic parameters whereas 3MB had no significant effects at the concentrations used. Schultz *et al*., treated plants with 3MB and reported small but significant changes in photosynthetic parameters indicating that the negative impacts of 2TBC might be compound specific. Additionally, the inhibitors were applied to plants using different delivery methods. In Chapter 3 PARP inhibitors were sprayed onto leaves of plants in soil whereas in Schultz *et al*., they were added to the growth media and taken up by the roots. This could have led to varying degrees of the compounds been taken up by a plant in relation to the amounts applied. Finally,

Schultz *et al*., grew plants in media, in Petri dishes whereas in this thesis plants were growth in pots, in soil, so the conditions each experiment were different. For example, plants grown in Petri dishes will experience greater relative humidity in comparison to soil-based experiments, which has obvious implications in drought experiments.

In relation to the initial hypothesis that PARP inhibition might lead to enhanced photosynthetic performance and growth, the evidence from work in Chapter 3 suggested that this was not the case. No significant growth enhancement was recorded following PARP inhibitor application under any condition, at any concentration used and relative growth rate was slowed in many cases, which also supports work in Chapter 4. Results from Schultz *et al*., (2012) suggested that 3MB treatment significantly enhanced growth relative to untreated plants under a range of abiotic stresses. However, they also showed using a dose response assay that higher compound concentrations inhibited growth. These results demonstrate that the impacts of PARP inhibitors are concentration dependent.

Pham *et al*., (2015) investigated the impact of single mutations in the three Arabidopsis *PARP* genes on F_v/F_m and ETR. Unfortunately the group mislabelled the germplasm they used and did not follow the TAIR nomenclature, which is listed in Table 11. For consistency, the labelling used by Pham *et al*., (2015) is ignored and the TAIR nomenclature is used throughout, including for experimental work later in this chapter. The group reported small but significant decreases in F_v/F_m and ETR in *parp*1 and *parp*2 plants which is consistent with the results of 2TBC treated plants in Chapter 3. *PARP*3 is primarily located and expressed in seeds and is implicated in dormancy rather than stress response, explaining why there was no significant change in ETR in these plants (Hunt & Gray, 2009). The impact of *PARP* knockout on photosynthetic induction was investigated further in this chapter to determine if the impacts of genetic PARP-deficiency were similar to those resulting from chemical PARP inhibitor application.

Table 11. Gene nomenclature used in Pham *et al*., (2015) (Figure 108) in comparison to the TAIR gene loci and nomenclature.

Gene knockout name used in Pham *et al*., (2015)	Germplasm	TAIR locus	TAIR gene name
*parp*1	SAIL_632_D07	At5g22470	*PARP3*
*parp*2	SALK_111410	At2g31320	*PARP1*
*parp*3	SAIL_1250_B03	At4g02390	*PARP2*

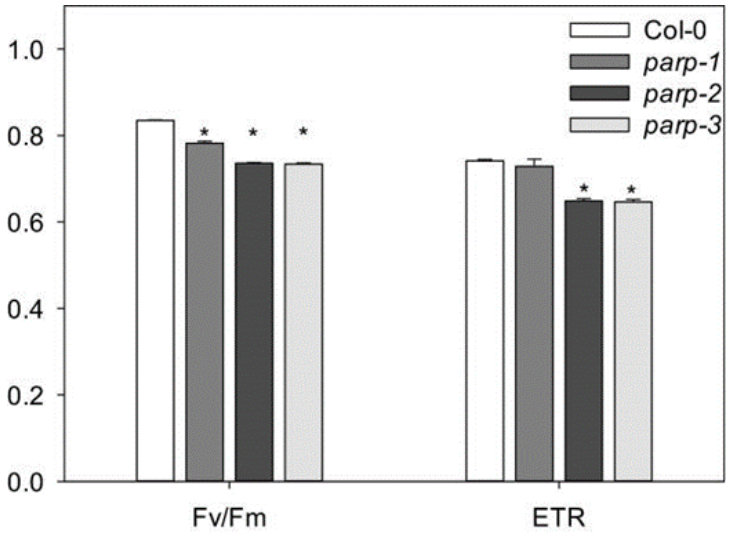

Figure 108. F_v/F_m and electron transport rate (ETR) in Arabidopsis *parp* single mutant lines in comparison to wild-type (Col-0). According to the standard TAIR nomenclature the group incorrectly classified their mutant lines. Refer to Table 11 for the correct classification. * denotes values are significantly different from the wild type, $P < 0.05$, Student's t-test. Values are the mean (n=7) ± SE. Taken from Pham *et al*., (2015).

Pham *et al*., (2015) also measured gas exchange parameters at different irradiances but reported that *parp* plants exhibited unaltered stomatal conductance and carbon assimilation rates. However, gas exchange analysis in chapter 3 indicated that the reduced ΦPSII during induction was caused by lower stomatal conductance in PARP inhibitor treated plants. A reduction in stomatal conductance can result in internal CO_2 limitation and the downregulation of photosynthetic electron transport (Baker, 2008; Foyer *et al*., 2012). Downregulation can be an adaptive plant response to prevent the over-reduction of the electron transport chain which can lead to the generation of harmful radical species that damage the photosynthetic machinery

(Zivcak *et al.*, 2013). Furthermore, PARP activity has been implicated in ABA-responsive stress-induced gene expression. Vanderauwera *et al*., (2007) claimed that PARP-deficient plants had elevated ABA levels and an overrepresentation of ABA-responsive genes in response to high light exposure.

ABA is perceived by PYR/PYL/RCARs (pyrabactin resistance/pyrabactin resistance-like/regulatory component of ABA receptor) receptors which bind to PP2Cs (protein phosphatase 2Cs), releasing SnRK2 kinases to phosphorylate downstream target proteins (Figure 109A-B) (Okamoto *et al*., 2013; Danquah *et al*., 2014). As a consequence of this ABA induces changes in gene expression and stomatal closure (Figure 109A-B; Figure 110). As well as increasing the degree of stomatal closure, which would be of benefit to a plant experiencing drought stress, increased levels of ABA could lead to the increased expression of ABA-responsive genes. Although ABA is required for normal growth, high levels are known to inhibit growth (Xiong & Zhu, 2003). This initially appears counterintuitive to the hypothesis that PARP-deficiency, which has been shown to increase cellular ABA levels, enhances growth. However, Vanderauwera *et al*., (2007) reported a moderate increase in ABA and a mild perturbation of ABA signalling in PARP-deficient plants. They claimed that their PARP-deficient plant lines were able to maintain signal transduction pathways and keep developmental cues in place whilst conferring stress-tolerance with no yield penalty. They went on to say that in field trials, PARP-deficient transgenic corn and oilseed rape plants had similar yields to wild-type controls under unstressed conditions (unpublished data as referred to in Vanderauwera *et al*., (2007)). Additionally, the PARP-deficient lines had ~ 40-60% higher yield than wild-types when the plants were exposed to drought stress.

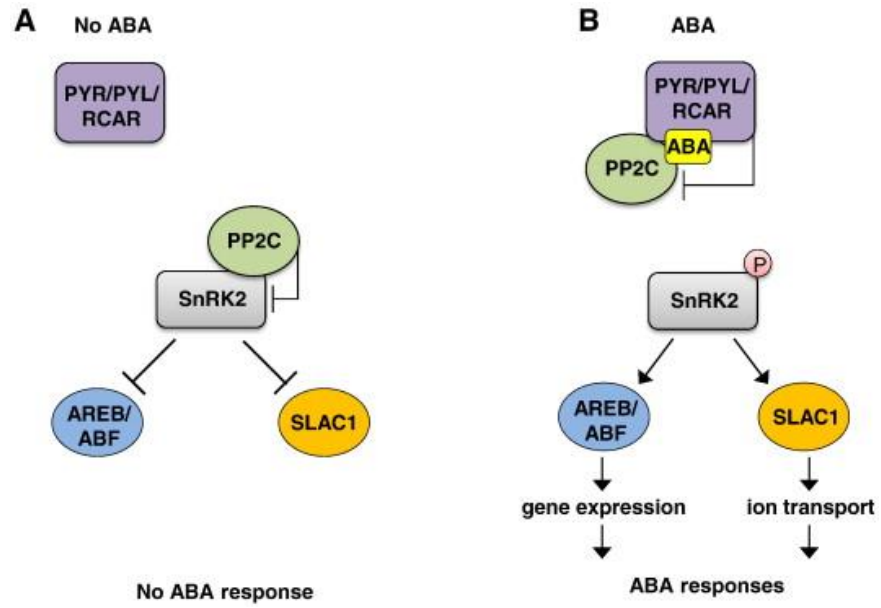

Figure 109A-B. (A) In the absence of ABA PP2Cs inactivate SnRK2 kinases. Without activation SnRk2s cannot transmit signals to target proteins. (B) ABA binds to PYR/PYL/RCAR receptors which in turn bind to PP2Cs, releasing SnRK2 kinases to phosphorylate downstream targets (e.g. AREB/AEF transcription factors, S-type anion channels (SLAC1)). Taken from (Danquah *et al*., 2014).

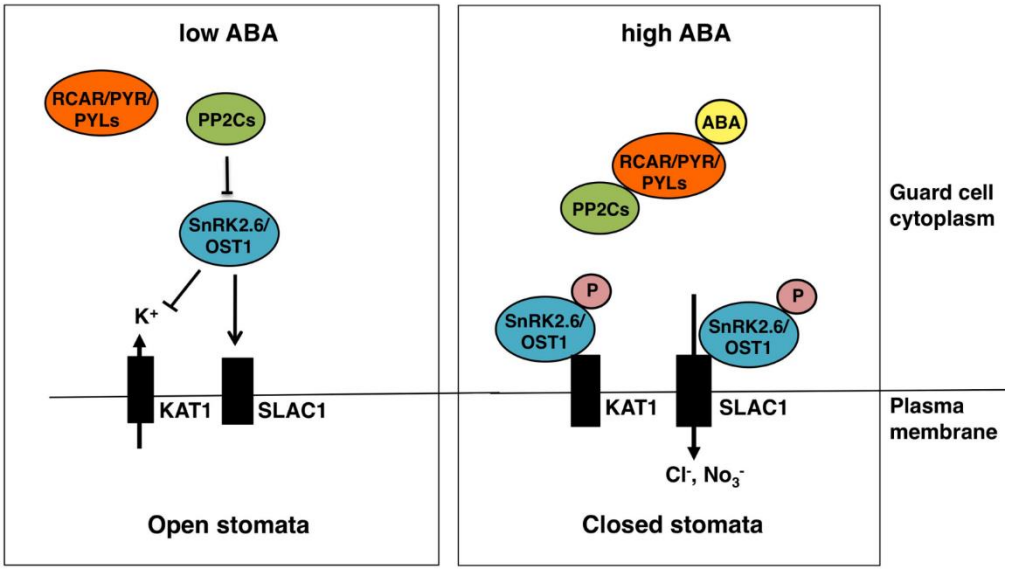

Figure 110. ABA signalling in guard cells showing the involvement of OST1 in the signal transduction pathway. When ABA levels are high PP2Cs are inactivated and SnRK2s are released (as described in Figure 109A-B). In the presence of ABA, OST1 activates KAT1 and SLAC1 ion channels which leads to ion efflux from the guard cells and results in stomatal closure. Taken from (Fernando & Schroeder, 2016).

Arabidopsis *ost*1-2 have an impaired ability to limit their transpiration under drought stress. *OST1* encodes a serine/threonine protein kinase which is a positive regulator of ABA-mediated stomatal response (Acharya *et al*., 2013). The position of OST1 in the ABA signal transduction pathway is shown in Figure 110. *ost*1-2 mutants are insensitive to ABA-induced stomatal closure and ABA-inhibition of light-induced stomatal opening (Mustilli *et al*., 2002). However, stomatal regulation by light or CO_2 remains unaffected suggesting that the gene is involved in ABA signalling. Accordingly, these plants should go through induction more quickly than wild-type plants because electron transport will not be hindered by CO_2 limitation. Additionally, *ost*1-2 plant should lose viability more quickly than wild-type plants when exposed to drought stress because they are unable to limit water loss. Finally, if PARP inhibition augments stomatal closure by increasing ABA levels, inhibitor application would not be expected to prolong viability of *ost*1-2 plants. If the mode of action of PARP inhibition is unrelated to ABA survival might be differentially altered.

The aim of this chapter was to use *parp* mutant lines to investigate if photosynthetic induction was altered under unstressed and drought stress conditions, and to determine if any changes were similar to those seen following application of 2TBC. Additionally, gas exchange analysis was performed to investigate the relationship between PARP inhibition, photosynthesis, ABA and stomatal closure.

5.1.1. Aims

- To determine if *PARP* mutants have altered photosynthesis during induction under well-watered and droughted conditions and to see how closely any changes in physiology resemble those resulting from 2TBC application. (Complemented mutant lines could enhance the design of the experiment).
- To determine if *PARP* mutants have altered survival rate in response to critical drought.
- To determine if the application of a PARP inhibitor could prolong survival of droughted wild-type and *ost*1-2 plants.

- To determine if PARP inhibitors alter stomatal opening/closing kinetics in response to light transitions under drought stress.
- To determine if PARP inhibitors have an anti-transpirant effect under well-watered and water-stressed conditions.

5.1.2. Objectives

- Apply drought to *B. napus* and Arabidopsis plants by withholding water.
- Use continuous, non-invasive chlorophyll fluorescence imaging to quantify the impact of *PARP* knockout on induction kinetics in response to drought in Arabidopsis.
- Measure survival of different Arabidopsis lines (wild-type, *parp*1, *parp*2, *parp*1*parp*2 and *ost*1-2).
- Treat droughted wild-type and *ost*1-2 plants with a PARP inhibitor and quantify survival.
- Measure changes in conductance during cycles of light and dark to quantify the impact of a PARP inhibitor on stomatal response in *B. napus*.
- Measure conductance in well-watered plants to assess if a PARP inhibitor induces stomatal closure in *B. napus*.

5.2. Materials and methods

5.2.1. Plant material

For photosynthetic measurements Arabidopsis *open-stomata*1-2 (*ost*1-2; At4g33950), *parp*1 (At2g31320) and *parp*2 (At4g02390) seeds were sourced from NASC (UK). *parp*1*parp*2 seeds were provided by Professor Andrew Bent from The University of Wisconsin-Madison (USA). Wild-type (Col-0) were also used. Unless stated seeds were cold stratified at 4 °C for 4 days before plating out onto soil in individual pots (6 cm diameter; LBS Horticulture; UK) containing M3 compost (Levington; UK) and grown for 27 days before measurements began and treatments were performed.

For gas exchange analysis *B. napus* (Temple; Elsoms; UK) seeds were germinated on wet filter paper in the dark at 22 °C for 4 days. Seedlings were transplanted into pots (10 x 10 x 10 cm; LBS Horticulture; UK) containing M3 compost (Levington; UK) and grown for 15 days before drought was initiated and treatments were performed.

All plants were grown in a greenhouse chamber under natural light with supplemental light at 200 µmol m^{-2} s^{-1}, during a 16/8 hour day/night photoperiod, at 25/20 °C and a relative humidity of 35-55%. Well-watered plants were watered every 2 days. In all cases drought was initiated by withholding water and quantified by calculating the % soil water content where saturated pot = 100% and oven-dried soil = 0%. Plants were moved daily to minimise the effects of light gradients.

5.2.2. Compound preparation

Stock solution containing the PARP inhibitor 2TBC (Bayer Crop Science; Germany) was prepared by dissolving 0.032 g 2TBC in 3.6 ml acetone and 400 µl DMSO. This solution was added to 394 ml of deionised water and 2 ml of the adjuvant methyl ester of rapeseed oil (MERO; Bayer Crop Science; Germany) to give a solution containing 364 µM of inhibitor. The mock solution contained acetone, DMSO and MERO in the same concentrations but no inhibitor. ABA was dissolved in methanol

to make a 50 mM stock solution which was diluted in dH_2O and 0.1% of the adjuvant Triton-X 100 was added to give a final concentration of 100 μM ABA (as described in Hopper *et al*., 2014). Chemicals were sourced from Sigma-Aldrich (USA) unless stated. All solutions were sprayed to run-off when stated. Untreated plants were unsprayed.

5.2.3. Chlorophyll fluorescence imaging

Chlorophyll fluorescence analysis with Arabidopsis wild-type and mutant lines was carried out on the PlantScreen™ Robotic XYZ System with a kinetic chlorophyll fluorescence camera and FluorCam 7 Software (Photon Systems Instruments; Czech Republic). Plants were dark-adapted for 5 min and induction was measured for 12 min at 400 μmol m^{-2} s^{-2} PAR. The scanner was 50 cm above pot height. The irradiance at pot level was measured using a light meter with an SK215 PAR quantum sensor (Skye Instruments; UK). The spectral data was measured using spectroradiometer (MK350S; URPTek; Taiwan). Measurements of F_v/F_m, ΦPSII and NPQ were taken daily between 12-3 pm for the duration of the experiment. Plants were randomised before measurements began but then remained in a fixed position throughout.

For NPQ measurements in 5.3.4, *B. napus* plants were dark-adapted for 5 min and NPQ was measured during 5 min of illumination at 400 μmol PAR m^{-2} s^{-1} using the scanner system detailed above.

5.2.4. Leaf gas exchange measurements

Gas exchange was measured on *B. napus* plants using an LI-6800 gas analyser with a leaf chamber fluorometer (Licor; USA). All measurements were recorded with 400 μmol m^{-2} s^{-1} PAR during light periods, 400 μmol mol^{-1} CO_2, 25 °C leaf temperature and ~ 50% relative humidity.

For the extended protocol in 5.3.2, plants were germinated and grown for 15 days before drought was initiated and treatments were performed. Measurements took place 4-5 days later when the soil water content in well-watered samples was > 90% and between 14-22% in droughted plants. The gas analyser was situated in the greenhouse where plants were growing. Measurements occurred across 4 consecutive days using 2 batches of plants to ensure comparable phenological states and soil water contents. The order of measuring was designed to minimise the impact of diurnal effects on stomatal conductance; one replicate of each treatment was measured at 9 am, one at ~ noon and the other after 3 pm. The top most expanded true leaf was measured which was leaf three or four in all cases.

For the 5 min protocol in 5.3.3, plants were sown and grown for 15 days before treatment. F_v'/F_m', ΦPSII, stomatal conductance and carbon assimilation were recorded during 5 min of illumination. F_v'/F_m' is the light-adapted maximum efficiency of photosystem II and is measured by applying a saturating flash to measure F_m' then immediately turning off the lights to measure F_0.

5.2.5. Image acquisition

Digital images of plants were acquired using an EOS REBEL T1i/EOS 500D camera (Canon; Japan).

5.2.6. Statistical analysis

Minitab was used perform Student's t-tests and one- and two-way ANOVAs (Minitab 17; Minitab, Inc; USA). Data were tested for equal variance. Where necessary Dunnett's, Tukey's or Games-Howell multiple comparisons tests were performed. The % survival of treatments were tested for significance using the log-rank (Mantel-Cox) method. GraphPad Prism 7 software was used to construct graphs and charts (GraphPad Software, Inc; USA).

5.3. Results

5.3.1. The impact of *PARP* on the efficiency of photosynthesis in *A. thaliana*

In Chapter 3 2TBC application reduced ΦPSII during induction in Arabidopsis and *B. napus* under unstressed and water stressed conditions. However, 3MB and lower concentrations of 2TBC did not significantly alter ΦPSII indicating the effect was compound and dose dependent. Arabidopsis *parp* lines were compared to wild-type plants to determine if *PARP* knockout perturbed induction parameters under drought in the same way as 2TBC application. *ost*1-2 mutants, which should increase ΦPSII during induction more quickly because of increased internal CO_2 availability, were used as an additional control. Seeds were cold stratified for 4 days at 4 °C, placed onto soil in individual pots and grown for 27 days before drought was initiated and measurements began (day 0). Well-watered plants were watered every 2 days throughout. Plants were dark-adapted for 5 min and values of F_v/F_m, ΦPSII and NPQ were recorded after 5 min induction.

Figure 111A-F shows how the parameters changed as the experiment progressed. Parameters were analysed for statistically significant differences between other genotypes of the same irrigation profile using one way ANOVAs with Tukey's multiple comparisons test. Under well-watered conditions F_v/F_m, ΦPSII and NPQ values were comparable between all genotypes throughout, except in *ost*1-2 plants which had significantly higher ΦPSII values than wild-types at each measuring point and significantly lower NPQ between days 3 and 4 ($P < 0.05$). Relative to wild-type samples all *parp* knockout plants had unaltered F_v/F_m, ΦPSII and NPQ values. Drought began to have a significant impact after 4 days of water withholding. In comparison to well-watered wild-type samples, droughted wild-type and *parp*1*parp*2 plants had significantly lower values of ΦPSII after 4 days ($P < 0.05$). After 5 days, ΦPSII values were significantly lower in droughted plants of all genotypes compared to well-watered wild-types (Table 12) and these differences persisted thereafter ($P < 0.05$; one-way ANOVA with Dunnett's multiple comparisons test). Over the course of the first 8 days of withholding water from droughted plants the soil water content

declined from 100% to < 10%, however there were no significant differences in values ΦPSII or NPQ between droughted wild-types and any other genotype except *ost*1-2. These plants had higher values of ΦPSII between 3-4 days and lower NPQ between 3-5 days ($P < 0.05$) (Figure 111B, D, F).

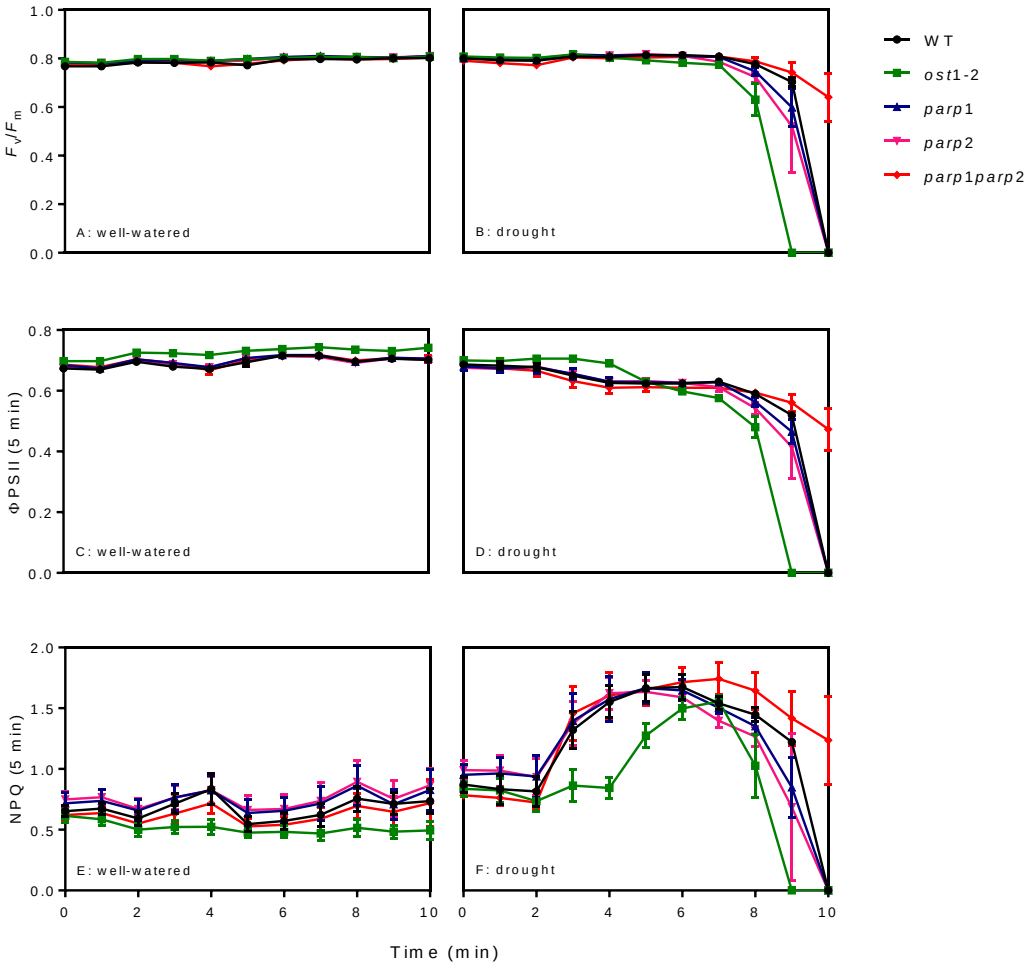

Figure 111A-F. F_v/F_m, ΦPSII and NPQ in (A+C+E) well-watered and (B+D+F) droughted Arabidopsis plants. ΦPSII and NPQ values were collected after 5 min induction. WT = wild-type, *ost*1-2 = *open stomata*1-2, *parp*1 and *parp*2 = single mutants, *parp*1*parp*2 = double mutant. Water was withheld from droughted plants on day 0. Statistically significant differences are referred to in the text. Values are the mean (n=5) ± SE.

Table 12. Average values (± SE) of ΦPSII (after 5 min induction) after 4 and 5 days from Figure 111C-D. * denotes significantly different from well-watered wild-type ($P < 0.05$; one-way ANOVA with Dunnett's multiple comparisons test).

Irrigation - genotype	Day 4 ΦPSII (± SE)	Day 5 ΦPSII (± SE)
Well-watered wild-type	0.67 (0.012)	0.69 (0.013)
Drought wild-type	0.62 (0.009)*	0.62 (0.007)*
Drought *ost*1-2	0.69 (0.009)	0.62 (0.011)*
Drought *parp*1	0.63 (0.013)	0.62 (0.009)*
Drought *parp*2	0.63 (0.009)	0.62 (0.008)*
Drought *parp*1*parp*2	0.61 (0.018)*	0.61 (0.014)*

The values of ΦPSII were higher than expected for induction in Arabidopsis at 400 µmol PAR m^{-2} s^{-1}. To assess the setup in more detail the light spectrum of the scanner system was measured using a spectroradiometer and compared to a reading from the bench-top WALZ system. Analysis suggested that there was a large amount of both blue and green in the scanner light (Figure 112). In the WALZ system the light was mostly blue which plants preferentially absorb for photochemistry. ΦPSII measures the proportion of absorbed light that is used in photochemistry. The elevated values of ΦPSII seen in Figure 111C-D are likely a result of less blue light been absorbed, so a greater proportion of the total was used in photosynthetic electron transport and ΦPSII increased. This highlights the dangers of instrumental differences between experiments. This experiment should be repeated at a higher effective irradiance.

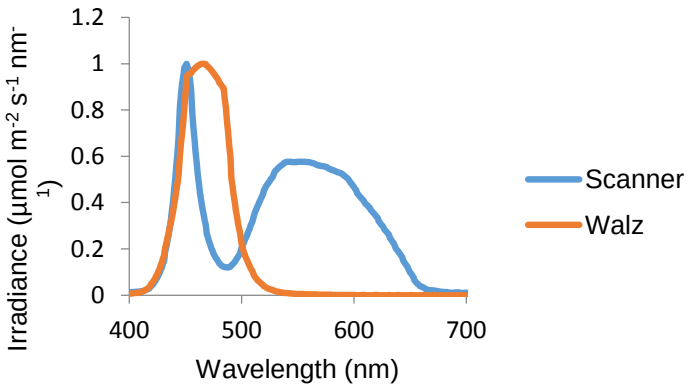

Figure 112. Spectral read-out for the scanner and WALZ systems. The amount of photosynthetic photon flux was normalised to one at different wavelengths for each system.

After 8 days of withholding water plants began to lose viability (Figure 113). All *ost*1-2 plants had lost viability after 9 days reflecting their inability to respond to ABA and close stomata. Wild-type, *parp*1 and *parp*2 plants lost viability at different rates between 8-9 days but all plants were dead on day 10. The decline of viability from day 8 onwards was consistent with decreases in ΦPSII and NPQ, although the average F_v/F_m of surviving plants remained > 0.5 on day 9 (Figure 111B, D, F). In contrast to other genotypes 100% of *parp*1*parp*2 plants were alive after 9 days, which decreased to 60% after 10 days, 20% after 11 days and finally to 0% after 12 days (Figure 113). The results of a survival curve analysis suggested that the enhanced survival on day 10 was statistically significant ($P < 0.05$). Additionally, surviving plants had relatively high values of F_v/F_m at each time point indicating that plants were photosynthetically capable. This coincides with previous results where PARP inhibitor application increased survival and also suggests that there is functional redundancy in the single mutants.

To determine if 2TBC affected survival in response to severe drought could be prolonged in wild-type and *ost*1-2, plants were treated to run-off with 364 μM 2TBC on day 0. After 9 days of water withholding wild-type unsprayed and wild-type + 2TBC plants had 60% survival rates (Figure 114). However, all wild-type unsprayed plants were dead 1 day later, whereas 40% of those sprayed with 2TBC remained alive. A survival analysis revealed this difference was not statistically significant. Wild-type treated plants then lost viability after 11 days. Spraying had less of an impact on *ost*1-2 plants. Relative to untreated plants, 2TBC increased survival of *ost*1-2 plants by 20% after 9 days ($F_v/F_m = 0.29$) although this was not statistically significant. Figure 115A-B shows how F_v/F_m changed in all samples throughout the experiment. Inhibitor application had no impact on viability under well-watered conditions and all plants had F_v/F_m values > 0.7 throughout. These findings indicate that PARP deficiency resulting from either *parp*1*parp*2 knockout or chemical inhibitor application prolonged survival of plants to drought stress. 2TBC application did not appear to rescue the *ost*1-2 phenotype and extend survival indicating that PARP activity may be linked to ABA.

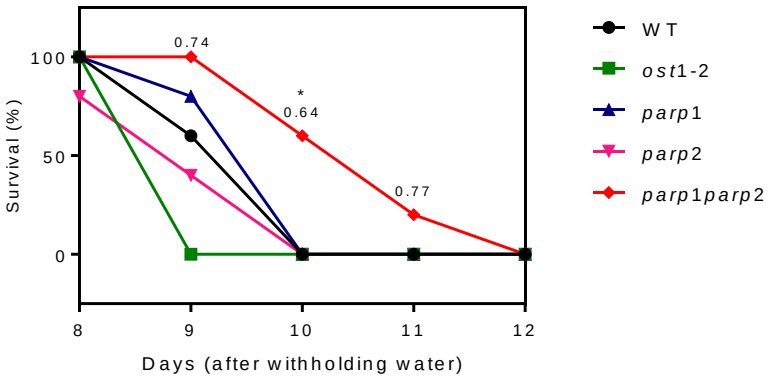

Figure 113. % survival (out of 5 replicates) of droughted plants over the latter stages of the experiment shown in Figure 111A-F. For survival F_v/F_m > 0.1. The numbers above the *parp*1*parp*2 line (pink) represent average F_v/F_m of surviving plants. * indicates significantly different from WT (P < 0.05), log-rank (Mantel-Cox) method of survival curve comparison.

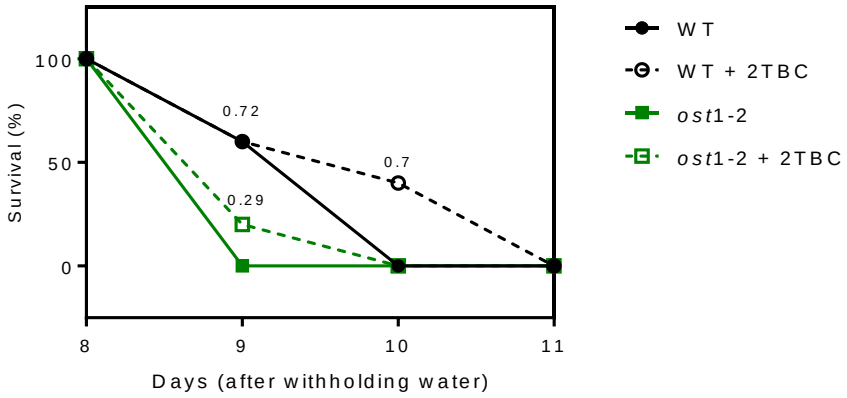

Figure 114. % survival (out of 5 replicates) of droughted plants over the latter stages of the experiment shown in Figure 111A-F and Figure 113. For survival F_v/F_m > 0.1. Additional wild-type and *ost*1-2 plants were treated with 364 µM 2TBC (dashed lines) to run-off on day 0. The numbers above the dashed lines represent average F_v/F_m values for the plants treated with inhibitor.

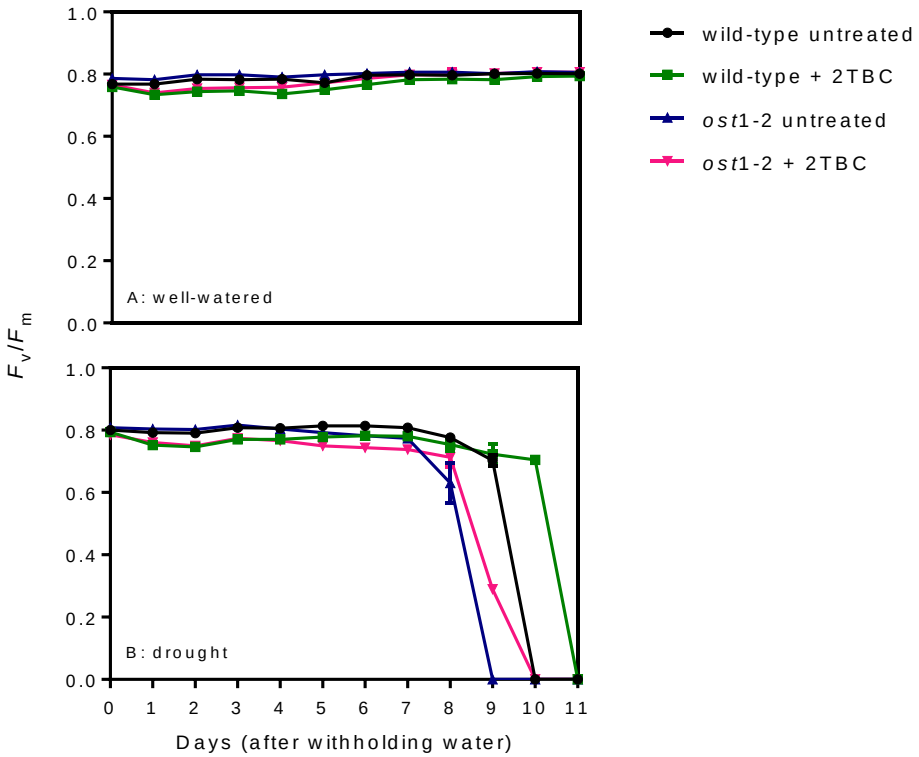

Figure 115A-B. F_v/F_m values of (A) well-watered and (B) droughted plants colour coded by genotype and treatment (control untreated or + 2TBC). Only values for surviving plants (F_v/F_m > 0.1) are shown. Values are the mean (n=5 in all cases for well-watered plants, see Figure 114 for survival % for droughted plants) ± SE.

Work in Chapter 3 suggested that application of the PARP inhibitor 2TBC reduced ΦPSII during induction under both well-watered and droughted conditions. However these changes were not observed for 3MB treated plants. In this chapter, genetic knockout of one or more *PARP* genes implicated in stress response did not result in ΦPSII changes relative to wild-type plants. However, plants treated with chemical PARP inhibitor (2TBC or 3MB) and double knockout lines all showed enhanced survival in response to critical drought stress. This is potentially a result of an increase in cellular ABA so gas exchange was measured to further investigate the interaction between drought, chemical PARP inhibiton and stomatal conductance.

5.3.2. The impact of PARP inhibitors on stomatal response to light transitions under drought stress in *B. napus*

Gas analysis work in 2.3.7 and 3.3.5 linked drought-induced reductions in ΦPSII during induction to reduced stomatal conductance. Because of the reduction of ΦPSII at high 2TBC concentrations, a potential anti-transpirant mode of action of PARP inhibitors was hypothesised. A protocol to assess stomatal response to consecutive periods of darkness and then light was defined to determine if PARP inhibitor application had any effect on stomatal conductance in response to drought and light/dark transitions. The protocol consisted of 5 min dark-adaption, 30 min illumination at 400 µmol PAR m^{-2} s^{-1}, then a 40 min extended dark period. At the time of measuring the soil water content in well-watered and droughted plants was > 90% and between 14-22% respectively.

Figure 116A-F shows the how stomatal conductance changed over the course of the experiment in response to drought and 2TBC application. In well-watered untreated plants stomatal conductance ranged from 0.4-0.6 mmol m^{-2} s^{-1} at the start of measuring (Figure 116A). During the 5 min dark-adaption period conductance decreased slightly. After the light was turned on, stomata began to open and conductance increased over the illumination period in a relatively uniform manner in all samples. All samples had higher values of conductance after 30 min of illumination than at the start of the period. At the point of light/dark transition when the light was switched off there was some fluctuation in the samples. Conductance began to decrease after the light was switched off, linearly in two samples and in a more biphasic manner in the other. The decrease in conductance plateaued in all samples towards the end of this dark period. Mock treated plants followed a similar pattern (Figure 116B).

Application of 2TBC led to increased variation (Figure 116C). Two samples had starting conductance values of > 0.8 mmol m^{-2} s^{-1} with one sample < 0.3 mmol m^{-2} s^{-1}. Two plants responded to the 5 min dark-adaption with an extended period of stomatal closure relative to untreated plants (Figure 116A, C). The sample which had a starting conductance of < 0.3 mmol m^{-2} s^{-1} did not close stomata in response to dark perhaps

indicating that the plants ability to respond to light/dark transitions was inhibited. After the light was switched on the kinetics of 2TBC treated plants resembled those of untreated samples. However, in comparison to untreated plants, two 2TBC treated samples had higher 'maximum' values following the illumination period, although the values were not larger than those the same plants had at the start of measuring (-5 min). Similarly, the kinetics of closure after the light was turned off were comparable between 2TBC and untreated plants, with different end values achieved.

Drought increased the variation among samples. In comparison to untreated plants, droughted plants had a much greater range of starting conductance values (Figure 116D). There was a strong impact of time of day on conductance at the start of measuring and throughout. The sample measured at ~ 9 am had a starting value of 0.74 mmol m^{-2} s^{-1}, whereas the samples measured at ~ noon and after 3 pm had values of 0.48 and 0.14 mmol m^{-2} s^{-1} respectively. Following dark-adaption when the light was turned on conductance increased in well-watered untreated plants. Again there was some fluctuation at the point of light/dark transition following the 30 min illumination period. Conductance in darkness decreased steadily in the two samples measured earliest in the day, whereas stomata were more responsive in the 3 pm sample and conductance decreased more quickly before steady-state was achieved. Following 40 min of darkness the conductance values of the 9 am, noon and 3 pm samples were 0.6, 0.32 and 0.08 mmol m^{-2} s^{-1} respectively. Two droughted mock treated samples responded in a similar manner to untreated plants whereas one had a small response to illumination and conductance decreased rapidly after the light was turned off (Figure 116E). Under droughted conditions 2TBC treated plants showed similar kinetics to untreated plants although the changes in conductance over periods of illumination or darkness were greater in 2TBC samples (Figure 116F).

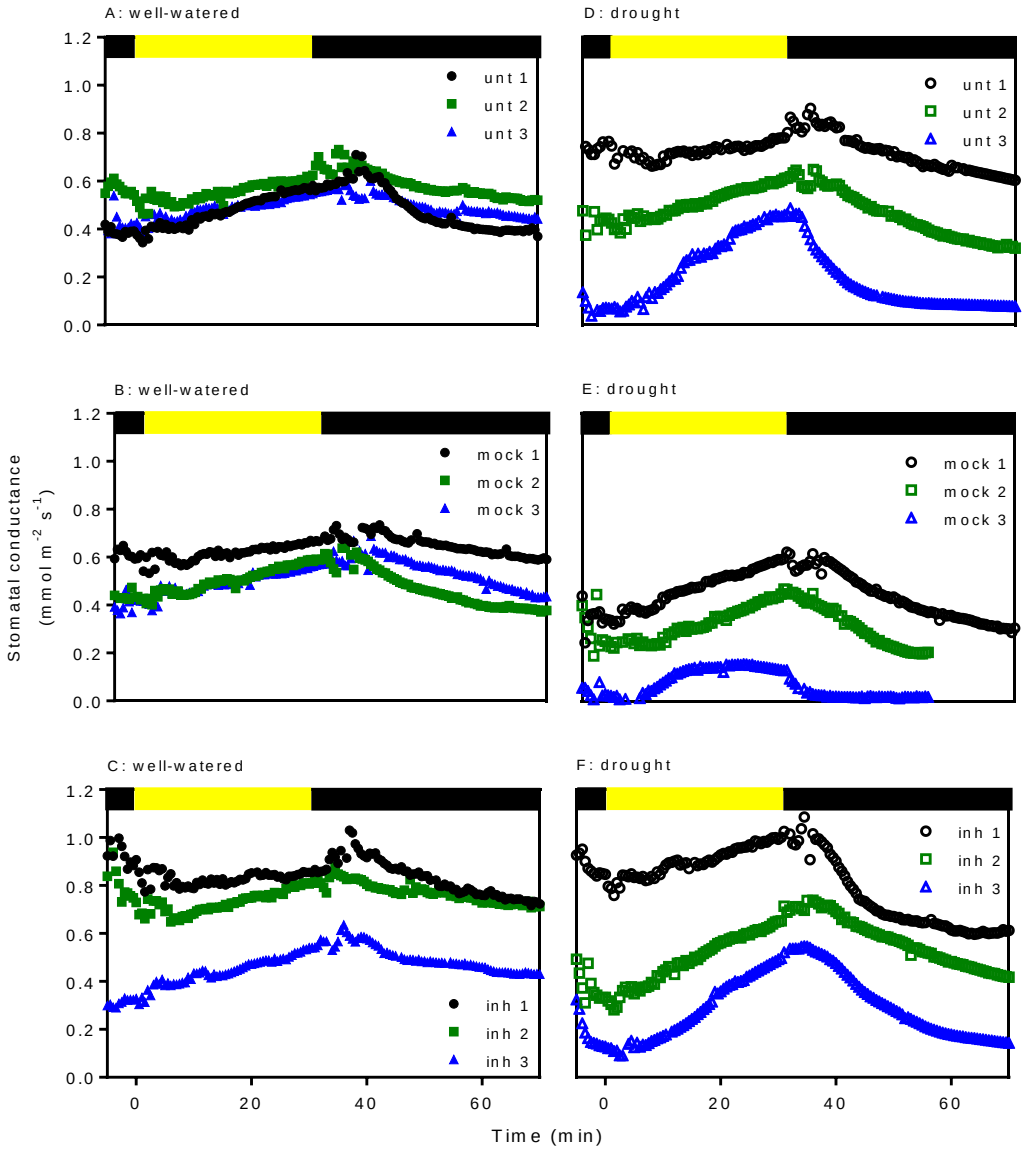

Figure 116A-F. Stomatal conductance in (A-C) well-watered and (D-F) droughted *B. napus* plants. The protocol included 5 min dark-adaption, 30 min high-light induction then 40 min darkness. The black and yellow blocks at the top of each plot represent dark and light periods respectively. Plants were untreated (A+D) or treated with either mock solution (B+E) or 364 µM 2TBC (C+F) to run off. Replicates were measured at different times of day to minimise diurnal effects: at 9 am (black symbols), ~ noon (green symbols) and after 3 pm (blue symbols). The soil water content of all well-watered plants was > 90% whereas in ranged between 14-22% in droughted samples.

Figure 117A-D shows data following the initial 5 min dark-adaption period extracted from the conductance curves in Figure 116A-F. Starting conductance was measured to assess how plants responded to 5 min dark-adaption in the gas analyser chamber having been exposed to growth irradiance in the greenhouse. Relative to well-

watered plants, droughted samples had increased variation in values of conductance following dark-adaption (Figure 117A). Variation was also quite large within 2TBC treatments. After 30 min illumination well-watered and droughted untreated plants had similar average values of conductance, as did well-watered and droughted 2TBC plants (Figure 117B). Droughted mock treated plants had lower values than the corresponding well-watered samples. In the data in Figure 117A-B, neither drought nor chemical treatment had a significant impact on mean values. The average change in conductance (Δg_s) over the period of illumination was recorded for each treatment. There was a significant impact of drought on Δg_s with well-watered plants having lower Δg_s values than droughted samples (P = 0.042) (Figure 117C). There was no additional impact of any chemical treatment. Interestingly, the time taken to achieve 50% of the Δg_s was similar in all plants with no significant impact of drought or chemical treatment (Figure 117D). This suggests that droughted plants were more responsive to light because they achieved a greater Δg_s in a similar amount of time it took well-watered plants to reach a smaller Δg_s.

Figure 118A-D shows measurements during the dark period following 30 min of illumination extracted from the conductance curves in Figure 116A-F. Figure 118A is a copy of Figure 117B for reference. Relative to well-watered plants, drought significantly reduced values of conductance at the end of the 40 min dark period (P = 0.025), although there was no additional impact of chemical spraying (Figure 118B). Additionally, there was more variation in the values of conductance at the end of the 40 min dark period in droughted samples than in well-watered plants. Conductance decreased in all plants after the light was turned off (Figure 118C). During the 40 min dark period all well-watered plants had comparable Δg_s values. Drought significantly increased Δg_s values relative to well-watered samples (P = 0.001) but there was no significant impact of any chemical treatment. This complements data in Figure 117C which shows that droughted plants responded more to light and dark than well-watered plants. In all cases the time taken to 50% of Δg_s was significantly lower in droughted plants than in well-watered plants (P = 0.015), but there was no additional effect of treatment (Figure 118D). This suggests that droughted plants responded to darkness much more quickly than well-watered plants.

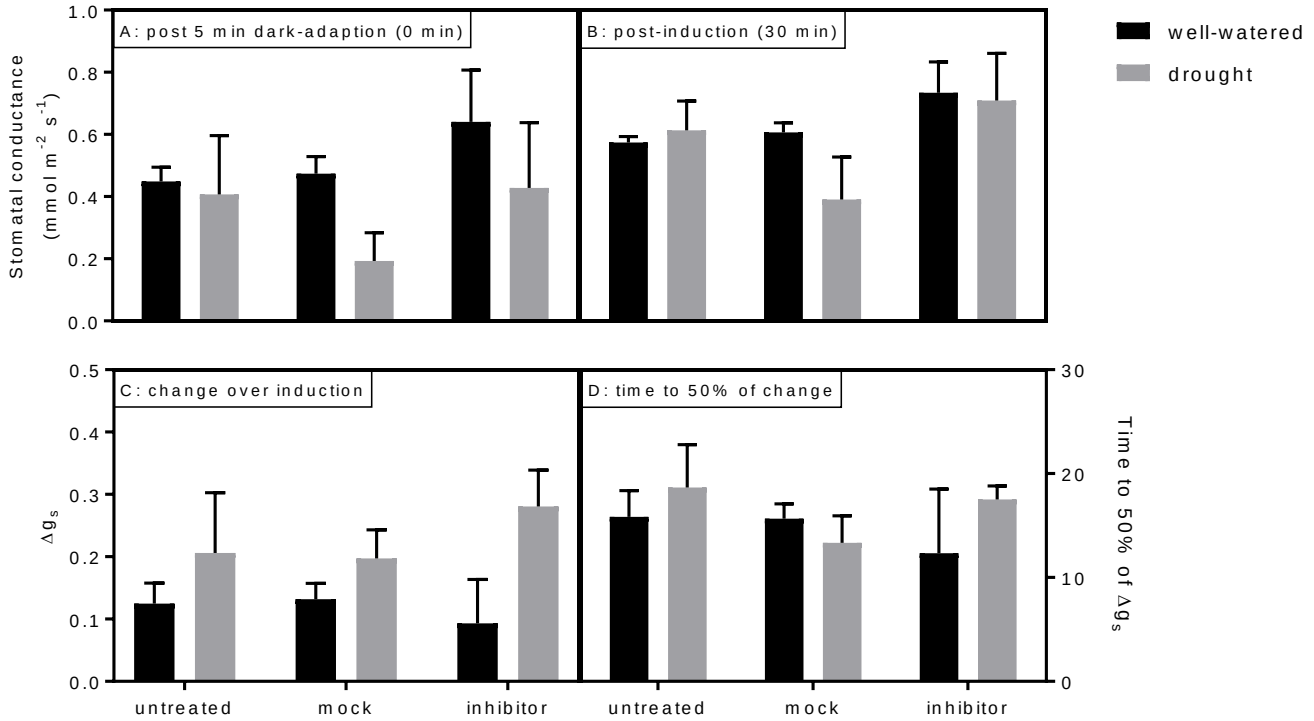

Figure 117A-D. Stomatal conductance (g_s) following (A) 5 min dark-adaption and (B) 30 min of high light induction, (C) the change in g_s between 0-30 min (Δg_s) and (D) the time taken to reach 50% of the Δg_s in well-watered (black bars) and droughted (grey bars) *B. napus* plants. Plants were dark-adapted for 5 min before induction was measured at 400 µmol PAR m^{-2} s^{-1}. Means of each treatment were tested for significant differences using a two-way ANOVA with an interaction term. Significant differences are referred to in the text. Values are the mean (n=3) ± SE and correspond to the raw data in Figure 116A-F.

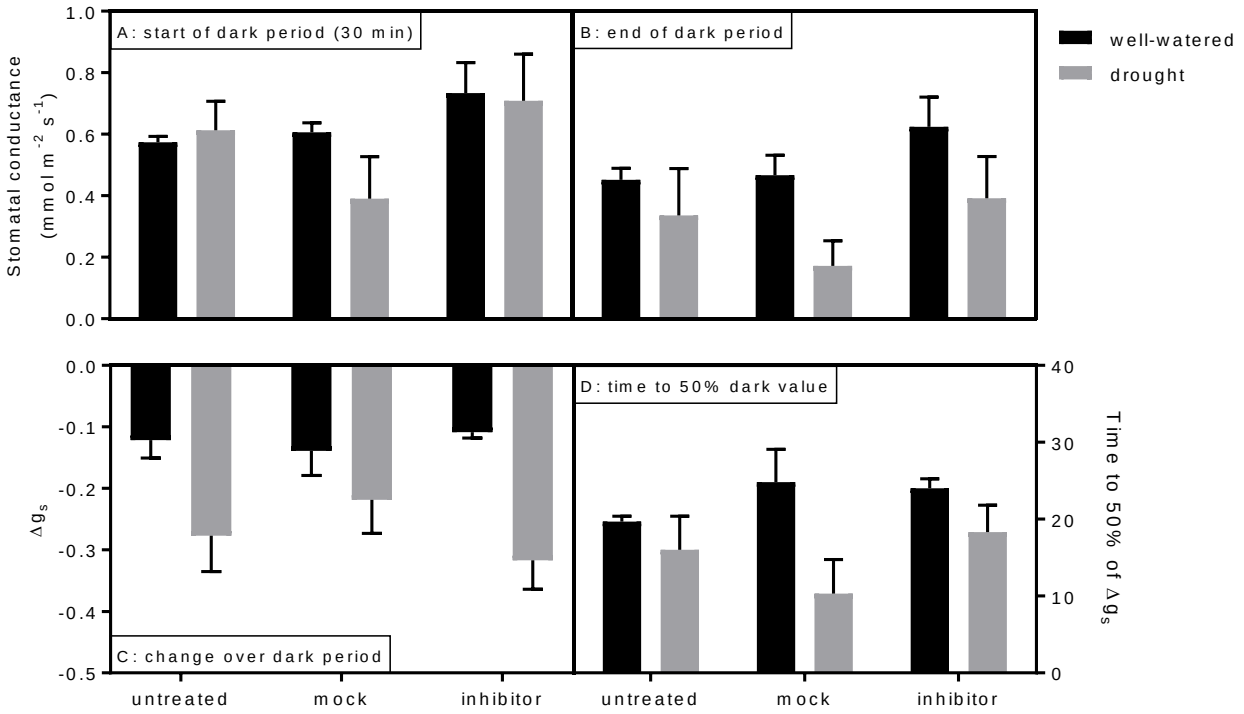

Figure 118A-D. Stomatal conductance (g_s) at the end of (A) 30 min high light induction and (B) the following extended dark period, (C) the change in g_s over this period (Δg_s) and (D) the time taken to reach 50% of the Δg_s in well-watered (black bars) and droughted (grey bars) *B. napus* plants. Means of each treatment were tested for significant differences using a two-way ANOVA with an interaction term. Significant differences are referred to in the text. Values are the mean (n=3) ± SE and correspond to the raw data in Figure 116A-F.

These results indicate that drought and inhibitor application increased the variation between samples within treatments. Also, droughted plants responded to light and dark to a greater extent and more quickly than well-watered samples. However, no significant impacts resulting from PARP inhibitor treatment were observed in any of the measurements suggesting that 2TBC did not alter stomatal responsiveness. There was a strong diurnal effect under drought conditions and, because the protocol was lengthy, considerable variation in soil water content was unavoidable even though two batches of plants were used.

5.3.3. The impact of 2TBC application on stomatal conductance and photosynthesis in well-watered *B. napus* plants

To investigate if 2TBC had an anti-transpirant effect a shorter protocol was defined. For this experiment *B .napus* plants were germinated on wet filter paper for 4 days then seedlings were transplanted into soil in individual pots and grown for 15 days then treated. Plants were either untreated or sprayed to run-off with mock solution, 364 μM 2TBC, or 100 μM ABA which served as a positive control. Gas exchange analysis was performed 2 hours after treatment on light-adapted, well-watered plants. All measurements were complete within 2 hours of treatment. F_v'/F_m', ΦPSII, stomatal conductance and carbon assimilation were recorded after 5 min of illumination at 400 μmol PAR m^{-2} s^{-1}. Pictures of the condition of the plants immediately prior to measurement are shown in Figure 119 to show that there were no visual signs of damage following chemical treatment. The aim of the experiment was to determine if 2TBC reduced stomatal conductance.

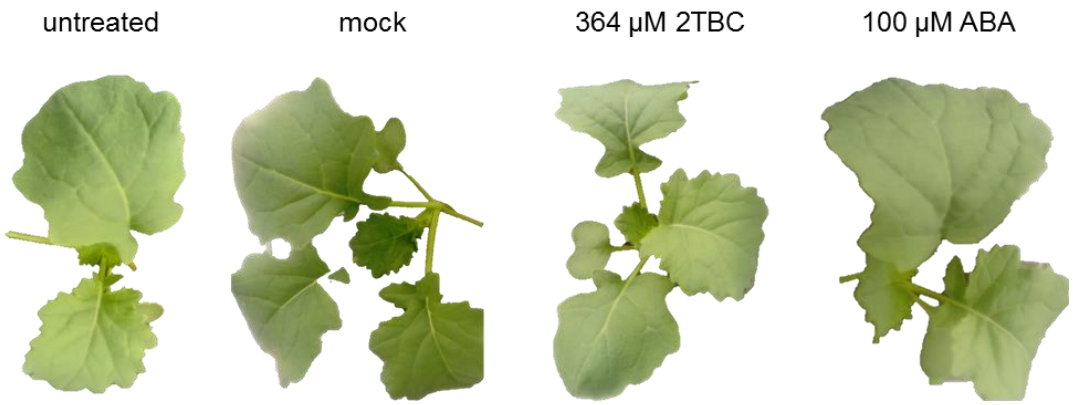

Figure 119. Pictures of *B. napus* plants prior to measuring (in Figure 120A-D). Samples were representative.

Untreated plants had F_v'/F_m' values of 0.74 but chemical treatment led to reductions from this value (Figure 120A). Mock treated plants had an average of 0.72 although this was not significantly different from the untreated value. However, both 2TBC and ABA significantly reduced F_v'/F_m' to 0.65 and 0.71 respectively ($P < 0.05$). In comparison to untreated plants, all treatments led to significant reductions in ΦPSII ($P < 0.05$) (Figure 120B). Untreated plants had ΦPSII values of 0.61 whereas it was reduced to 0.58, 0.4 and 0.54 in mock, 2TBC and ABA treated samples respectively ($P < 0.05$). Untreated and mock treated plants had similar values of stomatal conductance, which were 0.56 and 0.49 respectively (Figure 120C). However, conductance was significantly reduced to 0.31 in 2TBC treated samples and 0.13 in ABA treated plants ($P < 0.05$). This indicates that both of these compounds had an anti-transpirant impact and that ABA had a stronger effect on conductance than 2TBC. The changes in conductance were somewhat reflected in altered carbon assimilation. Relative to untreated plants, mock treatment significantly reduced carbon assimilation ($P < 0.05$) (Figure 120D). Additionally, assimilation in 2TBC and ABA treated plants was significantly lower than in untreated samples ($P < 0.05$). 2TBC and ABA treated plants had similar values of assimilation however conductance was reduced to a much greater extent in samples sprayed with ABA. These results further suggest that 2TBC damages plants and impairs their ability to photosynthesise.

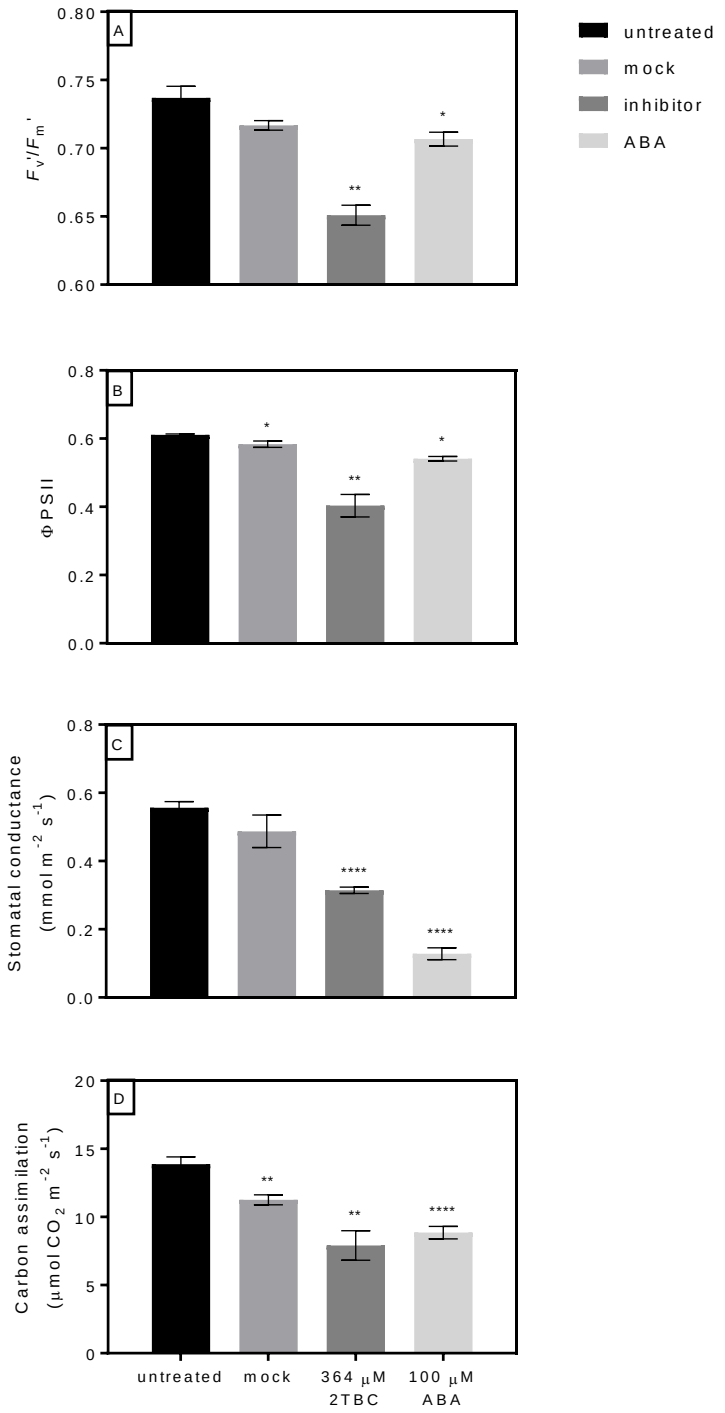

Figure 120A-D. (A) F_v'/F_m', (B) ΦPSII, (C) stomatal conductance and (D) carbon assimilation in well-watered *B. napus* plants. F_v'/F_m' was recorded by the application of a saturating flash to measure F_m', immediately after which the light was turned off to measure F_0. Other parameters were recorded after 5 min of illumination at 400 µmol PAR m^{-2} s^{-1}. Means were tested for significance in comparison to untreated using Student's t-tests. **** = P < 0.0001, ** = P < 0.005 and * = P < 0.05. Values are the mean (n=3-5) ± SE.

5.3.4. The impact of 2TBC and ABA on non-photochemical quenching

Measurements in Figure 120A-D were obtained from light-adapted samples. It is not possible to quantify NPQ on light-adapted samples because a reference measurement of dark-adapted F_m is necessary for the accurate determination of this parameter. To examine how these treatments affected NPQ the previous experimental setup was repeated and plants were sown, grown and treated as described in 5.3.3. In this experiment plants were dark-adapted for 5 min before NPQ was recorded after 5 min of illumination. Measurements were made 2 hours post-treatment and repeated daily over the course of the following 3 days.

Figure 121A shows how NPQ changed during the 5 min illumination period in plants when they were measured 2 hours after treatment. NPQ increased in untreated plants during the first 1 min of illumination but declined thereafter, reaching steady-state after ~ 3 min. Mock treated plants showed similar NPQ changes. However, treatment with 2TBC reduced the extent of the initial rise and plants achieved steady-state after ~ 2 min at lower values than plants of all other treatments. ABA treatment had the opposite effect. Although the initial rise in NPQ was smaller than in untreated plants it was sustained throughout the illumination period. NPQ was significantly lower in 2TBC treated plants than in untreated or ABA treated plants between 0.5-2 min ($P < 0.05$). At the end of the illumination period NPQ was significantly higher in ABA treated plants than in any other treatment ($P < 0.05$). These results, in conjunction with those in Figure 120A-D, suggest that 2TBC was damaging plants and prevented them from regulating energy dissipation. In contrast, ABA treated plants had higher NPQ values relative to untreated plants ($P < 0.05$) (Figure 121A-D). This is likely to be a compensatory mechanism as ABA has been shown to decrease ΦPSII (Figure 120B). Untreated, mock and ABA treated plants had similar NPQ induction kinetics when measured 1, 2 and 3 days(s) after treatment (Figure 121B-D). This suggests that the impact of ABA had worn off after 24 hours. In contrast, the impact of 2TBC on NPQ was still present 3 days after treatment. In these plants NPQ was significantly lower between 0.5-1 min, and from 2 min onwards in comparison to all other treatments, which did not significantly differ from each other ($P < 0.05$). This

further substantiates the suggestion that 2TBC damages plants as repairing the photosynthetic machinery can take considerable time.

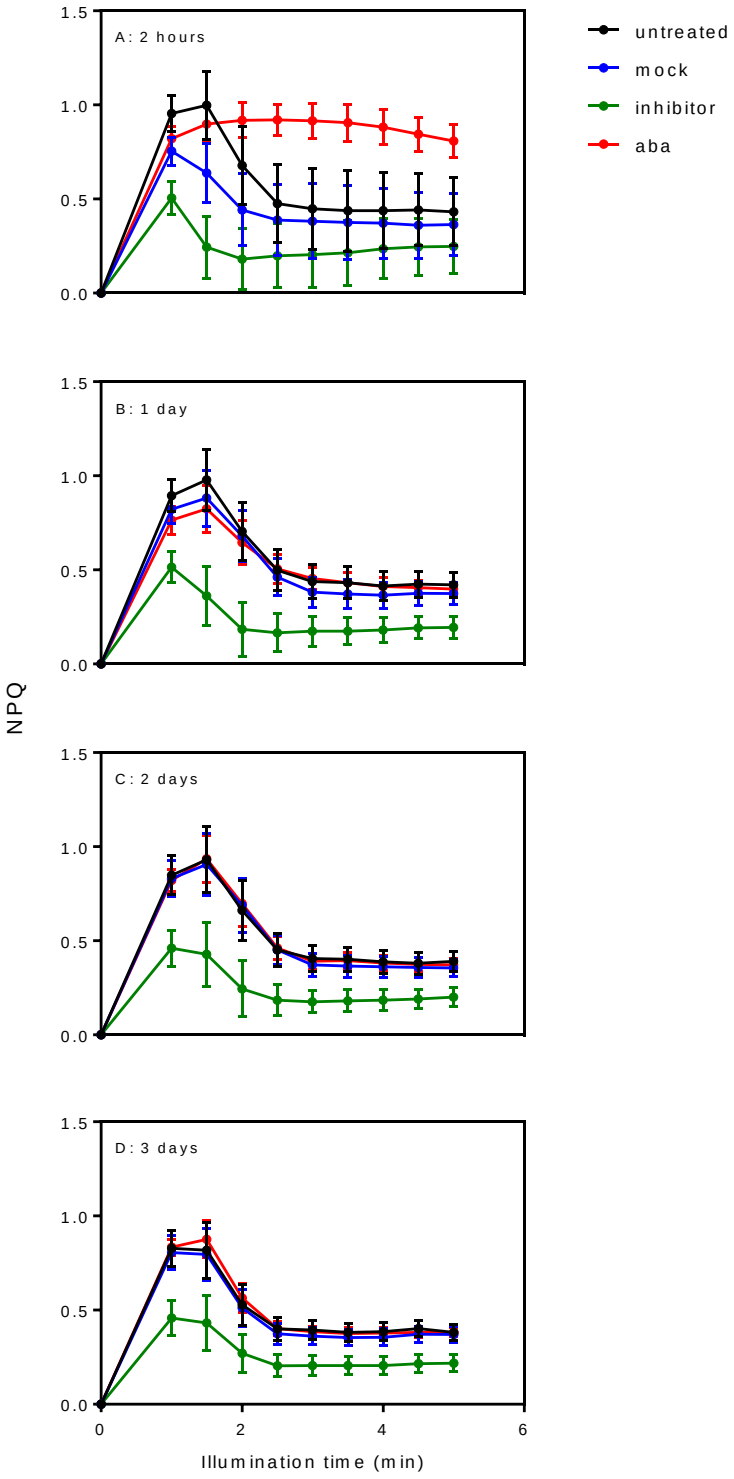

Figure 121A-D. NPQ in well-watered *B. napus* plants (A) 2 hours, then (B) 1, (C) 2 and (D) 3 days following treatment. Measurements were made on dark-adapted plants during min high-light induction. Inhibitor = 364 µM 2TBC, ABA = 100 µM abscisic acid. For statistical analysis data were tested for equal variance and one-way ANOVAs using either Tukey's or Games-Howell multiple comparisons test were performed. Significant results are referred to in the text. Values are the mean (n=5) ± SE.

5.4. Discussion

Results from Chapter 3 showed that application of 2TBC or 3MB reproducibly enhanced survival to critical drought stress. Block *et al*., (2004) and Schultz *et al*., (2012) indicated that PARP-deficient plants had increased abiotic stress tolerance which supports the enhanced survival effects seen in PARP inhibitor treated plants in Chapter 3. In this chapter, *parp*1*parp*2 showed prolonged survival to drought and wild-type plants treated with 2TBC survived for longer than untreated plants (Figure 113; Figure 114). Interestingly, the single *parp* mutants did not exhibit significantly prolonged survival likely as a result of the functional redundancy of the *PARP* family, which chemical inhibition overcomes (Figure 113) (Briggs & Bent, 2011).

Schultz *et al*., (2012) reported small but significant increases in ΦPSII in 3MB treated unstressed plants (Figure 107), which contradicts results from Chapter 3 where 2TBC or 3MB did not lead to increased ΦPSII under any conditions, at any concentration tested. This indicated that the impact of PARP inhibitors might be compound or concentration dependent, or both. Additionally, differences between each experimental setup may have influenced the results. To investigate the impact of PARP-deficiency on photosynthesis further, parameters were measured in Arabidopsis *parp* mutant lines. Pham *et al*., (2015) reported that F_v/F_m and electron transport rate were significantly reduced in *parp*1 and *parp*2 plants relative to wild-types (Figure 108). However, *parp* knockout did not significantly alter F_v/F_m, ΦPSII or NPQ relative to wild-types, except in response to severe drought when *parp*1*parp*2 plants survived for longer (Figure 111A-F). Due to instrumental differences which impacted on measurements of photosynthetic parameters, this experiment should be repeated.

Vanderauwera *et al*., (2007) reported that PARP-deficiency led to a moderate increase in ABA levels, transcript levels of ABA-responsive genes and ABA signal transduction. ABA is an important phytohormone which regulates physiology, growth and development (Shinozaki & Yamaguchi-Shinozaki, 2006). During water scarcity, ABA synthesis increases and perception is processed through complex signalling networks to achieve a variety of responses (Raghavendra *et al*., 2010; Sah

et al., 2016). For example, in the short-term ABA is known to induce stomatal closure and inhibit stomatal opening by causing the osmotic shrinking of guard cells, thereby reducing water loss (Acharya *et al.*, 2013). In the longer-term ABA can reprogram and inhibit growth.

Protein kinases such as OST1 play crucial role in ABA signalling (Mustilli *et al*., 2002; Acharya *et al*., 2013). *ost*1-2 mutants are insensitive to ABA-induced stomatal closure (Figure 110). Therefore, internal CO_2 concentration should not be limiting to photosynthesis and plants went through induction more quickly than wild-type plants, resulting in increased values of ΦPSII and lower NPQ (Figure 111A-F). Of course these plants also lost viability in response to drought more quickly than wild-types because of their inability to conserve water (Figure 113). Interestingly, the phenotype could not be rescued by the application of 2TBC indicating that PARPs may interact with ABA. This suggests that any anti-transpirant mode of action of PARP inhibitors is likely to be the result of ABA-related stomatal closure as opposed to the compounds forming films around leaves for example.

The increased ABA levels and related gene expression changes reported by Vanderauwera *et al*., (2007) is in agreement with the enhanced stress tolerance observed in PARP-deficient plants observed by Block *et al*., (2004) and Schultz *et al*., (2012), and the enhanced survival seen in this chapter and in Chapter 3. However, whilst ABA is required for normal growth processes, high levels are known to inhibit growth (Xiong & Zhu, 2003; Raghavendra *et al*., 2010). That said, Vanderauwera *et al*., (2007) reported only a small increase in ABA in PARP-deficient plants and explained that this more moderate perturbation could lead to enhanced growth. This might also have been the case for the growth enhancement reported in 3MB treated plants in Schultz *et al*., (2012), because the inhibitor concentration was small enough (200 μM) to lead to minor ABA increases. However, no growth enhancement was seen following 2TBC or 3MB application in Chapter 3. Because the growth reduction was less severe at lower inhibitor concentrations, this suggests that the higher concentration (typically 364 μM) either had a direct damaging effect or reduced growth because of a large increase in ABA resulting from PARP deficiency. Further

work should be done to determine effective working concentrations for the inhibitors.

To investigate the relationship between drought, PARP inhibition and stomatal response (and thus ABA) gas exchange was measured. Reduced ΦPSII in 2TBC treated plants in Chapter 3 could have been a result of ABA-induced stomatal closure and subsequent CO_2 limitation. Relative to untreated samples, both ABA and 2TBC application resulted in reduced stomatal conductance, ΦPSII and assimilation 2 hours after treatment of well-watered plants (Figure 120C-D). This suggests that these compounds had an anti-transpirant effect. Interestingly, 2TBC treatment led to a larger reduction in ΦPSII than ABA (Figure 120B). ABA and 2TBC treated plants had similar levels of carbon assimilation despite conductance been much lower in ABA plants. This may further indicate that 2TBC was damaging plants and inhibiting the photosynthetic processes. In a follow up experiment, ABA treated plants had elevated NPQ after 2 hours of treatment which then returned to the same values as untreated plants after 24 hours (Figure 121A-D). 2TBC treated plants showed a lasting impact on photosynthesis however and had reduced NPQ which persisted for 3 days. Overall these results indicate that 2TBC was having a damaging impact on the plants. Furthermore, the compound had a two-fold impact – an ABA-like effect and a damaging effect, which were occurring simultaneously.

Potentially protective compounds may act to augment plant stress responses, as in the case with chitosan inducing stomatal closure (Iriti *et al.*, 2009). An additional gas analysis was performed to investigate if 2TBC altered stomatal response to light and dark transitions. There was no significant impact on the rate or opening or closing of stomata in 2TBC treated plants relative to untreated samples under well-watered or droughted conditions, indicating the compound did not make stomata more responsive to light or dark (Figure 116A-F). There was a significant impact of time of day on stomatal conductance in droughted samples however, so any potentially smaller compound effects may have been masked. These extended gas analyses can prove difficult due to length of time needed to measure one replicate. Access to multiple gas analysers may solve this problem. Additionally thermal imaging could be used to quantify how plants respond over the course of a day, as in the case of canopy

temperature measurement, although this technique can be difficult under changing light conditions (Li *et al*., 2014).

The results from this chapter further suggest that high concentrations of 2TBC causes damage to plants, and reduces photosynthetic capabilities and stomatal conductance. Additionally, the inhibitor did not make stomata more responsive to light or dark under either unstressed or drought stressed conditions. More work needs to be done to determine effective working concentrations for inhibitors. However, there is clearly a relationship between PARP deficiency and survival in response to critical stress. Genetic and chemical PARP deficiency have reproducibly prolonged survival, perhaps as a result of enhanced stress tolerance through increased ABA levels and ABA-responsive gene expression. This suggests that PARP inhibition has a protective effect under certain conditions. Inevitably though, compounds which cause significant damage to plants are not commercially marketable. 2TBC has a potential anti-transpirant mode of action although it is likely that the reduced stomatal conductance seen in treated plants was as a result of elevated ABA or direct damage, or both. It might be possible to determine what causes the damaging impact of 2TBC, so that this effect can be minimised whilst preserving the protective effect. This relies on the two effects not being intrinsically linked. An example of this is the exogenous application of the defence response priming agent ß-aminobutyric acid (BABA), which protects plants against a range of stresses but inhibits growth (Luna *et al*., 2014; Schwarzenbacher *et al*., 2014). The compound has potential application in crop protection strategies but only when plants are experiencing stress, as application under non-stressed conditions would be detrimental. If the negative impact of 2TBC can be reduced (or removed) the compound could be used to augment plant response to stress.

In summary:

- Genetic PARP-deficiency enhanced survival to severe drought stress.
- PARP inhibitor application reduced stomatal conductance but did not affect the rate of stomatal opening or closing following dark/light transitions.

Chapter 6

6. General Discussion

6.1. Photosynthetic induction was a sensitive, early-onset indicator of drought

The work presented in Chapter 2 used non-invasive imaging techniques to quantify the impact of drought on plant physiology and growth. In particular, I used chlorophyll fluorescence imaging to define protocols to rapidly and reproducibly quantify drought stress in plants. Various studies have quantified F_v/F_m and other steady-state parameters when measuring abiotic stress response (Woo *et al*., 2008; Jansen *et al*., 2009; Sperdouli & Moustakas, 2012; Zivcak *et al*., 2013; Su *et al*., 2015). In Chapter 2 I showed that steady-state measurements were only indicative of severe drought and remained unperturbed at moderate stress intensities. Photosynthetic induction proved to be a more sensitive indicator of mild drought stress, which is perhaps unsurprising given the dynamic nature of the underlying processes involved. During photosynthetic induction of a dark-adapted plant, rates of electron transport increase, a transthylakoid pH gradient develops, metabolites and enzymes for the Calvin cycle are recruited and activated, and stomata begin to open (Baker, 2008*a*; Murchie & Lawson, 2013*b*). These processes can be sensitive to the onset of drought stress. For example, droughted plants will reduce stomatal opening which can lead to an internal CO_2 limitation and reduced carbon assimilation. Reduced biochemical demand for the metabolites required for carbon fixation can lead to a downregulation of electron transport, which may reduce ΦPSII and ETR, unless the activities of alternative electron sinks are increased to compensate (Flexas *et al*., 1998; Santos *et al*., 2009; Brestic & Zivcak, 2013). ROS generation resulting from the over-reduction of the electron transport chain can reduce photosynthetic efficiency and damage the apparatus (Tripathy & Oelmüller, 2012). Drought has also been shown to negatively impact RuBP regeneration and Rubisco activity (Gimenez *et al*., 1992; Parry *et al*., 2002). All of these impacts can slow the rate at which droughted plants go through induction and can manifest as changes in the parameters measured using chlorophyll fluorescence.

In several independent experiments in Chapter 2 I showed that drought significantly altered photosynthetic parameters when measured during induction. During the first

5 min of illumination, droughted Arabidopsis and *B. napus* plants had significantly lower values of ΦPSII and higher values of NPQ in comparison to controls. The onset of these changes was consistent with the decline of soil water content to ~ 20% in both species. This slowing of the rate of increase of ΦPSII was attributed to stomatal closure and internal CO_2 limitation in a separate gas exchange analysis in 2.3.7. This was concurrent with increased leaf temperature in droughted plants measured using thermal imaging in 2.3.3. However, steady-state photosynthesis was not perturbed until soil water content had declined further. Growth was also inhibited later than changes in photosynthetic induction first occurred. So although growth parameters were easy to measure, they were not as early-onset as the changes in induction.

These findings suggested that parameters measured during photosynthetic induction were sensitive, early-onset indicators of drought stress, whereas steady-state changes were more indicative of severe stress. I showed that the classically used parameter F_v/F_m proved to be more of a measure of viability than an indicator of moderate drought. Using chlorophyll fluorescence imaging, backed up by gas exchange analysis and thermal imaging, I developed a protocol for the rapid quantification of early-onset drought stress in Arabidopsis and *B. napus*. *T. aestivum* proved to be more drought tolerant and harder to measure because of its vertical growth pattern. Using this protocol, a reproducible measure of drought was obtainable in 10 min (at most), soon after water withholding. This protocol was used in Chapter 3 to quantify the impact of PARP inhibitors on photosynthesis.

6.2. PARP-deficiency enhanced survival of Arabidopsis in response to drought

In Chapter 3 I showed that application of the chemical PARP inhibitors 2TBC and 3MB reproducibly enhanced survival of Arabidopsis in response to severe drought stress. This was particularly the case at higher concentrations of the compounds. Because higher concentrations conferred higher survival rates than lower concentrations, this suggests that the compounds had a direct protective effect. Later in 5.3.1, survival

assays showed that Arabidopsis *parp*1*parp*2 plants had significantly prolonged survival under drought conditions than wild-types. In contrast, single *parp* mutants did not significantly alter survival, which further demonstrates the functional redundancy of the *PARP* family and verifies why chemical inhibitors have application in plant biology (Briggs & Bent, 2011; Schulz *et al.*, 2012). Several studies have suggested that genetically or chemically-induced PARP-deficiency confers enhanced abiotic stress tolerance (Block *et al*., 2004; Vanderauwera *et al*., 2007; Schulz *et al*., 2012). The work in this thesis supports this. Enhanced tolerance to drought likely prolonged the survival of PARP-deficient plants. This could have been as a result of the maintenance of energy homeostasis or elevated ABA-levels, or both (Block *et al*., 2004; Vanderauwera *et al*., 2007).

6.3. PARP inhibitors had negative impacts on photosynthesis and growth in short-term assays with Arabidopsis and *B. napus*

Survival in response to severe stress was an important benefit of PARP inhibitor treatment. However, work in 3.3.1 and 3.3.5 showed application of higher concentrations of 2TBC led to significant changes in photosynthetic induction in Arabidopsis and *B. napus*. In particular, high 2TBC concentrations reduced ΦPSII and NPQ throughout induction in both well-watered and droughted samples. Additionally, F_v/F_m was reduced and ΦNO was elevated indicating plants were damaged. High values of ΦNO indicate that the plant is unable to regulate energy dissipation (Kramer *et al*., 2004; Sperdouli & Moustakas, 2012). High compound concentrations also led to impaired growth and visual signs of damage. These findings show that 2TBC had a damaging impact on plant health at higher concentrations. These changes were not observed to the same extent at lower 2TBC concentrations, or at all for any of the concentrations of 3MB tested, indicating that the effects were compound specific. These findings support results from Schulz *et al*., (2012) who observed growth penalties at high compound concentrations, but enhanced growth at lower concentrations, indicating that there was a trade-off of chemical application. Additionally, Vanderauwera *et al*., (2007) suggested that

increased stress tolerance can often come at the expense of growth. In particular, high levels of ABA have been shown to inhibit growth processes (Xiong & Zhu, 2003). It is possible that in addition to a direct damaging effect, increased ABA led to growth suppression in PARP inhibitor treated plants. Alternatively, the damage might result from a different underlying mechanism that could, in theory, be separated from protective effects. It is therefore necessary to determine appropriate working concentrations for these compounds and better understand their mode of action.

6.4. 2TBC enhanced seed yield of Arabidopsis because more plants survived critical drought

In 3.3.3, the impact of 2TBC on Arabidopsis seed yield was measured. Under droughted conditions 2TBC treatment led to a higher overall yield relative to other treatments because more plants survived the drought. This was as opposed to individual plants producing more seed. Under well-watered conditions 2TBC had an associated cost as application led to a small reduction in average seed yield per plant. These findings demonstrate that there is often a trade-off when applying agro-chemicals (Aktar *et al*., 2009). Experimental setups of this nature, where an absolute drought is applied for a short period during the vegetative growth stage of a plant, is not necessarily representative of the type of stress plants would experience in the field. Additionally in Chapter 2 yield parameters were unaffected by a moderate drought, suggesting that the stress intensity was too mild or that plants had enough time to recover before harvest. Applying more severe stress intensities runs the risk of masking subtle compound effects. Furthermore, Arabidopsis is not necessarily a good model for investigating yield parameters due to the indeterminate nature of the inflorescence and because not all of the underlying determinants of yield are fully understood (Van Daele *et al.*, 2012). To determine if PARP inhibitors had application in an agricultural context, it was necessary to measure the impact of the compounds on the yield of an economically important crop species.

6.5. PARP and PSII inhibitors reduced growth and yield of *T. aestivum* in a long-term trial

In Chapter 4 the impact of PARP and PSII inhibitors on the yield of *T. aestivum* was quantified in response to a drought which was applied over the whole life cycle of the plants. I showed that PARP and PSII inhibitors had either no significant impact on growth and yield, or negative impacts. No compound led to a significant enhancement of growth or yield at any application point. This is in contrast to Vanderauwera *et al*., (2007) who suggested that yield was unaltered in PARP-deficient plants. Block and Metzlaff claimed that corn and oilseed rape PARP-deficient plants showed similar yields to wild-types under unstressed conditions, and ~ 40-60% higher yields under drought stress (unpublished results referred to in Vanderauwera *et al*., (2007)). However, these studies used genetic knockdown of PARP activity, not exogenous chemical application, demonstrating that different routes of reducing PARP activity have different effects. Genetic applications are not on the European agenda for the foreseeable future however, hence why there was a need to quantify the impacts of chemical inhibitors.

6.6. There was a strong relationship between *T. aestivum* growth and yield under drought stress which was used to predict the impact of compounds on yield

The results in Chapter 4 showed that there was a strong linear relationship between growth and yield under drought stress when compounds were applied at the mid-point application. During the vegetative growth period plants assimilate reserves which are relocated to the grain during grain filling (Pheloung & Siddique, 1991; Schnyder, 1993). Stress which reduces assimilation during growth can have an adverse impact on yield. However, this is likely to be less influential than stress during reproductive development itself, which is what plants experienced in this experiment (Yang & Zhang, 2006; Dolferus *et al*., 2011). The relationship between maximum OSA and yield meant that it was possible to predict the impact that a compound had on

yield ~ 40 days earlier than measuring at harvest. Additionally, by fitting a generalised additive model (GAM) to the growth data it was possible to detect compound-induced changes in growth ~ 10 days after application at the mid-point. This ability to predict the impact of compounds on yield much earlier than harvest measurements is a key finding of this work and of great potential industrial application. A critique of the majority of studies investigating the impacts of PARP inhibitors is that they have not been representative enough of whole-plant conditions in the field. The work in Chapter 4 quantified the impact of known PARP inhibitors on yield and found the effect to generally be small or negative.

6.7. PARP inhibitors reduced stomatal conductance but did not alter the kinetics of stomatal opening or closing

2TBC application had consistently reduced photosynthetic capability in Arabidopsis and *B. napus*. The work in 3.3.5 showed that this was partly a result of reduced stomatal conductance and internal CO_2 limitation. Application of 2TBC and ABA significantly reduced stomatal conductance in well-watered *B. napus* plants, suggesting that 2TBC had an anti-transpirant mode of action. However, 2TBC also caused dramatic reductions in F_v'/F_m' and ΦPSII further indicating that there was also a damaging impact. This was supported by a subsequent analysis in 5.3.4 which showed that NPQ was severely reduced in 2TBC sprayed plants, an effect that persisted 3 days after treatment. However, 2TBC did not make stomata more responsive to periods of light or dark, as might have been the case for a compound which augmented stress response. These results show that 2TBC had a two-fold impact, one brought about by a direct damaging effect and one through reduced stomatal conductance, likely as a result of increased ABA levels. Elevated ABA levels in PARP-deficient plants will increase stomatal closure and augment drought survival (Raghavendra *et al*., 2010; Tombesi *et al*., 2015; Bauer *et al*., 2017). There are associated costs of application to photosynthesis and growth. It is possible that the protective and the damaging effects are separable. If the mechanism of the damaging effect can be elucidated, it might be possible to reduce whilst still maintaining the

survival impact. An example of such work involves that defence priming agent BABA discussed in 5.4.

6.8. The use of PARP inhibitors is not agriculturally viable

From an agricultural perspective chemical PARP inhibitors are not commercially viable because they have a mammalian target (Briggs & Bent, 2011). In addition, this work has shown that there are costs associated with compound application, particularly under unstressed conditions. Although drought can be predicted to a certain extent, it is very undesirable from an agricultural point of view for any compound to cause damage and inhibit photosynthesis and growth under non-stressed conditions. This work showed that PARP inhibition has a clear impact on survival in response to critical drought stress. However, if a crop is stressed to such an extent that it is hours (or a few days) away from death, the quality of the crop product is likely to be so low that it is unmarketable anyway.

6.9. Where are we now?

Before this project began it was understood that PARP-deficient plants are more tolerant to a range of abiotic stresses (Block *et al.*, 2004; Jansen *et al*., 2009; Schulz *et al*., 2012). Block *et al*., (2004) argued that plants with enhanced stress tolerance are less sensitive to adverse conditions, which indirectly increases their growth potential. Furthermore, they reported that plants with reduced PARP activity had higher energy use efficiency and hypothesised that the reduction of energy consuming processes could enhance growth, and allow plants to acclimate to moderate stresses. Several studies then reported that PARP-deficiency enhanced growth under non-stressed and stressed conditions, although these studies were typically short-term *in vitro* assays (Jansen *et al*., 2009; Schulz *et al*., 2012, 2014). Unpublished results in Vanderauwera *et al*., (2007) reported that PARP-deficient plants had higher yields than wild-types under drought stress. However, this group used genetic approaches to reduce PARP activity. At the time of starting this work

there was an increasing need to measure the impact of chemical PARP inhibitors on growth and yield in whole plants. The results from this work support the widely reported increased stress tolerance of PARP-deficient plants. There was a clear enhancement of survival to critical stress suggesting PARP inhibitors augmented stress response. However, there were costs associated with chemical treatment which impaired photosynthesis and reduced growth and yield. These negative impacts were observed under well-watered and drought stressed conditions further highlighting the cost associated with application. Therefore PARP inhibitors are unlikely to be agriculturally useful and agronomically effective.

6.10. In summary

There was a clear benefit of PARP inhibitor application on survival. However, it was hypothesised that PARP inhibitors might present an avenue to preserve or enhance photosynthesis, growth and yield under moderate stress. In fact, under both moderate drought and well-watered conditions, high concentrations of 2TBC had negative impacts. These were less marked at lower concentrations or when using 3MB. The associated negative effects of 2TBC are likely two-fold, partly resulting from a direct damaging effect and partly through increased ABA levels. A major achievement of this work is the development of a rapid method to assess the impact of potential compounds on photosynthesis. Additionally, the impact of potential compounds on yield can be predicted ~ 45-50 days earlier than harvest using measurements of maximum OSA and data modelling, which is of great potential application in agro-chemistry.

6.11. Future perspectives

- The level of poly (ADP-ribosyl)ation (PAR) in untreated and treated plants should be quantified using a PAR assay for each compound to ensure that it is inhibiting PARP *in planta*.
- Working concentrations for each PARP inhibitor should be precisely determined.

- The impact of *parp* knockout on photosynthesis should be investigated.
- Thermal imaging should be used to probe the impact of PARP inhibitors on stomatal conductance and leaf temperature in response to drought stress.
- The impact of ABA on stomatal responsiveness to light/dark transitions should be measured and could serve as a point of comparison for the testing of other compounds.

References

Abdipour M, Ebrahimi M, Izadi A, Mastrangelo A, NAJAFIAN G, ARSHAD Y & Mirniyam G (2016). *Association between Grain Size and Shape and Quality Traits, and Path Analysis of Thousand Grain Weight in Iranian Bread Wheat Landraces from Different Geographic Regions*.

Access A (2015). Methylated Rape Seed Oil. *Generic Agrochem Portal*. Available at: http://www.agchemaccess.com/Methylated_rape_seed_oil.

Achard P, Gusti A, Cheminant S, Alioua M, Dhondt S, Coppens F, Beemster GTS & Genschik P (2017). Gibberellin Signaling Controls Cell Proliferation Rate in Arabidopsis. *Curr Biol* **19,** 1188–1193.

Acharya BR, Jeon BW, Zhang W & Assmann SM (2013). Open Stomata 1 (OST1) is limiting in abscisic acid responses of Arabidopsis guard cells. *New Phytol* **200,** 1049–1063.

AHDB (2015). *Wheat growth guide*. Warwickshire. Available at: https://cereals.ahdb.org.uk/media/185687/g66-wheat-growth-guide.pdf.

Aktar MW, Sengupta D & Chowdhury A (2009). Impact of pesticides use in agriculture: their benefits and hazards. *Interdiscip Toxicol* **2,** 1–12.

Alatorre-Cobos F, Calderón-Vázquez C, Ibarra-Laclette E, Yong-Villalobos L, Pérez-Torres C-A, Oropeza-Aburto A, Méndez-Bravo A, González-Morales S-I, Gutiérrez-Alanís D, Chacón-López A, Peña-Ocaña B-A & Herrera-Estrella L (2014). An improved, low-cost, hydroponic system for growing Arabidopsis and other plant species under aseptic conditions. *BMC Plant Biol* **14,** 69.

Allen GJ, Muir & Sanders D (1995). Release of Ca2+ from individual plant vacuoles by both InsP3 and cyclic ADP-ribose. *Science (80-)* **268,** 735 LP-737.

Alonso-Blanco C, Blankestijn-de Vries H, Hanhart CJ & Koornneef M (1999). Natural allelic variation at seed size loci in relation to other life history traits of Arabidopsis thaliana. *Proc Natl Acad Sci* **96,** 4710–4717.

Altman NS (1992). An Introduction to Kernel and Nearest-Neighbor Nonparametric Regression. *Am Stat* **46,** 175–185.

Amor Y, Babiychuk E, Inzé D & Levine A (1998). The involvement of poly(ADP-ribose) polymerase in the oxidative stress responses in plants. *FEBS Lett* **440,** 1–7.

Arena C, Mistretta C, Di Natale E, Faraone Mennella MR, De Santo AV & De Maio A (2011). Characterization and role of poly(ADP-ribosyl)ation in the Mediterranean species Cistus incanus L. under different temperature conditions. *Plant Physiol Biochem* **49,** 435–440.

Armstrong S & Clough J (2009). Crop protection chemicals. *R Soc Chem*. Available at: https://eic.rsc.org/feature/crop-protection-chemicals/2020121.article.

Arnon DI & Tang GM-S (1985). Uncouplers enhance photosynthetic electron

transport from water to NADP+ in the presence of plastoquinone inhibitors. *Biochim Biophys Acta - Bioenerg* **809,** 167–172.

Asada K, Neubauer C, Heber U & Schreiber U (1990). Methyl Viologen-Dependent Cyclic Electron Transport in Spinach Chloroplasts in the Absence of Oxygen. *Plant Cell Physiol* **31,** 557–564.

Ashraf M & Harris PJC (2013). Photosynthesis under stressful environments: An overview. *Photosynthetica*; DOI: 10.1007/s11099-013-0021-6.

Asseng S & van Herwaarden AF (2003). Analysis of the benefits to wheat yield from assimilates stored prior to grain filling in a range of environments*. *Plant Soil* **256,** 217–229.

Atkinson NJ & Urwin PE (2012). The interaction of plant biotic and abiotic stresses: from genes to the field. *J Exp Bot* **63,** 3523–3543.

Babiychuk E, Cottrill PB, Storozhenko S, Fuangthong M, Chen Y, O'Farrell MK, Van Montagu M, Inzé D & Kushnir S (1998). Higher plants possess two structurally different poly(ADP-ribose) polymerases. *Plant J* **15,** 635–645.

Baerenfaller K et al. (2012). Systems-based analysis of Arabidopsis leaf growth reveals adaptation to water deficit. *Mol Syst Biol* **8,** 606.

Baker NR (2008*a*). Chlorophyll Fluorescence: A Probe of Photosynthesis In Vivo. *Annu Rev Plant Biol* **59,** 89–113.

Baker NR (2008*b*). Chlorophyll fluorescence: a probe of photosynthesis in vivo. *Annu Rev Plant Biol* **59,** 89–113.

Bauer H, Ache P, Lautner S, Fromm J, Hartung W, Al-Rasheid KAS, Sonnewald S, Sonnewald U, Kneitz S, Lachmann N, Mendel RR, Bittner F, Hetherington AM & Hedrich R (2017). The Stomatal Response to Reduced Relative Humidity Requires Guard Cell-Autonomous ABA Synthesis. *Curr Biol* **23,** 53–57.

Benavente E, García-Toledano L, Carrillo JM & Quemada M (2013). Thermographic Imaging: Assessment of Drought and Heat Tolerance in Spanish Germplasm of Brachypodium Distachyon. *Procedia Environ Sci* **19,** 262–266.

Benlloch R, Berbel A, Serrano-Mislata A & Madueño F (2007). Floral Initiation and Inflorescence Architecture: A Comparative View. *Ann Bot* **100,** 659–676.

Block M De, Verduyn C, Brouwer D De & Cornelissen M (2004). Poly(ADP-ribose) polymerase in plants affects energy homeostasis, cell death and stress tolerance. *Plant J* **41,** 95–106.

Bonhomme L, Valot B, Tardieu F & Zivy M (2012). Phosphoproteome Dynamics Upon Changes in Plant Water Status Reveal Early Events Associated With Rapid Growth Adjustment in Maize Leaves. *Mol Cell Proteomics* **11,** 957–972.

Boyer JS (1982). Plant Productivity and Environment. *Science (80-)* **218,** 443 LP-448.

Boyer JS & Westgate ME (2004). Grain yields with limited water. *J Exp Bot* **55,** 2385–2394.

Brady SM, Sarkar SF, Bonetta D & McCourt P (2003). The ABSCISIC ACID INSENSITIVE 3 (ABI3) gene is modulated by farnesylation and is involved in auxin signaling and lateral root development in Arabidopsis. *Plant J* **34,** 67–75.

Bresson J, Vasseur F, Dauzat M, Koch G, Granier C & Vile D (2015). Quantifying spatial heterogeneity of chlorophyll fluorescence during plant growth and in response to water stress. *Plant Methods* **11,** 23.

Brestic M & Zivcak M (2013). PSII Fluorescence Techniques for Measurement of Drought and High Temperature Stress Signal in Crop Plants: Protocols and Applications BT - Molecular Stress Physiology of Plants. In, ed. Rout GR & Das AB, pp. 87–131. Springer India, India. Available at: https://doi.org/10.1007/978-81-322-0807-5_4.

Briggs AG & Bent AF (2011). Poly(ADP-ribosyl)ation in plants. *Trends Plant Sci* **16,** 372–380.

Burghardt M, Riederer M (2003) Ecophysiological relevance of cuticular transpiration of deciduous and evergreen plants in relation to stomatal closure and leaf water potential. *J Exp Bot* **54,** 1941-1949

C. Pheloung P & Siddique K (1991). *Contribution of Stem Dry-Matter to Grain-Yield in Wheat Cultivars*.

Calatayud a., Roca D & Martínez PF (2006). Spatial-temporal variations in rose leaves under water stress conditions studied by chlorophyll fluorescence imaging. *Plant Physiol Biochem* **44,** 564–573.

Camargo A V, Mott R, Gardner KA, Mackay IJ, Corke F, Doonan JH, Kim JT & Bentley AR (2016). Determining Phenological Patterns Associated with the Onset of Senescence in a Wheat MAGIC Mapping Population . *Front Plant Sci* **7,** 1540. Available at: http://journal.frontiersin.org/article/10.3389/fpls.2016.01540.

Chaves MM (2002). How Plants Cope with Water Stress in the Field? Photosynthesis and Growth. *Ann Bot* **89,** 907–916.

Chaves MM, Flexas J & Pinheiro C (2008). Photosynthesis under drought and salt stress: regulation mechanisms from whole plant to cell. *Ann Bot* **103,** 551–560.

Chaves MM, Flexas J & Pinheiro C (2009). Photosynthesis under drought and salt stress: regulation mechanisms from whole plant to cell. *Ann Bot* **103,** 551–560.

Chaves MM & Oliveira MM (2004). Mechanisms underlying plant resilience to water deficits: prospects for water-saving agriculture. *J Exp Bot* **55,** 2365–2384.

Choe S, Fujioka S, Noguchi T, Takatsuto S, Yoshida S & Feldmann KA (2001). Overexpression of DWARF4 in the brassinosteroid biosynthetic pathway results in increased vegetative growth and seed yield in Arabidopsis. *Plant J* **26,** 573–582.

Choudhury FK, Rivero RM, Blumwald E & Mittler R (2017). Reactive oxygen species, abiotic stress and stress combination. *Plant J* **90,** 856–867.

Claeys H, Skirycz A, Maleux K & Inzé D (2012). DELLA Signaling Mediates Stress-Induced Cell Differentiation in Arabidopsis Leaves through Modulation of Anaphase-Promoting Complex/Cyclosome Activity. *Plant Physiol* **159,** 739 LP-747.

Clauw P, Coppens F, De Beuf K, Dhondt S, Van Daele T, Maleux K, Storme V, Clement L, Gonzalez N & Inzé D (2015). Leaf Responses to Mild Drought Stress in Natural Variants of Arabidopsis. *Plant Physiol* **167,** 800–816.

Conn SJ, Hocking B, Dayod M, Xu B, Athman A, Henderson S, Aukett L, Conn V, Shearer MK, Fuentes S, Tyerman SD & Gilliham M (2013). Protocol: optimising hydroponic growth systems for nutritional and physiological analysis of Arabidopsis thaliana and other plants. *Plant Methods* **9,** 4.

CristinaRodriguez M, Petersen M & Mundy J (2010). Mitogen-Activated Protein Kinase Signaling in Plants. *Annu Rev Plant Biol* **61,** 621–649.

Van Daele I, Gonzalez N, Vercauteren I, de Smet L, Inzé D, Roldán-Ruiz I & Vuylsteke M (2012). A comparative study of seed yield parameters in Arabidopsis thaliana mutants and transgenics. *Plant Biotechnol J* **10,** 488–500.

Danquah A, de Zelicourt A, Colcombet J & Hirt H (2014). The role of ABA and MAPK signaling pathways in plant abiotic stress responses. *Biotechnol Adv* **32,** 40–52.

Dean RL & Miskiewicz E (2003). Rates of electron transport in the thylakoid membranes of isolated, illuminated chloroplasts are enhanced in the presence of ammonium chloride. *Biochem Mol Biol Educ* **31,** 410–417.

Desikan R, Cheung M, Bright J, Henson D, Hancock JT & Neill SJ (2004). ABA, hydrogen peroxide and nitric oxide signalling in stomatal guard cells. *J Exp Bot* **55,** 205–212.

Dinakar C, Djilianov D & Bartels D (2012). Photosynthesis in desiccation tolerant plants: Energy metabolism and antioxidative stress defense. *Plant Sci* **182,** 29–41.

Dolferus R, Ji X & Richards RA (2011). Abiotic stress and control of grain number in cereals. *Plant Sci* **181,** 331–341.

Dong L, Tu W, Liu K, Sun R, Liu C, Wang K & Yang C (2015). The PsbS protein plays important roles in photosystem II supercomplex remodeling under elevated light conditions. *J Plant Physiol* **172,** 33–41.

Dorostkar S, Pakniyat H, Ahmadi M, Aliakbari M, Sobhanian N, Ghorbani R & Eskandari M (2015). *Study of relationship between grain yield and yield components using multivariate analysis in barley cultivars (Hordeum vulgare International Journal of Agronomy and Agricultural Research (IJAAR)*.

Doucet-Chabeaud G, Godon C, Brutesco C, de Murcia G & Kazmaier M (2001). Ionising radiation induces the expression of PARP-1 and PARP-2 genes in Arabidopsis. *Mol Genet Genomics* **265,** 954–963.

Dubois M, Claeys H, Van den Broeck L & Inzé D (2017). Time of day determines

Arabidopsis transcriptome and growth dynamics under mild drought. *Plant Cell Environ* **40,** 180–189.

Dubois M, Skirycz A, Claeys H, Maleux K, Dhondt S, De Bodt S, Vanden Bossche R, De Milde L, Yoshizumi T, Matsui M & Inzé D (2013). ETHYLENE RESPONSE FACTOR6 Acts as a Central Regulator of Leaf Growth under Water-Limiting Conditions in Arabidopsis. *Plant Physiol* **162,** 319 LP-332.

European Union (2009). DIRECTIVE 2009/128/EC OF THE EUROPEAN PARLIAMENT AND OF THE COUNCIL of 21 October 2009 establishing a framework for Community action to achieve the sustainable use of pesticides. *Off J Eur Union* **309,** 71–86.

Evans N, Baierl A, Semenov MA, Gladders P & Fitt BDL (2008). Range and severity of a plant disease increased by global warming. *J R Soc Interface* **5,** 525 LP-531.

Farooq M, Hussain M & Siddique KHM (2014). Drought Stress in Wheat during Flowering and Grain-filling Periods. *CRC Crit Rev Plant Sci* **33,** 331–349.

Federal Biological Research Centre for Agriculture and (2001). *The extended BBCH-scale: growth stages of mono-and dicotyledonous plants*. Germany.

Fedoroff N V, Battisti DS, Beachy RN, Cooper PJM, Fischhoff DA, Hodges CN, Knauf VC, Lobell D, Mazur BJ, Molden D, Reynolds MP, Ronald PC, Rosegrant MW, Sanchez PA, Vonshak A & Zhu J-K (2010). Radically Rethinking Agriculture for the 21st Century. *Science (80-)* **327,** 833 LP-834.

Fernando VCD & Schroeder DF (2016). Role of ABA in Arabidopsis Salt, Drought, and Desiccation Tolerance. In, ed. Shanker AK & Shanker CBT-A and BS in P-RA and FP, p. Ch. 22. InTech, Rijeka. Available at: http://dx.doi.org/10.5772/61957.

Fischer RA (2008). The importance of grain or kernel number in wheat: A reply to Sinclair and Jamieson. *F Crop Res* **105,** 15–21.

Fisher LHC, Han J, Corke FMK, Akinyemi A, Didion T, Nielsen KK, Doonan JH, Mur LAJ & Bosch M (2016). Linking Dynamic Phenotyping with Metabolite Analysis to Study Natural Variation in Drought Responses of Brachypodium distachyon . *Front Plant Sci* **7,** 1751. Available at: http://journal.frontiersin.org/article/10.3389/fpls.2016.01751.

Flexas J, Bota J, Escalona JM, Sampol B & Medrano H (2002). Effects of drought on photosynthesis in grapevines under field conditions: an evaluation of stomatal and mesophyll limitations. *Funct Plant Biol* **29,** 461–471.

Flexas J, Escalona J & Medrano H (1998). *Down-regulation of photosynthesis by drought under field conditions in grapevine leaves*.

Flexas J & Medrano H (2002). Drought-inhibition of Photosynthesis in C3 Plants: Stomatal and Non-stomatal Limitations Revisited. *Ann Bot* **89,** 183–189.

Foley J a. et al. (2011). Solutions for a cultivated planet. *Nature* **478,** 337–342.

Food and Agriculture Organization of the United Nations (2016). *The State of Food*

and Agriculture: Climate Change, Agriculture and Food Security. Rome. Available at: http://www.fao.org/3/a-i6030e.pdf.

Foyer CH, Neukermans J, Queval G, Noctor G & Harbinson J (2012). Photosynthetic control of electron transport and the regulation of gene expression. *J Exp Bot* **63,** 1637–1661.

Foyer CH & Noctor G (2003). Redox sensing and signalling associated with reactive oxygen in chloroplasts, peroxisomes and mitochondria. *Physiol Plant* **119,** 355–364.

Fraire-velázquez S, Rodríguez-guerra R & Sánchez-Calderón (2011). Abiotic and Biotic Stress Response Crosstalk in Plants. *Tech*346.

Franks SJ (2011). Plasticity and evolution in drought avoidance and escape in the annual plant Brassica rapa. *New Phytol* **190,** 249–257.

Fuerst EP & Norman MA (1991). Interactions of Herbicides with Photosynthetic Electron Transport. *Weed Sci* **39,** 458–464.

Fujii T, Yokoyama E, Inoue K & Sakurai H (1990). The sites of electron donation of Photosystem I to methyl viologen. *Biochim Biophys Acta - Bioenerg* **1015,** 41–48.

Furbank RT & Tester M (2011). Phenomics – technologies to relieve the phenotyping bottleneck. *Trends Plant Sci* **16,** 635–644.

Gatehouse AMR, Ferry N, Edwards MG & Bell HA (2011). Insect-resistant biotech crops and their impacts on beneficial arthropods. *Philos Trans R Soc B Biol Sci* **366,** 1438 LP-1452.

Genty B, Briantais J-M & Baker NR (1989). The relationship between the quantum yield of photosynthetic electron transport and quenching of chlorophyll fluorescence. *Biochim Biophys Acta - Gen Subj* **990,** 87–92.

Gimenez C, Mitchell VJ & Lawlor DW (1992). Regulation of Photosynthetic Rate of Two Sunflower Hybrids under Water Stress. *Plant Physiol* **98,** 516–524.

Gornall J, Betts R, Burke E, Clark R, Camp J, Willett K & Wiltshire A (2010). Implications of climate change for agricultural productivity in the early twenty-first century. *Philos Trans R Soc B Biol Sci* **365,** 2973–2989.

Goss R, Opitz C, Lepetit B & Wilhelm C (2008). The synthesis of NPQ-effective zeaxanthin depends on the presence of a transmembrane proton gradient and a slightly basic stromal side of the thylakoid membrane. *Planta* **228,** 999–1009.

Griffiths S, Wingen L, Pietragalla J, Garcia G, Hasan A, Miralles D, Calderini DF, Ankleshwaria JB, Waite ML, Simmonds J, Snape J & Reynolds M (2015). Genetic Dissection of Grain Size and Grain Number Trade-Offs in CIMMYT Wheat Germplasm ed. Yan L. *PLoS One* **10,** e0118847.

Großkinsky DK, Svensgaard J, Christensen S & Roitsch T (2015). Plant phenomics and the need for physiological phenotyping across scales to narrow the genotype-

to-phenotype knowledge gap. *J Exp Bot* **66,** 5429–5440.

Herms S, Seehaus K, Koehle H & Conrath U (2002). A strobilurin fungicide enhances the resistance of tobacco against tobacco mosaic virus and Pseudomonas syringae pv tabaci. *Plant Physiol* **130,** 120–127.

Hopper DW, Ghan R & Cramer GR (2014). A rapid dehydration leaf assay reveals stomatal response differences in grapevine genotypes. *Hortic Res* **1,** 2.

Horton P, Johnson MP, Perez-Bueno ML, Kiss AZ & Ruban A V. (2008). Photosynthetic acclimation: Does the dynamic structure and macro-organisation of photosystem II in higher plant grana membranes regulate light harvesting states? *FEBS J* **275,** 1069–1079.

Humplík JF, Lazár D, Husičková A & Spíchal L (2015). Automated phenotyping of plant shoots using imaging methods for analysis of plant stress responses - a review. *Plant Methods* **11,** 29.

Hunt L & Gray JE (2009). The relationship between pyridine nucleotides and seed dormancy. *New Phytol* **181,** 62–70.

Hunt L, Lerner F & Ziegler M (2004). NAD – new roles in signalling and gene regulation in plants. *New Phytol* **163,** 31–44.

Ikejima M, Noguchi S, Yamashita R, Ogura T, Sugimura T, Gill DM & Miwa M (1990). The zinc fingers of human poly(ADP-ribose) polymerase are differentially required for the recognition of DNA breaks and nicks and the consequent enzyme activation. Other structures recognize intact DNA. *J Biol Chem* **265,** 21907–21913.

Iriti M, Picchi V, Rossoni M, Gomarasca S, Ludwig N, Gargano M & Faoro F (2009). Chitosan antitranspirant activity is due to abscisic acid-dependent stomatal closure. *Environ Exp Bot* **66,** 493–500.

Janků J., Bartovská L., Soukup J., Jursík M. HK (2012). Density and surface tension of aqueous solutions of adjuvants used for tank-mixes with pesticides. *Plant, Soil Environ* **58,** 568–572.

Jansen M, Gilmer F, Biskup B, Nagel KA, Rascher U, Fischbach A, Briem S, Dreissen G, Tittmann S, Braun S, De Jaeger I, Metzlaff M, Schurr U, Scharr H & Walter A (2009). Simultaneous phenotyping of leaf growth and chlorophyll fluorescence via GROWSCREEN FLUORO allows detection of stress tolerance in Arabidopsis thaliana and other rosette plants. *Funct Plant Biol* **36,** 902–914.

Jia Q, Dulk-Ras A den, Shen H, Hooykaas PJJ & de Pater S (2013). Poly(ADP-ribose)polymerases are involved in microhomology mediated back-up non-homologous end joining in Arabidopsis thaliana. *Plant Mol Biol* **82,** 339–351.

Jones H, Serraj R, R. Loveys B, Xiong L, Wheaton A & Price A (2009). *Thermal infrared imaging of crop canopies for remote diagnosis and quantification of plant responses to water stress in the field*.

Karpinska B, Wingsle G & Karpinski S (2000). Antagonistic Effects of Hydrogen

Peroxide and Glutathione on Acclimation to Excess Excitation Energy in Arabidopsis. *IUBMB Life* **50,** 21–26.

Kereïche S, Kiss AZ, Kouřil R, Boekema EJ & Horton P (2010). The PsbS protein controls the macro-organisation of photosystem II complexes in the grana membranes of higher plant chloroplasts. *FEBS Lett* **584,** 759–764.

Kohli A, Sreenivasulu N, Lakshmanan P & Kumar PP (2013). The phytohormone crosstalk paradigm takes center stage in understanding how plants respond to abiotic stresses. *Plant Cell Rep* **32,** 945–957.

Kornas A, Kuźniak E, Ślesak I & Miszalski Z (2010). The key role of the redox status in regulation of metabolism in photosynthesizing organisms. *Acta Biochim Pol* **57,** 143–151.

Kramer DM, Avenson TJ & Edwards GE (2004*a*). Dynamic flexibility in the light reactions of photosynthesis governed by both electron and proton transfer reactions. *Trends Plant Sci* **9,** 349–357.

Kramer DM, Johnson G, Kiirats O & Edwards GE (2004*b*). New Fluorescence Parameters for the Determination of QA Redox State and Excitation Energy Fluxes. *Photosynth Res* **79,** 209.

Krasensky J & Jonak C (2012). Drought, salt, and temperature stress-induced metabolic rearrangements and regulatory networks. *J Exp Bot* **63,** 1593–1608.

Kuchel H, Williams KJ, Langridge P, Eagles HA & Jefferies SP (2007). Genetic dissection of grain yield in bread wheat. I. QTL analysis. *Theor Appl Genet* **115,** 1029–1041.

Lamb RS, Citarelli M & Teotia S (2012). Functions of the poly(ADP-ribose) polymerase superfamily in plants. *Cell Mol Life Sci* **69,** 175–189.

Langridge P, Paltridge N & Fincher G (2006). Functional genomics of abiotic stress tolerance in cereals. *Brief Funct Genomics* **4,** 343–354.

LAWLOR DW (2002). Limitation to Photosynthesis in Water-stressed Leaves: Stomata vs. Metabolism and the Role of ATP. *Ann Bot* **89,** 871–885.

Lawlor DW & Cornic G (2002). Photosynthetic carbon assimilation and associated metabolism in relation to water deficits in higher plants. *Plant Cell Environ* **25,** 275–294.

Lawson T, Kramer DM & Raines CA (2012). Improving yield by exploiting mechanisms underlying natural variation of photosynthesis. *Curr Opin Biotechnol* **23,** 215–220.

Lepiniec L, Babiychuk E, Kushnir S & Montagu M Van (1995). Characterization of an Arabidopsis thaliana cDNA homologue to animal poly (ADP-ribose) polymerase. *FEBS Lett* **364,** 103–108.

Li L, Zhang Q & Huang D (2014). A review of imaging techniques for plant phenotyping. *Sensors (Basel)* **14,** 20078–20111.

Lopes MS & Reynolds MP (2012). Stay-green in spring wheat can be determined by

spectral reflectance measurements (normalized difference vegetation index) independently from phenology. *J Exp Bot* **63,** 3789–3798.

Luna E, Beardon E, Ravnskov S, Scholes J & Ton J (2015). Optimizing Chemically Induced Resistance in Tomato Against Botrytis cinerea. *Plant Dis* **100,** 704–710.

Luna E, van Hulten M, Zhang Y, Berkowitz O, López A, Pétriacq P, Sellwood MA, Chen B, Burrell M, van de Meene A, Pieterse CMJ, Flors V & Ton J (2014). Plant perception of β-aminobutyric acid is mediated by an aspartyl-tRNA synthetase. *Nat Chem Biol* **10,** 450–456.

Mahajan S & Tuteja N (2005). Cold, salinity and drought stresses: An overview. *Arch Biochem Biophys* **444,** 139–158.

Martin LBB, Romero P, Fich EA, Domozych D, Rose JKC (2017) Cuticle Biosynthesis is Developmentally Regulated by Abscisic Acid. *Plant Phys* DOI: 10.1104/pp.17.00387

Martinez-Medina A, Flors V, Heil M, Mauch-Mani B, Pieterse CMJ, Pozo MJ, Ton J, van Dam NM & Conrath U (2017). Recognizing Plant Defense Priming. *Trends Plant Sci* **21,** 818–822.

Massacci A, Nabiev SM, Pietrosanti L, Nematov SK, Chernikova TN, Thor K & Leipner J (2008). Response of the photosynthetic apparatus of cotton (Gossypium hirsutum) to the onset of drought stress under field conditions studied by gas-exchange analysis and chlorophyll fluorescence imaging. *Plant Physiol Biochem* **46,** 189–195.

Maxwell K & Johnson GN (2000). Chlorophyll fluorescence - a practical guide. *J Exp Bot* **51,** 659–668.

Mazzucotelli E, Mastrangelo AM, Crosatti C, Guerra D, Stanca AM & Cattivelli L (2008). Abiotic stress response in plants: When post-transcriptional and post-translational regulations control transcription. *Plant Sci* **174,** 420–431.

McIntyre CL, Mathews KL, Rattey A, Chapman SC, Drenth J, Ghaderi M, Reynolds M & Shorter R (2010). Molecular detection of genomic regions associated with grain yield and yield-related components in an elite bread wheat cross evaluated under irrigated and rainfed conditions. *Theor Appl Genet* **120,** 527–541.

Merlot S, Mustilli A-C, Genty B, North H, Lefebvre V, Sotta B, Vavasseur A & Giraudat J (2002). Use of infrared thermal imaging to isolate Arabidopsis mutants defective in stomatal regulation. *Plant J* **30,** 601–609.

Miralles D & Slafer G (2007). *Sink limitations to yield in wheat : how could it be reduced?*

Mittler R (2006). Abiotic stress, the field environment and stress combination. *Trends Plant Sci* **11,** 15–19.

Mittler R & Blumwald E (2010). Genetic Engineering for Modern Agriculture: Challenges and Perspectives. *Annu Rev Plant Biol* **61,** 443–462.

Miyake C (2010). Alternative Electron Flows (Water-Water Cycle and Cyclic Electron Flow Around PSI) in Photosynthesis: Molecular Mechanisms and Physiological Functions. *Plant Cell Physiol* **51,** 1951–1963.

Murata N, Takahashi S, Nishiyama Y & Allakhverdiev SI (2007). Photoinhibition of photosystem II under environmental stress. *Biochim Biophys Acta - Bioenerg* **1767,** 414–421.

Murchie EH & Lawson T (2013*a*). Chlorophyll fluorescence analysis: A guide to good practice and understanding some new applications. *J Exp Bot* **64,** 3983–3998.

Murchie EH & Lawson T (2013*b*). Chlorophyll fluorescence analysis: a guide to good practice and understanding some new applications. *J Exp Bot* **64,** 3983–3998.

Mustilli A-C, Merlot S, Vavasseur A, Fenzi F & Giraudat J (2002). Arabidopsis OST1 Protein Kinase Mediates the Regulation of Stomatal Aperture by Abscisic Acid and Acts Upstream of Reactive Oxygen Species Production. *Plant Cell* **14,** 3089 LP-3099.

Nakasu EYT, Edwards MG, Fitches E, Gatehouse JA & Gatehouse AMR (2014). Transgenic plants expressing ω-ACTX-Hv1a and snowdrop lectin (GNA) fusion protein show enhanced resistance to aphids. *Front Plant Sci* **5,** 673.

Navarro L, Bari R, Achard P, Lisón P, Nemri A, Harberd NP & Jones JDG (2017). DELLAs Control Plant Immune Responses by Modulating the Balance of Jasmonic Acid and Salicylic Acid Signaling. *Curr Biol* **18,** 650–655.

Oerke EC & Dehne HW (2004). Safeguarding production - Losses in major crops and the role of crop protection. *Crop Prot* **23,** 275–285.

Okamoto M, Peterson FC, Defries A, Park S-Y, Endo A, Nambara E, Volkman BF & Cutler SR (2013). Activation of dimeric ABA receptors elicits guard cell closure, ABA-regulated gene expression, and drought tolerance. *Proc Natl Acad Sci U S A* **110,** 12132–12137.

Ort DR & Baker NR (2002). A photoprotective role for O2 as an alternative electron sink in photosynthesis? *Curr Opin Plant Biol* **5,** 193–198.

PARRY MAJ, ANDRALOJC PJ, KHAN S, LEA PJ & KEYS AJ (2002). Rubisco Activity: Effects of Drought Stress. *Ann Bot* **89,** 833–839.

Pham PA, Wahl V, Tohge T, de Souza LR, Zhang Y, Do PT, Olas JJ, Stitt M, Araújo WL & Fernie AR (2015). Analysis of knockout mutants reveals non-redundant functions of poly(ADP-ribose)polymerase isoforms in Arabidopsis. *Plant Mol Biol* **89,** 319–338.

Pinheiro C & Chaves MM (2011). Photosynthesis and drought: can we make metabolic connections from available data? *J Exp Bot* **62,** 869–882.

Porcar-Castell A, Tyystjarvi E, Atherton J, van der Tol C, Flexas J, Pfundel EE, Moreno J, Frankenberg C & Berry JA (2014). Linking chlorophyll a fluorescence to photosynthesis for remote sensing applications: mechanisms and challenges. *J Exp Bot* **65,** 4065–4095.

Quick WP & Horton P (1984). Studies on the Induction of Chlorophyll Fluorescence in Barley Protoplasts. II. Resolution of Fluorescence Quenching by Redox State and the Transthylakoid pH Gradient. *Proc R Soc London Ser B Biol Sci* **220,** 371 LP-382.

Raghavendra AS, Gonugunta VK, Christmann A & Grill E (2010). ABA perception and signalling. *Trends Plant Sci* **15,** 395–401.

Rahaman MM, Chen D, Gillani Z, Klukas C & Chen M (2015). Advanced phenotyping and phenotype data analysis for the study of plant growth and development. *Front Plant Sci* **6,** 619.

REYNOLDS MP, PELLEGRINESCHI A & SKOVMAND B (2005). Sink-limitation to yield and biomass: a summary of some investigations in spring wheat. *Ann Appl Biol* **146,** 39–49.

Rissel D, Heym P, Thor K, Brandt W, Wessjohann L & Peiter E (2017). No silver bullet - Canonical Poly(ADP-Ribose) Polymerases (PARPs) are no universal factors of abiotic and biotic stress resistance of Arabidopsis thaliana . *Front Plant Sci* **8,** 59. Available at: http://journal.frontiersin.org/article/10.3389/fpls.2017.00059.

Rizhsky L, Liang H & Mittler R (2002). The Combined Effect of Drought Stress and Heat Shock on Gene Expression in Tobacco. *Plant Physiol* **130,** 1143 LP-1151.

Rizhsky L, Liang H, Shuman J, Shulaev V, Davletova S, Mittler R, Rizhsky L., Liang H., Shuman J., Shulaev V., Davletova S. & R. M (2004). When Defense Pathways Collide. The Response of Arabidopsis to a Combination of Drought and Heat Stress. *Plant Physiol* **134,** 1683–1696.

Roach T & Krieger-Liszkay AK (2014). Regulation of Photosynthetic Electron Transport and Photoinhibition. *Curr Protein Pept Sci* **15,** 351–362.

Roychoudhury A, Paul S & Basu S (2013). Cross-talk between abscisic acid-dependent and abscisic acid-independent pathways during abiotic stress. *Plant Cell Rep* **32,** 985–1006.

Ruban A V (2016). Nonphotochemical Chlorophyll Fluorescence Quenching: Mechanism and Effectiveness in Protecting Plants from Photodamage. *Plant Physiol* **170,** 1903–1916.

Sah SK, Reddy KR & Li J (2016). Abscisic Acid and Abiotic Stress Tolerance in Crop Plants. *Front Plant Sci* **7,** 571.

Saibo NJM, Lourenço T & Oliveira MM (2009). Transcription factors and regulation of photosynthetic and related metabolism under environmental stresses. *Ann Bot* **103,** 609–623.

Sánchez J-P, Duque P & Chua N-H (2004). ABA activates ADPR cyclase and cADPR induces a subset of ABA-responsive genes in Arabidopsis. *Plant J* **38,** 381–395.

Santino A, Taurino M, De Domenico S, Bonsegna S, Poltronieri P, Pastor V & Flors V (2013). Jasmonate signaling in plant development and defense response to multiple (a)biotic stresses. *Plant Cell Rep* **32,** 1085–1098.

Santos M, Ribeiro R, C. Machado E & Pimentel C (2009). *Photosynthetic parameters and leaf water potential of five common bean genotypes under mild water deficit*.

SCHNYDER H (1993). The role of carbohydrate storage and redistribution in the source-sink relations of wheat and barley during grain filling — a review. *New Phytol* **123,** 233–245.

Schulz P, Jansseune K, Degenkolbe T, Meret M, Claeys H, Skirycz A, Teige M, Willmitzer L & Hannah MA (2014). Poly(ADP-Ribose)polymerase activity controls plant growth by promoting leaf cell number. *PLoS One*; DOI: 10.1371/journal.pone.0090322.

Schulz P, Neukermans J, Van Der Kelen K, Mühlenbock P, Van Breusegem F, Noctor G, Teige M, Metzlaff M & Hannah MA (2012). Chemical PARP Inhibition Enhances Growth of Arabidopsis and Reduces Anthocyanin Accumulation and the Activation of Stress Protective Mechanisms. *PLoS One* **7,** e37287.

Schwarzenbacher RE, Luna E & Ton J (2014). The discovery of the BABA receptor: scientific implications and application potential. *Front Plant Sci* **5,** 304.

Shao H-B, Chu L-Y, Jaleel CA & Zhao C-X (2008). Water-deficit stress-induced anatomical changes in higher plants. *C R Biol* **331,** 215–225.

Shikanai T (2014). Central role of cyclic electron transport around photosystem I in the regulation of photosynthesis. *Curr Opin Biotechnol* **26,** 25–30.

Shinozaki K & Yamaguchi-Shinozaki K (2006). Gene networks involved in drought stress response and tolerance. *J Exp Bot* **58,** 221–227.

Sinclair TR & Jamieson PD (2006). Grain number, wheat yield, and bottling beer: An analysis. *F Crop Res* **98,** 60–67.

Skirycz A & Inzé D (2010). More from less: plant growth under limited water. *Curr Opin Biotechnol* **21,** 197–203.

Sperdouli I & Moustakas M (2012). Spatio-temporal heterogeneity in Arabidopsis thaliana leaves under drought stress. *Plant Biol* **14,** 118–128.

Statista (2016). Major global crop losses due to drought in 2012, by region (in billion U.S. dollars). Available at: https://www.statista.com/statistics/260693/global-key-crop-losses-due-to-drought/.

Steyn WJ, Wand SJE, Holcroft DM & Jacobs G (2002). Anthocyanins in vegetative tissues: a proposed unified function in photoprotection. *New Phytol* **155,** 349–361.

Su L, Dai Z, Li S & Xin H (2015). A novel system for evaluating drought-cold tolerance of grapevines using chlorophyll fluorescence. *BMC Plant Biol* **15,** 82.

Sun X, Shantharaj D, Kang X & Ni M (2010). Transcriptional and hormonal signaling control of Arabidopsis seed development. *Curr Opin Plant Biol* **13,** 611–620.

Sunkar R, Chinnusamy V, Zhu J & Zhu J-K (2007). Small RNAs as big players in plant

abiotic stress responses and nutrient deprivation. *Trends Plant Sci* **12,** 301–309.

SUZUKI N, KOUSSEVITZKY S, MITTLER R & MILLER G (2012). ROS and redox signalling in the response of plants to abiotic stress. *Plant Cell Environ* **35,** 259–270.

TAIR (n.d.). The Arabidopsis Information Resource.

Takahashi S & Badger MR (2011). Photoprotection in plants: A new light on photosystem II damage. *Trends Plant Sci* **16,** 53–60.

Takeno K (2016). Stress-induced flowering: the third category of flowering response. *J Exp Bot* **67,** 4925–4934.

The Royal Society (2009). *Reaping the benefits: science and the sustainable intensification of global agriculture*. London. Available at: https://royalsociety.org/~/media/Royal_Society_Content/policy/publications/2009/4294967719.pdf.

Tombesi S, Nardini A, Frioni T, Soccolini M, Zadra C, Farinelli D, Poni S & Palliotti A (2015). Stomatal closure is induced by hydraulic signals and maintained by ABA in drought-stressed grapevine. *Sci Rep* **5,** 12449.

Tripathy BC & Oelmüller R (2012). Reactive oxygen species generation and signaling in plants. *Plant Signal Behav* **7,** 1621–1633.

United Nations Department of Economic and Social Affairs (2015). *World Population Prospects: The 2015 Revision, Key findings and Advance Tables*. New York. Available at: https://esa.un.org/unpd/wpp/publications/files/key_findings_wpp_2015.pdf.

Valliyodan B & Nguyen HT (2006). Understanding regulatory networks and engineering for enhanced drought tolerance in plants. *Curr Opin Plant Biol* **9,** 189–195.

Vanderauwera S, De Block M, Van de Steene N, van de Cotte B, Metzlaff M & Van Breusegem F (2007). Silencing of poly(ADP-ribose) polymerase in plants alters abiotic stress signal transduction. *Proc Natl Acad Sci U S A* **104,** 15150–15155.

Vanková R, Dobrá J & Štorchová H (2012). Recovery from drought stress in tobacco: An active process associated with the reversal of senescence in some plant parts and the sacrifice of others. *Plant Signal Behav* **7,** 19–21.

VILE D, PERVENT M, BELLUAU M, VASSEUR F, BRESSON J, MULLER B, GRANIER C & SIMONNEAU T (2012). Arabidopsis growth under prolonged high temperature and water deficit: independent or interactive effects? *Plant Cell Environ* **35,** 702–718.

Walz (2017). ImagingWin Software.

Wan Y, Poole RL, Huttly AK, Toscano-Underwood C, Feeney K, Welham S, Gooding MJ, Mills C, Edwards KJ, Shewry PR & Mitchell RAC (2008). Transcriptome analysis of grain development in hexaploid wheat. *BMC Genomics* **9,** 121.

Wang W, Vinocur B & Altman A (2003). Plant responses to drought, salinity and

extreme temperatures: towards genetic engineering for stress tolerance. *Planta* **218,** 1–14.

Wickham H (2009). *ggplot2: Elegant Graphics for Data Analysis*. Springer-Verlag, New York. Available at: http://ggplot2.org.

Woo NS, Badger MR & Pogson BJ (2008). A rapid, non-invasive procedure for quantitative assessment of drought survival using chlorophyll fluorescence. *Plant Methods* **4,** 27.

Wu Y, Kuzma J, Maréchal E, Graeff R, Lee HC, Foster R & Chua N-H (1997). Abscisic Acid Signaling Through Cyclic ADP-Ribose in Plants. *Science (80-)* **278,** 2126 LP-2130.

Xiong L & Zhu J-K (2003). Regulation of Abscisic Acid Biosynthesis. *Plant Physiol* **133,** 29–36.

Xu P, Tian L, Kloz M & Croce R (2015). Molecular insights into Zeaxanthin-dependent quenching in higher plants. *Sci Rep* **5,** 13679.

Yamori W (2016). Photosynthetic response to fluctuating environments and photoprotective strategies under abiotic stress. *J Plant Res* **129,** 379–395.

Yang J & Zhang J (2006). Grain filling of cereals under soil drying. *New Phytol* **169,** 223–236.

Yano R, Nakamura M, Yoneyama T & Nishida I (2005). Starch-Related α-Glucan/Water Dikinase Is Involved in the Cold-Induced Development of Freezing Tolerance in Arabidopsis. *Plant Physiol* **138,** 837–846.

Zhang H & Sonnewald U (2017). Differences and commonalities of plant responses to single and combined stresses. *Plant J* **90,** 839–855.

Zhang, Zhu GY, Tian RY, Dai RH & Y.R. (2003). Cleavage of poly(ADP-ribose) polymerase during apoptosis induced by nicotinamide at high concentrations in tobacco suspension cells. *Plant Growth Regul*93–98.

Zhu J-K (2002). Salt and Drought Stress Signal Transduction in Plants. *Annu Rev Plant Biol* **53,** 247–273.

Zivcak M, Brestic M, Balatova Z, Drevenakova P, Olsovska K, Kalaji HM, Yang X & Allakhverdiev SI (2013). Photosynthetic electron transport and specific photoprotective responses in wheat leaves under drought stress. *Photosynth Res* **117,** 529–546.

Appendix

Chapter 4 supplementary information

Table 1. The conditions selected to simulate those summer wheat experiences in the field. The climate model contained 50 years of data from 50 weather stations in wheat growing areas worldwide.

Month	Real time	Duration (hours)	Temp (°C)	Humidity (%)	Light intensity (% of max; 350 μmol m^{-2} s^{-1})
March	0500-0600	01:00	2	90	25
	0600-0630	00:30	2	86	25
	0630-0700	00:30	3	82	25
	0700-0730	00:30	4	75	25
	0730-0900	01:30	8	50	50
	0900-0930	00:30	8	50	75
	0930-1000	00:30	8	50	75
	1000-1130	01:30	8	50	50
	1130-1200	00:30	8	50	25
	1200-1230	00:30	8	50	25
	1230-1300	00:30	7	50	25
	1300-1400	01:00	7	50	25
	1400-0500	15:00	2	90	0
April	0500-0600	01:00	4	90	25
	0600-0630	00:30	5	86	25
	0630-0700	00:30	6	82	25
	0700-0730	00:30	7	75	25
	0730-1030	03:00	14	50	50
	1030-1100	00:30	14	50	75
	1100-1130	00:30	14	50	75
	1130-1430	03:00	14	50	50
	1430-1500	00:30	14	50	25
	1500-1530	00:30	14	50	25
	1530-1600	00:30	14	50	25
	1600-1700	01:00	13	50	25
	1700-0500	12:00	4	90	0
May	0500-0600	01:00	8	90	25
	0600-0630	00:30	9	86	25
	0630-0700	00:30	10	82	25

	0700-0730	00:30	11	75	25
	0730-1100	03:30	18	50	50
	1100-1200	01:00	18	50	75
	1200-1300	01:00	18	50	75
	1300-1630	03:30	18	50	50
	1630-1700	00:30	18	50	25
	1700-1730	00:30	18	50	25
	1730-1800	00:30	18	50	25
	1800-1900	01:00	18	50	25
	1900-0500	10:00	8	90	0
June	0500-0600	01:00	10	90	25
	0600-0630	00:30	11	86	25
	0630-0700	00:30	12	82	25
	0700-0730	00:30	13	75	25
	0730-0815	00:45	15	63	50
	0815-1145	03:30	22	50	75
	1145-1315	01:30	22	50	100
	1315-1645	03:30	22	50	75
	1645-1730	00:45	22	50	50
	1730-1800	00:30	22	50	25
	1800-1830	00:30	22	50	25
	1830-1900	00:30	22	50	25
	1900-2000	01:00	22	50	25
	2000-0500	09:00	10	90	0
July	0500-0600	01:00	12	90	25
	0600-0630	00:30	13	86	25
	0630-0700	00:30	14	82	25
	0700-0730	00:30	15	75	25
	0730-0815	00:45	17	67	50
	0815-1145	03:30	25	50	75
	1145-1415	02:30	26	50	100
	1415-1745	03:30	25	50	75
	1745-1830	00:45	24	50	50
	1830-1900	00:30	24	50	25
	1900-1930	00:30	24	50	25
	1930-2000	00:30	24	50	25
	2000-2100	01:00	24	50	25

	2100-0500	08:00	12	90	0
August	0500-0600	01:00	12	90	25
	0600-0630	00:30	13	86	25
	0630-0700	00:30	14	82	25
	0700-0730	00:30	15	75	25
	0730-0815	00:45	17	67	50
	0815-1145	03:30	26	50	75
	1145-1315	01:30	28	50	100
	1315-1645	03:30	26	50	75
	1645-1730	00:45	25	50	50
	1730-1800	00:30	24	50	25
	1800-1830	00:30	24	50	25
	1830-1900	00:30	24	50	25
	1900-2000	01:00	24	50	25
	2000-0500	09:00	12	90	0
Sept	0500-0600	01:00	10	90	25
	0600-0630	00:30	11	86	25
	0630-0700	00:30	12	82	25
	0700-0730	00:30	13	75	25
	0730-0815	00:45	15	63	50
	0815-1145	03:30	22	50	75
	1145-1315	01:30	22	50	100
	1315-1645	03:30	23	50	75
	1645-1730	00:45	23	50	50
	1730-1800	00:30	23	50	25
	1800-1830	00:30	23	50	25
	1830-1900	00:30	23	50	25
	1900-2000	01:00	23	50	25
	2000-0500	09:00	10	90	0

Programme section	**Total days conditions simulated in climate chamber**
March	7
April	14
May	14
June	14
July	14
August	14

September	14 (+)
Length of climate programme	**90-100 d**

Table 2. The BBCH scale for the description of phenological growth stages of cereals including wheat. The first and second numbers in each two letter code correspond to the principal and secondary growth stages respectively. Adapted from Federal Biological Research Centre for Agriculture and Forestry, (2001).

BBCH scale: cereals (including wheat; *Triticum aestivum*)	
Code	Description
Principal growth stage 0: Germination	
00	Dry seed (caryopsis)
01	Beginning of seed imbibition
03	Seed imbibition complete
05	Radicle emerged from caryopsis
06	Radicle elongated, root hairs and/or side roots visible
07	Coleoptile emerged from caryopsis
09	Emergence: coleoptile penetrates soil surface (cracking stage)
Principal growth stage 1: Leaf development	
10	First leaf through coleoptile
11	First leaf unfolded
12	2 leaves unfolded
13	3 leaves unfolded
1.	Stage continues until…
19	9 or more leaves unfolded
Principal growth stage 2: Tillering	
20	No tillers
21	Beginning of tillering: first tiller detectable
22	2 tillers detectable
23	3 tillers detectable
2.	Stage continues until…
29	End of tillering. Maximum number of tillers detectable
Principal growth stage 3: Stem elongation	

30	Beginning of stem elongation: pseudostem and tillers erect, first internode begins to elongate, top of inflorescence at least 1 cm above tillering node
31	First node at least 1 cm above tillering node
32	Node 2 at least 2 cm above node 1
33	Node 3 at least 2 cm above node 2
3.	Stage continues until….
37	Flag leaf visible, still rolled
39	Flag leaf stage: flag leaf fully unrolled, ligule just visible
Principal growth stage 4: Booting	
41	Early boot stage: flag leaf sheath extending
43	Mid boot stage: flag leaf sheath just visibly swollen
45	Late boot stage: flag leaf sheath swollen
47	Flag leaf sheath opening
49	First awns visible
Principal growth stage 5: Inflorescence emergence, heading	
51	Beginning of heading: tip of florescence emerged from sheath, first spikelet just visible
52	20 % of inflorescence emerged
53	30 % of inflorescence emerged
54	40 % of inflorescence emerged
55	Middle of heading: half of inflorescence emerged
56	60 % of inflorescence emerged
57	70 % of inflorescence emerged
58	80 % of inflorescence emerged
59	End of heading: inflorescence fully emerged
Principal growth stage 6: Flowering, anthesis	
61	Beginning of flowering: first anthers visible
65	Full flowering: 50% of anthers mature
69	End of flowering: all spikelets have completed flowering but some dehydrated anthers may remain
Principal growth stage 7: Development of fruit	

71	Watery ripe: first grains have reached half their final size
73	Early milk
75	Medium milk: grain content milky, grains reached final size, still green
77	Late milk
Principal growth stage 8: Ripening	
83	Early dough
85	Soft dough: grain content soft but dry. Fingernail impression not held
87	Hard dough: grain content solid. Fingernail impression held
89	Fully ripe: grain hard, difficult to divide with thumbnail
Principal growth stage 9: Senescence	
92	Over-ripe: grain very hard, cannot be dented by thumbnail
93	Grains loosening in day-time
97	Plant dead and collapsing
99	Harvested product

R scripts used for analysis of Chapter 4 data

---

title: "Basic processing and outlier detection"

author: "Luke Cartwright"

date: "2017"

output:

  word_document:

    highlight: monochrome

```{r,warning=FALSE,message=FALSE}

rm(list=ls())

source("https://bioconductor.org/biocLite.R")

biocLite("zoo")

#or

#install.packages("directlabels")

library(ggplot2)

library(lubridate)

library(dplyr)

library(zoo)

library(gridExtra)

library(cowplot)

library(reshape2)

library(directlabels)

```

Set up standard files names and the subset to plot.

If you set the working directory then everything else is referenced relative to that

```{r}

#Big data file

input_file="./data/Halcon.csv"

#Information about the treatments

#Two sets of files are given - one filtered for outliers
```

#Running the code with this file changed makes it easy to exclude outliers

plant_codes_file="./data/Halcon_labels.csv"

#plant_codes_file="./data/Halcon_labels_filtered.csv"

#Yield data

yield_file="./data/Yield_data.csv"

```

Read in the data and associated files

```{r}

#read in the data - don't allow R to convert anything into factors

hdata<-read.csv(input_file,header=TRUE,stringsAsFactors = FALSE)

if(is.object(hdata)==FALSE) {stop(c("Can't open file:",input_file))}

#this file contains info about the plants used - all are factors

#change this from plant_codes to plant_codes_filtered to re-run the code with outliers excluded.

#Outliers are defined by the 'Inactive' field being set to y

plant_codes<-read.csv(plant_codes_file,header = TRUE,stringsAsFactors = TRUE)

#plant_codes<-read.csv(plant_codes_filtered,header = TRUE,stringsAsFactors = TRUE)

if(is.object(plant_codes)==FALSE) {stop(c("Can't open file:",plant_codes_file))}

```

Format the times so that they are in a standard format and relate this to days after germination)

Use POSIX format so that all of R's functions work properly.

POSIX comes in a variety of flavours, not all of which work well with downstream functions.

POSIXct seems compatible with most.

```{r}

#Data are provided as dates, but we want to express everything from a fixed starting point. In this case we use Days After Transfer (dat) when plants were moved into the system

#set the date of transfer in POSIX format (ignore the time zone)

dat_datetime<-as.POSIXct("25/02/2016 08:00:00",tz="","%d/%m/%Y %H:%M:%S")

#now set the factors manually - these are the experimental factors

```
hdata$number_of_trial<-as.factor(hdata$number_of_trial)

hdata$sideview<-as.factor(hdata$sideview)

#do some date and time wrangling to use POSIX dates

hdata$ptime<-paste(hdata$date_of_trial,hdata$clock_of_trial)

hdata$ptime<-as.POSIXct(hdata$ptime,tz="","%d/%m/%Y %H:%M:%S")

#now do some standard time processing

#use difftime to get the days after transfer

hdata$dat<-as.numeric(difftime(hdata$ptime,dat_datetime,units="days"))
```

We now do the same for the label file

We need to merge this into the main data file

```{r}
plant_codes$number_of_trial<-as.factor(plant_codes$number_of_trial)

plant_codes$Snapshot_ID_Tag<-as.factor(plant_codes$Snapshot_ID_Tag)

hdata<-merge(hdata,plant_codes,by="number_of_trial")

#Use subset to get rid of Inactive data

hdata<-subset(hdata,Inactive=="n")
```

Data are provided from two sideviews (SV1 and SV2).

It makes sense to average these.

```{R}
idata<-
summarise(group_by(hdata,Application,Irrigation,Compound_No,Snapshot_ID_Tag,date_of_trial),mean_Object_Sum_Area=mean(Object_Sum_Area),mean_area_yellow=mean(area_yellow),mean_area_green=mean(area_green),dat=mean(dat))


idata<-droplevels(idata)

#just in case there's missing data

idata<-na.omit(idata)
```

It is useful to inspect the raw data

```{R}
```

#plot the raw area data as a line for mean SV1 and SV2

p1<-
ggplot(data=idata,aes(x=dat,y=mean_Object_Sum_Area,color=Irrigation,group=Snapshot_ID_Tag))+
geom_line()

p1<-p1+scale_y_continuous(name="Object sum area")

p1<-p1+facet_grid(Compound_No~Application)

p1

```

We can see that the data are of different lengths - we'll set everything to the same

```{R}

subdata<-subset(idata,dat<=75)

subdata<-droplevels(subdata)

#just in case there's missing data

subdata<-na.omit(subdata)


#plot the  area data

p2<-
ggplot(data=subdata,aes(x=dat,y=mean_Object_Sum_Area,color=Irrigation,group=Snapshot_ID_Tag
))+geom_line()

p2<-p2+scale_y_continuous(name="Object sum area")

p2<-p2+facet_grid(Compound_No~Application)

p2

```

```{R}

#Plot green and yellow data

pgy<-ggplot(data=subdata)

pgy<-
pgy+geom_line(aes(x=dat,y=mean_area_green,group=Snapshot_ID_Tag),colour="forestgreen")

pgy<-
pgy+geom_line(aes(x=dat,y=mean_area_yellow,group=Snapshot_ID_Tag),colour="darkorange")


pgy<-pgy+scale_y_continuous(name="Mean area")

pgy<-pgy+facet_grid(Compound_No~Application)

pgy

```
```

It would be useful to always plot the control and drought control on the graphs.

```{R}

#get the control data into a separate dataset

cdata<-subset(subdata,(Compound_No=="Control" | Compound_No=="drought control"),select=c("dat","mean_Object_Sum_Area","Irrigation","Snapshot_ID_Tag"))

cdata<-droplevels(cdata)


#get the rest of the data for plotting

plotdata<-subset(subdata, !(Compound_No=="Control" | Compound_No=="drought control"),select=c("dat","mean_Object_Sum_Area","Irrigation","Snapshot_ID_Tag","Compound_No","Application"))

plotdata<-droplevels(plotdata)


#plot showing the control data as gray points

p3<-
ggplot(data=NULL,aes(x=dat,y=mean_Object_Sum_Area,color=Irrigation,group=Snapshot_ID_Tag))+geom_line(data=plotdata)+theme_bw()

p3<-p3+geom_point(data=cdata,colour="#C0C0C0",alpha=0.3)

p3<-p3+scale_y_continuous(name="Mean Object sum area")

p3<-p3+facet_grid(Compound_No~Application)

p3

```

Some outliers are obvious where plants failed to establish.

We can use the ratio of green to yellow

Calculate this on the main data set which is stored in subdata

```{R}

subdata$ratio_gy<-subdata$mean_area_green/subdata$mean_area_yellow


p4<-
ggplot(data=subdata,aes(x=dat,y=ratio_gy,color=Irrigation,group=Snapshot_ID_Tag))+geom_line()

p4<-p4+scale_y_continuous(name="Ratio green:yellow")

p4<-p4+facet_grid(Compound_No~Application)

p4

```

There's an outlier on BBCH12/13 well watered but we can't tell which

Therefore plot just this data set and show as IDs

```{R}

p5<-ggplot(data=subset(subdata,Compound_No=="Compound 4" & Application =="BBCH 12/13"),aes(x=dat,y=ratio_gy,color=Snapshot_ID_Tag))+geom_line()

p5<-p5+scale_y_continuous(name="Ratio yellow:green")

p5<-p5+facet_grid(~Irrigation)

p5+geom_dl(aes(label = Snapshot_ID_Tag), method = list(dl.combine("first.points", "last.points"), cex = 0.8))

```

Now it's obvious that 8869 is an outlier

Repeat this for all of the data that looks iffy and identify outliers.

```{R}

p6<-ggplot(data=subset(subdata,Compound_No=="Genapol" & Application =="BBCH 55/57"),aes(x=dat,y=ratio_gy,color=Snapshot_ID_Tag))+geom_line()

p6<-p6+scale_y_continuous(name="Ratio yellow:green")

p6<-p6+facet_grid(~Irrigation)

p6+geom_dl(aes(label = Snapshot_ID_Tag), method = list(dl.combine("first.points", "last.points"), cex = 0.8))

```

These outliers should be set to Inactive in the plant_codes_filtered file.

For now we'll create a list, delete them from subdata and then plot again.

```{R}

exclude_list<-c("8869","8920","8925","8829","8992","8869")

subdata<-subset(subdata,!Snapshot_ID_Tag %in% exclude_list)

p7<-ggplot(data=subdata,aes(x=dat,y=mean_Object_Sum_Area,color=Irrigation,group=Snapshot_ID_Tag))+geom_line()

p7<-p7+scale_y_continuous(name="Object sum area")

p7<-p7+facet_grid(Compound_No~Application)

p7

```

---

title: "Initial growth data analysis"

author: "Luke Cartwright"

date: "2017"

output: html_document

Standard code to clear the system and install required libraries

```{r,warning=FALSE}

rm(list=ls())

biocLite("mgcv")

#biocLite("lubridate")

#biocLite("zoo")

#install.packages("cowplot")

#install.packages("gridExtra")

library(ggplot2)

library(lubridate)

library(dplyr)

library(zoo)

library(gridExtra)

library(cowplot)

library(reshape2)

```

Set up standard files names and the subset to plot

```{r}

input_file="./data/Halcon.csv"

plant_codes="./data/Halcon_labels.csv"

plant_codes_filtered="./data/Halcon_labels_filtered.csv"

yield_file="./data/Yield_data.csv"

output_file="./output/Halcon_output.csv"

```

Read in the data

```{r}

#read in the data - don't allow R to convert anything into factors

hdata<-read.csv(input_file,header=TRUE,stringsAsFactors = FALSE)

if(is.object(hdata)==FALSE) {stop(c("Can't open file:",input_file))}


#this file contains info about the plants used - all are factors

#plant_codes<-read.csv(plant_codes,header = TRUE,stringsAsFactors = TRUE)

plant_codes<-read.csv(plant_codes_filtered,header = TRUE,stringsAsFactors = TRUE)


if(is.object(plant_codes)==FALSE) {stop(c("Can't open file:",plant_codes))}

```

Format the times so that they are in a standard format and relate this to days after germination - it's easy enough to change this to days after anything you like (e.g. start of the expt)

Use POSIX format so that all of R's functions work properly.

```{r}

#dat offset from first data point

#it's good to express everything as days after germination but 1st data point will not be dat

#set the date of transfer in POSIX format (ignore the time zone)

dat_datetime<-as.POSIXct("25/02/2016 08:00:00",tz="","%d/%m/%Y %H:%M:%S")


#now set the factors manually - these are the experimental factors

hdata$number_of_trial<-as.factor(hdata$number_of_trial)

hdata$sideview<-as.factor(hdata$sideview)


#do some date and time wrangling to use POSIX dates

hdata$ptime<-paste(hdata$date_of_trial,hdata$clock_of_trial)

hdata$ptime<-as.POSIXct(hdata$ptime,tz="","%d/%m/%Y %H:%M:%S")


#now do some standard time processing

#use difftime to get the days after germination

hdata$dat<-as.numeric(difftime(hdata$ptime,dat_datetime,units="days"))

```

We now do the same for the label file

We need to merge this into the main data file

```{r}

plant_codes$number_of_trial<-as.factor(plant_codes$number_of_trial)

plant_codes$Snapshot_ID_Tag<-as.factor(plant_codes$Snapshot_ID_Tag)

hdata<-merge(hdata,plant_codes,by="number_of_trial")

hdata<-subset(hdata,Inactive=="n")

```

```{R}

idata<-
summarise(group_by(hdata,Application,Irrigation,Compound_No,Snapshot_ID_Tag,date_of_trial),mean_Object_Sum_Area=mean(Object_Sum_Area),mean_area_yellow=mean(area_yellow),mean_area_green=mean(area_green),dat=mean(dat))

idata<-droplevels(idata)

#just in case there's missing data

idata<-na.omit(idata)

```

```{R}

#plot the raw area data as a line

p1<-
ggplot(data=idata,aes(x=dat,y=mean_Object_Sum_Area,color=Irrigation,group=Snapshot_ID_Tag))+
geom_line()

p1<-p1+scale_y_continuous(name="Object sum area")

p1<-p1+facet_grid(Compound_No~Application)

p1

```

We can see that the data are of different lengths - we'll set everything to the same

```{R}

subdata<-subset(idata,dat<=75)

subdata<-droplevels(subdata)

#just in case there's missing data

subdata<-na.omit(subdata)

#plot the raw area data as a line

p1<-
ggplot(data=subdata,aes(x=dat,y=mean_Object_Sum_Area,color=Irrigation,group=Snapshot_ID_Tag
))+geom_point()

p1<-p1+scale_y_continuous(name="Object sum area")

p1<-p1+facet_grid(Compound_No~Application)
```

p1

```

It would be useful to always plot the control and drought control on the graphs.

```{R}

#get the control data into a separate dataset

cdata<-subset(subdata,(Compound_No=="control" | Compound_No=="drought control"),select=c("dat","mean_Object_Sum_Area","Irrigation","Snapshot_ID_Tag"))

cdata<-droplevels(cdata)

#get the rest of the data for plotting

plotdata<-subset(subdata, !(Compound_No=="control" | Compound_No=="drought control"),select=c("dat","mean_Object_Sum_Area","Irrigation","Snapshot_ID_Tag","Compound_No","Application"))

plotdata<-droplevels(plotdata)


#plot showing the control data as gray points

p2<-ggplot(data=NULL,aes(x=dat,y=mean_Object_Sum_Area,color=Irrigation,group=Snapshot_ID_Tag))+geom_line(data=plotdata)+theme_bw()

p2<-p2+geom_point(data=cdata,colour="#C0C0C0",alpha=0.3)

p2<-p2+scale_y_continuous(name="Mean Object sum area")

p2<-p2+facet_grid(Compound_No~Application)

p2

```

The data set is very large, so for testing growth models we'll just look at a subset.

Choosing BBCH 12/13 and Compound 1 (at random)

```{R}

singledata<-subset(idata,Compound_No=="Compound 2" & Application=="BBCH 12/13" & Irrigation=="drought"&dat<=75)

singledata<-droplevels(singledata)

#just in case there's missing data

singledata<-na.omit(singledata)


p2<-ggplot(data=singledata,aes(x=dat,y=mean_Object_Sum_Area,color=Irrigation,group=Snapshot_ID_Tag))+geom_point()

p2<-p2+scale_y_continuous(name="Object sum area")

```
p2
#Plot on a log sccale
p2<-p2+scale_y_log10()
p2
p2a<-p2
p2a<-p2a+scale_x_continuous(limits=c(26,46))
p2a+stat_smooth(method="loess")+facet_wrap(~Snapshot_ID_Tag,scales="free")
```
Data look reasonably smooth on a log scale
Fit a 3 order polynomial through the data
```{R}
singledata$log_Object_Sum_Area<-log10(singledata$mean_Object_Sum_Area)
p3<-ggplot(data=singledata,aes(x=dat,y=log_Object_Sum_Area,color=Irrigation))+geom_point()
p3<-p3+facet_wrap(Irrigation~Snapshot_ID_Tag)
p3<-p3 + stat_smooth(method = "lm", formula = y ~ poly(x, 3), size = 1)
p3
```
Looks good - so do the fits properly
```{R}
for (compound in levels(subdata$Compound_No)){
 for (application in levels(subdata$Application)){
  fname<-(paste(compound,"_",gsub("/","_",application),".PNG",sep=""))
  d<-subset(subdata,Compound_No==compound & Application==application)
  if (dim(d)[1]>0){
   d$log_Object_Sum_Area<-log10(d$mean_Object_Sum_Area)

   p4<-ggplot(data=d,aes(x=dat,y=log_Object_Sum_Area,color=Snapshot_ID_Tag))+geom_point()
   #p4<-p4 + stat_smooth(method = "lm", formula = y ~ poly(x, 3), size = 1)
   p4<-p4+stat_smooth(method="gam",formula=y ~ s(x,k=5),size=1)
   p4<-p4+facet_wrap(Irrigation~Snapshot_ID_Tag)

   p4a<-ggplot(data=d,aes(x=dat,y=log_Object_Sum_Area,color=Snapshot_ID_Tag))+geom_point()
   #p4a<-p4a + stat_smooth(method = "lm", formula = y ~ poly(x, 3), size = 1)
```

```
    p4a<-p4a+stat_smooth(method="gam",formula=y ~ s(x,k=5),size=1)

    p4a<-p4a+facet_wrap(~Irrigation)

    p4a

    ggsave(paste("all_gam_",fname,sep=""),p4a,path="./output",width=50,height=30,units="cm")


    dmat<-
melt(d,id.vars=c("Snapshot_ID_Tag","dat","Irrigation"),measure.vars=c("mean_area_yellow","mean
_area_green"))

    p5<-
ggplot(dmat,aes(x=dat,y=value,fill=variable,color=variable))+theme_bw()+geom_line(size=2)+facet_
wrap(Irrigation~Snapshot_ID_Tag)

    p5<-p5+scale_color_manual(values=c("orange","green4"))


    p6<-(plot_grid(p4,p5))

    ggsave(fname,p6,path="./output",width=50,height=30,units="cm")

   }

 }

}
```

Manual inspection allows us to come up with an exclude list.

We'll remove this from the subdata dataset

I added y to the inactive columns of these and saved a new labels file

We can then run the whole pipeline again but change the labels file to _filtered

Now do all the fits properly

```{R}


for (snap in levels(subdata$Snapshot_ID_Tag)){

 print(paste(snap))

 d<-subset(subdata,Snapshot_ID_Tag==snap)

 #need to sort by dat to make this sensible!

 d<-d[order(d$dat),]

 d<-data.frame(d)

 if (dim(d)[1]>0){

  d$log_Object_Sum_Area<-log10(d$mean_Object_Sum_Area)

  model<-lm(log_Object_Sum_Area ~ poly(dat,3),data=d)
```

```
   print(summary(model)$r.squared)
  }
}

#Sanity check that we're not doing something stupid!
plot(d$dat,d$log_Object_Sum_Area)
lines(d$dat,predict(model))
#Get values by day
pdays<-data.frame("dat"=seq(1:75))
pdays$predict<-predict(model,pdays)
lines(pdays$dat,pdays$predict)
#get the maximum value
pdays[which.max(pdays$predict),]
plot(d$dat,resid(model))
#residuals aren't particularly well scattered

library(mgcv)
ct<-gam(d$mean_Object_Sum_Area ~ s(d$dat,k=6),family=Gamma(link=log),data=d)
ct
plot(ct,residuals=TRUE)
```

---

title: "Model fitting"

author: "Luke Cartwright"

date: '2017'

output:

word_document: default

html_document: default

You must install packages (just the once) using install.packages() or biocLite()

They need to be loaded every time.

```{r,warning=FALSE,message=FALSE}

rm(list=ls())

source("https://bioconductor.org/biocLite.R")

#biocLite("lubridate")

#or

install.packages("knitr")

library(ggplot2)

#library(lubridate)

library(dplyr)

library(zoo)

library(gridExtra)

library(cowplot)

library(reshape2)

library(directlabels)

library(plyr)

library(mgcv)

```

Set up standard files names and the subset to plot.

If you set the working directory then everything else is referenced relative to that

This data set has been analysed for outliers using the Basic Processing analysis

Therefore the filtered codes are used.

```{r}
#Big data file
input_file="./data/Halcon.csv"

#Information about the treatments
#Two sets of files are given - one filtered for outliers
#Running the code with this file changed makes it easy to exclude outliers

plant_codes_file="./data/Halcon_labels.csv"
#plant_codes_file="./data/Halcon_labels_filtered.csv"

#Yield data
yield_file="./data/Yield_data.csv"
```

Read in the data and associated files

```{r}
#read in the data - don't allow R to convert anything into factors
hdata<-read.csv(input_file,header=TRUE,stringsAsFactors = FALSE)
if(is.object(hdata)==FALSE) {stop(c("Can't open file:",input_file))}

#this file contains info about the plants used - all are factors
#change this from plant_codes to plant_codes_filtered to re-run the code with outliers excluded.
#Outliers are defined by the 'Inactive' field being set to y
plant_codes<-read.csv(plant_codes_file,header = TRUE,stringsAsFactors = TRUE)
if(is.object(plant_codes)==FALSE) {stop(c("Can't open file:",plant_codes_file))}
```

Format the times so that they are in a standard format and relate this to days after germination

```{r}
#Data are provided as dates, but we want to express everything from a fixed starting point. In this case we use Days After Transfer (dat) when plants were moved into the system
#set the date of transfer in POSIX format (ignore the time zone)
dat_datetime<-as.POSIXct("25/02/2016 08:00:00",tz="","%d/%m/%Y %H:%M:%S")
```

#now set the factors manually - these are the experimental factors

hdata$number_of_trial<-as.factor(hdata$number_of_trial)

hdata$sideview<-as.factor(hdata$sideview)

#do some date and time wrangling to use POSIX dates

hdata$ptime<-paste(hdata$date_of_trial,hdata$clock_of_trial)

hdata$ptime<-as.POSIXct(hdata$ptime,tz="","%d/%m/%Y %H:%M:%S")

#now do some standard time processing

#use difftime to get the days after transfer

hdata$dat<-as.numeric(difftime(hdata$ptime,dat_datetime,units="days"))

#```{r}

#Data are provided as dates, but we want to express everything from a fixed starting point. In this case we use Days After Transfer (dat) when plants were moved into the system

#set the date of transfer in POSIX format (ignore the time zone)

#dat_datetime<-as.POSIXct("25/02/2016 08:00:00",tz="","%d/%m/%Y %H:%M:%S")

#now set the factors manually - these are the experimental factors

#hdata$number_of_trial<-as.factor(hdata$number_of_trial)

#hdata$sideview<-as.factor(hdata$sideview)

#do some date and time wrangling to use POSIX dates

#hdata$ptime<-paste(hdata$date_of_trial,hdata$clock_of_trial)

#hdata$ptime<-as.POSIXct(hdata$ptime,tz="","%d/%m/%Y %H:%M:%S")

#now do some standard time processing

#use difftime to get the days after transfer

#hdata$dat<-as.numeric(difftime(hdata$ptime,dat_datetime,units="days"))

```

We now do the same for the label file

We need to merge this into the main data file

```{r}

```
plant_codes$number_of_trial<-as.factor(plant_codes$number_of_trial)

plant_codes$Snapshot_ID_Tag<-as.factor(plant_codes$Snapshot_ID_Tag)

hdata<-merge(hdata,plant_codes,by="number_of_trial")

#Use subset to get rid of Inactive data

hdata<-subset(hdata,Inactive=="n")
```

```{R}
idata<-dplyr::summarise(group_by(hdata,Application,Irrigation,Compound_No,Snapshot_ID_Tag,date_of_trial),mean_Object_Sum_Area=mean(Object_Sum_Area),mean_area_yellow=mean(area_yellow),mean_area_green=mean(area_green),dat=mean(dat))

idata<-droplevels(idata)

#just in case there's missing data

idata<-na.omit(idata)
```

Set everything to the same length

```{R}
subdata<-subset(idata,dat<=75)

subdata<-droplevels(subdata)

#just in case there's missing data

subdata<-na.omit(subdata)

#plot the  area data

p1<-ggplot(data=subdata,aes(x=dat,y=mean_Object_Sum_Area,color=Irrigation,group=Snapshot_ID_Tag))+geom_line()

p1<-p1+scale_y_continuous(name="Object sum area")

p1<-p1+facet_grid(Compound_No~Application)

p1

#plot the  green area data

#p1<-ggplot(data=subdata,aes(x=dat,y=mean_area_green,color=Irrigation,group=Snapshot_ID_Tag))+geom_line()

#p1<-p1+scale_y_continuous(name="Green area")

#p1<-p1+facet_grid(Compound_No~Application)

#p1
```

#plot the yellow area data

#p1<-
ggplot(data=subdata,aes(x=dat,y=mean_area_yellow,color=Irrigation,group=Snapshot_ID_Tag))+geom_line()

#p1<-p1+scale_y_continuous(name="yellow area")

#p1<-p1+facet_grid(Compound_No~Application)

#p1

```

It would be useful to always plot the control and drought control on the graphs.

```{R}

#get the control data into a separate dataset

cdata<-subset(subdata,(Compound_No=="Control" | Compound_No=="drought control"),select=c("dat","mean_Object_Sum_Area","Irrigation","Snapshot_ID_Tag"))

cdata<-droplevels(cdata)


#get the rest of the data for plotting

plotdata<-subset(subdata, !(Compound_No=="Control" | Compound_No=="drought control"),select=c("dat","mean_Object_Sum_Area","Irrigation","Snapshot_ID_Tag","Compound_No","Application"))

plotdata<-droplevels(plotdata)


#plot showing the control data as gray points

p2<-
ggplot(data=NULL,aes(x=dat,y=mean_Object_Sum_Area,color=Irrigation,group=Snapshot_ID_Tag))+geom_line(data=plotdata)+theme_bw()

p2<-p2+geom_point(data=cdata,colour="#C0C0C0",alpha=0.3)

p2<-p2+scale_y_continuous(name="Mean Object sum area")

p2<-p2+facet_grid(Compound_No~Application)

p2

```

Check the green/yellow ratio

```{R}

subdata$ratio_gy<-subdata$mean_area_green/subdata$mean_area_yellow

p3<-
ggplot(data=subdata,aes(x=dat,y=ratio_gy,color=Irrigation,group=Snapshot_ID_Tag))+geom_line()

p3<-p3+scale_y_continuous(name="Ratio yellow:green")

p3<-p3+facet_grid(Compound_No~Application)

p3

```

The data set is very large, so for testing growth models we'll just look at a subset.

Choosing BBCH 30/31 and Compound 2 (at random)

```{R}

singledata<-subset(subdata,Compound_No=="Comp 2" & Application=="BBCH 29/32" & dat<=75)

singledata<-droplevels(singledata)

#just in case there's missing data

singledata<-na.omit(singledata)


#plot the raw osa data for this subset

#p4<-
ggplot(data=singledata,aes(x=dat,y=mean_Object_Sum_Area,color=Irrigation,group=Snapshot_ID_Tag))+geom_point()+geom_line()

#p4<-p4+scale_y_continuous(name="Object sum area")

#p4

#plot the green:yellow ratio data for this subset

p4<-
ggplot(data=singledata,aes(x=dat,y=ratio_gy,color=Irrigation,group=Snapshot_ID_Tag))+geom_point()+geom_line()

p4<-p4+scale_y_continuous(name="Green:yellow pixel ratio")

p4

```

There is noise in the data and the variation increases with plant size. This is an obvious time when we should calculate the log of the data.

Do this for everything and subset again

NOTE: These are natural logs

```{R}

#log of the osa

#subdata$log_OSA<-log(subdata$mean_Object_Sum_Area)


#singledata<-subset(subdata,Compound_No=="Comp 2" & Application=="BBCH 29/32" & dat<=75)

#singledata<-droplevels(singledata)

#just in case there's missing data

```
#singledata<-na.omit(singledata)

#p5<-
ggplot(data=singledata,aes(x=dat,y=log_OSA,color=Irrigation,group=Snapshot_ID_Tag))+geom_point
()+geom_point()+geom_line()

#p5<-p5+scale_y_continuous(name="LOG (Object sum area)")

#p5

#log of green:yellow ratio data

subdata$log_ratio_gy<-log(subdata$ratio_gy)

singledata<-subset(subdata,Compound_No=="Comp 2" & Application=="BBCH 29/32" & dat<=75)

singledata<-droplevels(singledata)

#just in case there's missing data

singledata<-na.omit(singledata)

p5<-
ggplot(data=singledata,aes(x=dat,y=log_ratio_gy,color=Irrigation,group=Snapshot_ID_Tag))+geom_p
oint()+geom_point()+geom_line()

p5<-p5+scale_y_continuous(name="LOG (Green:yellow pixel ratio)")

p5
```

```

GAMs - General Additive Models. These have a variable smooth parameter which can capture the variations in growth rate but avoid noise.

GAMs can have different k values - so inspect the data to see what is approrpiate

There's a known issue with GAMs on time series data - the data are auto-correlated.

This means that if a value is high at one time point, it is likely to be high at the next (which is fairly obvious). This needs to be compensated for.

```{R}

#subset the first data set


d<-subset(singledata,Snapshot_ID_Tag==levels(singledata$Snapshot_ID_Tag)[1])

#We use the gamm function as this allows the autocorrelation correction

#The number of 'knots' is defined by k

#We use a gamma distribution as this is common for time series data

#We pass the raw OSA but tell the function to log it
```
```

```
g3<-gamm(d$mean_Object_Sum_Area ~ s(d$dat,k=3),data=d,family=Gamma(link="log"),correlation
= corCAR1(form = ~dat))

g4<-gamm(d$mean_Object_Sum_Area ~ s(d$dat,k=4),data=d,family=Gamma(link="log"),correlation
= corCAR1(form = ~dat))

g5<-gamm(d$mean_Object_Sum_Area ~ s(d$dat,k=5),data=d,family=Gamma(link="log"),correlation
= corCAR1(form = ~dat))

g6<-gamm(d$mean_Object_Sum_Area ~ s(d$dat,k=6),data=d,family=Gamma(link="log"),correlation
= corCAR1(form = ~dat))

g7<-gamm(d$mean_Object_Sum_Area ~ s(d$dat,k=7),data=d,family=Gamma(link="log"),correlation
= corCAR1(form = ~dat))

g8<-gamm(d$mean_Object_Sum_Area ~ s(d$dat,k=8),data=d,family=Gamma(link="log"),correlation
= corCAR1(form = ~dat))


dn3<-g3$gam

pobj3<-data.frame(fitted.values(dn3),residuals(dn3),d$mean_Object_Sum_Area,d$dat)

colnames(pobj3)<-c("Fit","Res","Obj_SA","days")

pobj3$k<-3


dn5<-g5$gam

pobj5<-data.frame(fitted.values(dn5),residuals(dn5),d$mean_Object_Sum_Area,d$dat)

colnames(pobj5)<-c("Fit","Res","Obj_SA","days")

pobj5$k<-5


dn7<-g7$gam

pobj7<-data.frame(fitted.values(dn7),residuals(dn7),d$mean_Object_Sum_Area,d$dat)

colnames(pobj7)<-c("Fit","Res","Obj_SA","days")

pobj7$k<-7


dn8<-g8$gam

pobj8<-data.frame(fitted.values(dn8),residuals(dn8),d$mean_Object_Sum_Area,d$dat)

colnames(pobj8)<-c("Fit","Res","Obj_SA","days")

pobj8$k<-8


pobj<-rbind(pobj3,pobj7)

pobj<-rbind(pobj,pobj5)
```

```
pobj<-rbind(pobj,pobj8)
pobj$k<-factor(pobj$k)

p1<-ggplot(data=pobj,aes(x=days,y=Fit,color=k,group=k))+geom_line()
p1<-p1+geom_point(aes(x=days,y=Obj_SA),colour="black")
p1<-p1+scale_y_continuous(name="Object sum area")
p1<-p1+scale_x_continuous(name="dat")
p1

pobj<-rbind(pobj8,pobj7)
pobj$k<-factor(pobj$k)

p1<-ggplot(data=pobj,aes(x=days,y=Fit,color=k,group=k))+geom_line()
p1<-p1+geom_point(aes(x=days,y=Obj_SA),colour="black")
p1<-p1+scale_y_continuous(name="Object sum area")
p1<-p1+scale_x_continuous(name="dat")
p1

p1log<-ggplot(data=pobj,aes(x=days,y=log(Fit),color=k,group=k))+geom_line()
p1log<-p1log+geom_point(aes(x=days,y=log(Obj_SA)),colour="black")
p1log<-p1log+scale_y_continuous(name="LOG (Object sum area)")
p1log<-p1log+scale_x_continuous(name="dat")
p1log

p1res<-ggplot(data=pobj,aes(x=days,y=Res,color=k,group=k))+geom_point()
p1res<-p1res+scale_y_continuous(name="Residuals")
p1res<-p1res+scale_x_continuous(name="dat")
p1res
plot_grid(p1,p1log)

p1<-p1+scale_y_continuous(name="Object sum area")
p1<-p1+facet_grid(Compound_No~Application)
p1
```

```
pgam<-ggplot(data=pobj,aes(x=days,y=Fit,group="k",colour="k"))+geom_line()
pgam

dn<-g4$gam
pobj<-data.frame(fitted.values(dn),residuals(dn),d$mean_Object_Sum_Area,d$dat)
colnames(pobj)<-c("Fit","Res","Obj_SA","days")
p4<-ggplot(data=pobj)+geom_point(aes(x=days,y=(Obj_SA)))+geom_line(aes(x=days,y=(Fit)))
p4

dn<-g5$gam
pobj<-data.frame(fitted.values(dn),residuals(dn),d$mean_Object_Sum_Area,d$dat)
colnames(pobj)<-c("Fit","Res","Obj_SA","days")
p5<-ggplot(data=pobj)+geom_point(aes(x=days,y=(Obj_SA)))+geom_line(aes(x=days,y=(Fit)))
p5

dn<-g6$gam
pobj<-data.frame(fitted.values(dn),residuals(dn),d$mean_Object_Sum_Area,d$dat)
colnames(pobj)<-c("Fit","Res","Obj_SA","days")
p6<-ggplot(data=pobj)+geom_point(aes(x=days,y=(Obj_SA)))+geom_line(aes(x=days,y=(Fit)))
p6

dn<-g7$gam
pobj<-data.frame(fitted.values(dn),residuals(dn),d$mean_Object_Sum_Area,d$dat)
colnames(pobj)<-c("Fit","Res","Obj_SA","days")
p7<-ggplot(data=pobj)+geom_point(aes(x=days,y=(Obj_SA)))+geom_line(aes(x=days,y=(Fit)))
p7

dn<-g8$gam
pobj<-data.frame(fitted.values(dn),residuals(dn),d$mean_Object_Sum_Area,d$dat)
colnames(pobj)<-c("Fit","Res","Obj_SA","days")
p8<-ggplot(data=pobj)+geom_point(aes(x=days,y=(Obj_SA)))+geom_line(aes(x=days,y=(Fit)))
p8
```

```
summary(g3$gam)

summary(g8$gam)



#Careful inspection shows that a 7 knot fit is about right

#Use plot for a quick look

par(mfrow=c(1,1))

plot(g3$gam)

plot(g3$lme)

plot(g7$gam)

plot(g7$lme)


#create a plotting object

dn<-g7$gam

pobj<-data.frame(fitted.values(dn),residuals(dn),d$mean_Object_Sum_Area,d$dat)

colnames(pobj)<-c("Fit","Res","Obj_SA","days")

p7<-ggplot(data=pobj)+geom_point(aes(x=days,y=log(Obj_SA)))+geom_line(aes(x=days,y=log(Fit)))

p7

ggsave("log_gam_k7.png",p7)

p8<-ggplot(data=pobj)+geom_point(aes(x=days,y=(Obj_SA)))+geom_line(aes(x=days,y=(Fit)))

p8

ggsave("gam.png",p8)


p9<-ggplot(data=pobj)+geom_point(aes(x=log(Fit),y=Res))

p9

ggsave("gam_resid.png",p9)

```

Do the same for the green:yellow ratio data

```{R}

d<-subset(singledata,Snapshot_ID_Tag==levels(singledata$Snapshot_ID_Tag)[1])

g3<-gamm(d$ratio_gy ~ s(d$dat,k=3),data=d,family=Gamma(link="log"),correlation = corCAR1(form = ~dat))
```

```
g4<-gamm(d$ratio_gy ~ s(d$dat,k=4),data=d,family=Gamma(link="log"),correlation = corCAR1(form = ~dat))

g5<-gamm(d$ratio_gy ~ s(d$dat,k=5),data=d,family=Gamma(link="log"),correlation = corCAR1(form = ~dat))

g6<-gamm(d$ratio_gy ~ s(d$dat,k=6),data=d,family=Gamma(link="log"),correlation = corCAR1(form = ~dat))

g7<-gamm(d$ratio_gy ~ s(d$dat,k=7),data=d,family=Gamma(link="log"),correlation = corCAR1(form = ~dat))

g8<-gamm(d$ratio_gy ~ s(d$dat,k=8),data=d,family=Gamma(link="log"),correlation = corCAR1(form = ~dat))


dn3<-g3$gam

pobj3<-data.frame(fitted.values(dn3),residuals(dn3),d$ratio_gy,d$dat)

colnames(pobj3)<-c("Fit","Res","ratio_gy","days")

pobj3$k<-3


dn5<-g5$gam

pobj5<-data.frame(fitted.values(dn5),residuals(dn5),d$ratio_gy,d$dat)

colnames(pobj5)<-c("Fit","Res","ratio_gy","days")

pobj5$k<-5


dn7<-g7$gam

pobj7<-data.frame(fitted.values(dn7),residuals(dn7),d$ratio_gy,d$dat)

colnames(pobj7)<-c("Fit","Res","ratio_gy","days")

pobj7$k<-7


dn8<-g8$gam

pobj8<-data.frame(fitted.values(dn8),residuals(dn8),d$ratio_gy,d$dat)

colnames(pobj8)<-c("Fit","Res","ratio_gy","days")

pobj8$k<-8


pobj<-rbind(pobj3,pobj7)

pobj<-rbind(pobj,pobj5)

pobj<-rbind(pobj,pobj8)

pobj$k<-factor(pobj$k)
```

```
p1<-ggplot(data=pobj,aes(x=days,y=Fit,color=k,group=k))+geom_line()
p1<-p1+geom_point(aes(x=days,y=ratio_gy),colour="black")
p1<-p1+scale_y_continuous(name="Green:yellow pixel ratio")
p1<-p1+scale_x_continuous(name="dat")
p1

p1log<-ggplot(data=pobj,aes(x=days,y=log(Fit),color=k,group=k))+geom_line()
p1log<-p1log+geom_point(aes(x=days,y=log(ratio_gy)),colour="black")
p1log<-p1log+scale_y_continuous(name="LOG (Green:yellow pixel ratio)")
p1log<-p1log+scale_x_continuous(name="dat")
p1log

p1res<-ggplot(data=pobj,aes(x=days,y=Res,color=k,group=k))+geom_point()
p1res<-p1res+scale_y_continuous(name="Residuals")
p1res<-p1res+scale_x_continuous(name="dat")
p1res

plot_grid(p1,p1log)

p1<-p1+scale_y_continuous(name="Green:yellow pixel ratio")
p1<-p1+facet_grid(Compound_No~Application)
p1
pgam<-ggplot(data=pobj,aes(x=days,y=Fit,group="k",colour="k"))+geom_line()
pgam

dn<-g4$gam
pobj<-data.frame(fitted.values(dn),residuals(dn),d$ratio_gy,d$dat)
colnames(pobj)<-c("Fit","Res","ratio_gy","days")
p4<-ggplot(data=pobj)+geom_point(aes(x=days,y=(ratio_gy)))+geom_line(aes(x=days,y=(Fit)))
p4

dn<-g5$gam
```

```
pobj<-data.frame(fitted.values(dn),residuals(dn),d$ratio_gy,d$dat)
colnames(pobj)<-c("Fit","Res","ratio_gy","days")
p5<-ggplot(data=pobj)+geom_point(aes(x=days,y=(ratio_gy)))+geom_line(aes(x=days,y=(Fit)))
p5

dn<-g6$gam
pobj<-data.frame(fitted.values(dn),residuals(dn),d$ratio_gy,d$dat)
colnames(pobj)<-c("Fit","Res","ratio_gy","days")
p6<-ggplot(data=pobj)+geom_point(aes(x=days,y=(ratio_gy)))+geom_line(aes(x=days,y=(Fit)))
p6

dn<-g7$gam
pobj<-data.frame(fitted.values(dn),residuals(dn),d$ratio_gy,d$dat)
colnames(pobj)<-c("Fit","Res","ratio_gy","days")
p7<-ggplot(data=pobj)+geom_point(aes(x=days,y=(ratio_gy)))+geom_line(aes(x=days,y=(Fit)))
p7

dn<-g8$gam
pobj<-data.frame(fitted.values(dn),residuals(dn),d$ratio_gy,d$dat)
colnames(pobj)<-c("Fit","Res","ratio_gy","days")
p8<-ggplot(data=pobj)+geom_point(aes(x=days,y=(ratio_gy)))+geom_line(aes(x=days,y=(Fit)))
p8
summary(g3$gam)
summary(g8$gam)

#Careful inspection shows that a 7 knot fit is about right
#Use plot for a quick look
par(mfrow=c(1,1))
plot(g3$gam)
plot(g3$lme)
plot(g7$gam)
plot(g7$lme)
```

```
#create a plotting object
dn<-g7$gam
pobj<-data.frame(fitted.values(dn),residuals(dn),d$ratio_gy,d$dat)
colnames(pobj)<-c("Fit","Res","ratio_gy","days")
p7<-ggplot(data=pobj)+geom_point(aes(x=days,y=log(ratio_gy)))+geom_line(aes(x=days,y=log(Fit)))
p7
ggsave("log_gam_k7.png",p7)
```

Check everything including the residuals

```{R}

for (compound in levels(subdata$Compound_No)){
 for (application in levels(subdata$Application)){
  fname<-(paste(compound,"_",gsub("/","_",application),".PNG",sep=""))
  d<-subset(subdata,Compound_No==compound & Application==application)
  if (dim(d)[1]>0){
    p10<-ggplot(data=d,aes(x=dat,y=log_OSA,color=Snapshot_ID_Tag))+geom_point()
    p10<-p10+stat_smooth(method="gam",formula=y ~ s(x,k=7),size=1)
    p10<-p10+facet_wrap(Irrigation~Snapshot_ID_Tag)

    p10a<-ggplot(data=d,aes(x=dat,y=log_OSA,color=Snapshot_ID_Tag))+geom_point()
    p10a<-p10a+stat_smooth(method="gam",formula=y ~ s(x,k=7),size=1)
    p10a<-p10a+facet_wrap(~Irrigation)
    p10a
    ggsave(paste("all_gam_",fname,sep=""),p10a,path="./output",width=50,height=30,units="cm")

    #get the yellow green data as well

    dmat<-
melt(d,id.vars=c("Snapshot_ID_Tag","dat","Irrigation"),measure.vars=c("mean_area_yellow","mean
_area_green"))
    p11<-
ggplot(dmat,aes(x=dat,y=value,fill=variable,color=variable))+theme_bw()+geom_line(size=2)+facet_
wrap(Irrigation~Snapshot_ID_Tag)
    p11<-p11+scale_color_manual(values=c("orange","green4"))
```

```
    p12<-(plot_grid(p10,p11))
    ggsave(fname,p12,path="./output",width=50,height=30,units="cm")
   }
 }
}
```

Now do all the fits properly

```{R}
#Create a function to do the fit
#Let it handle the logs

gammod<-function(df){
 gam(df$mean_Object_Sum_Area ~ s(dat,k=7),family=Gamma(link=log),data=df,correlation = corCAR1(form = ~dat))
}
#Use plyr to apply to each ID
gmodels<-dlply(subdata,"Snapshot_ID_Tag",gammod)

res_list=list()
fv_list<-list()

#loop through each model and get the residuals into a dataframe
for (i in 1:length(gmodels)){
 #residuals are
 res_list[[i]]<-residuals(gmodels[[i]])
 fv_list[[i]]<-fitted.values(gmodels[[i]])
}
names(res_list)<-levels(subdata$Snapshot_ID_Tag)
names(fv_list)<-levels(subdata$Snapshot_ID_Tag)

#we can now get these into a long list
res_list<-melt(res_list,value.name = "Res")
fv_list<-melt(fv_list,value.name="Fitted")
```

```
#merge by ID (which has been rename as L1)
fit_df<-data.frame(res_list,fv_list)
#change it back to ID and dump the second set
colnames(fit_df)[2]<-"Snapshot_ID_Tag"
fit_df$L1.1<-NULL
```

Now plot all the residuals

```{R}
for (compound in levels(subdata$Compound_No)){
 for (application in levels(subdata$Application)){
  fname<-(paste(compound,"_",gsub("/","_",application),"_residuals",".PNG",sep=""))
  d<-subset(subdata,Compound_No==compound & Application==application)
  if (dim(d)[1]>0){
    #plot these IDs
    ids=levels(droplevels(d$Snapshot_ID_Tag))
    e<-fit_df[fit_df$Snapshot_ID_Tag %in% ids,]
    e$Snapshot_ID_Tag<-factor(e$Snapshot_ID_Tag)
    p<-ggplot(data=e,aes(x=log10(Fitted),y=Res))+geom_point()+facet_wrap(~Snapshot_ID_Tag)
    plot(p)
    ggsave(fname,p,path="./output",width=50,height=30,units="cm")
 }
```

---

title: "Extraction from model"

author: "Luke Cartwright"

date: "2017"

output: html_document

```{r,warning=FALSE,message=FALSE}

rm(list=ls())

source("https://bioconductor.org/biocLite.R")

biocLite("lubridate")

#or

#install.packages("directlabels")

library(ggplot2)

library(lubridate)

library(dplyr)

library(zoo)

library(gridExtra)

library(cowplot)

library(reshape2)

library(directlabels)

library(plyr)

library(mgcv)

```

Set up standard files names and the subset to plot.

If you set the working directory then everything else is referenced relative to that

This data set has been analysed for outliers using the Basic Processing analysis

Therefore the filtered codes are used.

```{r}

#Big data file

input_file="./data/Halcon.csv"

#Information about the treatments

#Two sets of files are given - one filtered for outliers
```

#Running the code with this file changed makes it easy to exclude outliers

#plant_codes_file="./data/Halcon_labels.csv"

plant_codes_file="./data/Halcon_labels_filtered.csv"

#Yield data

yield_file="./data/Yield_data.csv"

```

Read in the data and associated files

```{r}

#read in the data - don't allow R to convert anything into factors

hdata<-read.csv(input_file,header=TRUE,stringsAsFactors = FALSE)

if(is.object(hdata)==FALSE) {stop(c("Can't open file:",input_file))}

#this file contains info about the plants used - all are factors

#change this from plant_codes to plant_codes_filtered to re-run the code with outliers excluded.

#Outliers are defined by the 'Inactive' field being set to y

plant_codes<-read.csv(plant_codes_file,header = TRUE,stringsAsFactors = TRUE)

if(is.object(plant_codes)==FALSE) {stop(c("Can't open file:",plant_codes_file))}

```

Format the times so that they are in a standard format and relate this to days after germination

```{r}

#Data are provided as dates, but we want to express everything from a fixed starting point. In this case we use Days After Transfer (dat) when plants were moved into the system

#set the date of transfer in POSIX format (ignore the time zone)

dat_datetime<-as.POSIXct("25/02/2016 08:00:00",tz="","%d/%m/%Y %H:%M:%S")

#now set the factors manually - these are the experimental factors

hdata$number_of_trial<-as.factor(hdata$number_of_trial)

hdata$sideview<-as.factor(hdata$sideview)

#do some date and time wrangling to use POSIX dates

hdata$ptime<-paste(hdata$date_of_trial,hdata$clock_of_trial)

hdata$ptime<-as.POSIXct(hdata$ptime,tz="","%d/%m/%Y %H:%M:%S")

#now do some standard time processing

#use difftime to get the days after transfer

hdata$dat<-as.numeric(difftime(hdata$ptime,dat_datetime,units="days"))

```

We now do the same for the label file

We need to merge this into the main data file

```{r}

plant_codes$number_of_trial<-as.factor(plant_codes$number_of_trial)

plant_codes$Snapshot_ID_Tag<-as.factor(plant_codes$Snapshot_ID_Tag)

hdata<-merge(hdata,plant_codes,by="number_of_trial")

#Use subset to get rid of Inactive data

hdata<-subset(hdata,Inactive=="n")

```

```{R}

idata<-
dplyr::summarise(group_by(hdata,Application,Irrigation,Compound_No,Snapshot_ID_Tag,date_of_trial),mean_Object_Sum_Area=mean(Object_Sum_Area),mean_area_yellow=mean(area_yellow),mean_area_green=mean(area_green),dat=mean(dat))

idata<-droplevels(idata)

#just in case there's missing data

idata<-na.omit(idata)

```

```{R}

subdata<-subset(idata,dat<=75)

subdata<-droplevels(subdata)

#just in case there's missing data

subdata<-na.omit(subdata)

```

It would be useful to always plot the control and drought control on the graphs.
```

```{R}

#get the control data into a separate dataset

cdata<-subset(subdata,(Compound_No=="Control" | Compound_No=="drought control"),select=c("dat","mean_Object_Sum_Area","Irrigation","Snapshot_ID_Tag"))

cdata<-droplevels(cdata)


#get the rest of the data for plotting

plotdata<-subset(subdata, !(Compound_No=="Control" | Compound_No=="drought control"),select=c("dat","mean_Object_Sum_Area","Irrigation","Snapshot_ID_Tag","Compound_No","Application"))

plotdata<-droplevels(plotdata)


#plot showing the control data as gray points

p2<-
ggplot(data=NULL,aes(x=dat,y=mean_Object_Sum_Area,color=Irrigation,group=Snapshot_ID_Tag))+geom_line(data=plotdata)+theme_bw()

p2<-p2+geom_point(data=cdata,colour="#C0C0C0",alpha=0.3)

p2<-p2+scale_y_continuous(name="Mean Object sum area")

p2<-p2+facet_grid(Compound_No~Application)

p2

```

Now do all the fits properly

```{R}

#Create a function to do the fit

#Let it handle the logs


gammod<-function(df){

  gam(df$mean_Object_Sum_Area ~ s(dat,k=7),family=Gamma(link=log),data=df,correlation = corCAR1(form = ~dat))

}

#Use plyr to apply to each ID

gmodels<-dlply(subdata,"Snapshot_ID_Tag",gammod)


res_list=list()

fv_list<-list()
```

```
#loop through each model and get the residuals into a dataframe
for (i in 1:length(gmodels)){
 #residuals are
 res_list[[i]]<-residuals(gmodels[[i]])
 fv_list[[i]]<-fitted.values(gmodels[[i]])
 }

names(res_list)<-levels(subdata$Snapshot_ID_Tag)
names(fv_list)<-levels(subdata$Snapshot_ID_Tag)

#we can now get these into a long list
res_list<-melt(res_list,value.name = "Res")
fv_list<-melt(fv_list,value.name="Fitted")

#merge by ID
fit_df<-data.frame(res_list,fv_list)
#change it back to ID and dump the second set
colnames(fit_df)[2]<-"Snapshot_ID_Tag"
fit_df$L1.1<-NULL
```

```{R}
#Pick the first model from gmodels
ex_model<-gmodels[1]

#use names to get the name of the model and subset on that
ex_data<-subset(fit_df,fit_df$Snapshot_ID_Tag==names(ex_model))

#get the raw data
orig_data<-subset(subdata,subdata$Snapshot_ID_Tag==names(ex_model))

#create an empty plot
```

```
ex_plot<-ggplot()

#draw the original data

ex_plot<-ex_plot+geom_point(data=orig_data,aes(x=dat,y=mean_Object_Sum_Area))


#predict new values form the model over a sensible range

new_data<-data.frame(dat=seq(5,75))

new_data$y<-predict(gmodels[[1]],new_data)

#draw the modelled data as a line

ex_plot<-ex_plot+geom_line(data=new_data,aes(x=dat,y=exp(y)))


#find the maximum value of the modelled data

out_mod<-new_data[which.max(new_data$y),]


#add this to the graph

ex_plot<-ex_plot+geom_point(data=out_mod,aes(x=dat,y=exp(y)),colour="red")+ggtitle("")

ex_plot<-ex_plot+scale_y_continuous(name="Object sum area")

ex_plot


#look at the corrected growth rates

#get the difference in growth rates - data are ln by default and time has been set at 1 day intervals so this is RGR

#create an empty plot

ex_plot<-ggplot()

#plot the modelled data which is LOG

ex_plot<-ex_plot+geom_line(data=new_data,aes(x=dat,y=y))

ex_plot


#find the max

out_mod<-new_data[which.max(new_data$y),]

ex_plot<-ex_plot+geom_point(data=out_mod,aes(x=dat,y=y),colour="red")+labs(y="LOG (Object sum area)")

ex_plot


#Calculate the Relative Growth Rate
```

#This is easy as we can calculate size at daily intervals

#The RGR therefore is simply the difference from one day to the next

rgr<-data.frame(rgr=diff(new_data$y))

rgr$dat<-new_data$dat[-1]

rgr_plot<-ggplot(data=rgr,aes(x=dat,y=rgr))+geom_line()+ggtitle("Relative growth rate")

rgr_plot

#Dylan suggested plotting Relative Growth Rate against LOG object size - it corrects for differences in growth assuming that growth rate is size dependent.

rgr$mean_Object_Sum_Area<-new_data$y[-1]

crgr_plot<-ggplot(data=rgr,aes(x=mean_Object_Sum_Area,y=rgr))+geom_line()

crgr_plot

```

```{R}

#Calculate the RGR for all of the data from the predictions

rgr_list=list()

new_data<-data.frame(dat=seq(5,75))

#loop through each model and get the predicted values into a dataframe

for (i in 1:length(gmodels)){

 new_data$pred<-predict(gmodels[[i]],new_data)

 rgr<-data.frame(rgr=diff(new_data$pred))

 rgr$dat<-seq(6,75)

 rgr_list[i]<-list(rgr)

}

names(rgr_list)<-levels(subdata$Snapshot_ID_Tag)

#we can now get these into a long list

df_rgr <- ldply(rgr_list, data.frame)

colnames(df_rgr)<-c("Snapshot_ID_Tag","rgr","dat")

df_rgr<-merge(df_rgr,plant_codes,by="Snapshot_ID_Tag")

```
ggplot(data=df_rgr,aes(x=dat,y=rgr,group=Snapshot_ID_Tag,color=Compound_No))+geom_line()+facet_grid(Irrigation~Application)
```

For now we'll just use the max OSA and the day that it took to get there as a parameter

```{R}
#for each ID in turn
#create a list of the correct length to hold the results
#it's much more efficient that way
days_max<-vector("list",length(levels(subdata$Snapshot_ID_Tag)))
#name the list elements as IDs
names(days_max)<-c(levels(subdata$Snapshot_ID_Tag))

for (ID in levels(subdata$Snapshot_ID_Tag)){
  #get the data
  d<-subset(subdata,Snapshot_ID_Tag==ID)
  #get the model
  ex_model<-gmodels[ID]
  #use names to get the name of the model and subset on that
  ex_data<-subset(fit_df,fit_df$Snapshot_ID_Tag==names(ex_model))
  #create new dat values for prediction
  new_data<-data.frame(dat=seq(5,75))
  #get predicted OSAs for these dats
  new_data$pred<-predict(gmodels[[ID]],new_data)
  #get the maximum value
  out_mod<-(new_data[which.max(new_data$pred),])
  #add it to the list
  days_max[ID]<-list(out_mod)
}
#convert the list into a dataframe
dmax<-ldply(days_max)
#Label the columns
colnames(dmax)<-c("Snapshot_ID_Tag","max_dat","max_osa")
#merge in information about the plants
dmax<-merge(x=dmax,y=plant_codes,by="Snapshot_ID_Tag",all.x=TRUE)
```

#plot the maximum OSA

maxOSA_plot<-
ggplot(data=dmax,aes(x=Irrigation,y=max_osa,colour=Compound_No))+facet_grid(~Application,scales="free_x")+geom_boxplot() +theme(axis.text.x = element_text(angle = 90, hjust = 1,vjust=0.5))+ylab("LOG Maximum object sum area")

maxOSA_plot

ggsave(filename="max_osa.png",plot=maxOSA_plot,width=34,height=20,units=c("cm"),dpi=600)

#For max OSA values stats

write.csv(dmax,file="max_osa.csv")

#plot the days it takes to reach that

#maxdat_plot<-
ggplot(data=dmax,aes(x=Compound_No,y=max_dat,colour=Compound_No))+geom_jitter(width=0.3,height=0)+facet_grid(~Application+Irrigation,scales="free_x")+geom_boxplot()+ theme(axis.text.x = element_text(angle = 90, hjust = 1))

#maxdat_plot

#plot the days it takes to reach that standardised

maxdat_plot<-
ggplot(data=dmax,aes(x=Irrigation,y=max_dat,colour=Compound_No))+facet_grid(~Application,scales="free_x")+geom_boxplot()+ theme(axis.text.x = element_text(angle = 90, hjust = 1,vjust=0.5))+ylab("Days to LOG max OSA")

maxdat_plot

ggsave(filename="time_max_osa.png",plot=maxdat_plot,width=34,height=20,units=c("cm"),dpi=600)

#are these derived parameters normally distributed?

ggplot(data=dmax,aes(max_osa,colour=Irrigation))+geom_density()

ggplot(data=dmax,aes(max_dat,colour=Irrigation))+geom_density()

```

The results seem to be normally distributed

Calculate growth rates for the periods before and after treatment

Growth rates for BBCH30/31

```{R}

#subset the data

sublist<-c("None","BBCH 29/32")

```
#Data30_31_data<-subdata[subdata$Application %in% sublist,]
Data30_31_data<-subset(subdata,Application=="BBCH 29/32")
Data30_31_data<-droplevels(Data30_31_data)
#fit the model
Data30_31_models<-dlply(Data30_31_data,"Snapshot_ID_Tag",gammod)
#30/31 application time is 36 dat
app_point=36
#get the data x days before and after
calc_diff_after=30
calc_diff_before=5
#for each ID in turn
#create a list of the correct length to hold the results
#it's much more efficient that way
ldat<-vector("list",length(levels(Data30_31_data$Snapshot_ID_Tag)))

names(ldat)<-c(levels(Data30_31_data$Snapshot_ID_Tag))

#step through each model in turn
for (ID in names(Data30_31_models)){
   ex_model<-Data30_31_models[[ID]]
   new_data<-data.frame(dat=seq(app_point-calc_diff_before,app_point+calc_diff_after))
   new_data$pred<-as.vector(predict(gmodels[[ID]],new_data))
   new_data$norm<-new_data$pred-new_data$pred[calc_diff_before+1]
   ldat[[ID]]<-new_data
   ldat[[ID]]$Snapshot_ID_Tag<-ID
}
#get the data as dataframes
ddat<-ldply(ldat)
#the IDs are replicated
ddat[1]<-NULL
ddat<-merge(ddat,plant_codes,by="Snapshot_ID_Tag")
```

Now start plotting

```{R}

pg<-ggplot(data=ddat,aes(x=dat,y=pred,colour=Compound_No))

pg<-pg+facet_wrap(~Irrigation)+geom_smooth()+geom_vline(xintercept = app_point)

pg

#ggsave("Modelled growth 30_31.png",pg)

```

The application point is midway - we can subtract the predicted value at day 36 from everything. Note - the data are LOG so we subtract them (the equivalent of dividing by unLOGed data)

```{R}

pg<-ggplot(data=ddat,aes(x=dat,y=norm,colour=Compound_No))

pg<-
pg+facet_wrap(~Irrigation)+geom_smooth()+geom_vline(xintercept=app_point)+theme_bw()+labs(y="LOG Normalised growth",title=(paste("Application:",app_point," dat",sep="")))

pg

ggsave(filename="LOG_normalised_midpoint.png",plot=pg,width=34,height=20,units=c("cm"),dpi=600)

```

The Genapol and Compound 4 growth rates are maintained under droughted conditions

This difference is evident ~10 days after treatment and continues until max OSA reached.

Growth rates for BBCH 12/13

```{R}

#subset the data

Data12_13_data<-subset(subdata,Application=="BBCH 13/21")

Data12_13_data<-droplevels(Data12_13_data)

#fit the model

Data12_13_models<-dlply(Data12_13_data,"Snapshot_ID_Tag",gammod)


#12/13 application time is 15 dat

app_point=15

#get the data x days before and after

calc_diff_after=30

calc_diff_before=5

#for each ID in turn

#create a list of the correct length to hold the results

#it's much more efficient that way
```

```
ldat<-vector("list",length(levels(Data12_13_data$Snapshot_ID_Tag)))

names(ldat)<-c(levels(Data12_13_data$Snapshot_ID_Tag))

#step through each model in turn
for (ID in names(Data12_13_models)){
   ex_model<-Data12_13_models[[ID]]
   new_data<-data.frame(dat=seq(app_point-calc_diff_before,app_point+calc_diff_after))
   new_data$pred<-as.vector(predict(gmodels[[ID]],new_data))
   new_data$norm<-new_data$pred-new_data$pred[calc_diff_before+1]
   ldat[[ID]]<-new_data
   ldat[[ID]]$Snapshot_ID_Tag<-ID
}
#get the data as dataframes
ddat<-ldply(ldat)
#the IDs are replicated
ddat[1]<-NULL
ddat<-merge(ddat,plant_codes,by="Snapshot_ID_Tag")

pg<-ggplot(data=ddat,aes(x=dat,y=norm,colour=Compound_No))
pg<-
pg+facet_wrap(~Irrigation)+geom_smooth()+geom_vline(xintercept=app_point)+theme_bw()+labs(y
="LOG Normalised growth",title=(paste("Application:",app_point," dat",sep="")))
pg
ggsave("Modelled normalised growth 12_13.png",pg)
```

Growth rates for BBCH 55/57

```{R}
#subset the data
Data55_57_data<-subset(subdata,Application=="BBCH 55/57")
Data55_57_data<-droplevels(Data55_57_data)
#fit the model
Data55_57_models<-dlply(Data55_57_data,"Snapshot_ID_Tag",gammod)
```

```
#55/57 application time is 50 dat
app_point=50
#get the data x days before and after
calc_diff_after=20
calc_diff_before=5
#for each ID in turn
#create a list of the correct length to hold the results
#it's much more efficient that way
ldat<-vector("list",length(levels(Data55_57_data$Snapshot_ID_Tag)))

names(ldat)<-c(levels(Data55_57_data$Snapshot_ID_Tag))

#step through each model in turn
for (ID in names(Data55_57_models)){
   ex_model<-Data55_57_models[[ID]]
   new_data<-data.frame(dat=seq(app_point-calc_diff_before,app_point+calc_diff_after))
   new_data$pred<-as.vector(predict(gmodels[[ID]],new_data))
   new_data$norm<-new_data$pred-new_data$pred[calc_diff_before+1]
   ldat[[ID]]<-new_data
   ldat[[ID]]$Snapshot_ID_Tag<-ID
}
#get the data as dataframes
ddat<-ldply(ldat)
#the IDs are replicated
ddat[1]<-NULL
ddat<-merge(ddat,plant_codes,by="Snapshot_ID_Tag")

pg<-ggplot(data=ddat,aes(x=dat,y=norm,colour=Compound_No))
pg<-
pg+facet_wrap(~Irrigation)+geom_smooth()+geom_vline(xintercept=app_point)+theme_bw()+labs(y
="LOG Normalised growth",title=(paste("Application:",app_point," dat",sep="")))
pg
ggsave(filename="LOG_normalised_early.png",plot=pg,width=34,height=20,units=c("cm"),dpi=600)
```

```

Is there an impact on Stay green

Calculate the % green at any time

```{R}

#Calculate the % green

subdata$pc_green<-
100*subdata$mean_area_green/(subdata$mean_area_green+subdata$mean_area_yellow)

app_point=50


Data55_57_data<-subset(subdata,Application=="BBCH 50/55")

Data55_57_data<-droplevels(Data55_57_data)

py<-ggplot(data=Data55_57_data,aes(x=dat,y=pc_green,colour=Compound_No))

py<-
py+facet_wrap(~Irrigation)+geom_smooth()+geom_vline(xintercept=app_point)+theme_bw()+labs(y
="% green pixels",title=(paste("Application:",app_point," dat",sep="")))

py

ggsave(filename="LOG_normalised_green.png",plot=py,width=34,height=20,units=c("cm"),dpi=600)

```

Not really

Overall - we have calculated maxOSA and the days it takes to get there.

We have shown that the midpoint applications leads to prolonged growth for tw treatments under droughted conditions

There is no stay green effect of late treatments

For simplicity we'll write the values to a file so that they can be read in again without the need for all of this code.

```{R}

write.csv(dmax,file="Max OSA and Max dat.csv")

```
```

---

title: "Stats analysis"

author: "Luke Cartwright"

date: "2017"

output: html_document

```{r,warning=FALSE,message=FALSE}

rm(list=ls())

source("https://bioconductor.org/biocLite.R")

biocLite("lubridate")

#or

install.packages("directlabels")

library(ggplot2)

library(lubridate)

library(dplyr)

library(zoo)

library(gridExtra)

library(cowplot)

library(reshape2)

library(directlabels)

library(plyr)

library(mgcv)

library(lmtest)

```

Set up standard files names and the subset to plot.

If you set the working directory then everything else is referenced relative to that

This data set has been analysed for outliers using the Basic Processing analysis

Therefore the filtered codes are used.

```{r}

#Big data file

input_file="./data/Halcon.csv"

#Information about the treatments

#Two sets of files are given - one filtered for outliers
```

#Running the code with this file changed makes it easy to exclude outliers

#plant_codes_file="./data/Halcon_labels.csv"

plant_codes_file="./data/Halcon_labels_filtered.csv"

#Yield data

yield_file="./data/Yield_data.csv"

#model data output from extract data routines

model_file="Max OSA and Max dat.csv"

```

Work out the application times

```{R}

#The time of transfer as a date

dat_datetime<-as.POSIXlt("25/02/2016 08:00:00",tz="","%d/%m/%Y %H:%M:%S")

#Somewhere to store the results

app_no<-c(1,2,3)

app_date<-c("11/03/2016 08:00:00","01/04/2016 08:00:00","15/04/2016 08:00:00")

Application=c("BBCH 12/13","BBCH 30/31","BBCH 55/57")

app_posix<-as.POSIXlt(app_date,tz="","%d/%m/%Y %H:%M:%S")

app_dat<-as.numeric(difftime(app_posix,dat_datetime,units="days"))

app<-data.frame(app_no,Application,app_dat)

app

#For simplicity round to 0 dp

app$app_dat<-round(app$app_dat,0)

app

```

Read in the plant codes, modelled data and yield files

```{r}

#this file contains info about the plants used - all are factors

#change this from plant_codes to plant_codes_filtered to re-run the code with outliers excluded.

#Outliers are defined by the 'Inactive' field being set to y

plant_codes<-read.csv(plant_codes_file,header = TRUE,stringsAsFactors = TRUE)

if(is.object(plant_codes)==FALSE) {stop(c("Can't open file:",plant_codes_file))}

model_data<-read.csv(model_file,header=TRUE,stringsAsFactors = FALSE)

#It reads the first rows as X so we'll dump that

model_data$X<-NULL

#Set the appropriate columns to factors

model_data$Snapshot_ID_Tag<-as.factor(model_data$Snapshot_ID_Tag)

model_data$number_of_trial<-as.factor(model_data$number_of_trial)

model_data$Treatment_Number<-as.factor(model_data$Treatment_Number)

model_data$Compound_Name_irrigation<-as.factor(model_data$Compound_Name_irrigation)

model_data$COMPOUND_NAME<-as.factor(model_data$COMPOUND_NAME)

model_data$Application<-as.factor(model_data$Application)

model_data$Irrigation<-as.factor(model_data$Irrigation)

model_data$Inactive<-as.factor(model_data$Inactive)

model_data$Compound_No<-as.factor(model_data$Compound_No)

#Read in the yield data

yield_data<-read.csv(file=yield_file,header=TRUE,sep=",",stringsAsFactors = FALSE)

#Set the factors

yield_data$Snapshot_ID_Tag<-as.factor(yield_data$Snapshot_ID_Tag)

#Merge the yield and model data together

all_data<-merge(model_data,yield_data,by="Snapshot_ID_Tag")

head(all_data)

#Some yield values are NA. As we are interested in yield predictors we may as well drop these,

all_data<-all_data[!is.na(all_data$WtTotal),]

```

Do some basic plots of the yield data

```{R}

#It's useful to put the controls first as many stats packages require the first sample to be the control. It also controls the plot order.

levels(all_data$Compound_No)

all_data$Compound_No<-relevel(all_data$Compound_No,ref="Control")

levels(all_data$Compound_No)

```
all_data$Application<-relevel(all_data$Application,ref="None")

p1<-ggplot(data=all_data,aes(x=Application,y=WtTotal))+
 theme_bw()+
 geom_boxplot(aes(fill=Compound_No),outlier.color = "red",outlier.size=3)+
 facet_wrap(~Irrigation)+
 ggtitle("Yield")+labs(y="Total grain weight (g)")
p1

p2<-ggplot(data=all_data,aes(x=Application,y=TKW))+
 theme_bw()+
 geom_boxplot(aes(fill=Compound_No),outlier.color = "red",outlier.size=3)+
 facet_wrap(~Irrigation)+
 ggtitle("TKW")+labs(y="TKW (g)")
p2

p3<-ggplot(data=all_data,aes(x=Application,y=GrainTotal))+
 theme_bw()+
 geom_boxplot(aes(fill=Compound_No),outlier.color = "red",outlier.size=3)+
 facet_wrap(~Irrigation)+
 ggtitle("Grain total")+labs(y="Grain total")
p3


```

It's very obvious there is an effect of drought - but let's do a test anyway

We want to compare the WtTotal between well watered and droughted plants for each compound and application

```{R}
#Do a quick plot and check for equal variances
plot(WtTotal ~ interaction(Compound_No,Application,Irrigation),data=all_data)
bartlett.test(WtTotal ~ interaction(Compound_No,Application,Irrigation),data=all_data)


lmMod<-lm(WtTotal ~Application*Compound_No*Irrigation,data=all_data)
lmMod
```

```
par(mfrow=c(2,2))
plot(lmMod)
bptest(lmMod)
wtBCMod<-BoxCoxTrans(all_data$WtTotal)
wtBCMod

all_data<-cbind(all_data,WtTotalBC=predict(wtBCMod,all_data$WtTotal))

lmModbc<-lm(WtTotalBC ~Application*Compound_No*Irrigation,data=all_data)
bptest(lmModbc)
plot(lmModbc)
```

The variances are highly uneven.

What about within an irrigation set?

```{R}
#Do a quick plot and check for equal variances
d_data=subset(all_data,Irrigation=="drought")
plot(WtTotal ~ interaction(Compound_No,Application),data=d_data)
bartlett.test(WtTotal ~ interaction(Compound_No,Application),data=d_data)

w_data=subset(all_data,Irrigation=="well watered")
plot(WtTotal ~ interaction(Compound_No,Application),data=w_data)
bartlett.test(WtTotal ~ interaction(Compound_No,Application),data=w_data)
```

Fits from the GAM fitted to Chapter 4 data

The treatment corresponding to each graph is labelled at the bottom of each page.

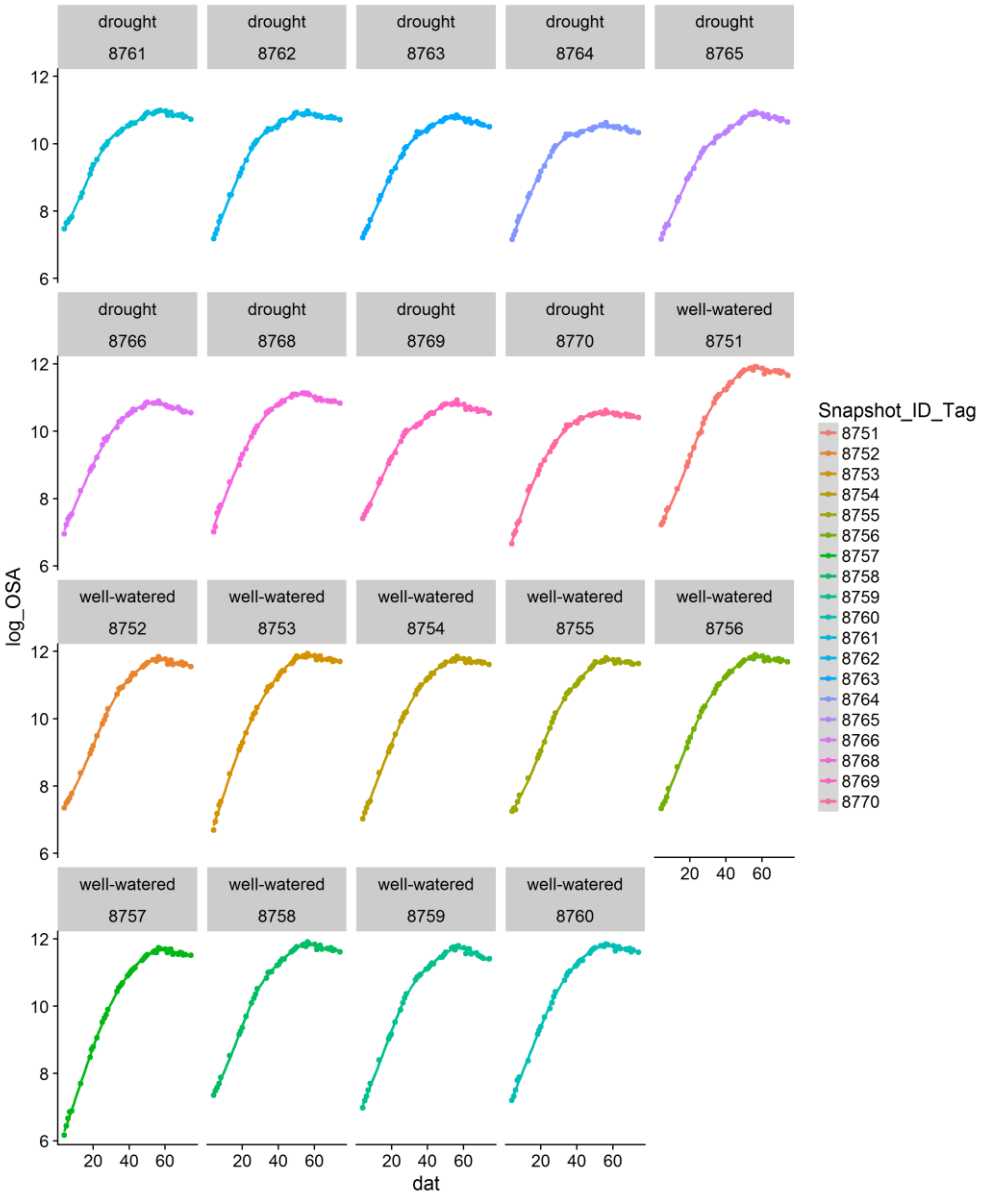

Untreated (control)

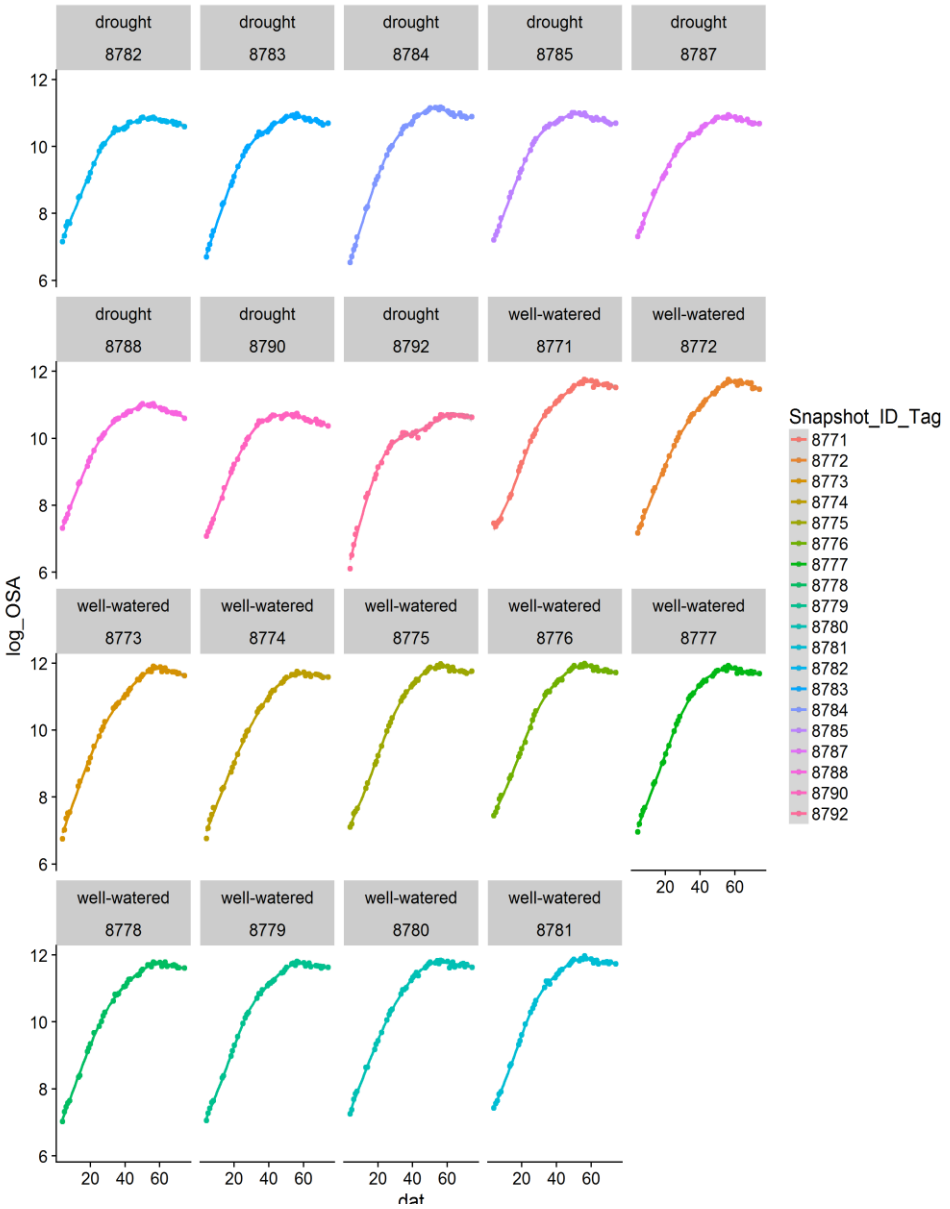

Early application: genapol

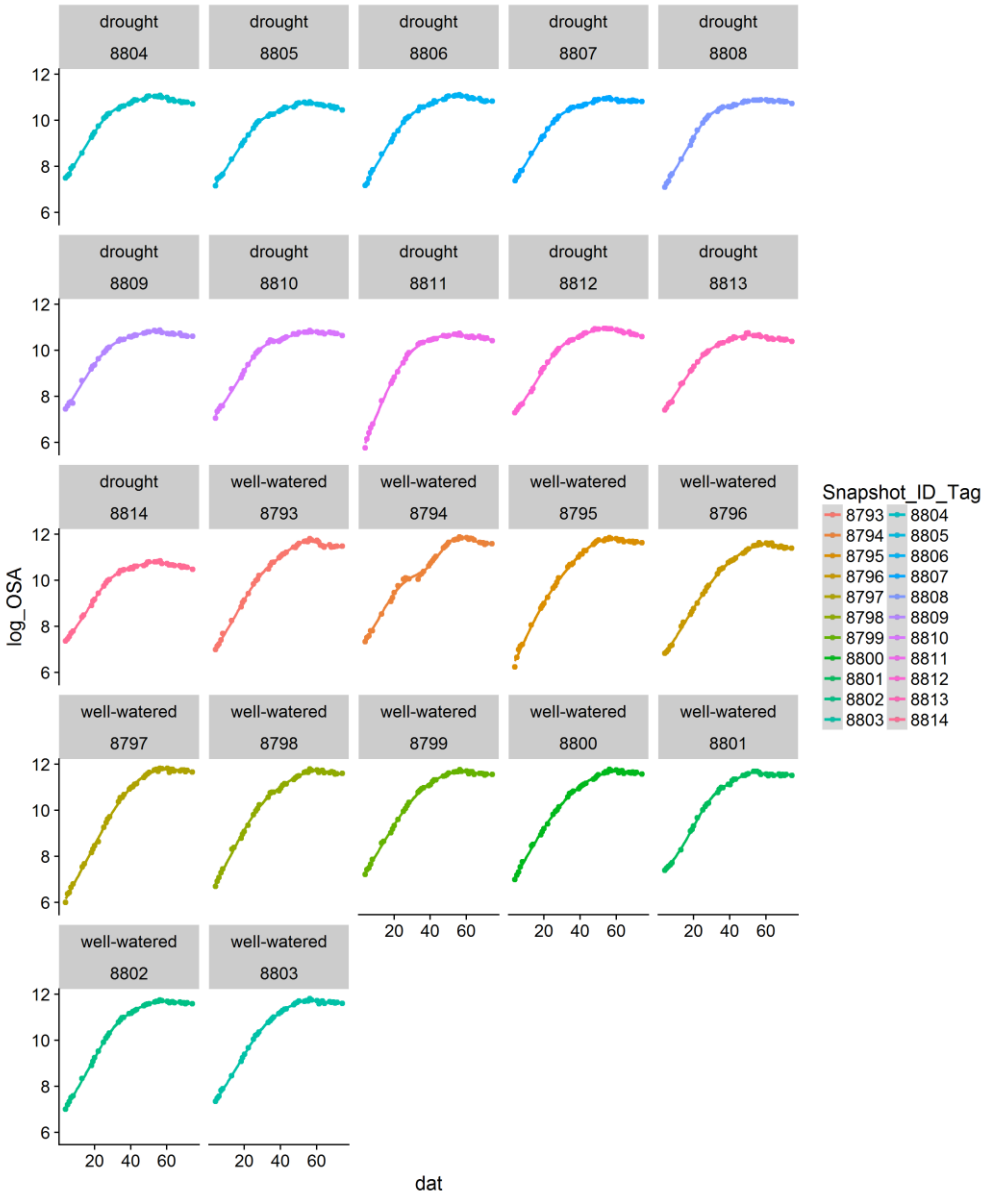

Early application: compound 1

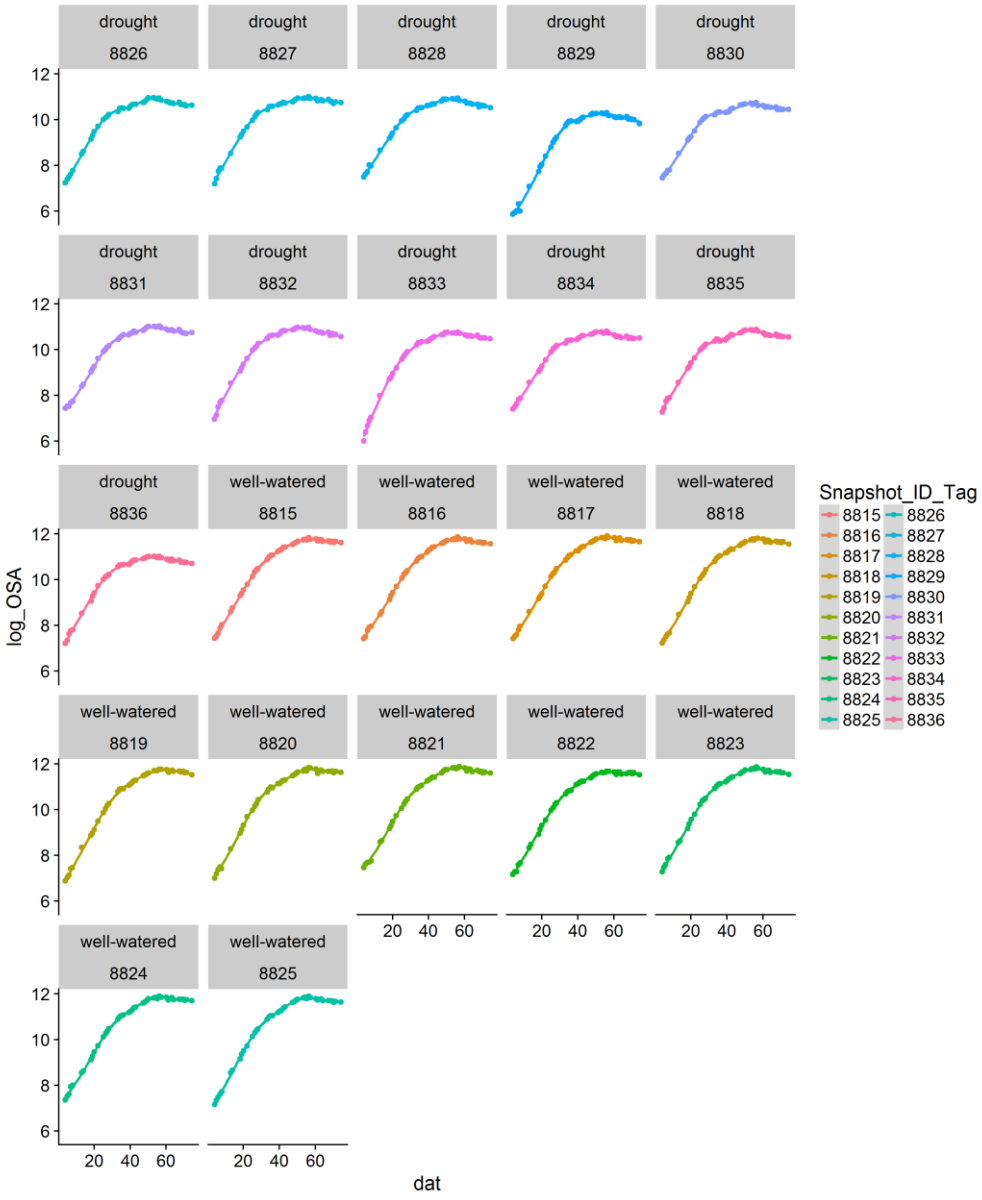

Early application: compound 2

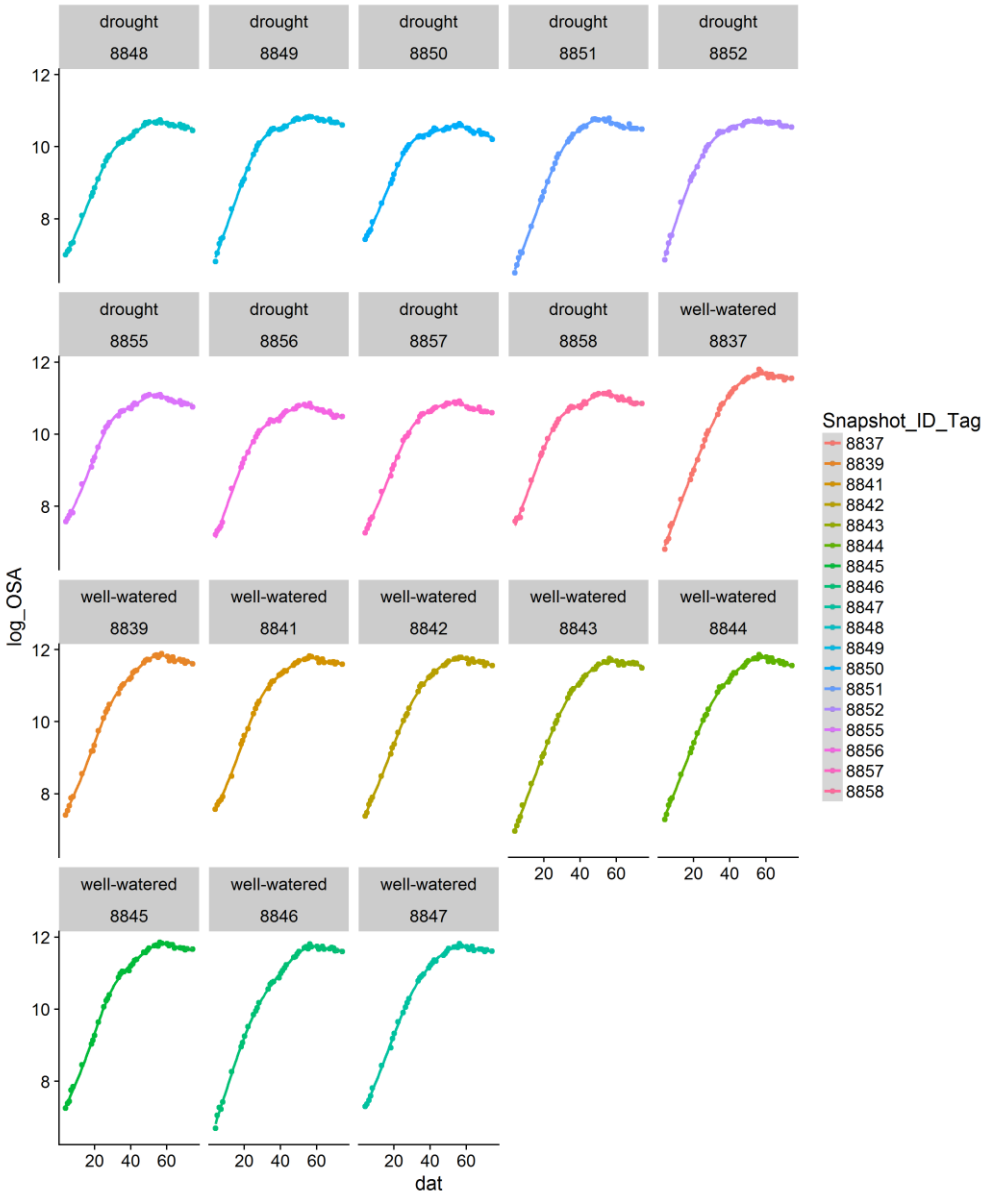

Early application: compound 3

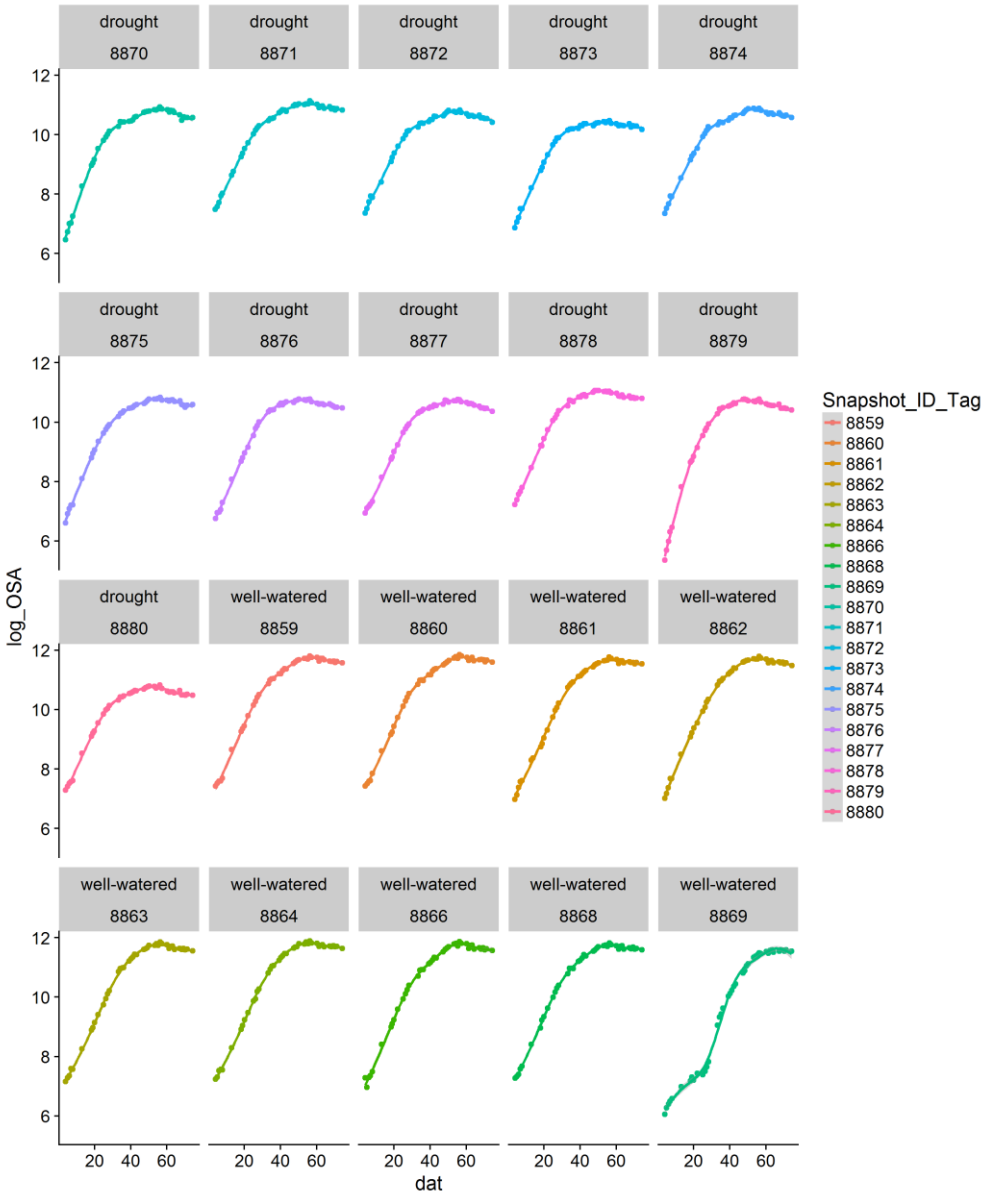

Early application: compound 4

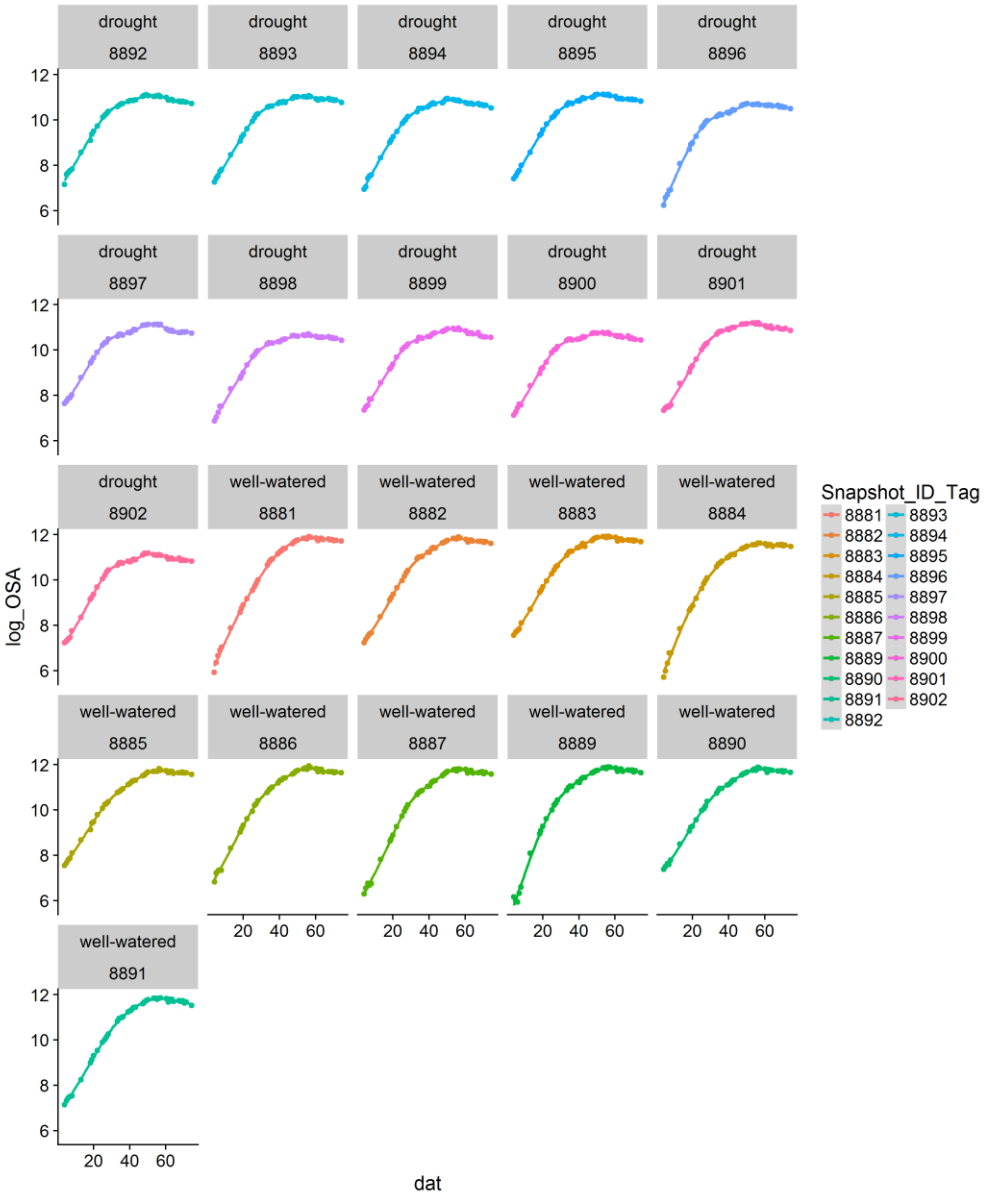

Mid-point application: genapol

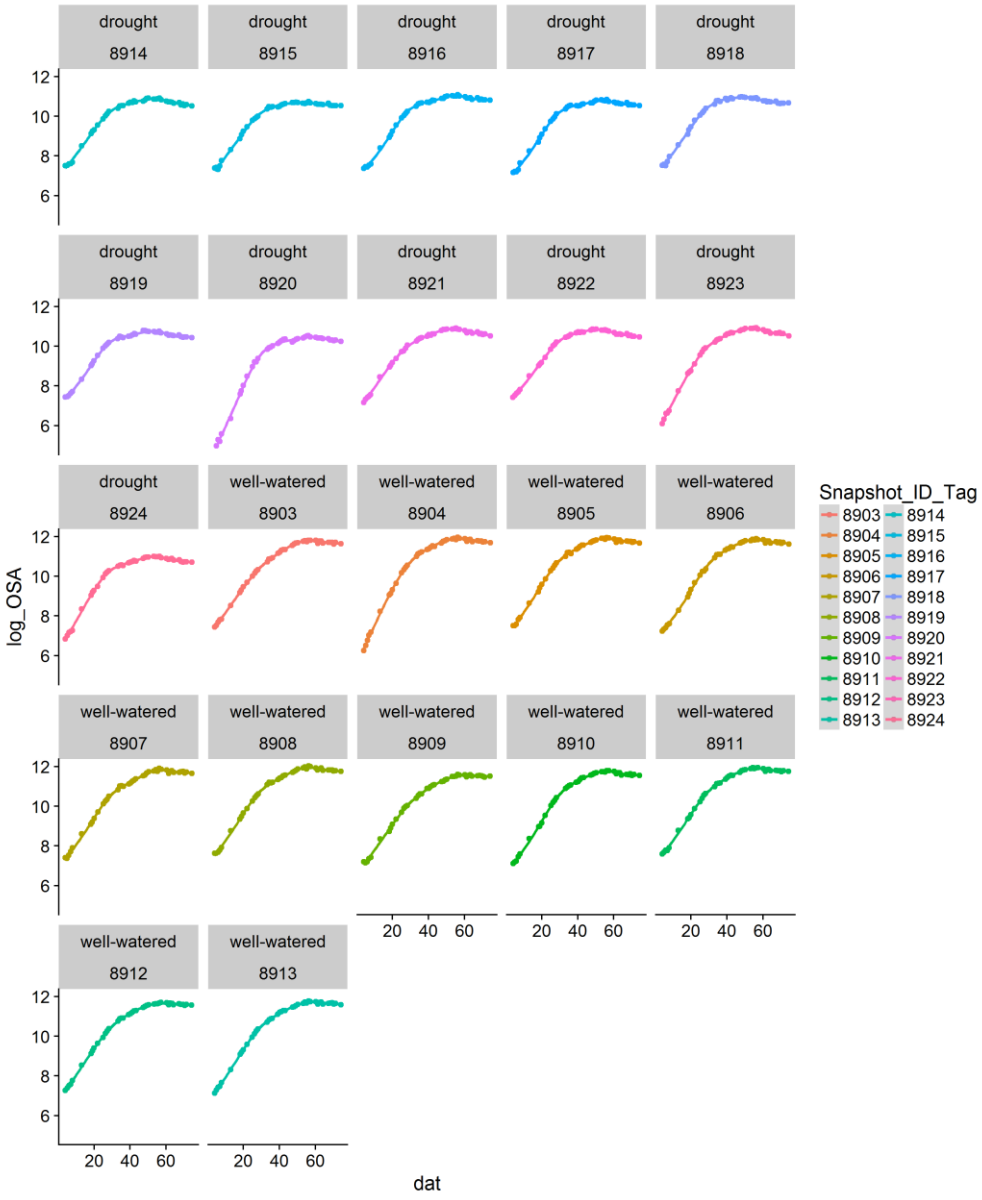

Mid-point application: compound 1

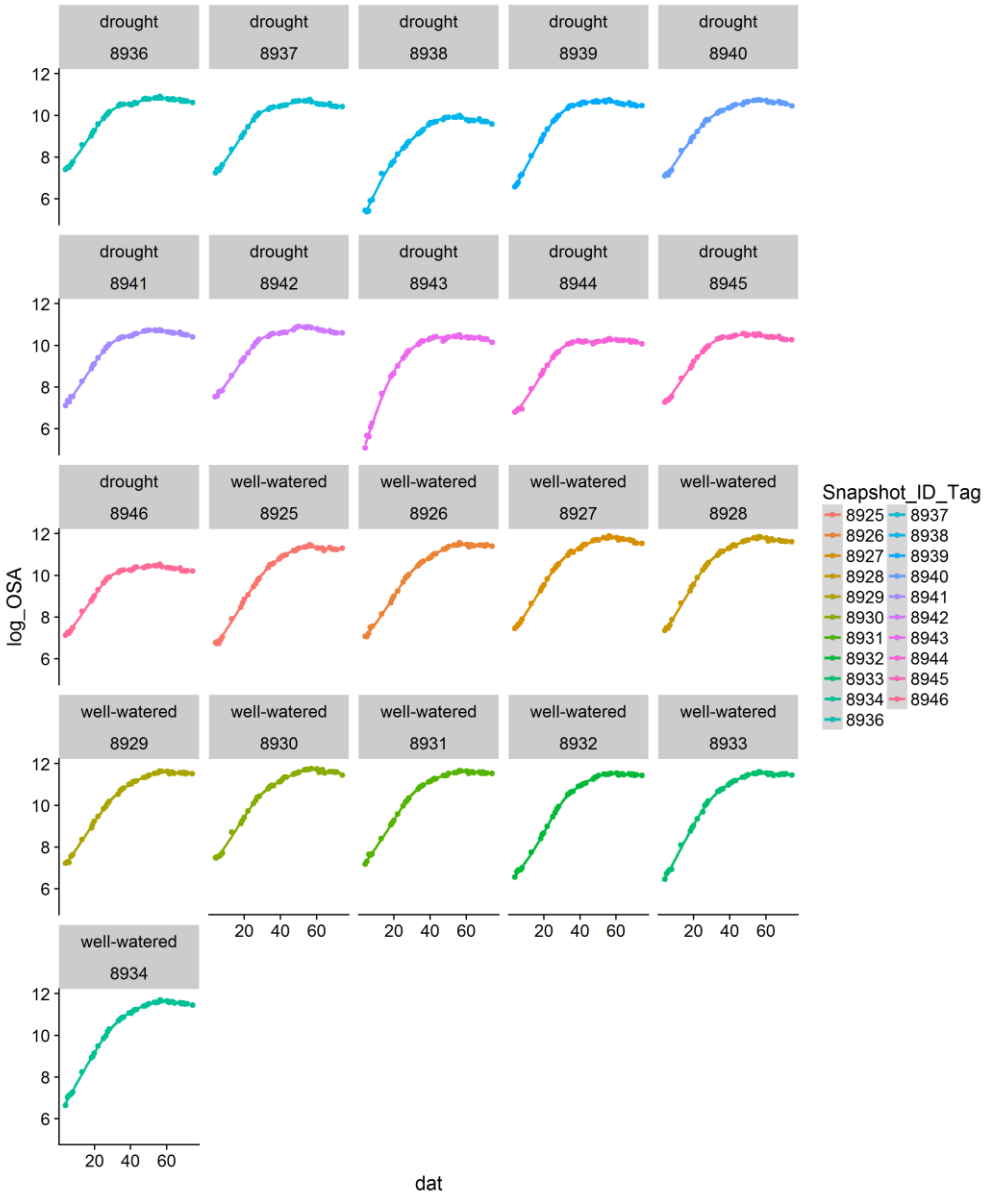

Mid-point application: compound 2

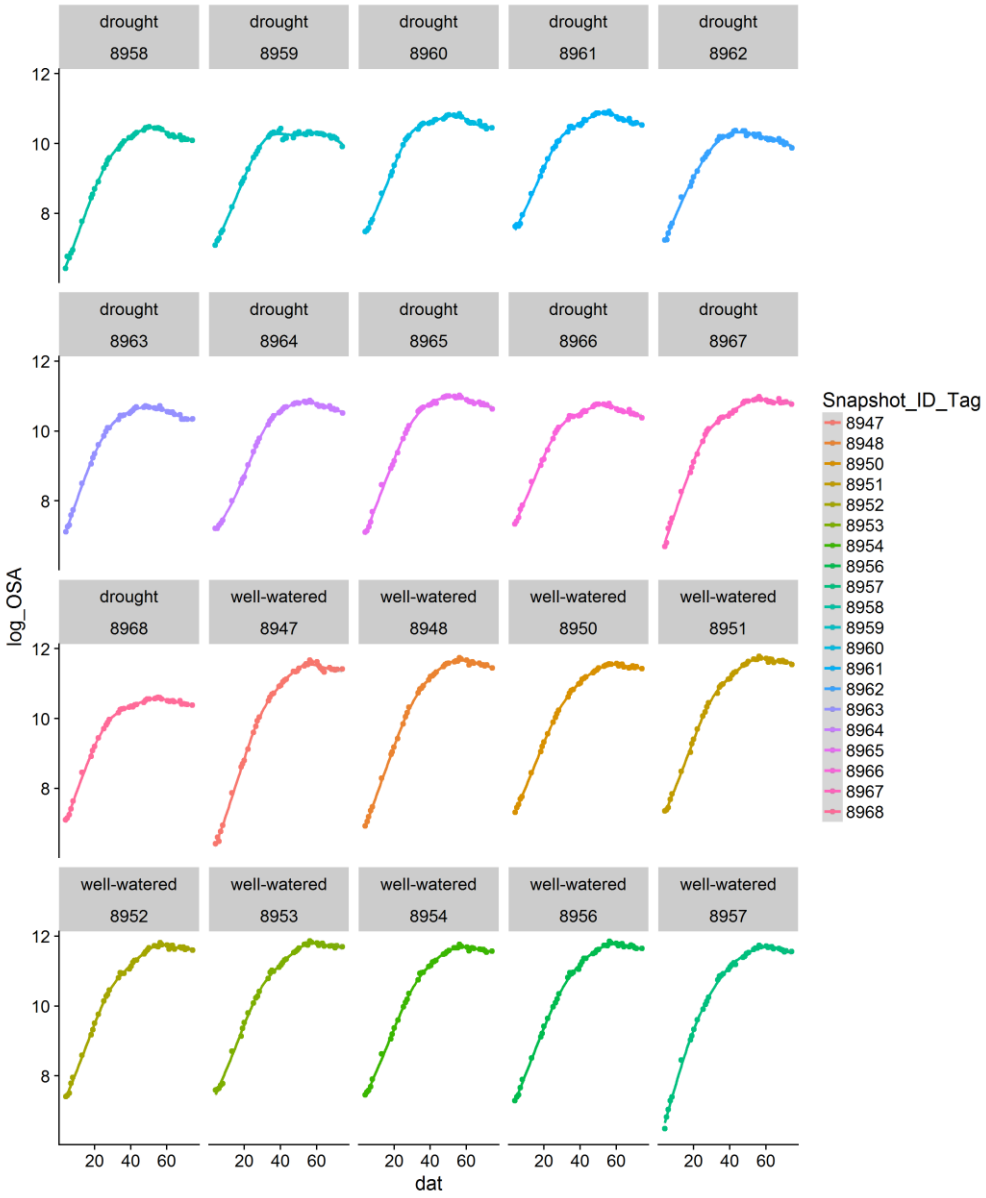

Mid-point application: compound 3

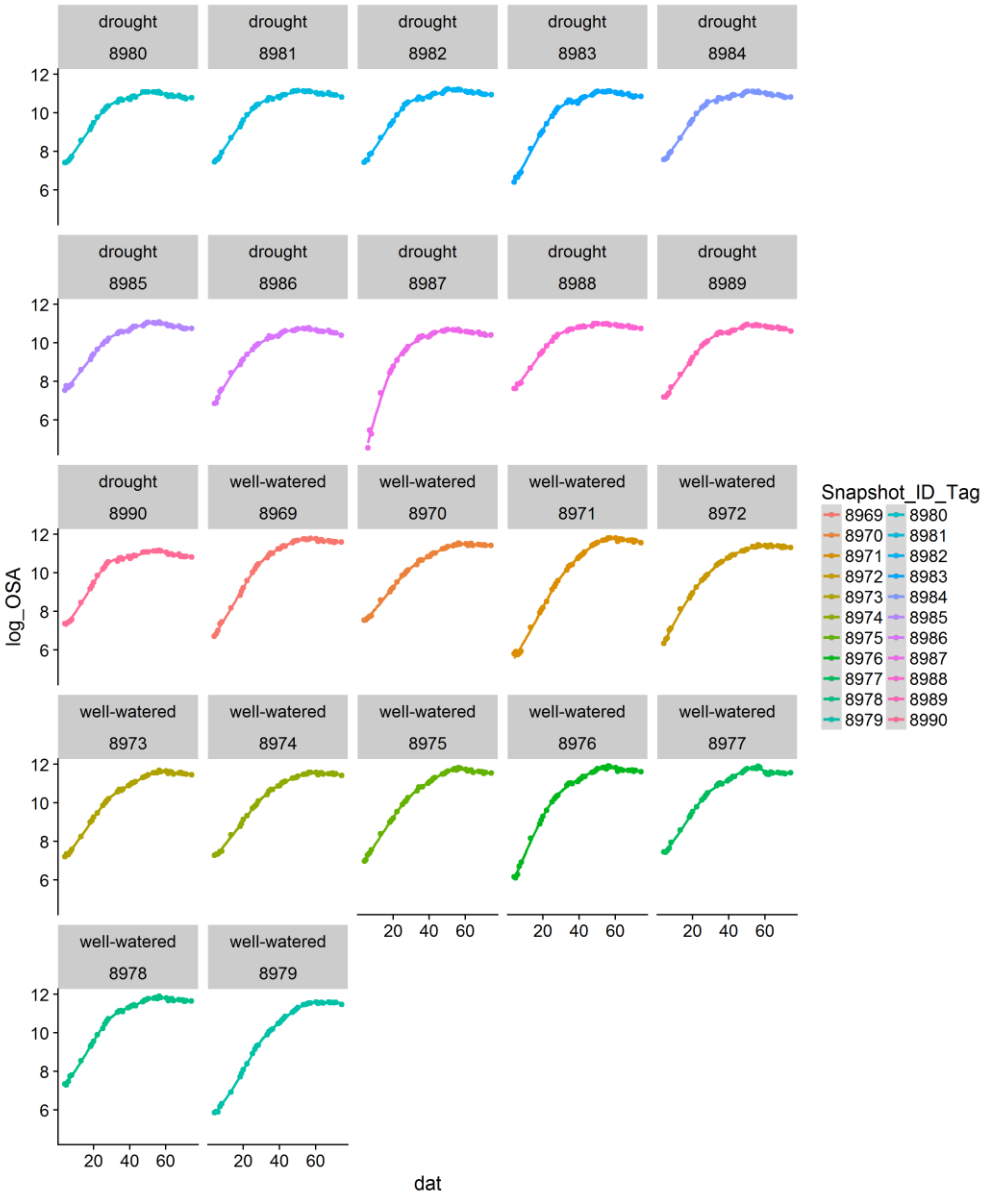

Mid-point application: compound 4

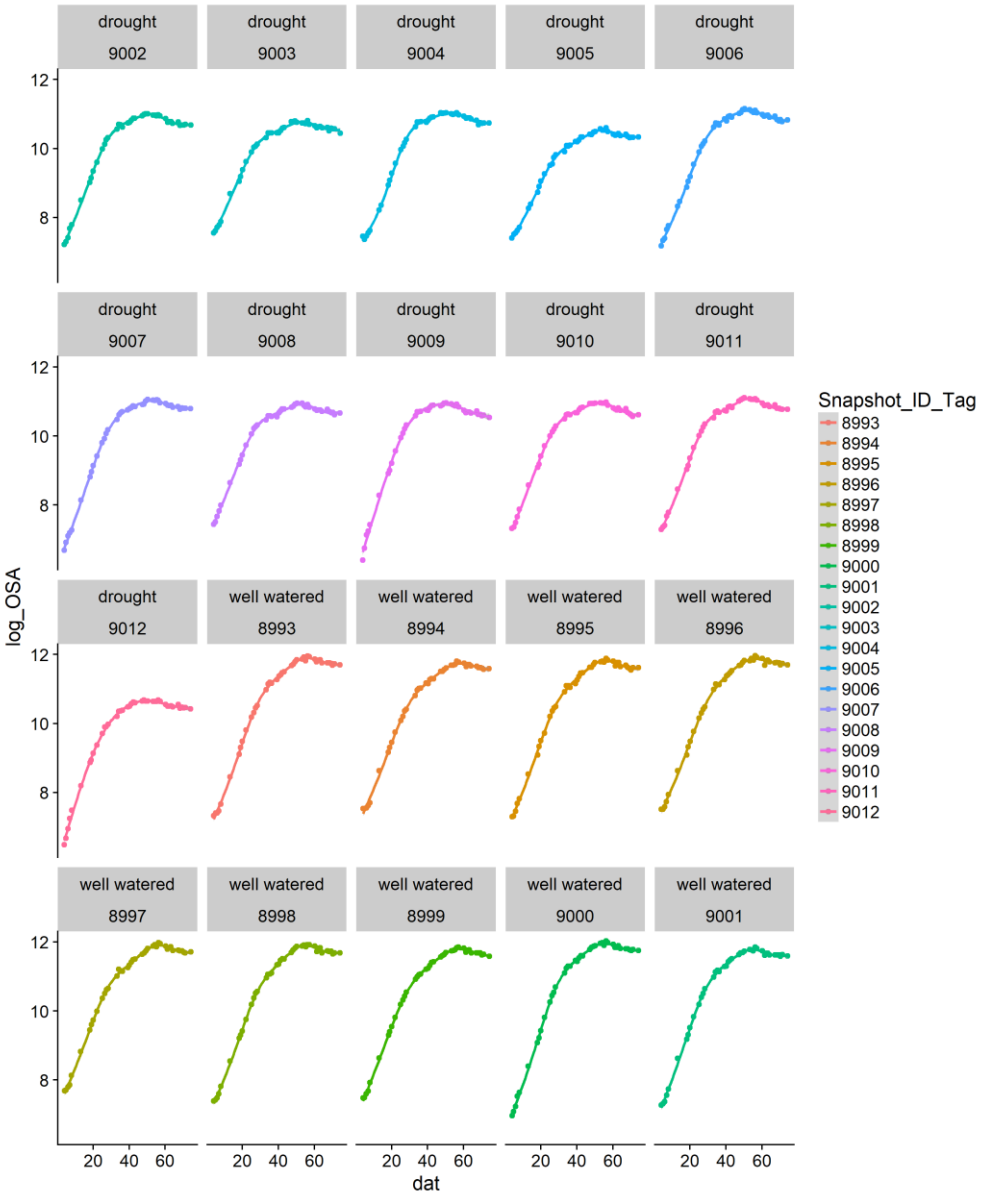

Late application: genapol

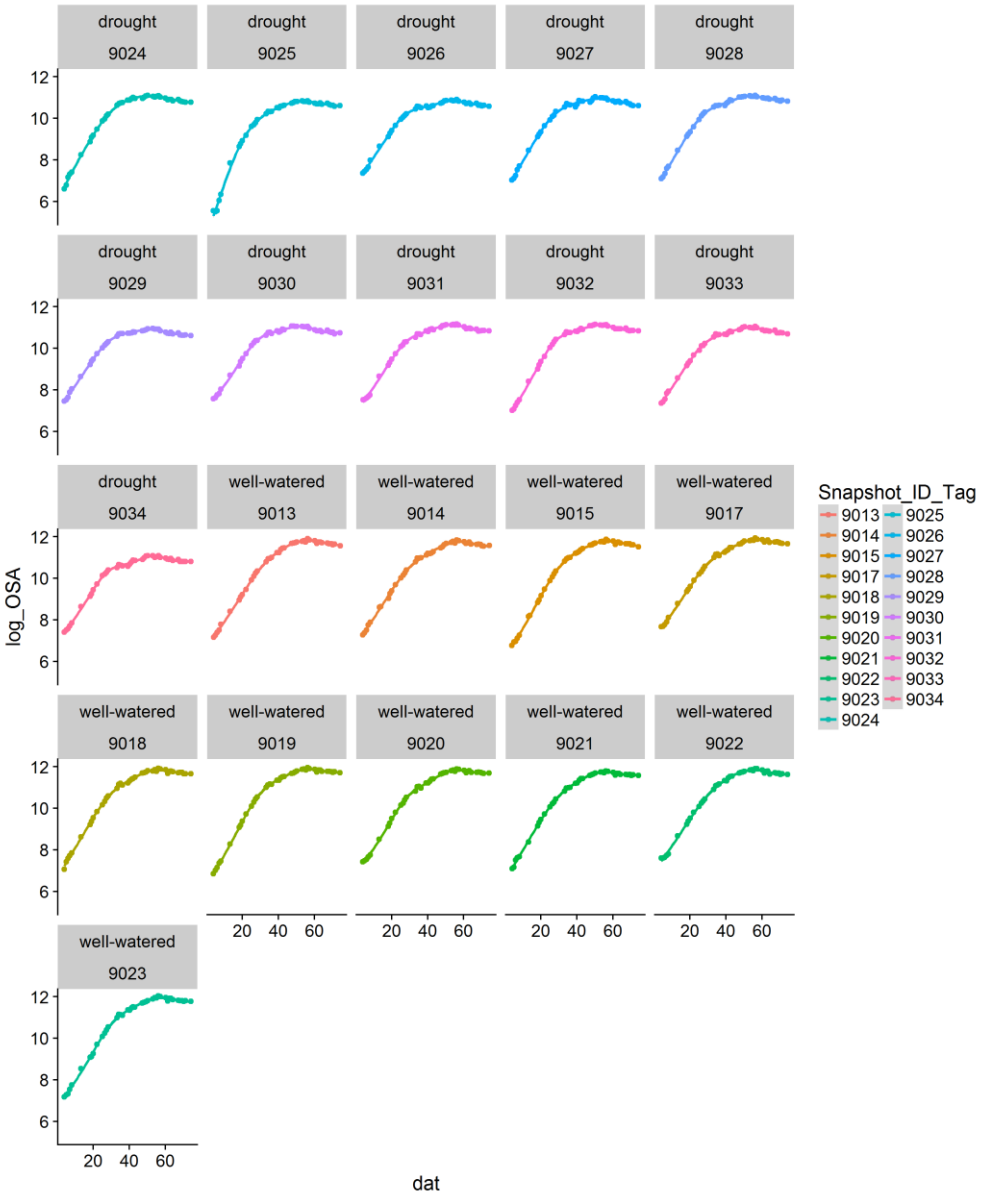

Late application: compound 1

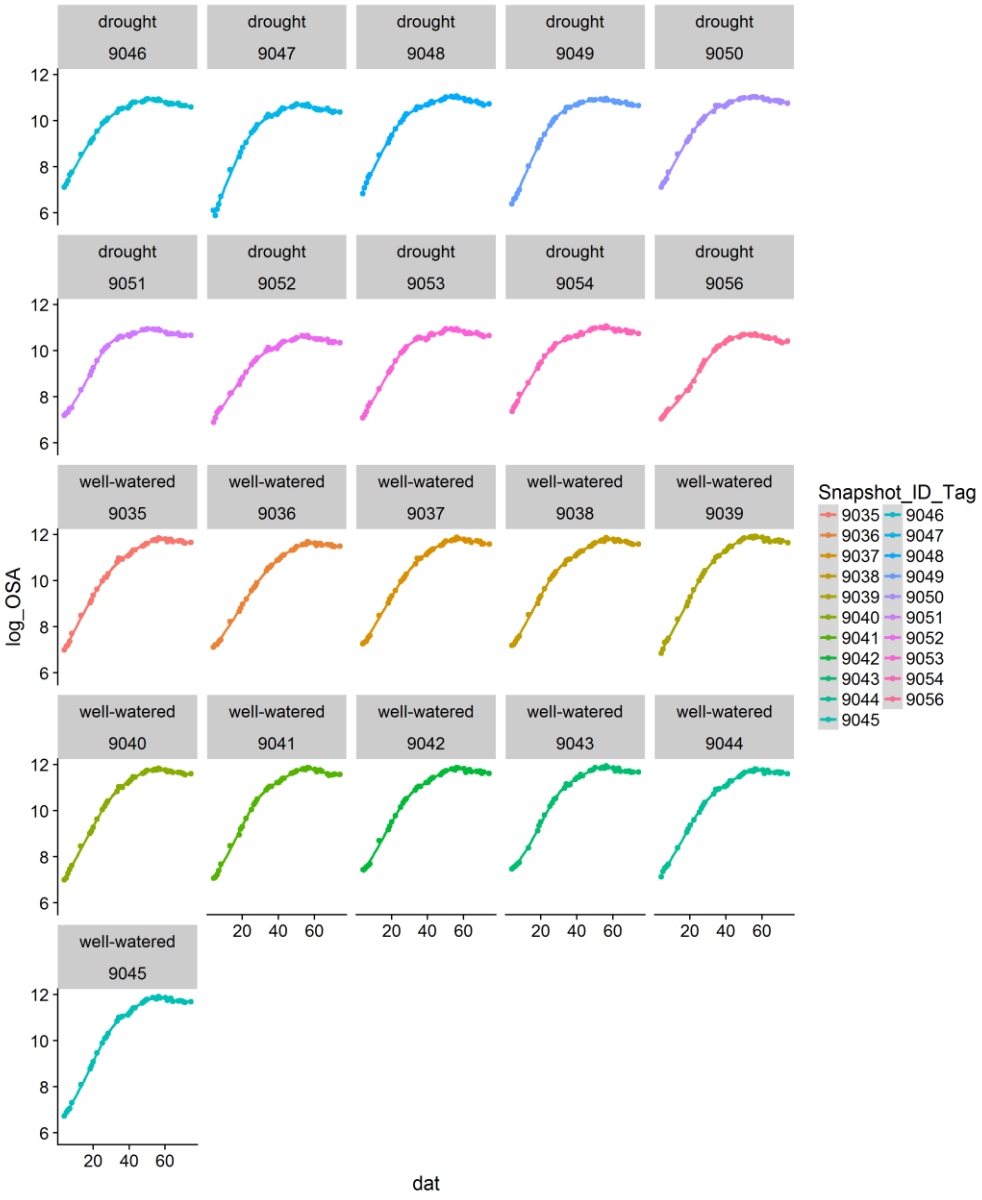

Late application: compound 2

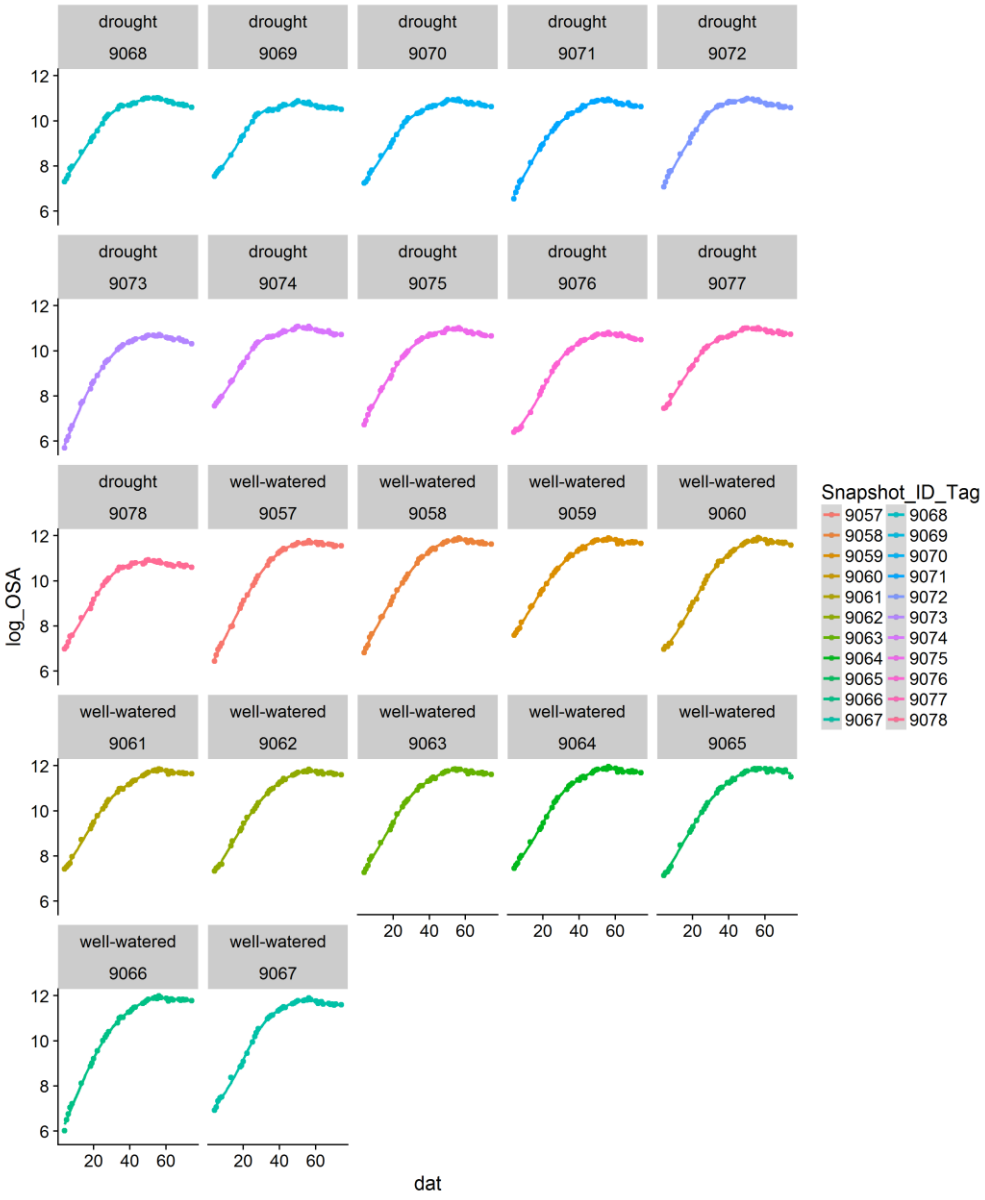

Late application: compound 3

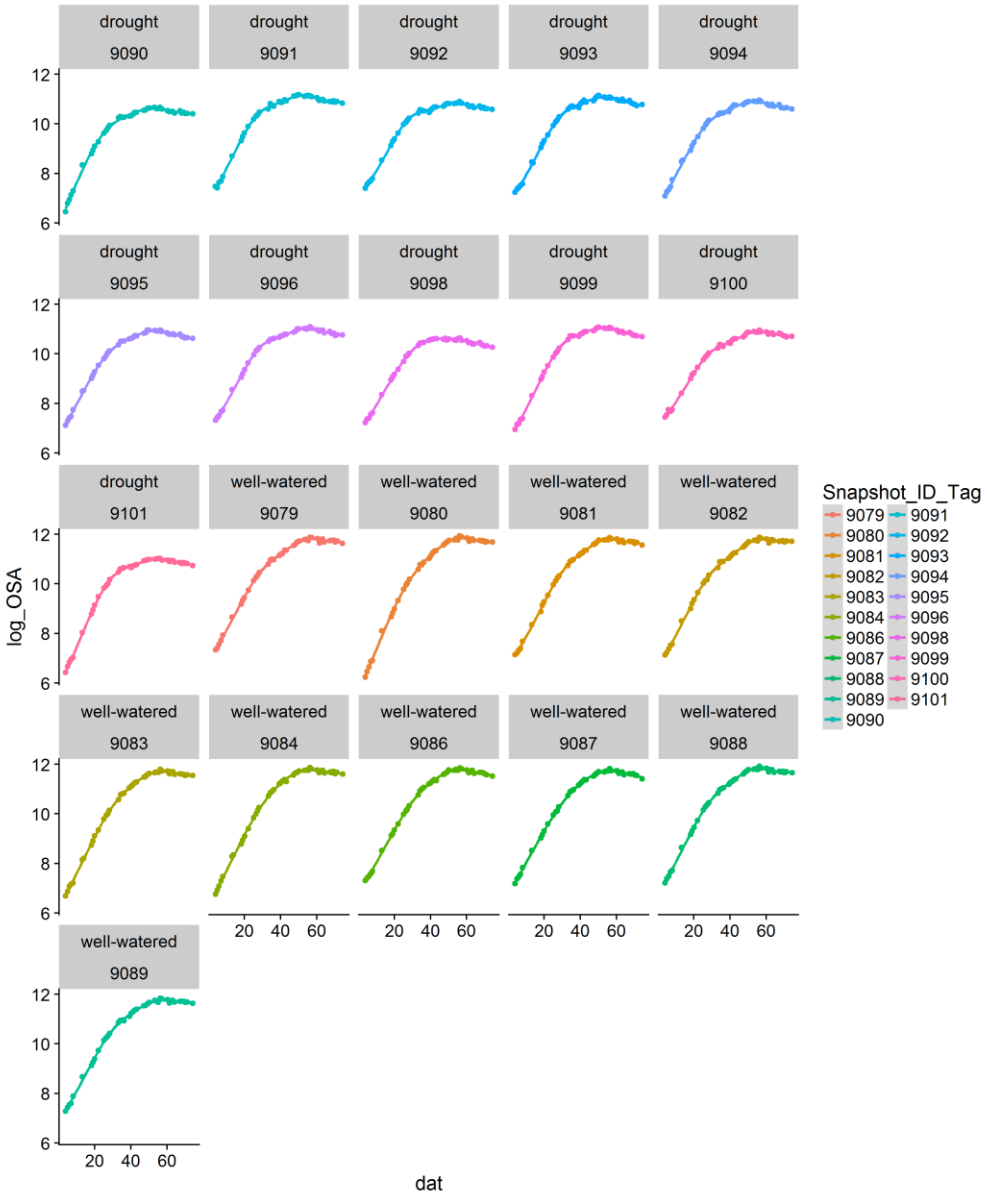

Late application: compound 4

Residuals from the GAM fits

The treatment corresponding to each graph is labelled at the bottom of each page.

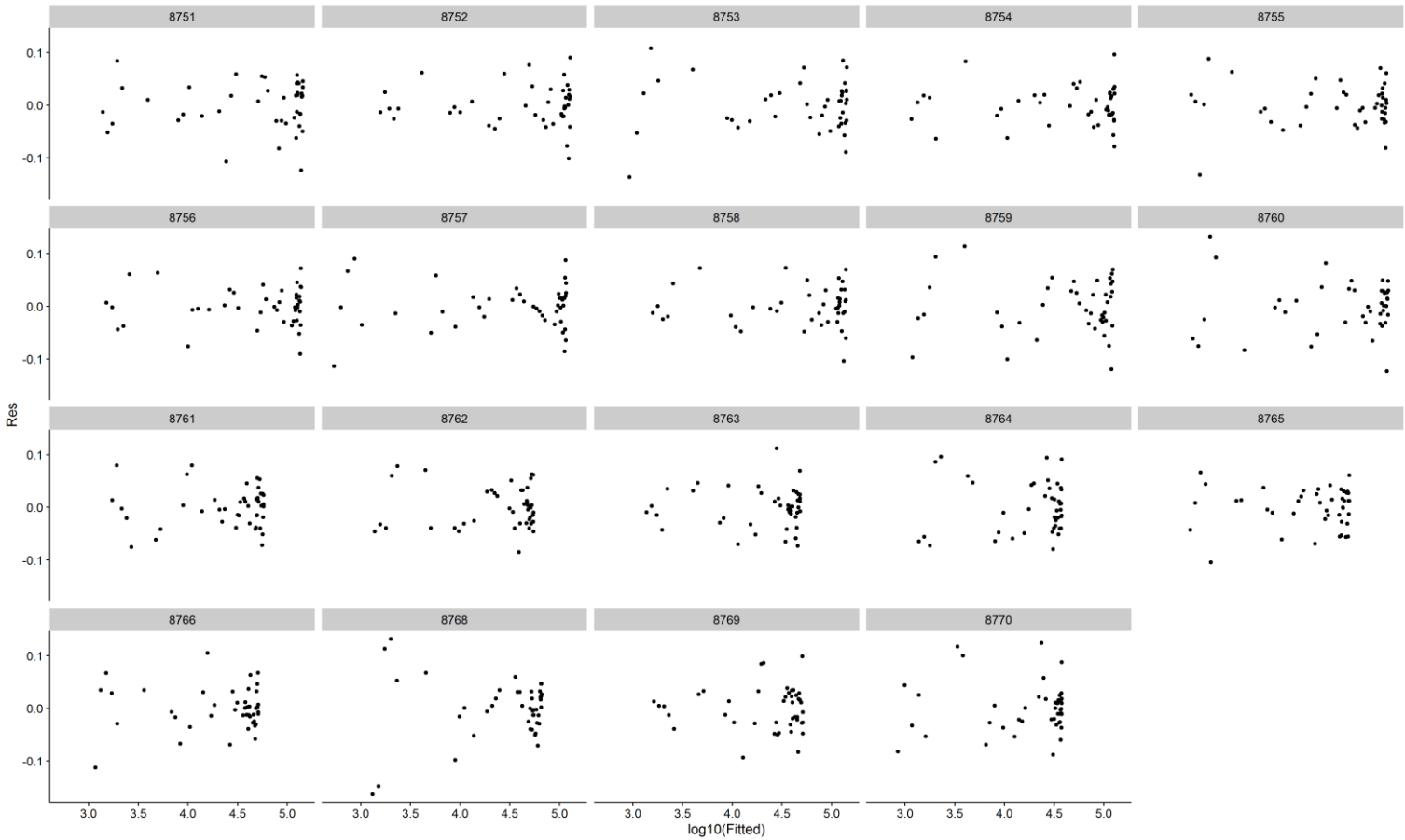

Untreated (control)

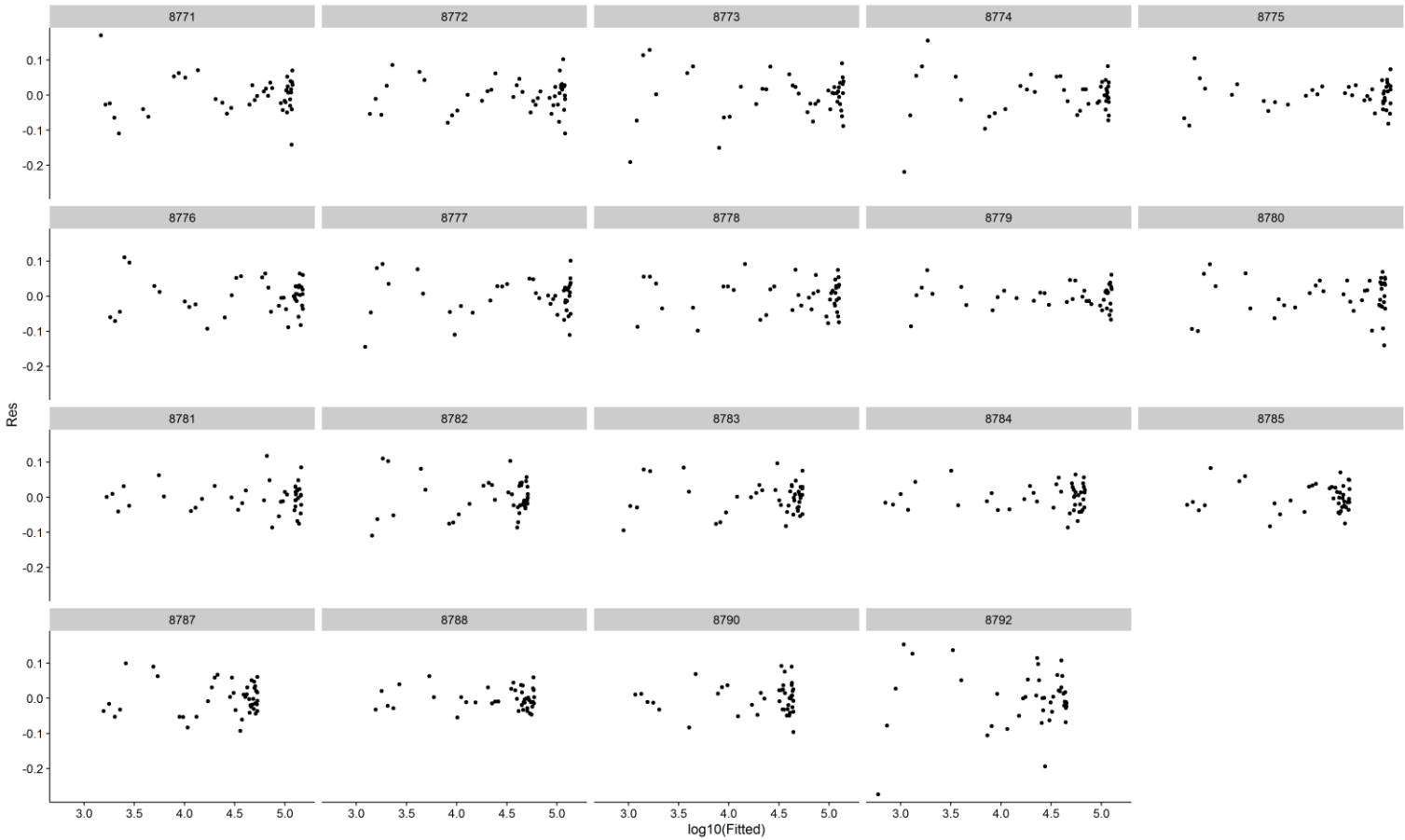

Early application: genapol

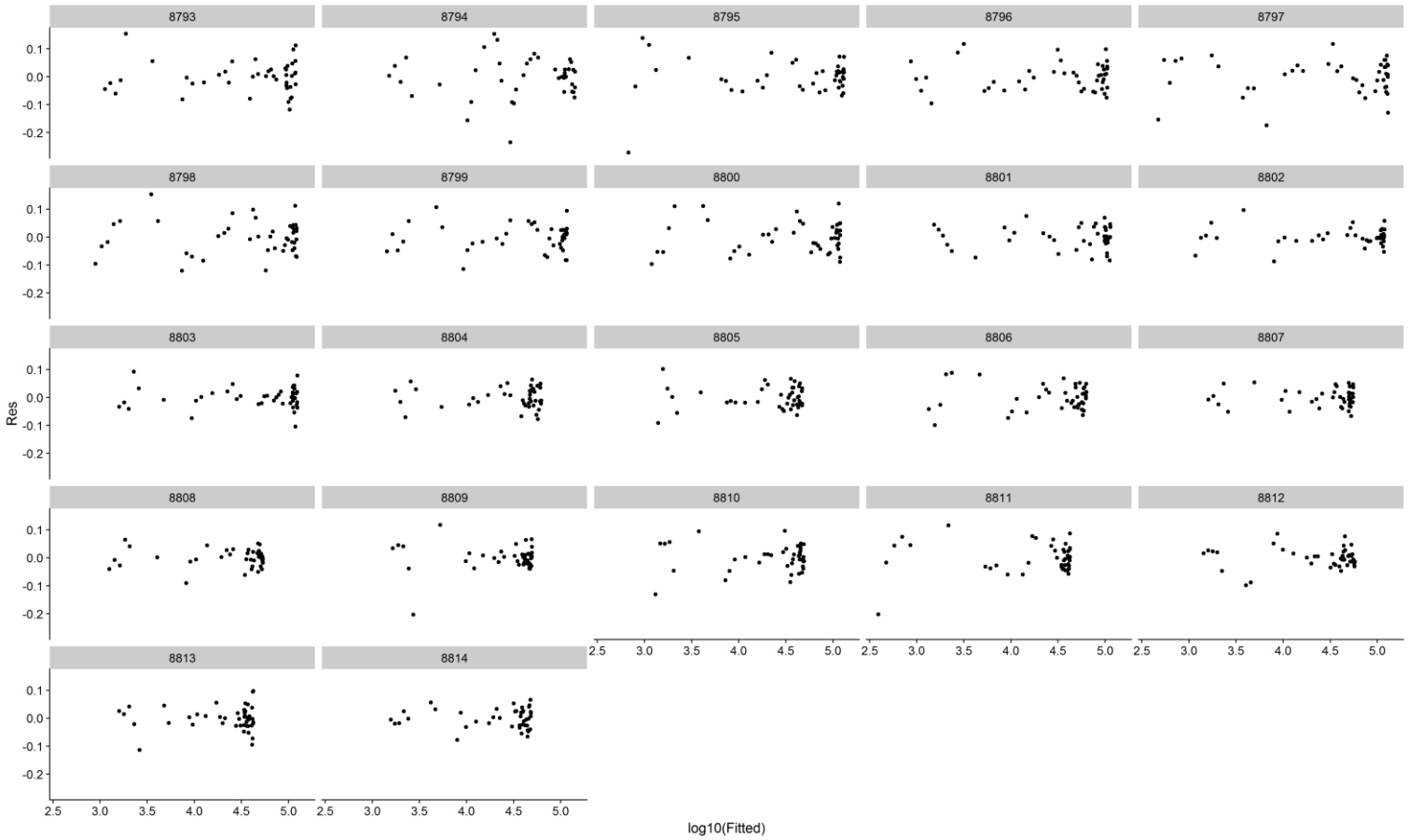

Early application: compound 1

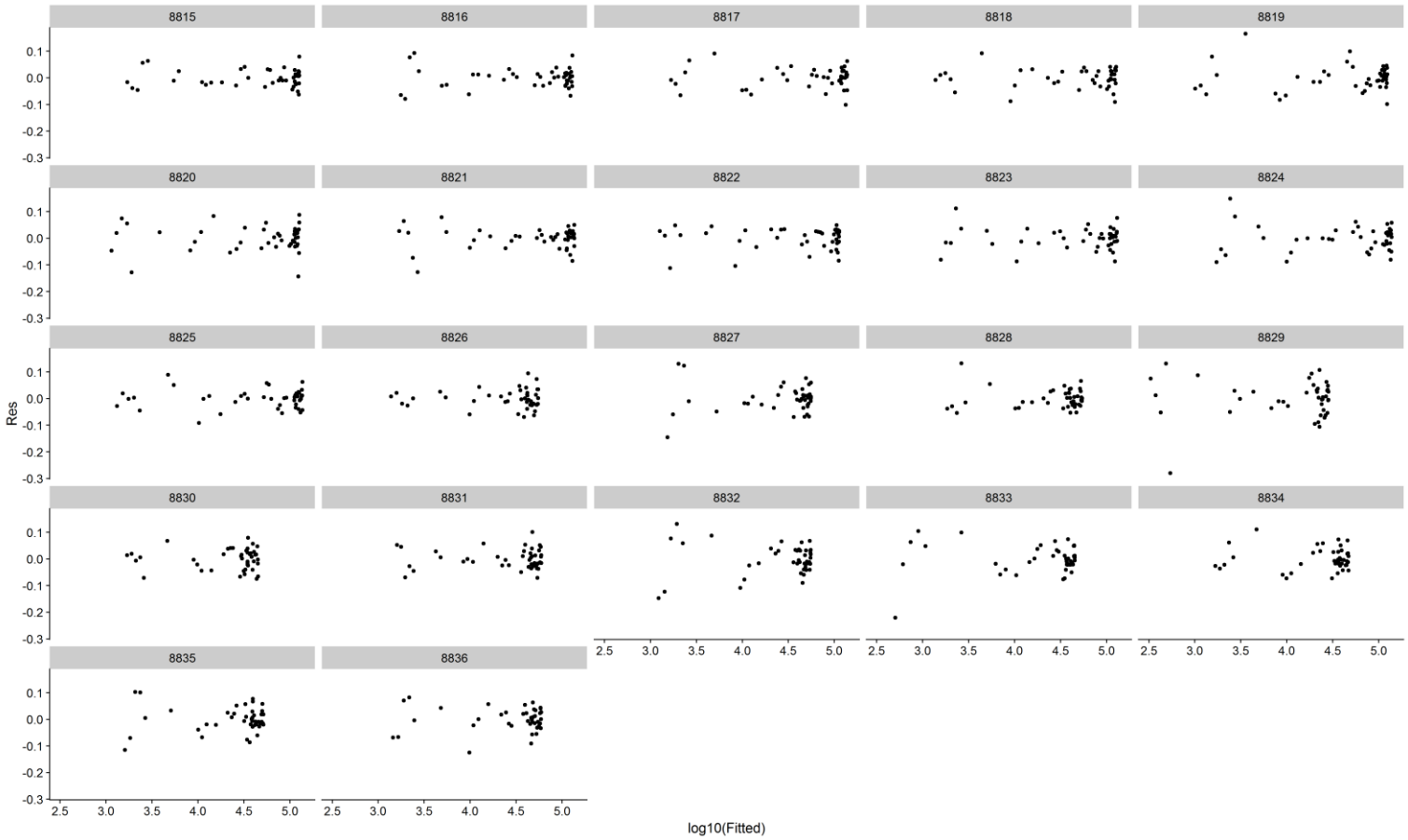

Early application: compound 2

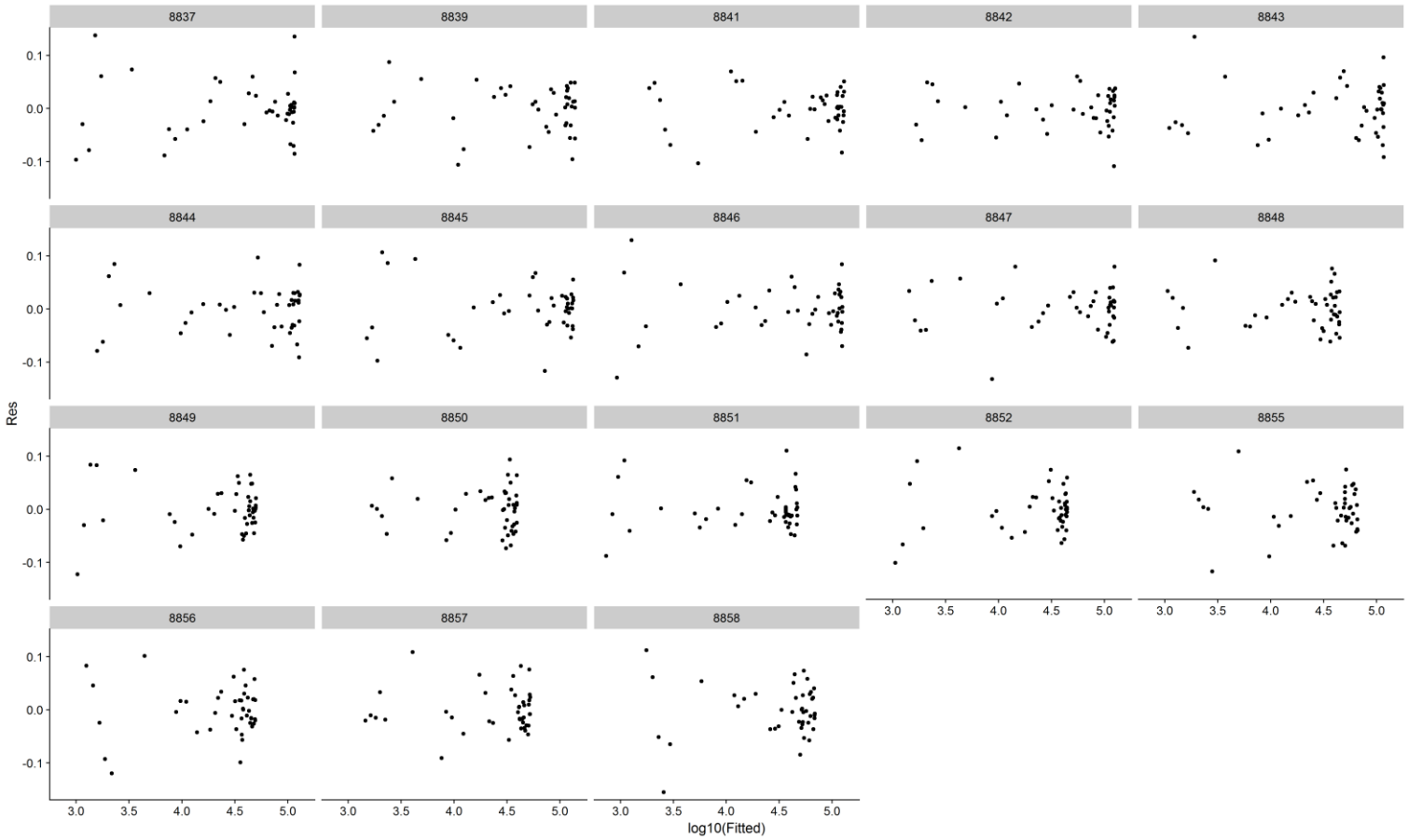

Early application: compound 3

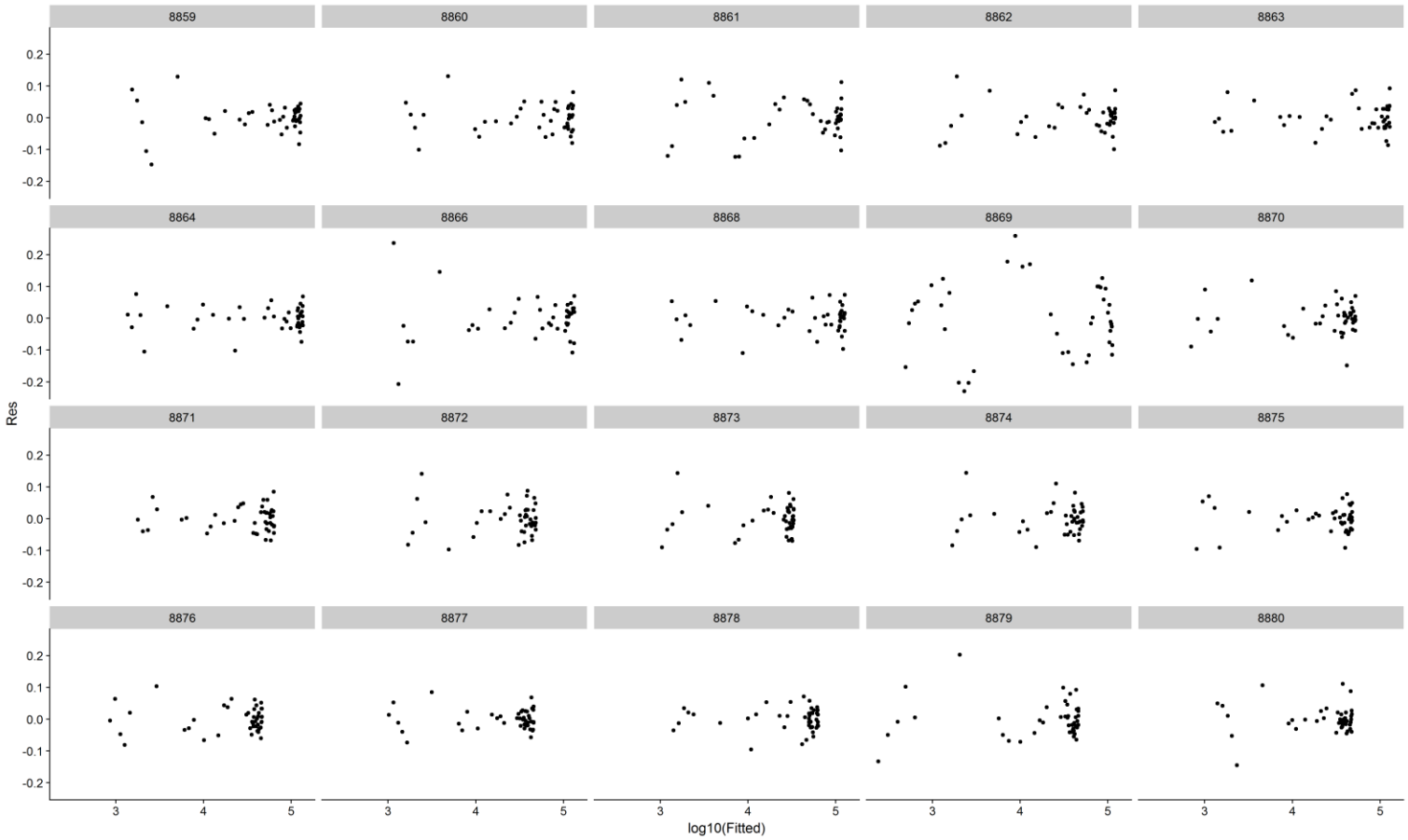

Early application: compound 4

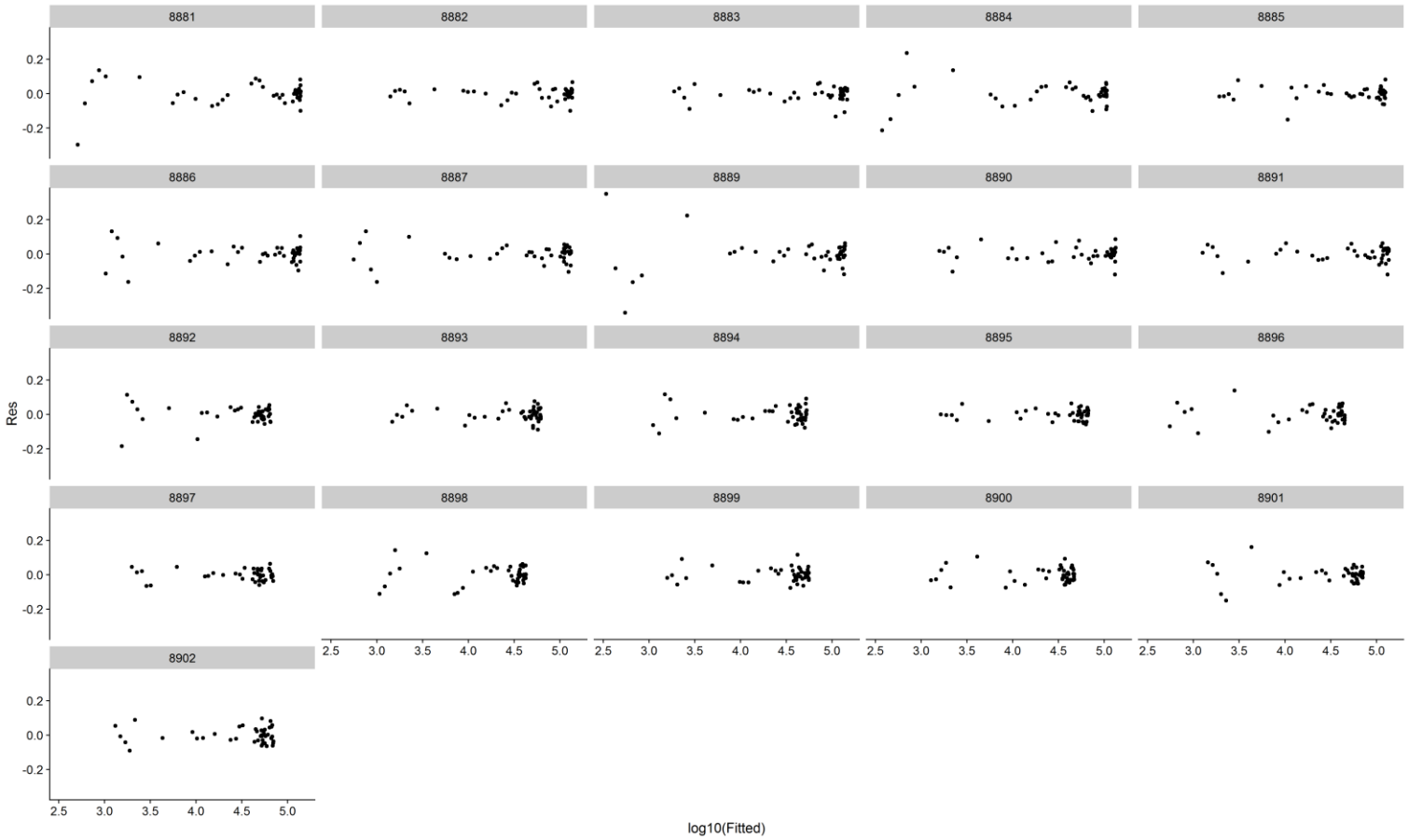

Mid-point application: genapol

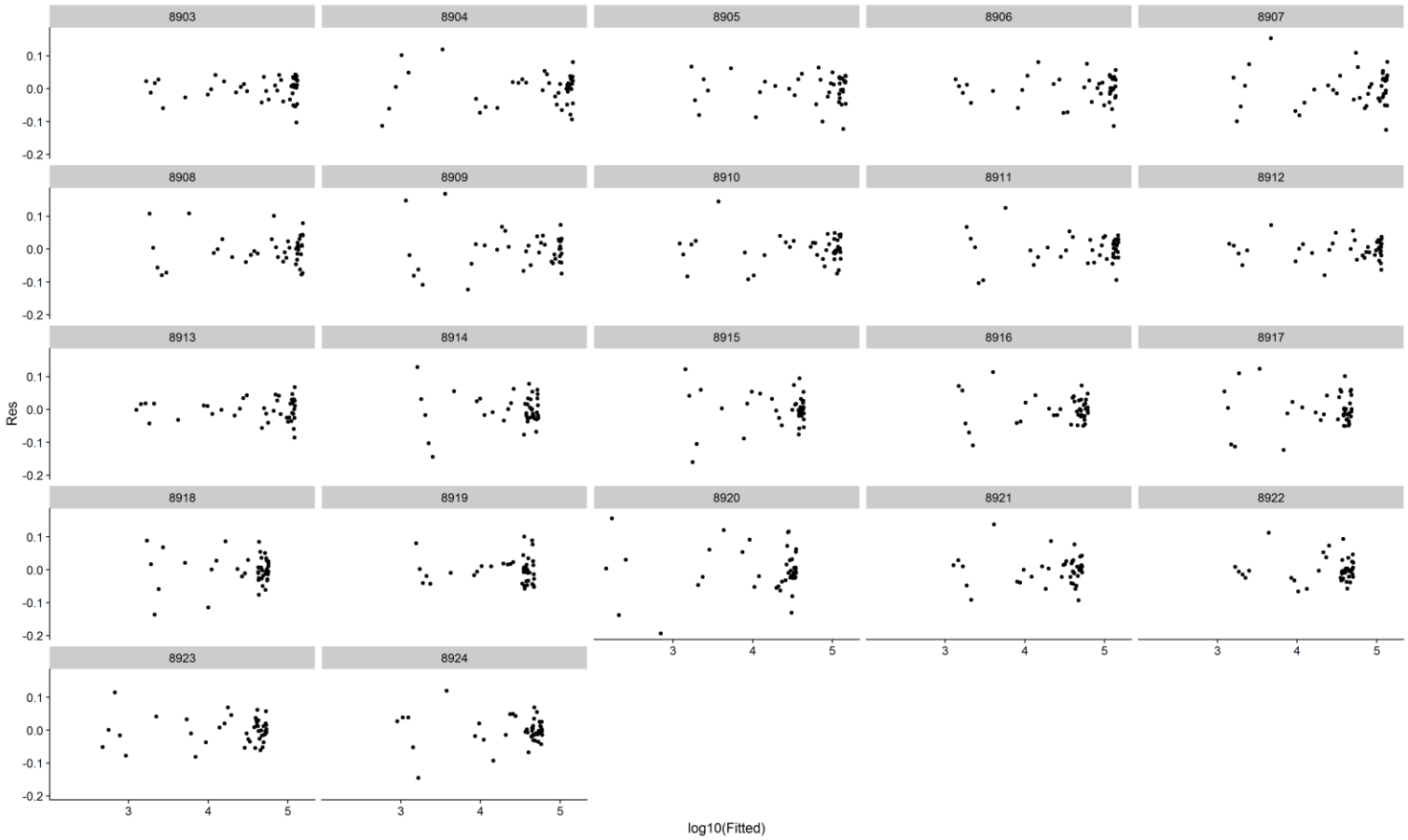

Mid-point application: compound 1

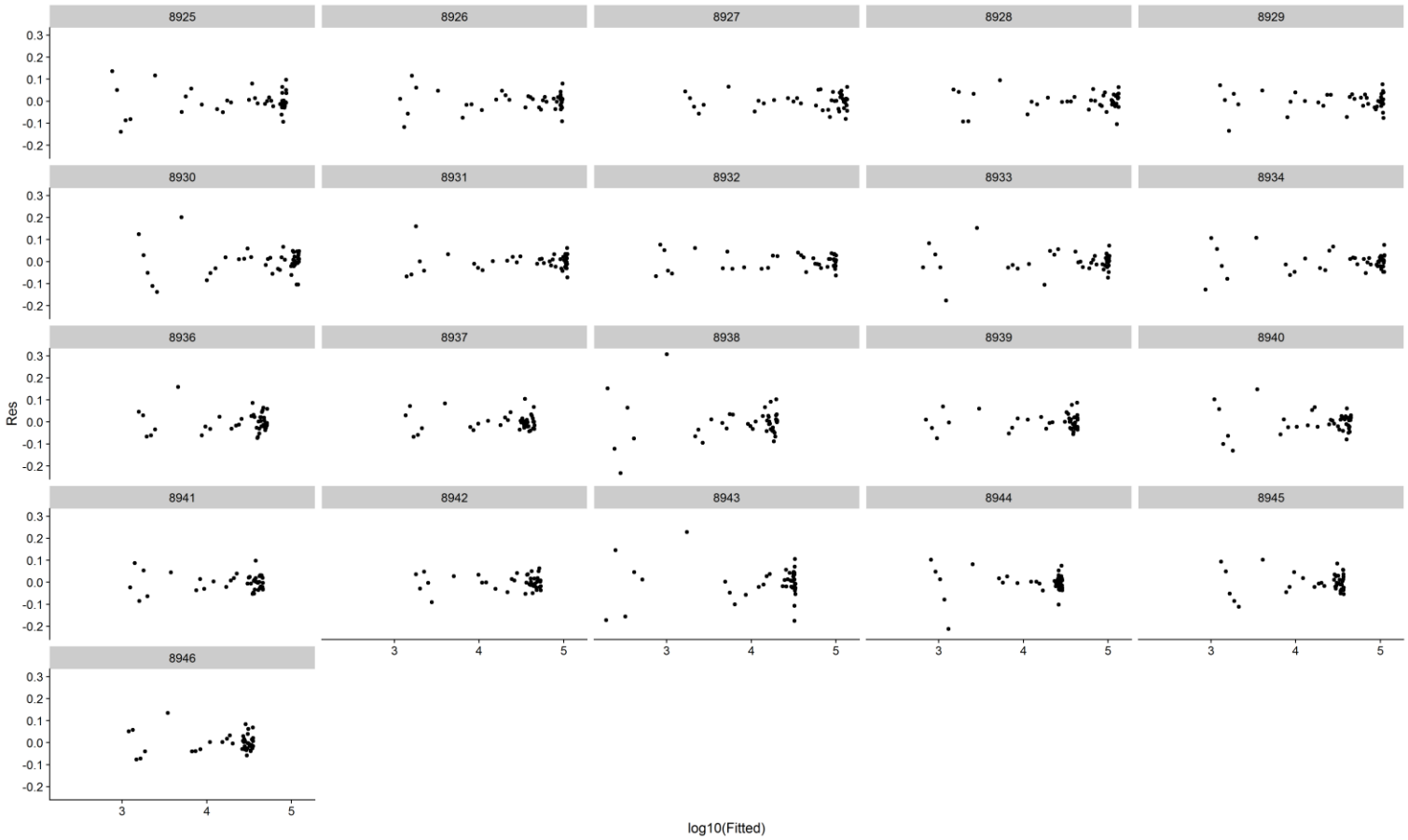

Mid-point application: compound 2

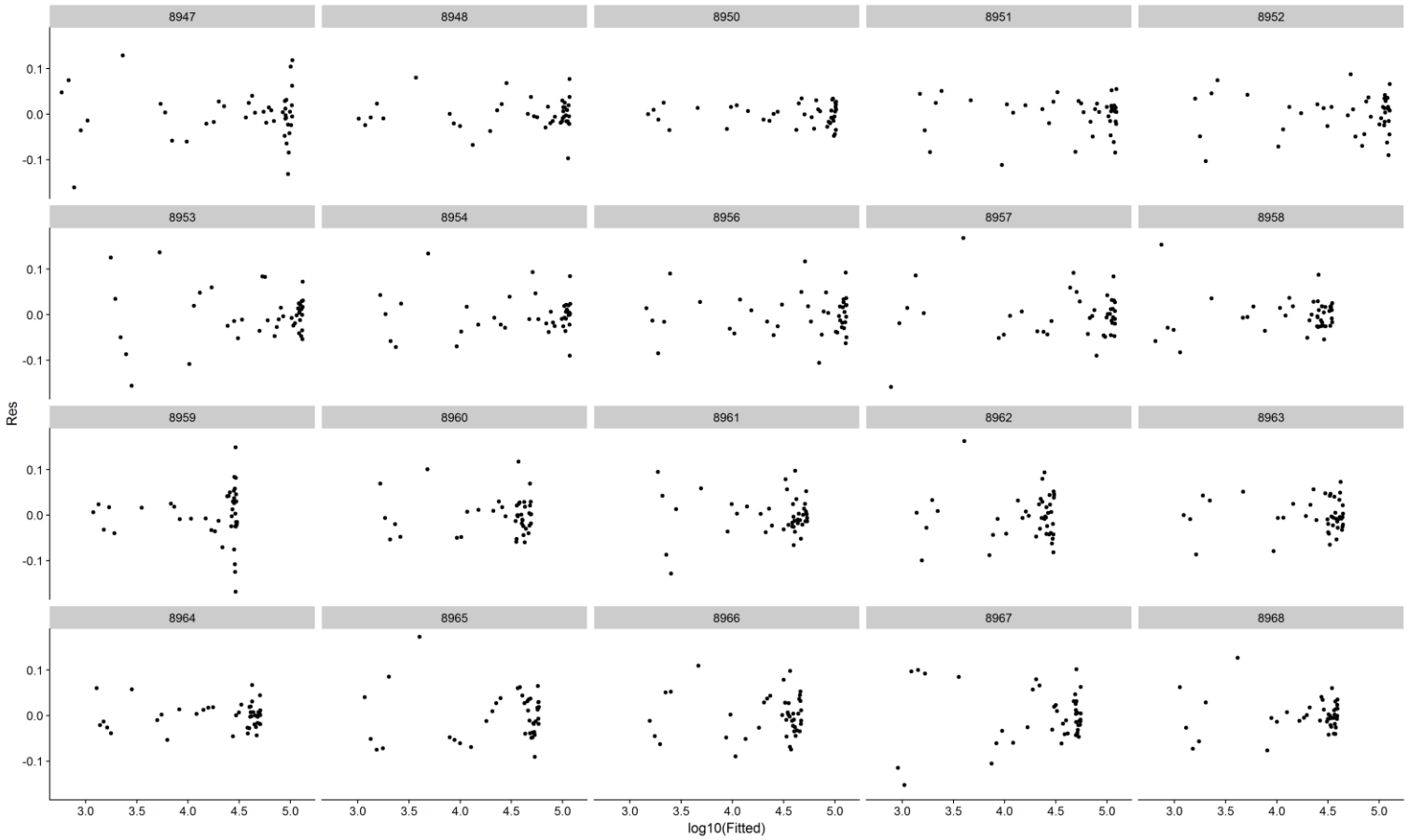

Mid-point application: compound 3

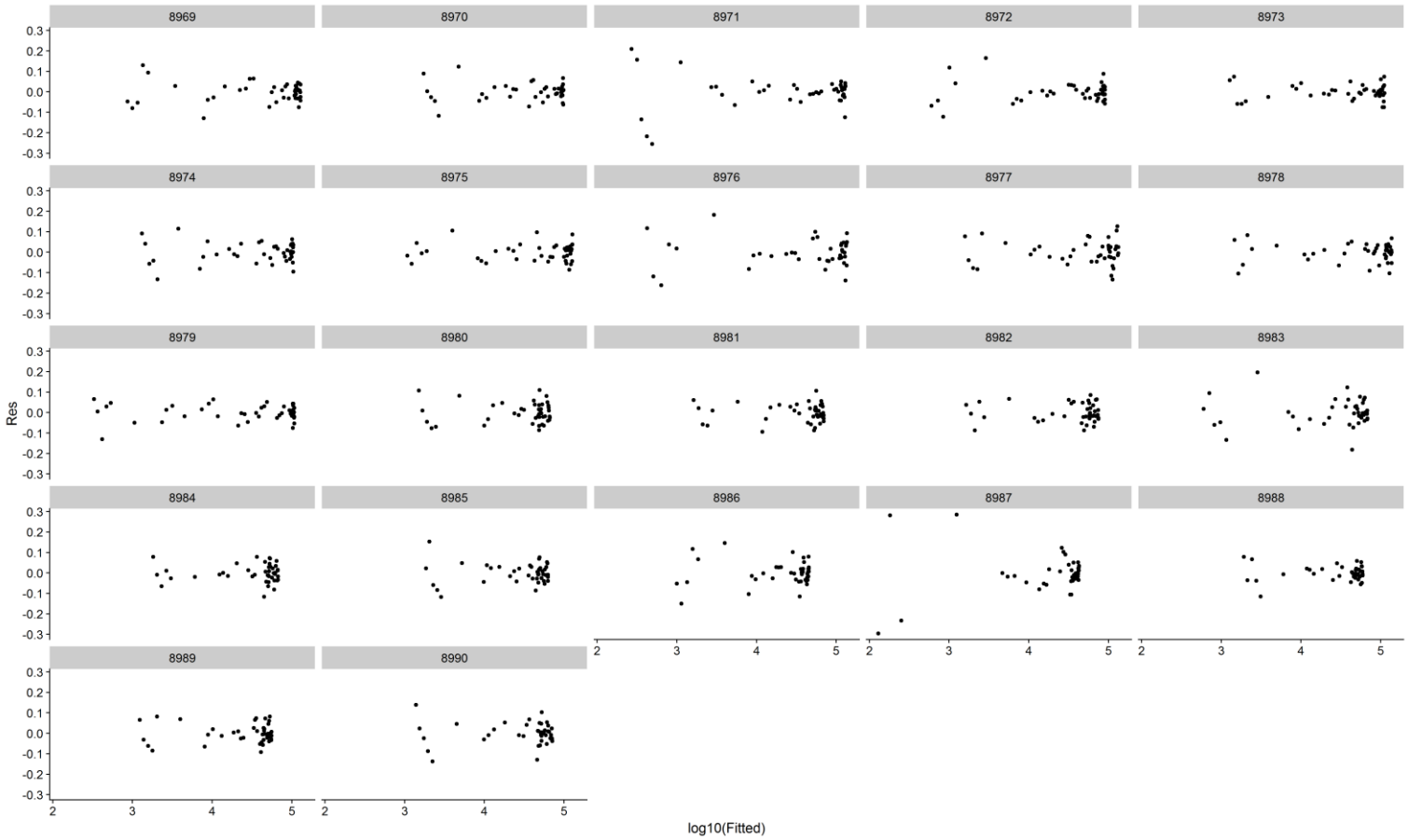

Mid-point application: compound 4

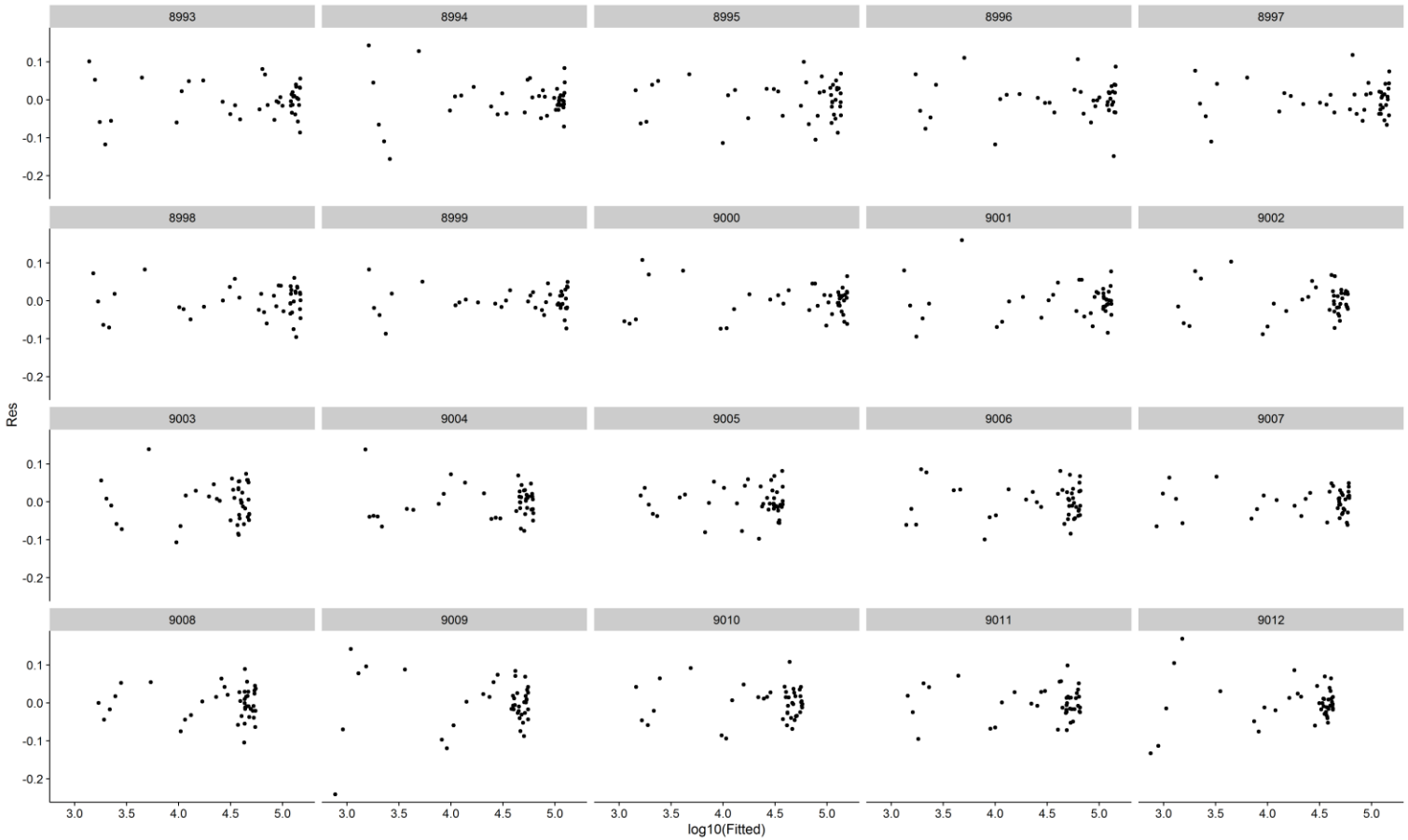

Late application: genapol

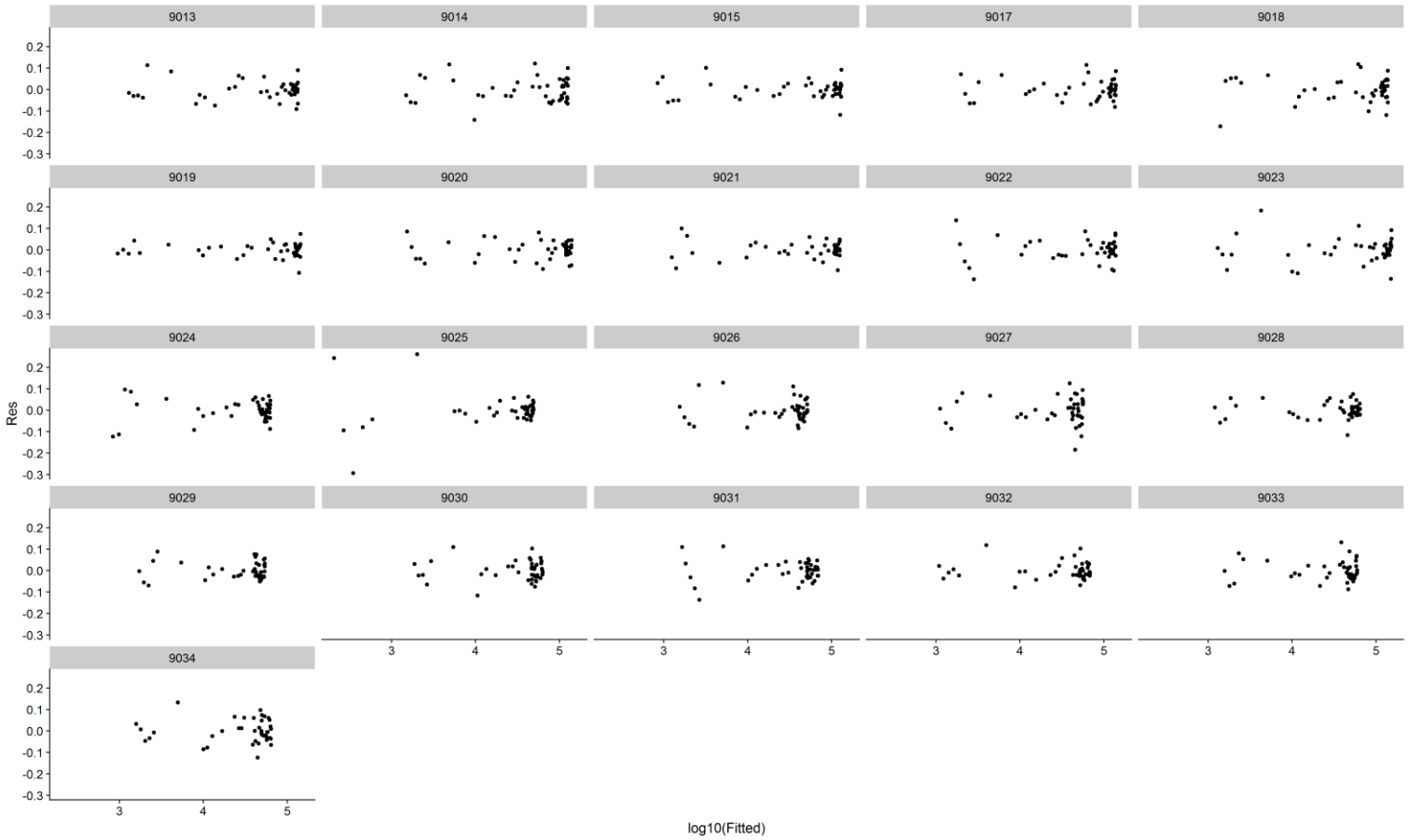

Late application: compound 1

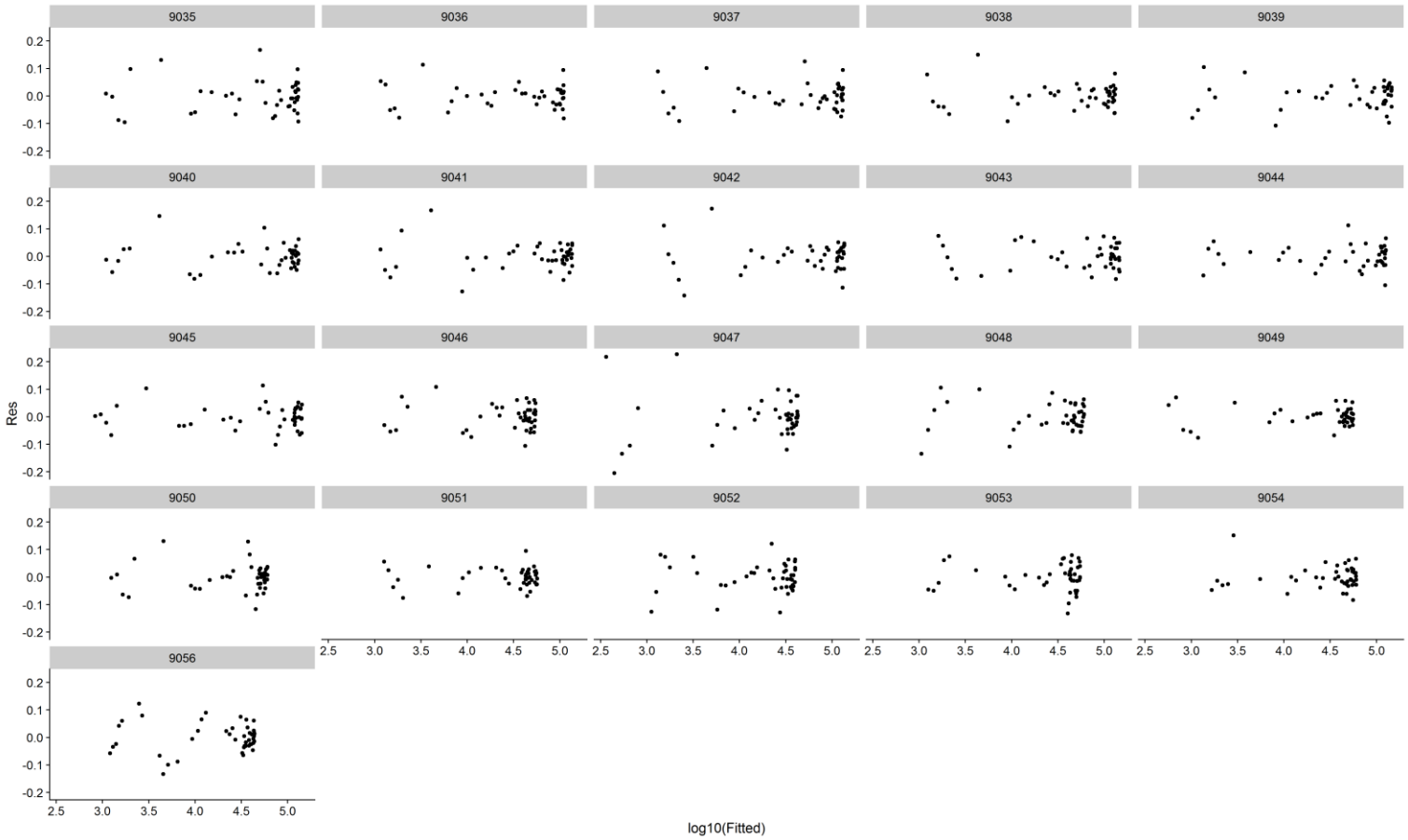

Late application: compound 2

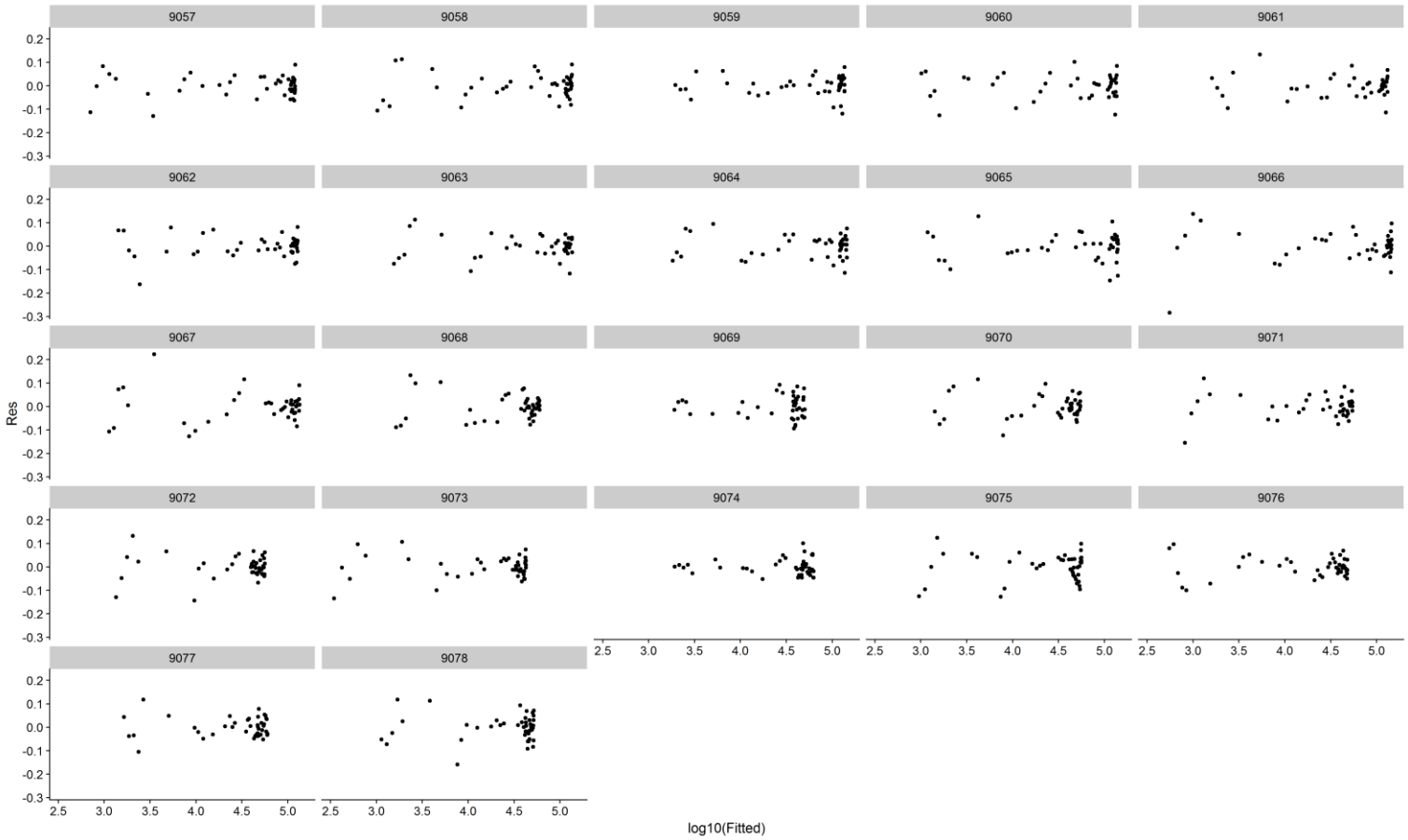

Late application: compound 3

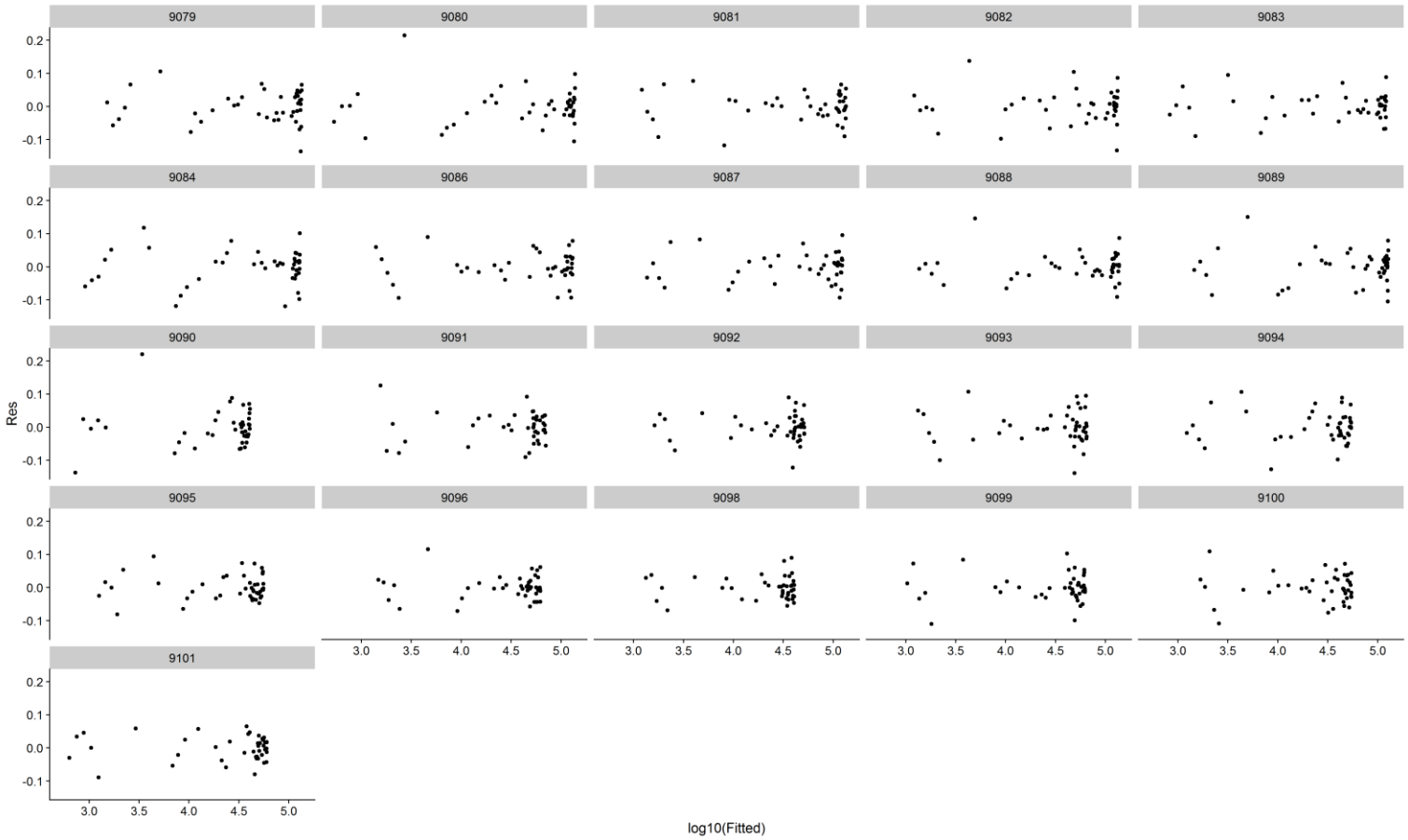

Late application: compound 4